Early Miocene Olistostrome Belt in Tanegashima and Re-exmamination of the Tectono-stratigraphic Setting of the Southern Shimanto Belt in North Ryukyu

福田, 泰英

https://doi.org/10.15017/1654978

出版情報：九州大学, 2015, 博士（理学）, 論文博士
バージョン：

Early Miocene Olistostrome Belt in Tanegashima and Re-examination of the Tectono-stratigraphic Setting of the Southern Shimanto Belt in North Ryukyu

Yasuhide FUKUDA

CONTENTS

Abstract

Ryukyu Arc is divided geotectonically into three regions, North, Central and South Ryukyus separated by arc-perpendicular depressions with some amounts of left-lateral displacement: the Tokara Channel on the north and Kerama Gap on the south. North Ryukyu has been considered as the most important key field to examine the different tectonic evolution between the proto-SW Japan and Ryukyu Arcs during Cenozoic. The Kumage Group in North Ryukyu has been believed to be an extent of the Southern Shimanto Belt in Kyushu from a similar lithologic facies and deformations. Many lines of evidence on fossil age, sedimentology and structural geology of the group have been required. Aims of this study were focused, therefore, to describe sedimentary facies, facies successions, and style of deformations in detail, and to obtain available planktonic foraminiferal remains through sampling of mudstone from many localities. As the result, this paper revised the previous Kumage Group and proposed a new tectono-stratigraphic division. Foraminiferal bio-chronological data was obtained on the precise timing of the formation of olistostrome belt constituting the outermost part of the Shimanto Belt.

The Kumage Complex occupies the north and central parts of Tanegashima and extends to the northwestern part of Yakushima on the southwest. The detailed analyses of depositional facies and deformation structures along the coastal regions and some on land exposures show clearly that the majority of clastic successions of the complex are composed of turbidites of deep-sea fan system with shelfal succession locally in the slump beds. The complex is subdivided into three units: the Hamatsuwaki, Fukago, and Sumiyoshi Units in the lower, middle, and upper parts, respectively. The Hamatsuwaki Unit is in fault contact with the Fukago Unit. Although it exposes restrictedly near Hamatsuwaki port, but presents a higher deformation grade than other units within this complex. Meso-scopic asymmetric folds with axial plane cleavages are developed, respectively. Due to the extensional strain parallel to cleavage plane, most of sandstone beds are converted to boudins. It is assumed that the Hamatsuwaki Unit was of accreted trench-fill deposits originally because of intense lateral shortening under high confining pressure. The Fukago and Sumiyoshi Units are thick-bedded clastic successions of deep-marine fan systems. The

Fukago Unit assigned to Middle Eocene to Oligocene in age from radiolarian fossils and is composed of sandstone-dominant facies in the lower to middle parts representing a thickening and coarsening upward succession in 10s to 100meters thick and of shale-dominant in the upper. The Sumiyoshi Unit, dominant in sandstone, is dated Early Miocene from foraminiferal bio-chronobiology. These units mentioned above are less deformed generally. Some large-scaled, asymmetric flexural-slip folds, in several kilometers scale, accompanied with high-angled thrust faults occur in the Fukago Unit partly. Four facies associations were distinguished in which axial and lateral flow directions were observed in the channeled and channeled lobe and the lobe and lobe-fringe facies associations, respectively. Facies and paleocurrent data indicate an elongated deep-marine forearc basin for the Kumage Complex.

The Kadokurazaki Complex, on the other hand, represents a very chaotic nature in lithology, stratification, and deformation styles. This complex is traceable to the southern part of Yakushima directly. It is made up of a large-scaled chaotic sedimentary mixture including many blocks or clasts in various size from 10s centimeters to 100s meters in length embedded in scaly mudstone as block-in-matrix fabric. Majority of blocks or clasts are of allochthonous, therefore, it is identified to an olistostrome because of a huge-scaled gravity mixture of various rocks. Mega-liths or sheeted blocks present a wide variety of clastic succession of deep-sea fan and shelf facies, and contain an oceanic rocks assemblage such as pillow basalt, volcanic breccia, and iron-ore deposits rarely. Majority of mega- and meso-liths are lithologically similar to the turbidite facies in the Kumage complex. Shallow-marine successions consisting of hyperpycnites and storm beds of shelf environment were found not only from some olistoliths in the Kadokurazaki Complex but also from slump sheets in the Kumage Complex. Thus, the facies analysis suggests that the almost of olistoliths in the Kadokurazaki Complex were derived from the Kumage Complex essentially. Geometric fold analysis for some sheeted olistoliths demonstrates the direction of sliding down from west or northwest.

In summary this study provided evidence for the development processes of tectono-stratigraphic setting of the Southern Shimanto Belt of North Ryukyu in relation to that of the Philippine Sea Plate as follows: First, it should be concluded that the tectono-stratigraphic setting of the Kumage and Kadokurazaki Complexes are correlative with the Hyuga and Nichinan Groups in Kyushu, but they do not continue to Central and South Ryukyus. Second, the Kumage Complex had been formed as a subduction complex during Middle Eocene to Oligocene through the convergent processes of the Philippine Sea Plate. Within the Kumage Complex, the Hamatsuwaki and Fukago Units could be reconstructed as the accretionary prism and forearc basin deposits, respectively. Third, the olistostromal Kadokurazaki Complex representing a huge collapse of forearc region was resulted from the re-subduction the Philippine Sea Plate just after the opening of the Shikoku Basin. The timing of the emplacement of olistostrome could be assigned precisely to the end of Early Miocene between the youngest age (N.4-N.6 zones: ca. 23-17.5Ma) of the complexes and the intrusive rocks (18.2Ma) prior to the shallow marine Kukinaga Formation in Middle Miocene. It is suggested strongly, therefore, that the opening of Japan Sea during 17 to 15Ma could be inferred as the most possible driving force for the extensive large-scaled failure and subsequent rapid elevation of forearc region.

1. Introduction

1.1 General information

(1) Convergent margin of the Philippine Sea Plate

Current plate boundaries and remnant spreading centers in the Philippine Sea are shown in Fig.1.1.1. The seafloor magnetic anomaly data and ODP/DSDP results show that the Daito Basin, the west Philippine Basin, the Shikoku-Parece Vela Basin and the Mariana Trough were formed since late Cretaceous (Seno & Maruyama, 1984, 1985). Honza & Fujioka (2004) assumed that "During the Late Cretaceous, the Daito Ridge and the Philippine Islands were positioned along the boundary between the Indian and Pacific Plates" from the result of the geological and geophysical surveys.

These ridges were separated from the western part of Mindanao Island due to spreading at the central part of the proto-Philippine Arc (Holloway, 1981; Haraguchi *et al.,* 2014). The Kita-Daito Ridge has been formed as remnant arc in the Western Philippine Basin. The Central Basin fault in the center of the West Philippine Basin initiated to spread in N-S direction during Eocene time (Karig, 1975; Watts *et al*., 1977; Scott & Kroenke, 1980; Seno & Maruyama, 1984, 1985). The evolution of the proto-Mariana Arc commenced in middle Eocene time. By late Oligocene, the Shikoku and Parece Vela basin had begun to spread, causing the proto Izu-Ogasawara Arc to be divided into the Izu-Bonin Arc and the Kyushu Palau Ridge.

With spreading of the West Philippine Basin, the proto Izu-Ogasawara Arc moved to the northeast. The north end of the proto arc probably was located in the Pacific Ocean between North Ryukyu and Kyushu at ca. 40 Ma (Seno & Maruyama, 1984, 1985).

In Central and North Ryukyu, the Philippine Sea Plate began to subduct along the Ryukyu trench, and the accretional wedge as the Kumage Group has been formed in North Ryukyu. It is suggested, therefore, that the sedimentary systems and geological features of the Southern Shimanto Belt have been directly affected by the motion of the Philippine Sea Plate during Middle Eocene to Early Miocene time. It is important to know about sedimentation system and

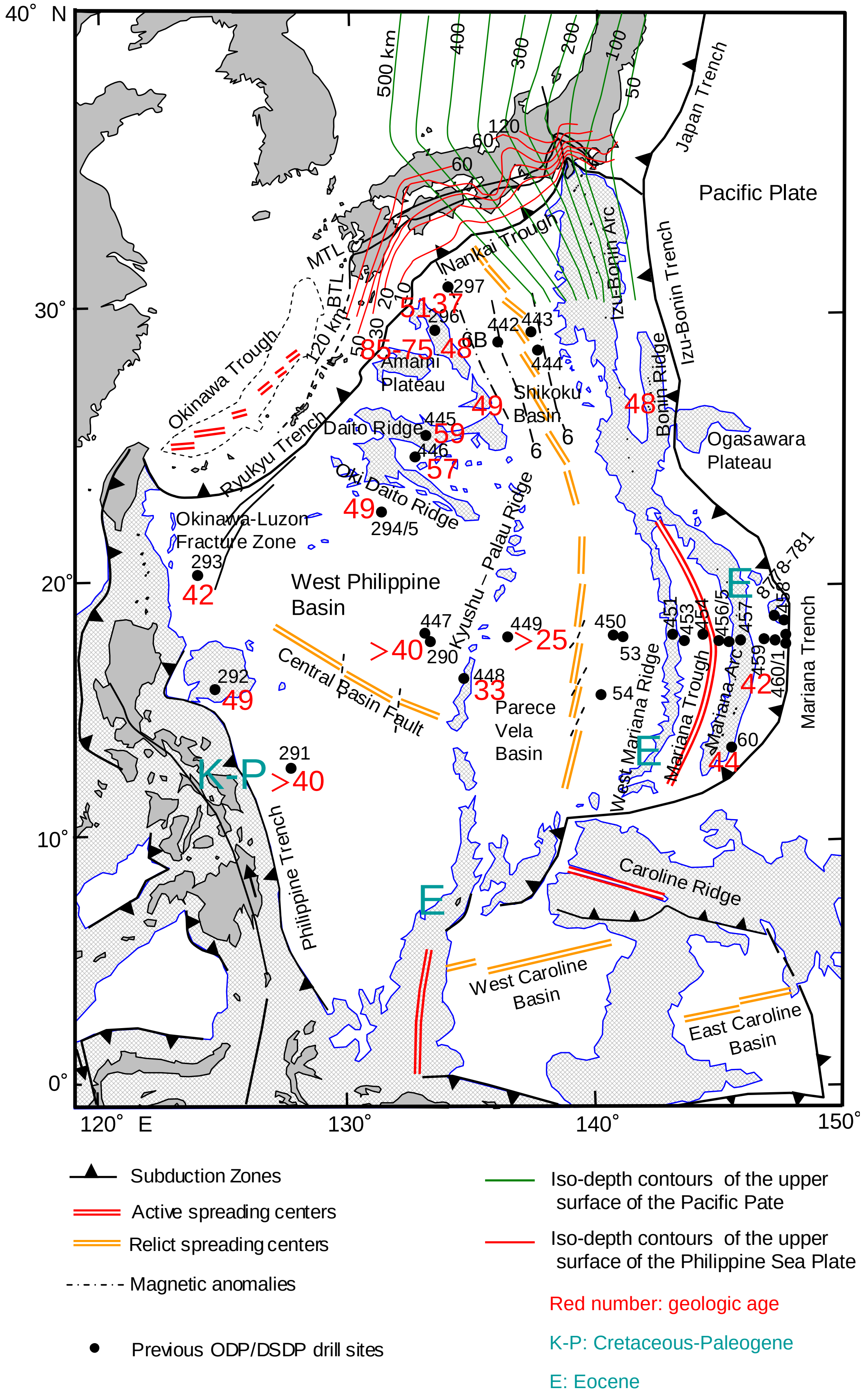

Fig.1.1.1 Current plate boundaries and relict spreading centers in the Philippine Sea Plate (modified after Taylor, B., 1992). Iso-depth contours of seismic center of the Pacific Plate and Philippine Sea Plate from Hasegawa et al (2010). Okinawa-Luzon Fracture Zone from Okino *et al*. (1999). Location of the Okinawa Trough from Letouzey and Kimura (1987). Geologic age (Ma) and epoch from compiled map by Seno & Maruyama (1984, 1985).

tectonics of the Southern Shimanto Belt in North Ryukyu, because it was located at the junction of the Southwest Japan Arc and the Ryukyu Arc.

(2) Geological outline of the Ryukyu Arc

The Ryukyu Arc was formed by the interaction of the Philippine Sea Plate and the Eurasian Plate since Paleocene. Now, the Ryukyu Island Arc is located at a convergent plate margin where the Philippine Sea Plate is subducting under the Eurasian Plate along the Ryukyu trench. The Okinawa Trough at the northwest side of the island arc is an active back arc basin after the deposition of Pliocene Shimajiri Group (Kamata & Kodama, 1994, 1999; Park, J.-O, *et al*., 1998).

Ryukyu Islands about 1200km long are an island chain of Ryukyu Arc lying from Kyushu to Taiwan. These arcuate islands are divided morphologically and geologically into three divisions separated at the Tokara Strait and Kerama Gap (Konishi,1965): North, Central and South Ryukyus (Kizaki, 1978, 1979, 1986).

The Southern Shimanto Belt is exposed in Tanegashima and Yakushima Islands of North Ryukyu, and Amami-Oshima and Okinawa Island of Central Ryukyu, but it does not occur in South Ryukyu.

In North-Central Ryukyu, the basement rocks are composed mainly of the Paleozoic-Mesozoic olistostromes comparable to the Chichibu Belt and the Shimanto Supergroup of Southwest Japan, represent the geotectonic arrangement of the outer Belt of Southwest Japan. The South Ryukyu Arc is characterized, on the other hand, by high-pressure metamorphic rocks (Yaeyama metamorphic rocks), Eocene volcanics (Nosoko volcanics), limestone (Miyara Group), and lower Miocene sediments (Yaeyama Group) (Kizaki, 1986).

1.2 General Geology

In South Kyushu and North-Central Ryukyu, the Shimanto Supergroup is divided into two sub-belts, such as the Northern and Southern Shimanto Belt (Fig.1.2.1). The Northern Sub-belt is

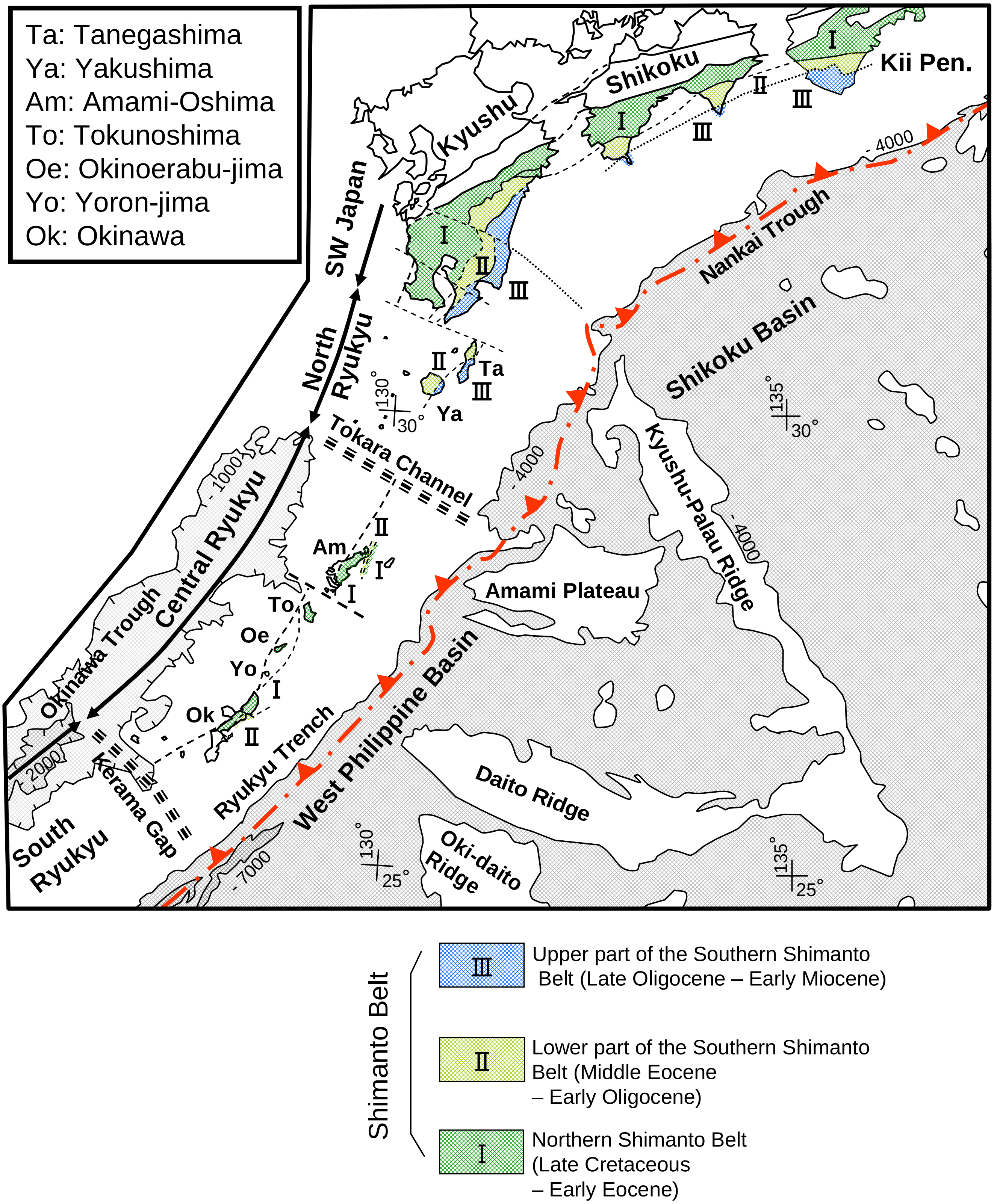

Fig.1.2.1 Tectonic division of the Shimanto Belt and between Southwest Japan and Central Ryukyu Arcs. After Sakai (1985, 1994).

occupied by the Lower Shimanto Supergroup composed of the subduction complex, ranging from late Cretaceous to early Paleogene in age (Sakai, 1992; Teraoka et al., 1999). The Southern Shimanto Belt is divided into the Middle Eocene to Early Oligocene Hyuga Group in the north region and the Late Oligocene to Early Miocene Nichinan Group in the south region.

The basement rocks of Tanegashima in North Ryukyu were named Kumage Group by Hanzawa (1935) and they are comparable to the Hyuga Group (Hashimoto, 1956) in Kyushu. The Kumage Group is distributed also in Yakushima and Magejima, west Tanegashima. In Central Ryukyu, there is the Wano Formation (Ishida, 1969) in the northern part of Amami-Oshima, and the Kayo Formation (Flint *et al*., 1959) in the east area of the central part of Okinawa Island.

In Ryukyu Islands, the Southern Sub-belt shows complicated structures and is generally poor in fossil evidences. However, these rocks have been considered to Middle Eocene to Oligocene age, based on fossil evidences (such as *Nummlites*, radiolarians and molluscs) (Ishida, 1969; Konishi, 1973; Hayasaka *et al*., 1980; Okada et al., 1982; Hayasaka *et al*., 1983; Hayasaka, 1988; Taira et al, 1988; Suzuki and Ujiie, 1985;Sakai, 1994; Saito *et al*., 2007).

The Wano Formation and the Kayo Formation of Central Ryukyu are considered to be Eocene in age based on the common occurrence of *Nummulites amakusaensis* Yabe and Hanzawa, 1925 (Suzuki & Ujiie, 1985). These strata are comparable to the fore arc basin fill deposits that composed of turbidite sequence accompanied by conglomerates in lower part. The geological structure represents a synclinorium which the axis-plane dips northwest-ward, and the east and west franks are cut by thrusts dipping towards NW in direction.

1.3 Objective of present investigation

The Southern Shimanto Belt in north-central Ryukyu has been regarded as the accretionary complex ranging from Eocene to Oligocene in age, though it is rather poor in fossil occurrence and intricate structure (Konishi, 1963; Hayasaka *et al*., 1980; Okada *et al*., 1982; Suzuki and Ujiie, 1985; Sakai, 1994; Saito *et al*., 2007). In addition, it has been pointed out that the Southern Shimanto Belt (Kumage Group) of North Ryukyu is similar to the Hyuga Group and the Nichinan Group based on the lithostratigraphic features and geological structure (Sakai, 1985, 1988, 1992, 1994).

However, the difference in sedimentary system and deformation structures between the Southern Shimanto Belt of North Ryukyu and Central Ryukyu have been recognized (Sakai, 1985, 1992, 1994; Saito, 2007). The former composed of turbidite sequence is characterized by coarsening- and thickening-upward cycles, but the latter shows fining- and thinning-upward cycles (Ishida, 1968; Sakai & Fukuda, 1994; Fukuda, 2008).

As for the lithostratigraphic and structural features, there is a similarity between the Southern Shimanto Belt of North Ryukyu and South Kyushu. From the geologic province point of view, both regions show same arrangement of the accretionary complexes in western region and olistostrome belt in eastern region. The Southern Shimanto Belt of North Ryukyu yields poor fossils, but involves particular importance to tectonic evolution.

It is still remained to solve the genetic period and process of the olistostromes which are not clear in North Ryukyu region. The main objectives of this study to decipher the above mentioned unsolved questions include the following:

1) to summarize the structural and sedimentological features of the Southern Shimanto Belt focusing on the oliststrome,
2) to carry out the geological age resolution of the Southern Shimanto Belt based on planktonic foraminifera, and
3) to make clear the timing of emplacement of olistostrome in North Ryukyu.

2. Geologic framework

2.1 Introduction

Tanegashima Area

In Tanegashima, the Southern Shimanto Belt exposes in the most part of the island except for the middle and southern part where shows rather sporadic distribution covered with the formations of Miocene and later ages (Hanzawa, 1935; Hashimoto, 1956; Okada & Whitaker 1974; Hayasaka *et al.*, 1980; Sakai, 1980; Okada *et al.*, 1982; Kuwazuru & Nagatsu, 2007; Saito *et al.*, 2007ab). The soutern Shimanto Belt is overlain by the Miocene Kukinaga Group with a large-scale clino-unconformity in the middle and southern part of the eastern areas (Fig.2.1.1, Table 2.1.1). The late Pliocene Masuda Formation is exposed in the central and southern parts of the island, and unconformably overlying with the erosional surface of Kumage and Kukinaga Groups (Hayasaka, 1969, 1973).

The geological map and profile of Tanegashima in this study are shown in Figs.2.1.2 and 2.1.3. As shown in Fig.2.1.2, some molluscan fossils comparable to the Ashiya fauna of Ashiya Group have been obtained from two localities of the Southern Shimanto Belt (Hayasaka *et al.*, 1980; Hayasaka, 1985).

An abundant occurrence of radiolarian fossils from the variegated shale interbedded in turbidite sequence in the central and southern part of the island has been reported (Okada *et al.*, 1982; Kuwazuru & Nagatu, 2007). The radiolarian fossils are assigned to the age from Middle Eocene to Early Oligocene.

In the northwest part of the Island, a rock body of lamprophyre (camptonite) is known to occur, showing a long and narrow distribution in the NNE-SSW direction (Taneda & Kinoshita, 1972; Yagi *et al.*, 1975). The length is up to 20km and the width changes between 6 and 12m. K-Ar age of this dyke rock indicates 16±2.0 Ma (Taneda & Kinoshita, 1972). However, Ogasawara (1997) carried out precise K-Ar dating of lamprophyre in the southern part of Nishinoomote and dyke rock of quartz porphyry of Shimamazaki in Minamitane area, and the obtained ages were 18.2 ± 0.9 Ma and 15.6 ±

0.8 Ma, respectively.

Yakushima Area

In Yakushima, the Southern Shimanto Belt is exposed along the coast of the island (see Fig.12 in the Appendix). Most of the formations were underwent contact metamorphism by Middle Miocene granite intrusion. The age of the granite intrusion is considered about 14 Ma (Shibata & Nozawa, 1968). Several quartz porphyry dikes are present on the northeastern margin of Yakushima and southwestern shore of Tanegashima. These dikes intruded in the Southern Shimanto Belt at the same time as Yakushima Granite emplacement (Ogasawara, 1997).

The stratigraphical and sedimentological studies of the basement rocks have been carried out by many workers (Hashimoto, 1956, Nagahama & Sakai, 1972; Sakai, 1980). However, fossils useful for geological age determination have been not found from the island. Recently, the radiolarian fossils have been obtained from the red mudstone distributed in the northeast of the island. Their assemblages indicate the middle to early Late Eocene (Saito *et al.*, 2007).

2.2 Overview of regional tectonic framework

Recently olistostromes have been recognized from extensive area of the southernmost part of the Shimanto Belt as well as Kyushu (H. Sakai, 1988abc; T. Sakai *et al*. 1992). It extends from the west Kanto region to Tanegashima and Yakushima in north Ryukyu. However, such a huge scale olistostrome has not been found from Central and South Ryukyu.

Since Middle Eocene, the Outer Zone of Ryukyu and Kyushu, corresponding to the continental margin, has been considered that was a convergent margin of the Philippine Sea Plate having replaced from the Pacific Plate (Seno & Maruyama, 1984; Byne & DiTullo, 1992).

North Ryukyu has been considered as the most important key area to examine the different tectonic evolution between the proto-SW Japan and Ryukyu Arcs during the Cenozoic. Therefore, clarification of the timing of olistostrome emplacement in North Ryukyu contributes valuable information for the behavior of the Philippine Sea Plate.

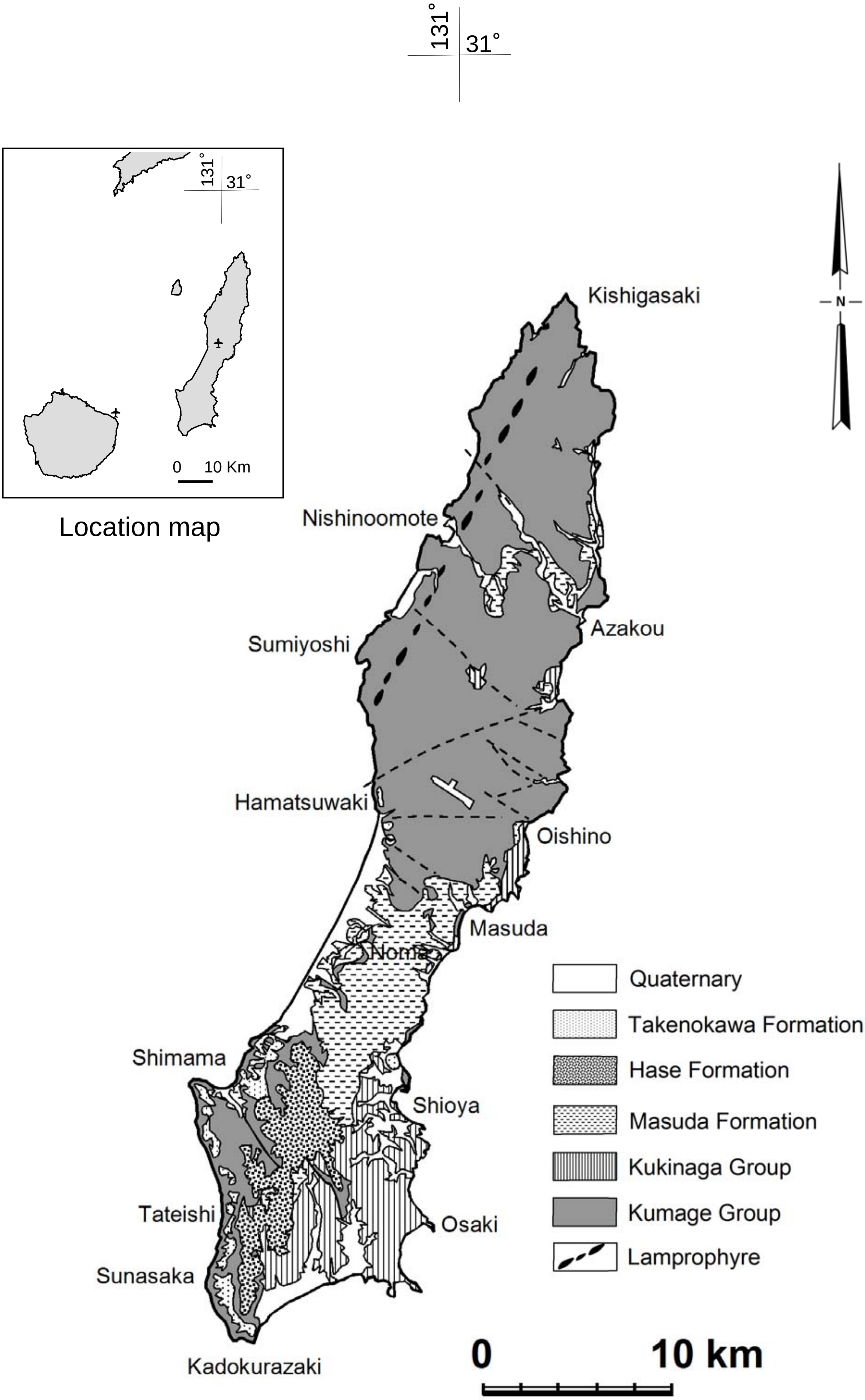

Fig.2.1.1 Geological map of Tanegashima Island.
From Hayasaka (1974) and Hayasaka *et al*. (1983).

Table 2.1.1 Stratigraphic Table of Paleogene to Quaternary sediments in Tanegashima (modified from Hayasaka et al., 1980, 1983).

Age	Group	Formation Complex	Thick-ness(m)	Lithology
Holocene	Alluvium		—	Sand, gravel and clay
	UC			
Pleistocene	Volcanic Ash		5	Loam
	UC			
	Takenokawa Formation		10	Reddish brown-colored sand, partially with clay and gravel beds.
	UC			
	Hase Formation		5	Subangular gravel (boulder to granule sizes) mainly of sandstone.
	UC			
Pliocene	Masuda Formation		20-100	Light brown, fine- to medium-grained, loose sandstone, partially with cross-bedded sandstone and fossil-bearing siltstone beds.
	UC			
Middle to early Late Miocene	Kukinaga Group	Osaki Formation	700	Reddish to yellowish brown, medium- to coarse-grained sandstone, often with thin granule conglomerate. Fossiliferous.
		Kawachi Formation	320	Bluish grey mudstone, with thin sandstone layers in its upper- and lowermost parts. Fossiliferous.
		Tashiro Formation	430	Conglomerate consisting of well-rounded cobbles and boulders mainly of sandstone.
	UC			
Middle Eocene to Early Miocene	Southern Shimanto Belt	Kadokurazaki Complex	700-1800	Chaotic deposits and large-scale slump sheets consisting of turbidie sequences.
		Kumage Complex	1800	Coherent turbidite sequences made up of thin- to thick-bedded sandstone, shale and variegated shale.

[UC: Unconformity]

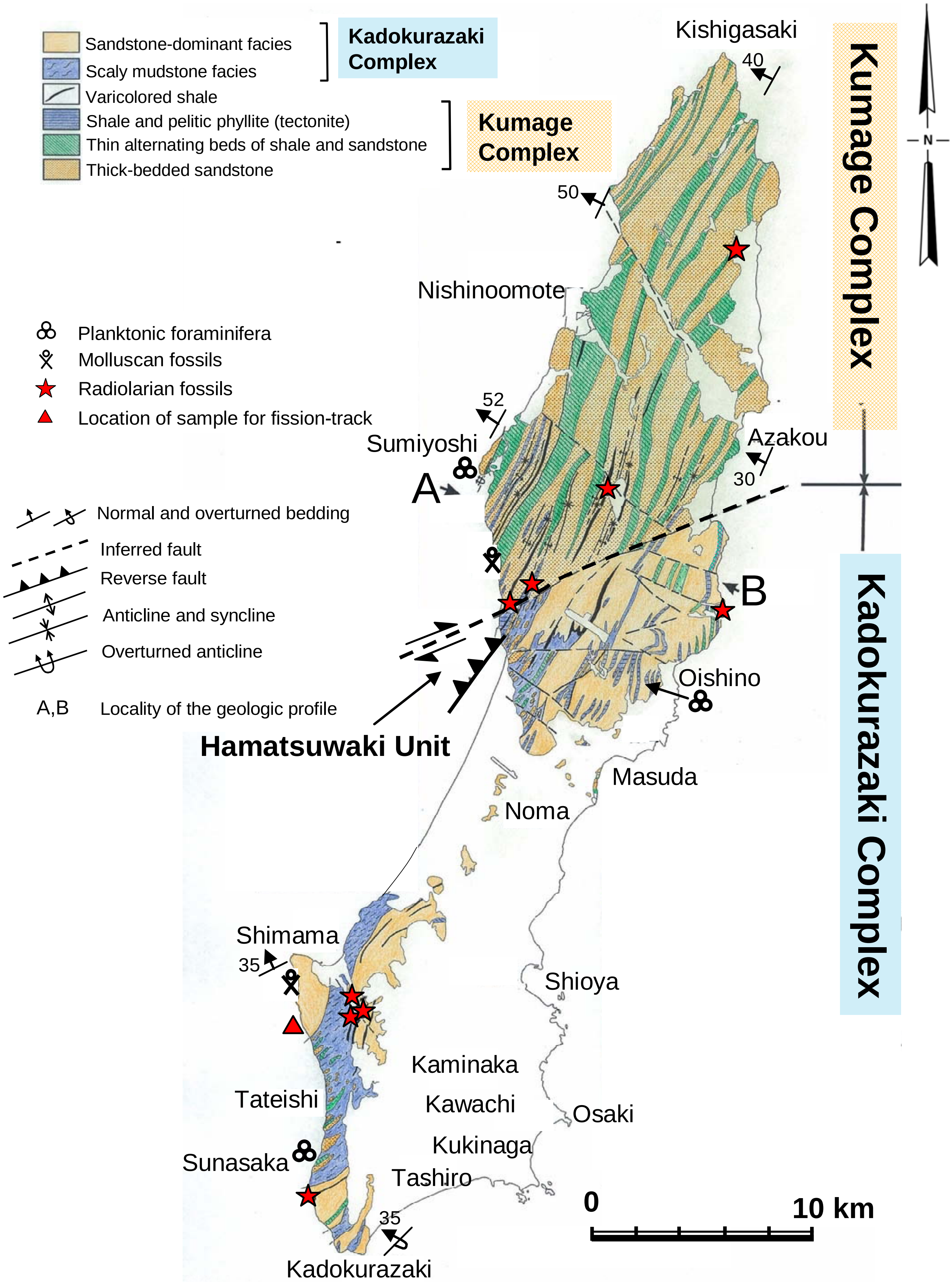

Fig. 2.1.2 Geological map of Tanegashima showing the distribution of the Kumage and Kadokurazaki Complexes. The geological map in northern part of Tanegashima was compiled from "*Geological map of Kagoshima Prefecture with Geological Sheet Map at 1:100,000* (Kagoshima Prefecture, 1990)".

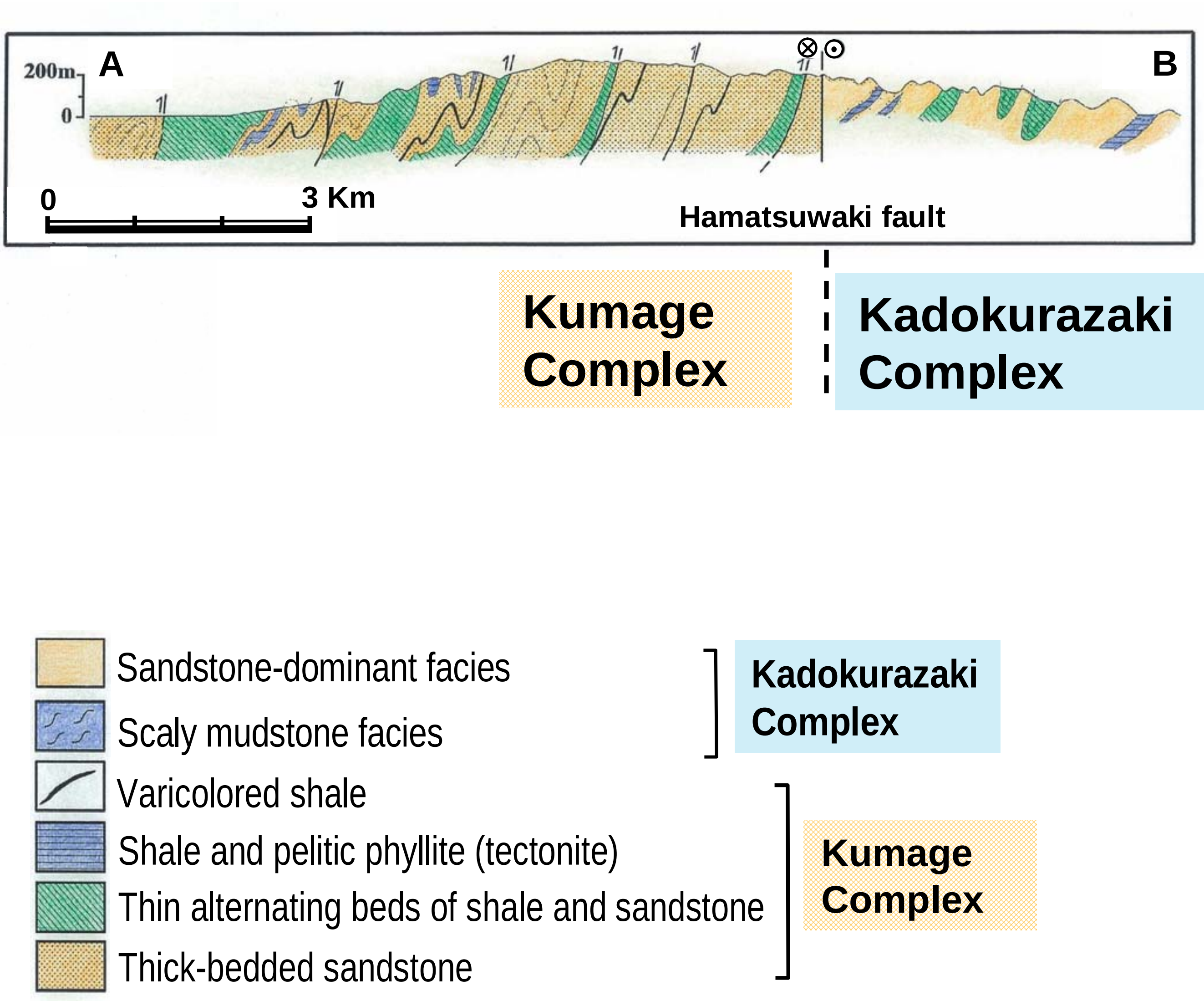

Fig. 2.1.3 Geologic profile of the northern part of Tanegashima.

3. Lithostratigraphy of the Southern Shimanto Belt in Tanegashima

The Southern Shimanto Belt of Tanegashima shows a general trend in NNE to SSW direction, nearly parallel to the long axis of the geomorphologic outline of the island (Fig.2.1.2) and dips intermediately to steeply (45-70°) westward in general (Fig.2.1.3).

Four formations were classified by Hayasaka *et al*. (1980): the Nijuban, the Hamatsuwaki, the Fukago and the Sumiyoshi in ascending order, mainly based on the sedimentary cycle of coarsening-upward (Fig.3.1.1, Table 3.1.1, Table 3.1.2).

On the other hand, Okada (1982) and Okada *et al.* (1982) recognized three formations, Kadokurazaki, Tateishi and Nishinoomote, from the base to the top bounded by thrust faults (Fig.3.1.1). These formations are characterized by a flysch facies with variegated shale, a chaotic facies and thick-bedded sandstone, respectively.

This study proposed that the Southern Shimanto Belt could be divided to two complexes; the Kumage and Kadokurazaki Complexes based on the characteristics of lithofacies and deformation structures (Fukuda & Sakai, 2009). The Kumage Complex represents a coherent nature and occupies the northern part of Tanegashima and the western part of Yakushima (Fig.12 in the Appendix). The Kadokurazaki Complex characterized by a chaotic body including large-scaled slumped blocks or sheets of turbidite sequences is exposed from the central to the southern part of Tanegashima and the eastern part of Yakushima. The Kumage and the Kadokurazaki Complexes are able to compare with the Hyuga Group and the Nichnan Group in Kyushu, respectively.

Main lithofaceis of Kumage Group

The characteristics of facies associations (FA1 to FA5) were discriminated based on facies analysis in the Kumage Complex (Fig.3.1.2, Table3.1.3). The relationships of the lithofacies and sedimentary environments are interpreted as follows:

・variegated shale (FA1)- abyssal plane.
・mudstone (FA2)- abyssal plain or trench floor.
・sand predominant alternation (FA3) – lobe.

- thick-bedded sandstone (FA4) - channel and channel-lobe transition.
- shale predominant alternation (FA5) - lobe fringe.

In the FA2 and FA3, coarsening- and thickening-upward mega-sequences are developed, frequently in the Kumage Complex probably related to the progradation of suprafans (Mutti & Normark, 1987; Pickering et al, 1989). Detailed geological maps and profiles in the middle and southern part of Tanegashima are shown in Figs.3.1.3-3.1.7.

Lithofacies and sedimentary features

In this study, eleven routes were selected to describe facies, deformation styles and making measured sections, as shown in Fig.3.1.8. Each column is shown in Figs.1-11 of the Appendix.

The Kumage Complex can be divided into three units bounded by thrust faults dipping steeply northwards. These units have similar lithologic characteristics of facies association, although there are some differences among individual sub-units.

On the other hand, the Kadokurazaki Complex is made up of chaotic rocks entirely and includes many large-scaled slump sheets. Large slump sheets were mostly derived from the Kumage Complex, however, some slump sheets and blocks are recognized as sliding mass from shelf deposits. In addition, slump sheets in the Kumage Complex exposed at Okigahamada show a characteristic of hyperpycnal flow deposits.

The Kumage Complex occupies the north and central parts of Tanegashima and extends to the northwestern part of Yakushima on the southwest. The detailed analyses of depositional facies and deformation structures along the coastal regions and some on land exposures show clearly that the majority of clastic successions of the complex are composed of turbidites in deep-sea fan system with localized shelfal succession in some slump beds. The complex is subdivided into three units: the Hamatsuwaki, Fukago, and Sumiyoshi Units in the lower, middle, and upper parts, respectively.

The Hamatsuwaki Unit is in fault contact with the Fukago Unit.

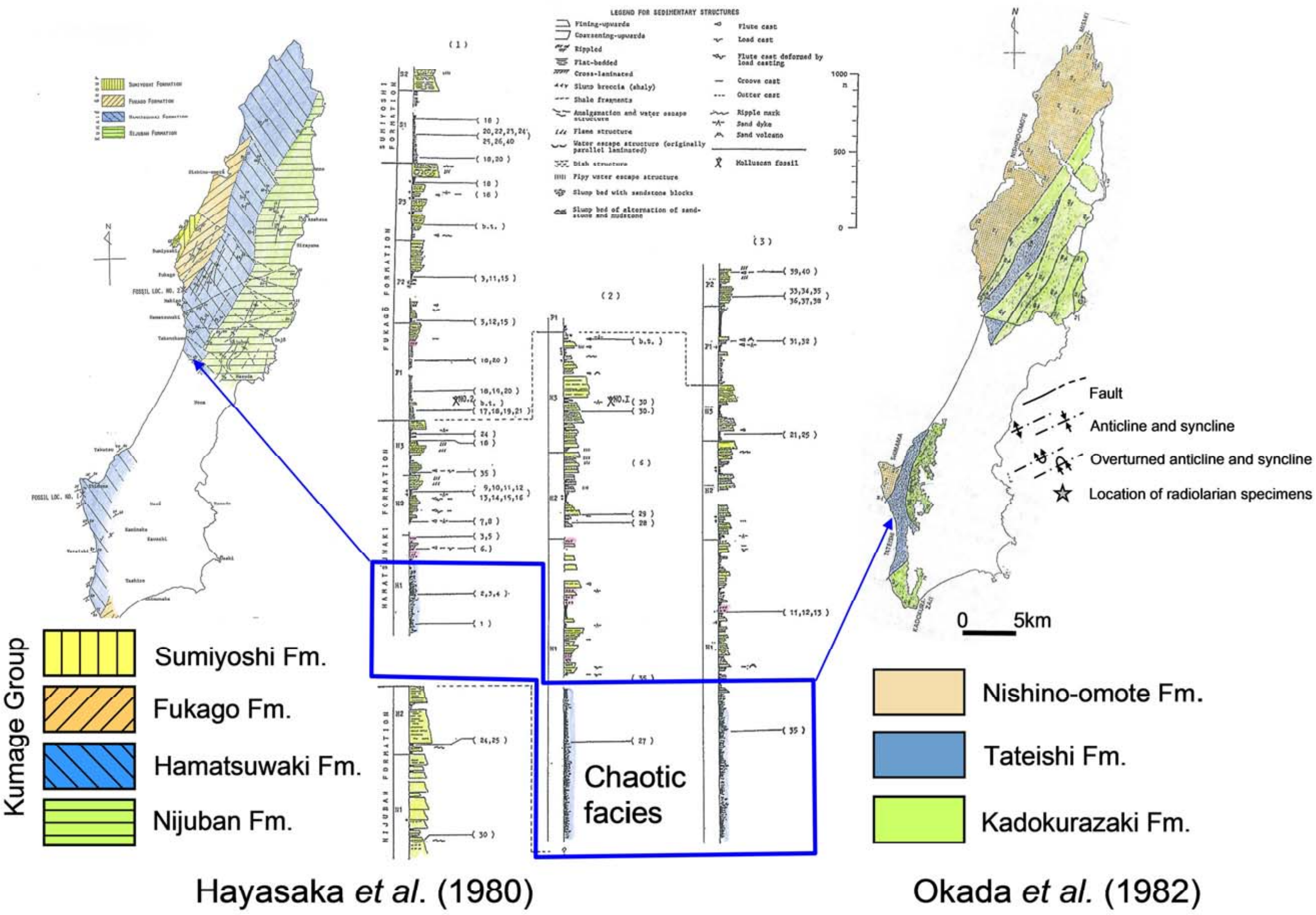

Fig.3.1.1 Comparison between two published geologic maps of the Southern Simanto Belt of Tanegashima. Columnar sections come from Hayasaka *et al*. (1980).

Table 3.1.1 Comparison of the newly defined tectono-stratigraphic units and sections with the previous lithostratigraphic divisions for the Southern Shimanto Belt along the west coastal region in the middle part of

Hayasaka *et al.*(1980)			Okada (1982)	This study		
Formation	Member	Lithofacies	Formation	Complex		Section
Sumiyoshi Fm.	S2	Thick-bedded sandstones	Nishino-omote Fm.	Kumage Complex	Sumiyoshi Unit	4
	S1	Thin-bedded alternation of sandstone and shale			Fukago Unit	3
Fukago Fm.	F3	Thick-bedded sandstones				
	F2	Predominantly sandy alternations				
	F1	Thin-bedded alternation of sandstone and shale				2
Hamatsuwaki Fm.	H3	Thick-bedded sandstones				
	H2	Predominantly sandy alternations	Kadokurazaki Fm.			
	H1	Large-scale slump beds and chaotic rocks	Tateishi Fm.		Hamatsuwaki Unit	1

Table 3.1.2 Comparison of the newly defined tectono-stratigraphic units and sections with the previous lithostratigraphic divisions for the Southern Shimanto Belt in the middle and southern regions of Tanegashima.

Hayasaka *et al.*(1980)			Okada (1982)	This study	
Formation	Member	Lithofacies	Formation	Complex	Section
Sumiyoshi Fm.	S2	Thick-bedded sandstones	Nishino-omote Fm.	Kadokurazaki Complex	11
	S1	Thin-bedded alternation of sandstone and shale			10
Fukago Fm.	F3	Thick-bedded sandstones			9
	F2	Predominantly sandy alternations			8
	F1	Thin-bedded alternation of sandstone and shale			7
Hamatsuwaki Fm.	H3	Thick-bedded sandstones			6
	H2	Predominantly sandy alternations			
	H1	Large-scale slump beds and chaotic rocks	Tateishi Fm.		5
Nijuban Fm.	N1	Thick sandstone	Kadokura-zaki Fm.		
	N2	Thick sandstone and sandy alternation			

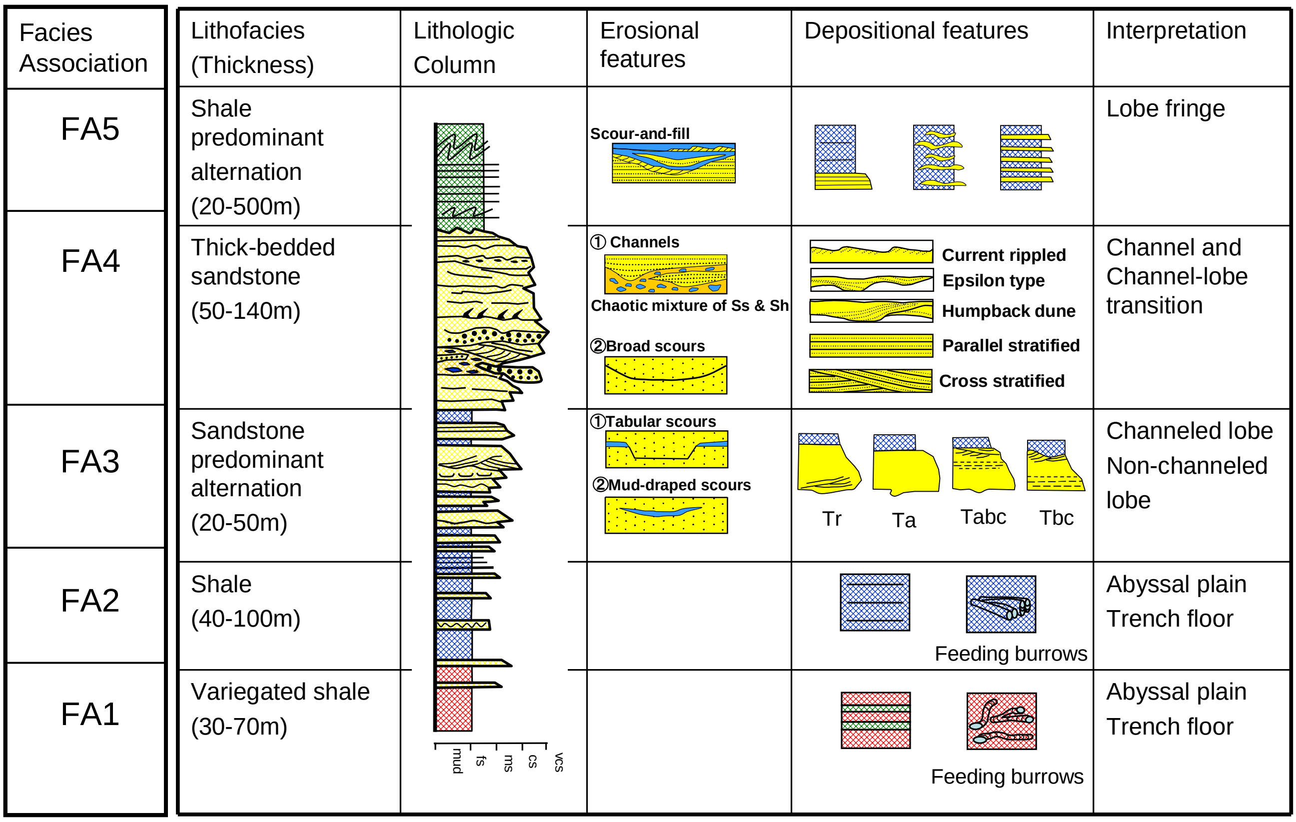

Fig.3.1.2 Representative facies associations distinguished in the Kumage Complex and their facies interpretations.

Table 3.1.3 Sedimentary features of coherent sequences of the Kumage Complex.

Facies Association	Lithofacies	Lithology	Sedimentary structures
FA5	Shale predominant alternation	Thick sequence of thinly bedded alternation of fine-grained sandstone (1-20cm thick) and shale (0.5-5cm thick). Slump structures occurred in the middle and upper part.	Current-rippled cross-lamination. Abundant small size of trace fossils and bioturbated muddy sandstone. Ichnofossil: *Terebellina*
FA4	Thick-bedded sandstone	Medium- to coarse-grained sandstone beds with subordinate shale beds and alternation of sandstone and shale, showing coarsening- and thickening upwards cycles of sedimentation. Mixed-layers of sandstone and shale breccia and slump beds occur adjacent to channel structures. Channel or channeled lobe sandstones comprise amalgamated coarse-grained to very coarse sandstone. Thin coal seams are occasionally found within sandstone sequences.	Channel-filled chaotic mixture of sandstone and shale, cross-lamination, ripple marks, sand volcanoes, flame structures, and various kind of water escape structure in the thick sandstone beds. Flute casts, horseshoe-shaped flute casts, groove casts, load casts and sandstone dykes in the alternation units. Inversely grading in thick-bedded sandstone.
FA3	Sandstone predominant alternation	Sandstone beds of various thicknesses accompanied with black shale and alternating beds of sandstone and shale, showing coarsening-upwards cycles of sedimentation. Thin beds of white tuff occur sporadically in this sandstone predominant alternation.	Gutter casts, flute cast, cross-lamination and various types of water escape structures in sandstone bed. Flysch trace fossils. Feeding burrows.
FA2	Shale	Bluish gray to black colored mudstone with thin interbeds of fine sandstone.	Feeding burrows.
FA1	Variegated shale	Red, green and yellow colored mudstone with thin-bedded turbidites.	Slump structures and sandstone dykes. Feeding burrows.

Table 3.1.4 Lithofacies and sedimentary features of the tectono-stratigraphic units and sections of the Kumage and Kadokurazaki Complexes in Tanegashima.

Complex	Unit	Section (Type locality)	Facies Association	Thickness (m)	Nature of Contact (L: Lower; U: Upper)	Lithofacies and Sedimentary features	Representative trace fossils	Mega-and Micro-Fossils	Geological Age
Kumage Complex	Hamatsuwaki Unit	**Section ①** Hamatsuwaki	FA1 FA2 FA3	300m	L: fault U: fault	Tectonite facies: composed intensely cleaved bluish-grey mudstone (FA2) and variegated shale (FA1) containing slumped beds and sandy turbidite (FA3).	Bioturbation HF burrows *Chondrirites* *Zoophycos*		
Kumage Complex	Fukago Unit	**Section ②** Hamatsuwaki - Makigo - Fukago	FA1 FA2 FA3 FA4 FA5	1470m	L: fault U: fault	Lower part: comprises sandstone dominant alternation (FA3) with shale (FA2) and with radiolarian- bearing variegated shale (FA1). Lower to middle part: consists many cycles of thickening and coarsening upward to asymmetric successions (Single cycle: 10-90m) (FA3, FA4). Upper part: comprises thinly bedded alternation of fine-grained sandstone and shale, and contains slumped ill-sorted muddy sandstone bed yielding molluscan fossils (FA5).	Bioturbation HF burrows *Chondrirites* IS burrows *Terebellina*	R M	Middle Eocene to Oligocene
Kumage Complex	Fukago Unit	**Section ③** Fukago - Sumiyoshi	FA1 FA2 FA3 FA4 FA5	2020m	L: fault U: fault	Lower part: consists of shale and turbidite succession with variegated shale (FA1). Middle part: comprises many cycles of coarsening-up (thickening-up) to asymmetric turbidite sequence produced by lobe deposition and switching (10-100m thick) (FA2, FA3, FA4). Upper part: consists of thinly bedded alternation of fine-grained sandstone and shale (FA5). Small-scale scour-and-fill structures occur partially in this alternation.	Bioturbation IS burrows *Terebellina*	Bf (*Glomospira*)	Unknown
Kumage Complex	Sumiyoshi Unit	**Section ④** Sumiyoshi	FA2 FA3	170m	L: fault U: unknown	Lowermost part: comprises mainly shale facies (FA2). Middle to upper part: consists of medium- to fine-grained sandstone beds characterized by fining-upward tendency (FA3). Epsilon cross-stratifications, humpback dunes, parallel stratifications and flame structures are found in thick-sandstone.		Pf Bf	Early Miocene
Kadokurazaki Complex		**Section ⑤** Tateishi - Sunasaka	Chaotic rocks	>1000m	L: fault (detachment) U: unknown	Chaotic deposits: shows block-in-matrix fabrics, characterizing deformed to chaotic rocks resulting from soft and hard sediment failures, transport and mud-diapiric processes. Allochtonous pillow lavas occur in scaly mud stone.	Ichnofossils: *Nereite* *Helminthopsis* *Paleophycus*	Pf	Early Miocene
Kadokurazaki Complex		**Section ⑥** Oishino	FA2,FA3, FA4,FA5, Diapiric mudstone	>350m	L: unknown U: unknown	This section comprises thick-bedded sandstone (FA4), sandy turbidite (FA3), thinly bedded alternation of sandstone and shale (FA5), mudstone (FA2) and diapiric-mudstone. These sedimentary successions crop out as southeasterly vergence recumbent anticline.	HF burrows	Pf	Early Miocene

Table 3.1.4(continued). Lithofacies and sedimentary features of the tectono-stratigraphic units and sections of the Kumage and Kadokurazaki Complexes in Tanegashima.

Kadokurazaki Complex	**Section ⑦** Shimama- Kaminaka	FA1 FA2 FA3	>370m	L: fault U: unknown	This section consists of sandy turbidite succession composed with coarsening-upward tendency (FA3), black colored shale (FA2) and variegated shale containing slumped sandstones (FA1).	HF burrows	R	Middle Eocene
	Section ⑧ Kihara- Oda	FA1 FA2 FA3 FA4	1200m	L: fault U: fault	This section shows a very thick stratified succession which is made up of slumped shale (FA2), variegated shale (FA1), sandy turbidite (FA3) and thick-bedded sandstone (FA4). Sandy turbidite and thick-bedded sandstone sequences have many cycles of thickening and coarsening upward to asymmetric successions (Individual sequence thickness: 10-110m). Sand volcanos less than 3cm in diameter occur, occasionally on the upper surfaces of sandy turbidite (FA3).	HF burrows	R	Middle Eocene to early Early Oligocene
	Section ⑨ Oda- Shimonishime	FA2 FA3 FA4 FA5	1000m	L: fault U: fault	This section mainly consist of sandy turbidite (FA3) and thick-bedded sandstone sequences (Individual thickness: 10-70m) (FA4). Shale dominant beds (FA2) and thinly alternation of fine-grained sandstone and shale (FA5) recognized in middle to upper part of this section. Small molluscan fossils are found in shale dominant beds (FA5).	HF burrows	M (*Nuculidae*?)	Unknown
	Section ⑩ Kadokurazaki	FA3 FA4	250m	L: fault U: unknown	This section comprises turbidite and thick-bedded sandstone sequences containing many cycles of thickening and coarsening upward to asymmetric successions (Individual cycle: 10-110m thick). These sandy turbidite sequences are occasionally intercalated with thin coal seams and ichnofossils such as Terebellina are found from the bottom surface of the thin sandstone alternated with shale in the upper part of this section.	HF burrows *Planolites* *Terebellina*	Not found	Unknown
	Section ⑪ Shimamazaki	FA2 FA3 FA4	1300m	L: fault U: unknown	This section mainly comprises sandy turbidite (FA3) and thick-bedded sandstone (FA4). The sequence of the coherent turbisites shows many sedimentary cycles containing a coarsening- and thickening-upward as well as fining- and thinning-upward cycles(Individual cycle: 10-130m thick). The lower part of this succession contains intercalation of shale beds with whitish tuffaceous sandstone giving an age of ca.49Ma. *Paleodictyon* ichnofossils occur in thin sandstone bed in the lowermost part of this succession. Molluscan fossils and vertical burrows bearing ill-sorted sandstone which are intercalated in the middle part of this succession.	*Paleodictyon* Feeding burrows V burrows Bioturbation	M	FT age (48.9±4.1Ma) early Middle Eocene to Oligocene

Abbreviation: R = Radiolarian fossils; P f =Planktonic foraminifera; B f = Benthic foraminifera; M =Molluscan fossils; HF burrows =Horizontal feeding burrows; V burrows = Vertical burrows; IS burrows= Inclined small burrows.

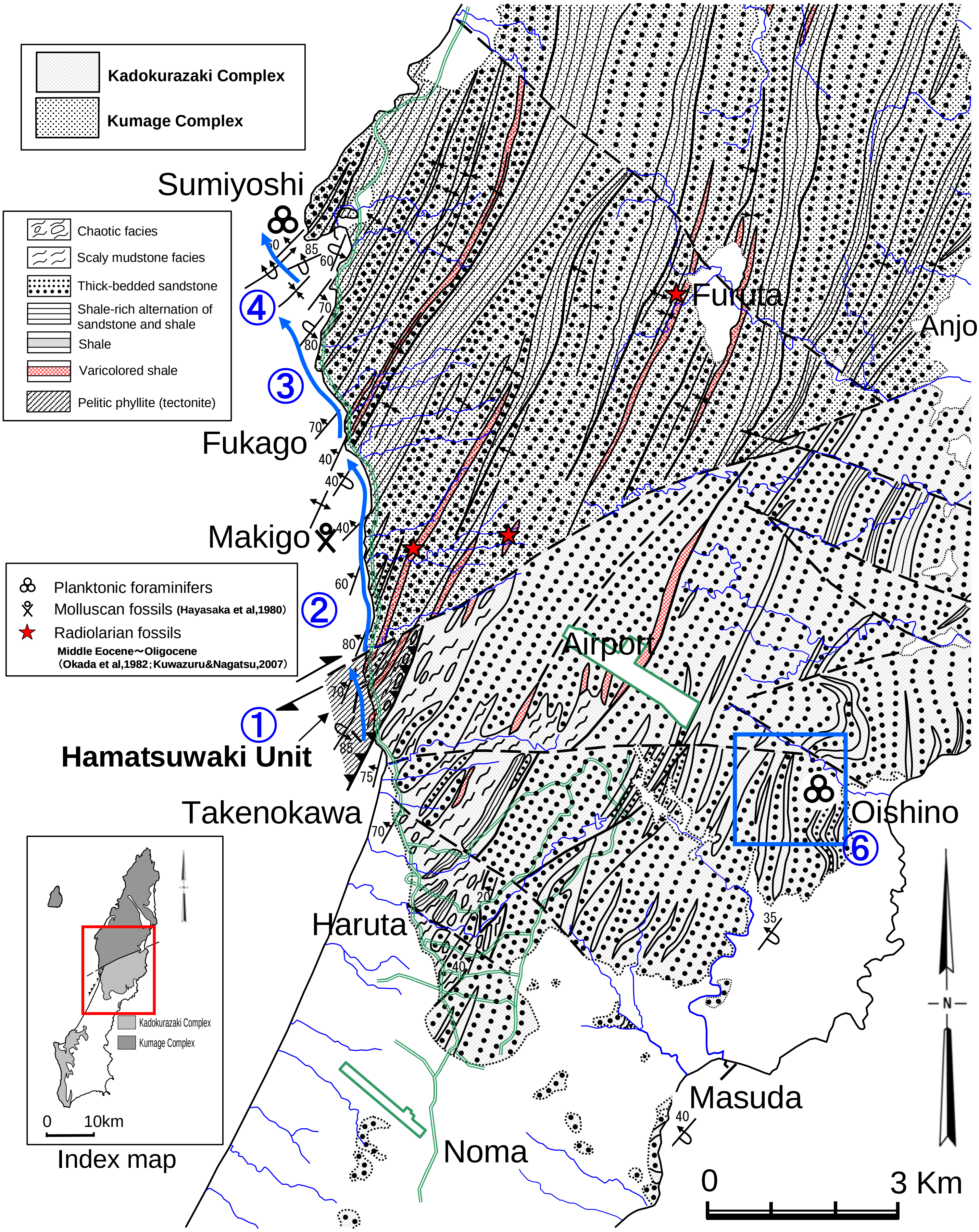

Fig.3.1.3 Geologic map showing the distribution the various facies of the Kumage and the Kadokurazaki complexes in the middle part of Tanegashima. Dotted lines stand for boundary between the basement rocks and overlying strata. Blue arrows and frame are localities of measured sections.

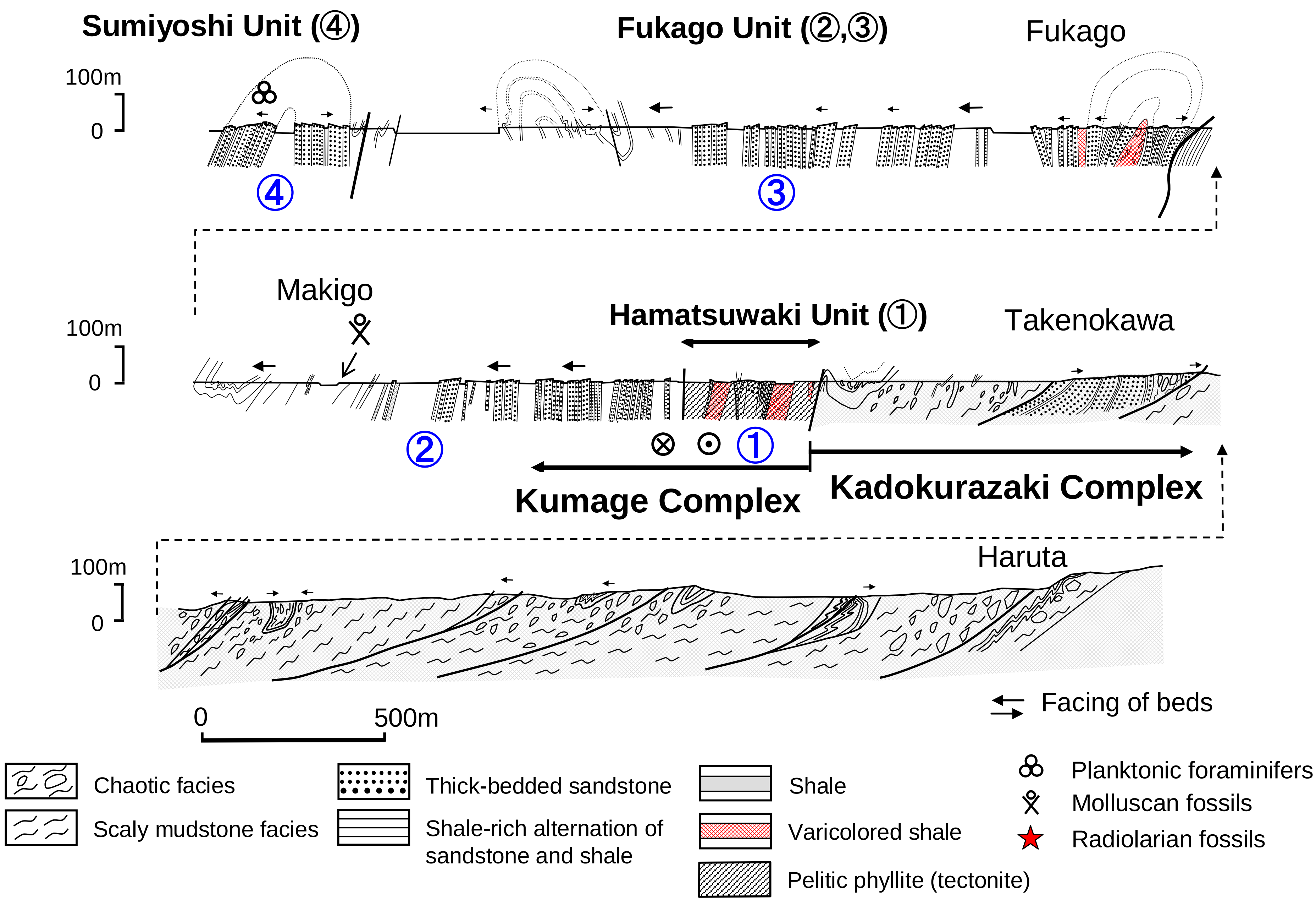

Fig.3.1.4 Nearly N-S oriented cross-section along the west coast area in the middle part of Tanegashima. Number ①-④ indicate measured sections.

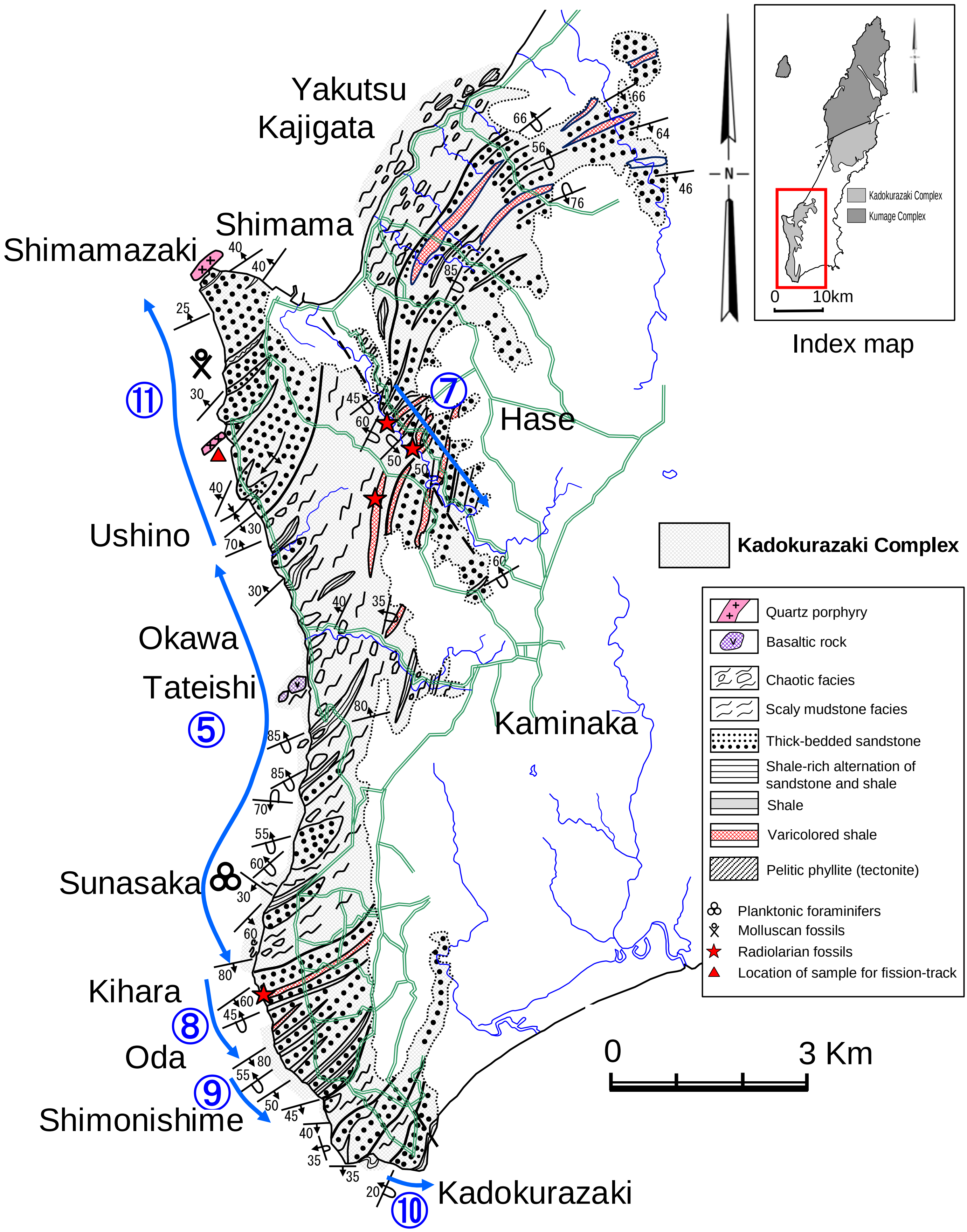

Fig.3.1.5 Map showing the distribution of chaotic rocks and large slump sheets of the Kadokurazaki Complex in the southern part of Tanegashima. Dotted lines stand for boundary between the basement rocks and overlying strata. Blue arrows and numbers are localities of measured sections.

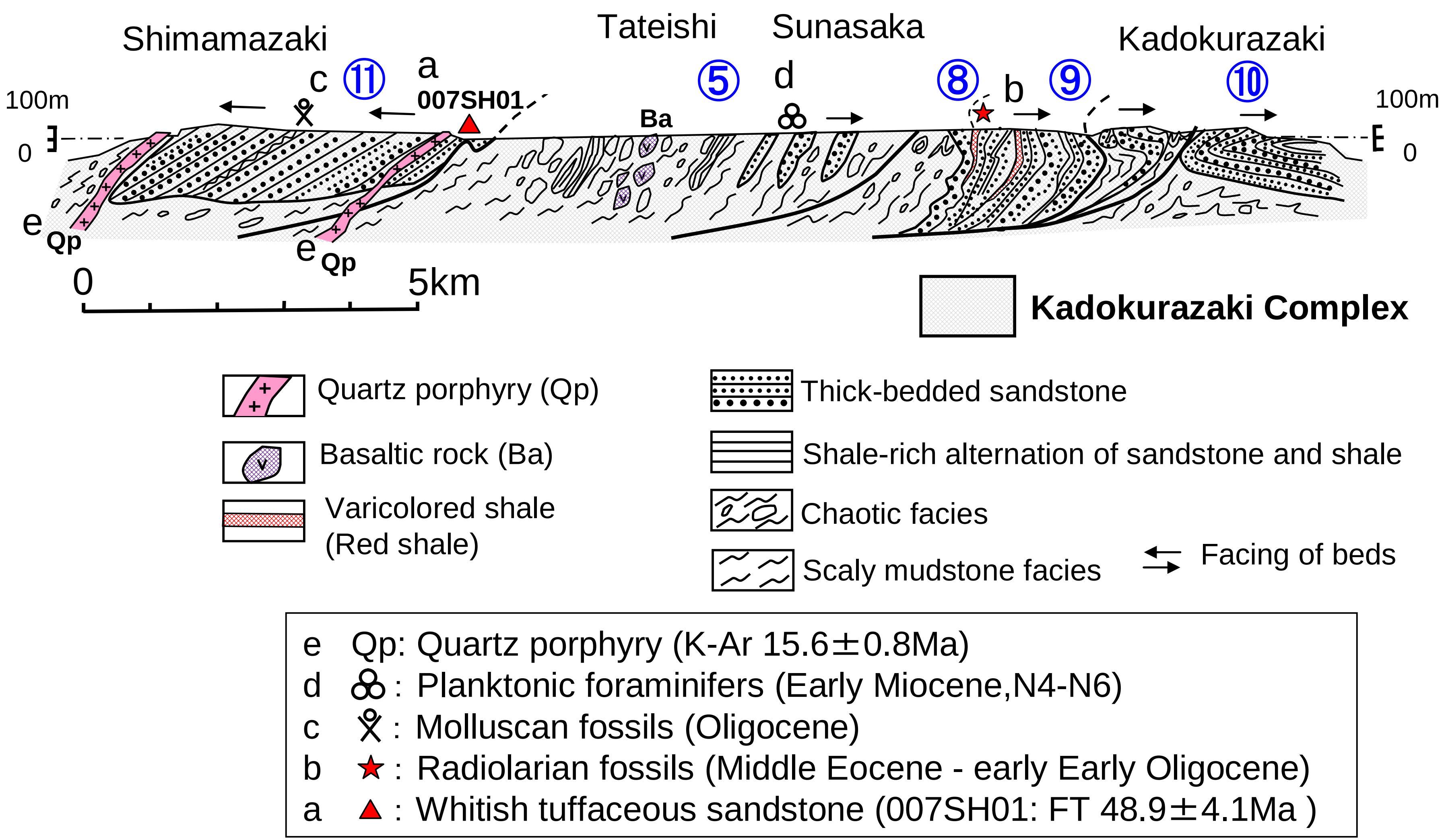

Fig.3.1.6 Geologic cross-section of the Kadokurazaki Complex along the west coast of southern Tanegashima. Number ⑤ and ⑧-⑪ indicate measured sections.

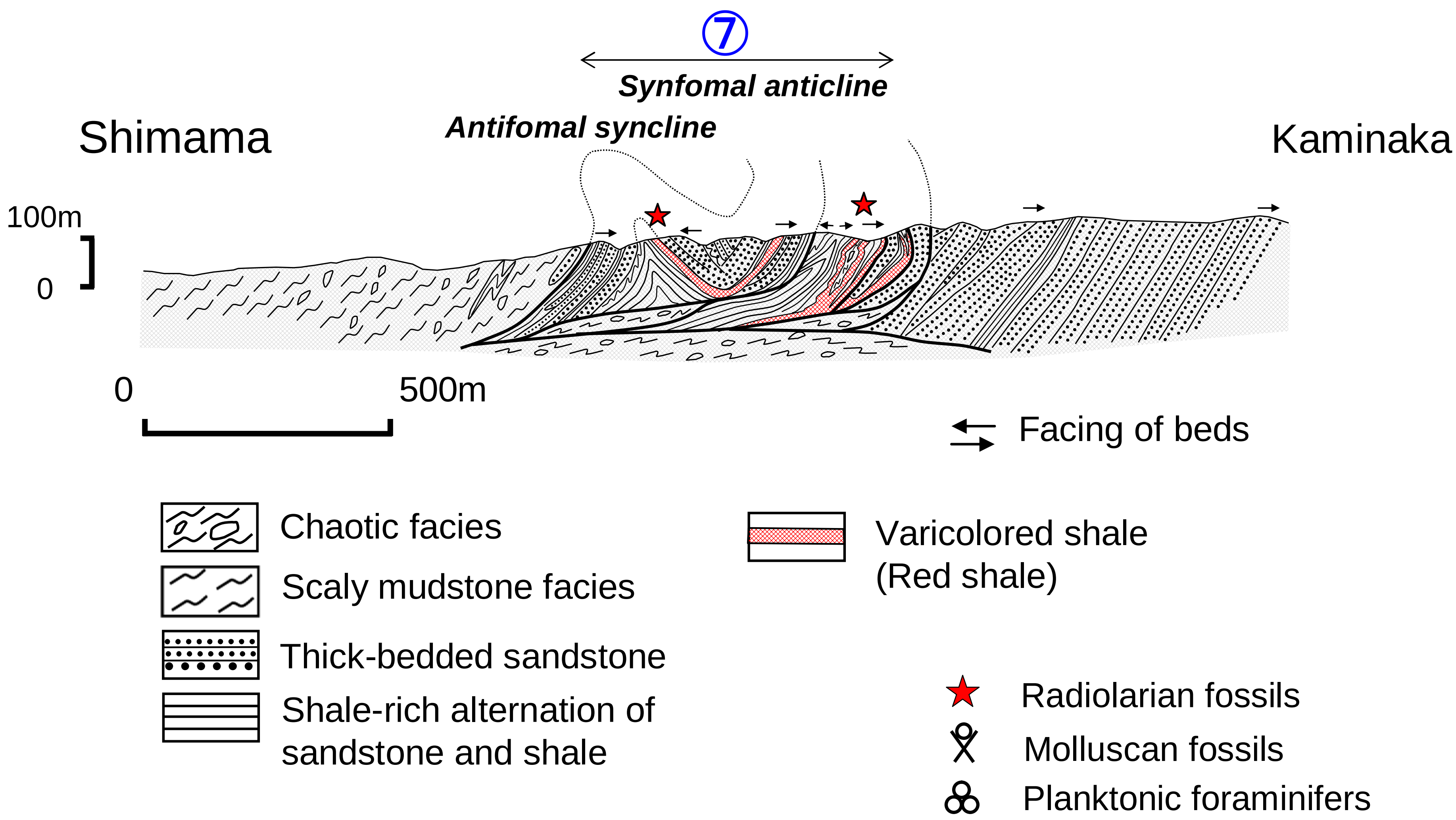

Fig.3.1.7 Geologic cross-section of the Kadokurazaki Complex in the Shimama-Kaminaka area in the southern part of Tanegashima. Number ⑦ indicates measured section.

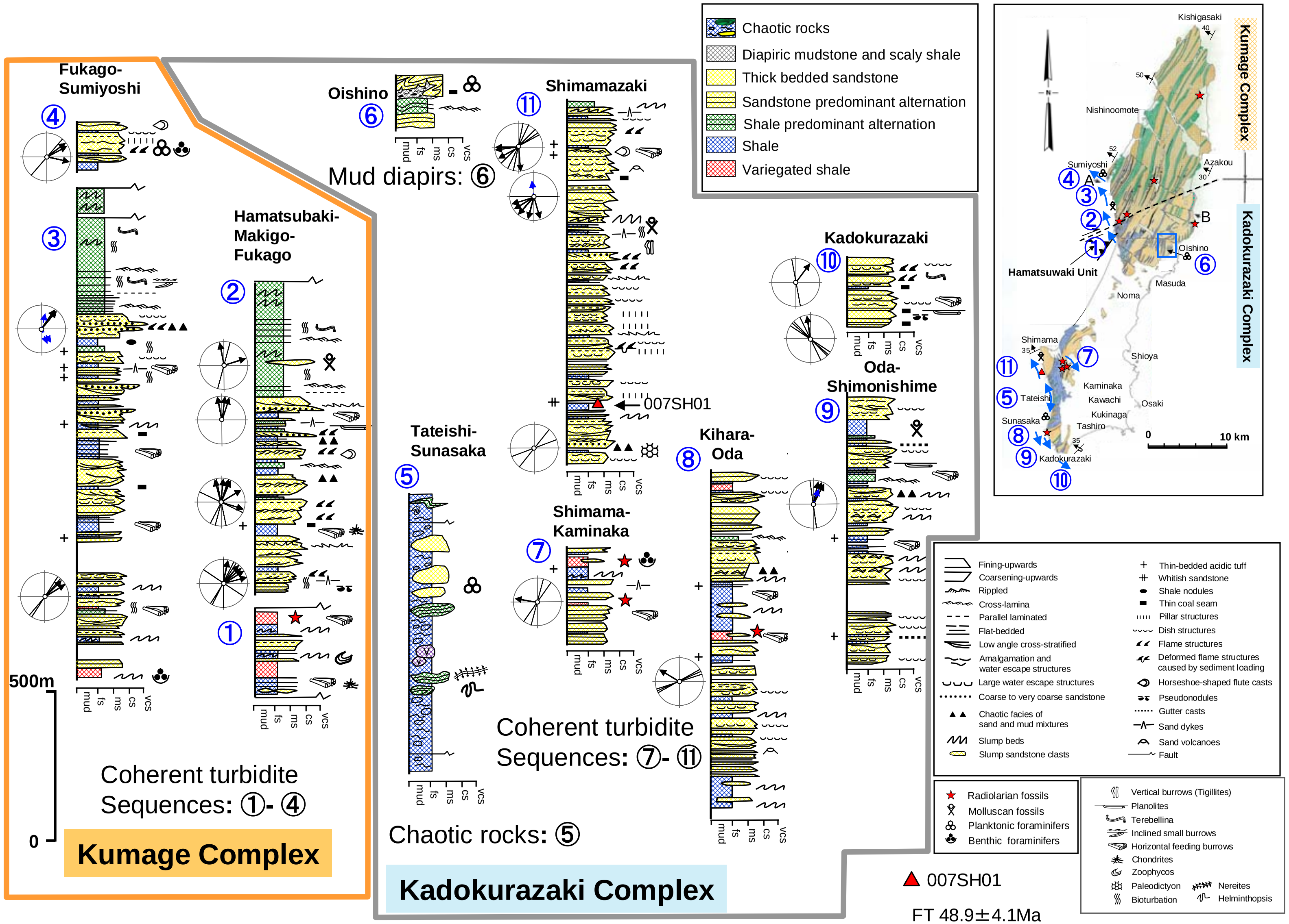

Fig.3.1.8 Correlation of turbidite sequences of the Kumage and Kadokurazaki Complexes in Tanegashima. Number 1-11 with circle are representative sections. 1 to 4: Kumage Complex, 5 to 10: Kadokurazaki complex

Although it exposes restrictedly near Hamatsuzaki port, but presents a higher deformation grade than other units within this complex. Mesoscopic asymmetric folds with axial plane cleavages are developed, penetravively. Due to the extensional strain parallel to cleavage plane, most of sandstone beds are converted to boudins. It is interpreted that the Hamatsuzaki Unit was of accreted trench-fill deposits originally because of intense lateral shortening under high confining pressure.

The Fukago and Sumiyoshi Units are thick-bedded clastic successions of deep-marine fan systems. The Fukago Unit is assigned to Middle Eocene to Oligocene in age based on the radiolarian fossils occurrence and is composed of sandstone-dominant facies in the lower to middle parts representing a thickening- and coarsening-upward succession in 10s to 100meters thick and of shale-dominant in the upper part.

The Sumiyoshi Unit, dominant in sandstone, is dated Early Miocene from foraminiferal bio-chronobiology. These units mentioned above are less deformed, generally. Some large-scaled, asymmetric flexural-slip folds in several kilometers scale accompanied with high-angled thrust faults occur in the Fukago Unit, partly. Four facies associations were distinguished in which axial and lateral flow directions were observed in the channel, channeled lobe and lobe-fringe facies associations, respectively. Facies and paleocurrent data indicate an elongated deep-marine forearc basin for the Kumage Complex.

3.1 Kumage Complex in Tanegashima

3.1.1 Coherent turbidite sequence

(1) Hamatsuwai Unit (Section ①)

The Hamatsuwaki Unit is exposed in the lowermost part of Kumage Complex at the west coast of the central part of Tanegashima. This unit consists mostly of pelitic phyllite involving variegated shale and is characterized by the development of isoclinal shear folds with slaty cleavages parallel to axis of folds. Majority of sandstones are included as tectonic lenses (Fig. 3.1.9). The cleavage is often cut by mud injection veins having been resulted from high pore fluid pressure within the accretionary wedge (Fig.3.1.9 B).

The lower part of this unit is fault in contact with the Kadokurazaki Complex (olistostrome), and this tectono-stratigraphic unit is overlain by a thick-bedded turbidite succession of deep-sea fan deposits being composed of the sandstone, sandy alternation and shale. A remarkable repetition of beds can be found due to folding and thrusting comparable to accretionary deformations. However, the boundary between the tectonite and turbidite sequence units is replaced by younger right-lateral-strike slip fault trending ENE-WSW (Hamatsuwaki fault) in direction (Fig.3.1.3). The total thickness of this unit is about 300 meters.

(2) Fukago Units (Section ②and ③)

As mentioned above, these units are distributed in the north of the Hamatsuwaki Fault. In the cross-section of this unit, sedimentary sequences show younging towards the west. East-westward trending strata show many asymmetric flexural-slip folds and are contacted with northeast-trending thrust faults at base, with repetitions of the same stratigraphic successions by imbricate thrusts.

The Section ② of the Fukago Unit represents many sedimentary cycles consisting of the facies association of the FA3 and FA4 that are generally characterized by a coarsening- and thickening-upward sequence. Uppermost thick turbidite sandstone of facies association FA4 is overlaid by thinly bedded alternation of fine-grained sandstone and shale. The total thickness probably exceeds 1400 meters. The thickness of sandstone beds from FA4 are generally 3 to 100 meter and ripples are observed on the top surface. Sand volcanoes, various dewatering structures and erosional structures are found in sand-dominated deep sea fan deposits comparable to channel, channel-lobe facies (Fig.3.1.10). Okada & Whitaker (1979) reported large sand volcanoes from the sandstone corresponding to this unit on the northeast coast of Tanegashima.

The lowest part of the Section ③ of the Fukago Unit begins with variegated shale (FA1) and passes into alternating beds of sandstone and shale showing a coarsening- and thickening-upward sequence (FA3 and FA4) in the middle and upper parts. Uppermost thick-bedded sandstone (FA4) is interpreted as channel and channel-lobe transition facies and is overlain by shale dominant alternation (FA5). The total thickness attains to about 2000 meters.

(3) Sumiyoshi Unit (Section ④)

The Sumiyoshi Unit (Section ④) is restricted in the western-most part of Tanegashima and is made up of massive shale (FA2) in the lower part and of thick sandstone dominant interbeds (FA3) in the top. Small-scale finning- and thinning upward cycles are developed well in middle to upper parts. Planktonic foraminiferal fossils referable to Early Miocene were found from shale bed intercalated with thick-bedded sandstone.

Epsilon cross-stratifications, antidunes, humpback dunes and parallel stratifications are found in thick-sandstone (Figs.3.1.11 and 3.1.12). Antidunes and humpback dunes which show the convex-up crossbedding and upstream-dipping (Fielding, 2006; Allen & Fielding, 2007) are observed in the middle-upper part of 1m thick sandstone bed. Antidune bedforms had been produced by the flume experiment under upper-flow-regime condition and it supports that sediments were supplied by high-speed flows (Bridge & Best, 1988; Yagishita et al, 1988; Yagishita, 1992; Stow, 2010).

In the Sumiyoshi Unit, paleocurrent directions are predominantly north-northeast in the sandy alternation of lobe facies, whereas in the thick-bedded sandstone show southeast-ward flow. The terrigenous sediments of the upper part of this unit were supplied by both lateral and axial flows.

The remarkable shift of paleoflow direction between the channel and channel lobe and the lobe facies within the fan system suggests that the elongated slope basin for the Sumiyoshi Unit in which the axial flow and lateral flow were dominated in channel-channel lobe and lobe facies, respectively.

3.1.2 Southern Shimanto Belt in Yakushima

According to Hashimoto (1956), the Kumage Group in Yakusima has been divided into four formations, the Mugio, Funayuki, Miyanoura and Isso Formations in ascending order. The Mugio Formation consists of muddy chaotic rocks including sandstone bodies. The Funayuki Formation is made up of scaly cleaved shale associated with varicolored shale and basaltic rocks as exotic blocks. The Miyanoura Formation is composed of thick sandstone and alternating beds of sandstone and shale bearing trace fossils of flysch. The Isso Formation consists of conglomeratic sequence and alternating beds of sandstone and shale.

Sakai (1980) studied on the allocthonous basaltic rocks occurred in the olistostrome of Tanegashima and Yakushima. More recently, Sakai (2010) recognized that the Kumage Group in Northern Ryukyu could be divided into two different series of lithostratigraphy: the coherent and chaotic series, mention above. With reference to the investigation in Tanegashima at my doctor’s course in Kyushu University, he proposed to call the Kumage and Kadokurazaki Complexes for the coherent and chaotic series shown in Fig.12 of the Appendix.

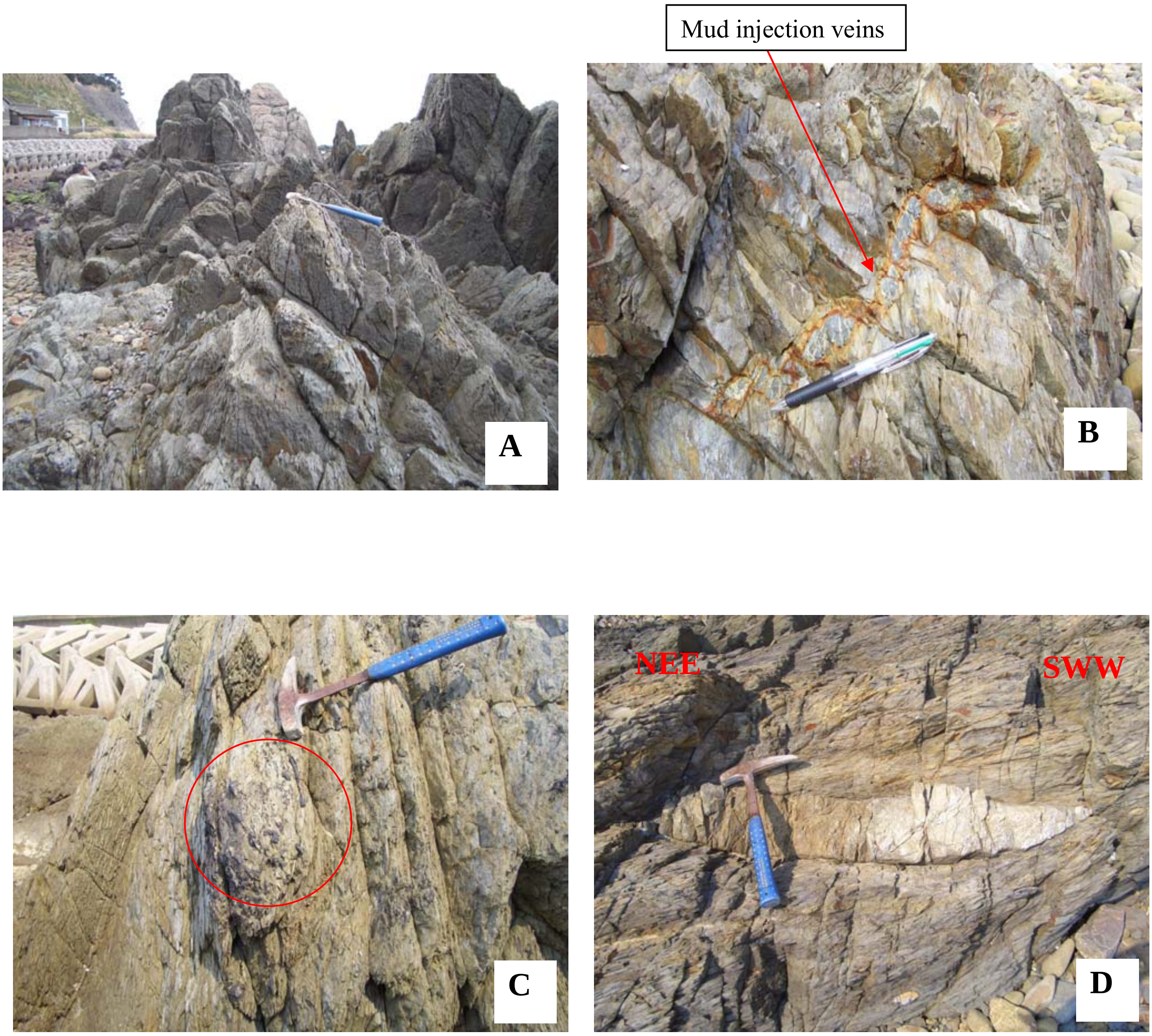

Fig.3.1.9 Pelitic phyllite is the Hamatsuwaki Unit (Section ①). A: Outcrop of bluish muddy rock characterized by pervasively developed slaty cleavage (strike N30°E/dip 65°W). B: Mud injection veins (arrowed) caused by high pore fluid pressure. C: Horizontal burrows (circled) recognized in the pelitic rock. D: Boudinaged sandstone lens in the pelitic phyllite indicating a general NEE-SWW extension direction. The locations of outcrop photos are shown in Fig. 3.1.13.

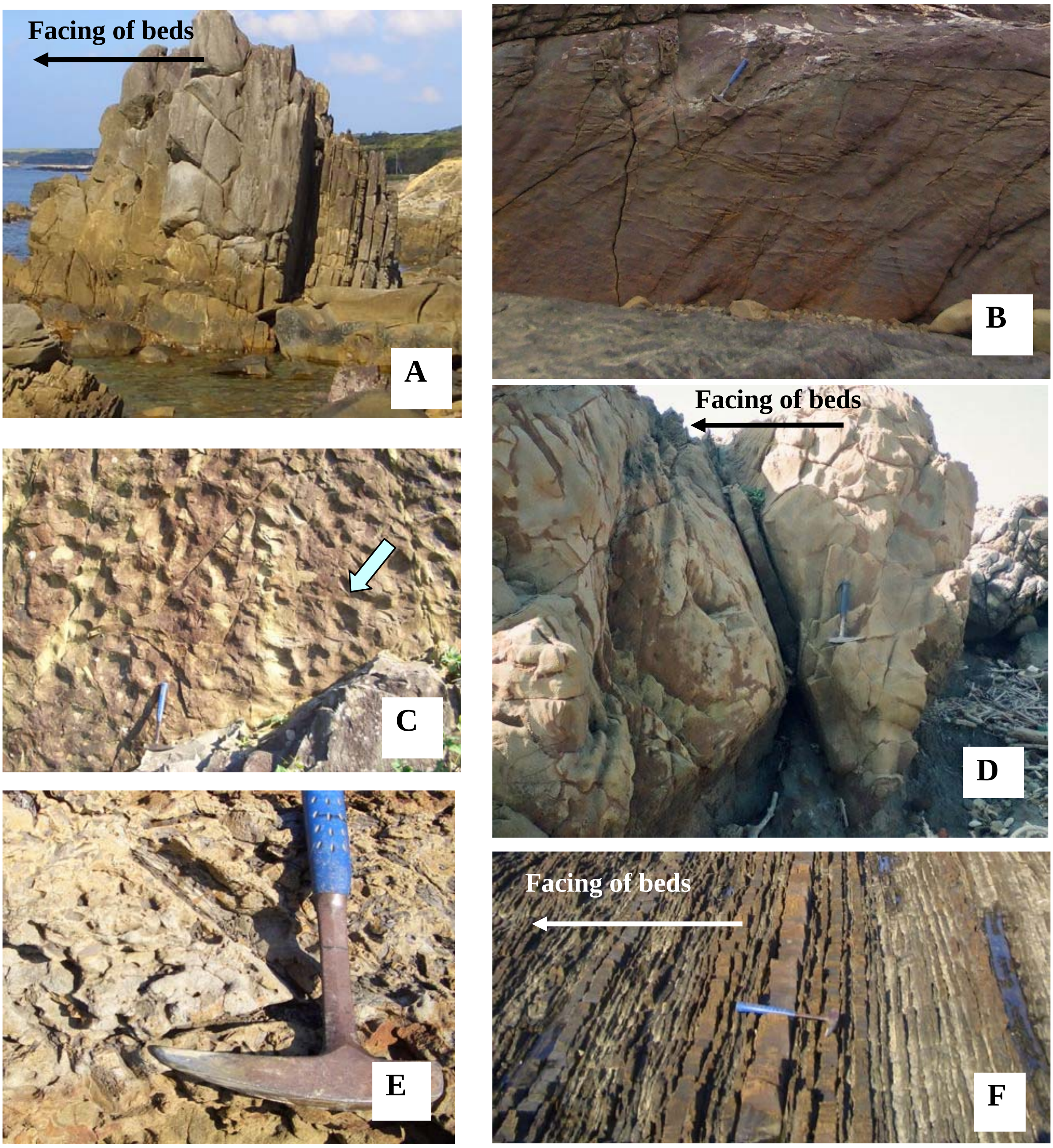

Fig.3.1.10 Outcrop photos show sedimentary features in the Section ② and ③). A: Coarseing- and thickening-upward cycle of coherent turbidite sequence in which arrow indicates a coarsening upward direction. B: Large groove casts on the bottom surface of the thick bedded sandstone. C: Lunate ripple marks on the top surface of thick bedded sandstone in which arrow indicates northward paleoflow. D: Channel structure observed at the bottom of the very thick sandstone. E: Coarse grained-sandstone with shale breccia probably caused by channel wall collapse. F: Thick sequence of thinly bedded alternation of fine-grained sandstone (1-20cm thick) and shale (0.5-5cm thick). The locations of outcrop photos are shown in Fig. 3.1.13.

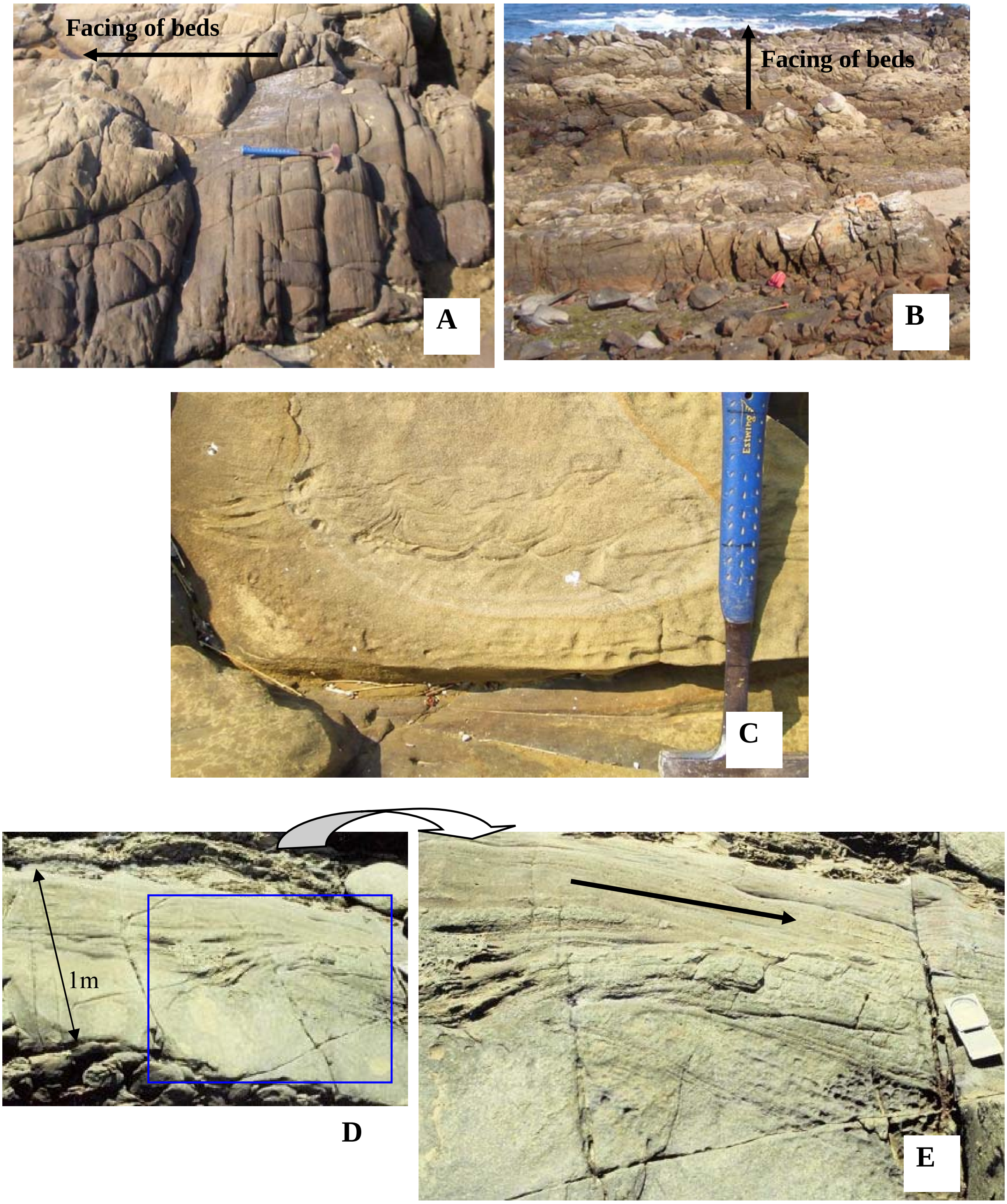

Fig.3.1.11 Outcrop photos show the sedimentary features of the Kumage Complex along the coast of Sumiyoshi (Section 4). A: Parallel lamination of thick bedded sandstone. B: Thick bedded sandstone with subordinate shale bed, and alternating beds of sandstone and shale from which some planktonic foraminiferal fossils of Early Miocene age obtained. C: Flame structure in medium grained- sandstone due to liquefaction. D and E: Antidune and humpback dune observed in the middle-upper part of 1m thick sandstone bed. These sedimentary structures imply sand deposition under upper-flow-regime conditions. Arrow indicates paleoflow direction. The locations of outcrop photos are shown in Fig. 3.1.13.

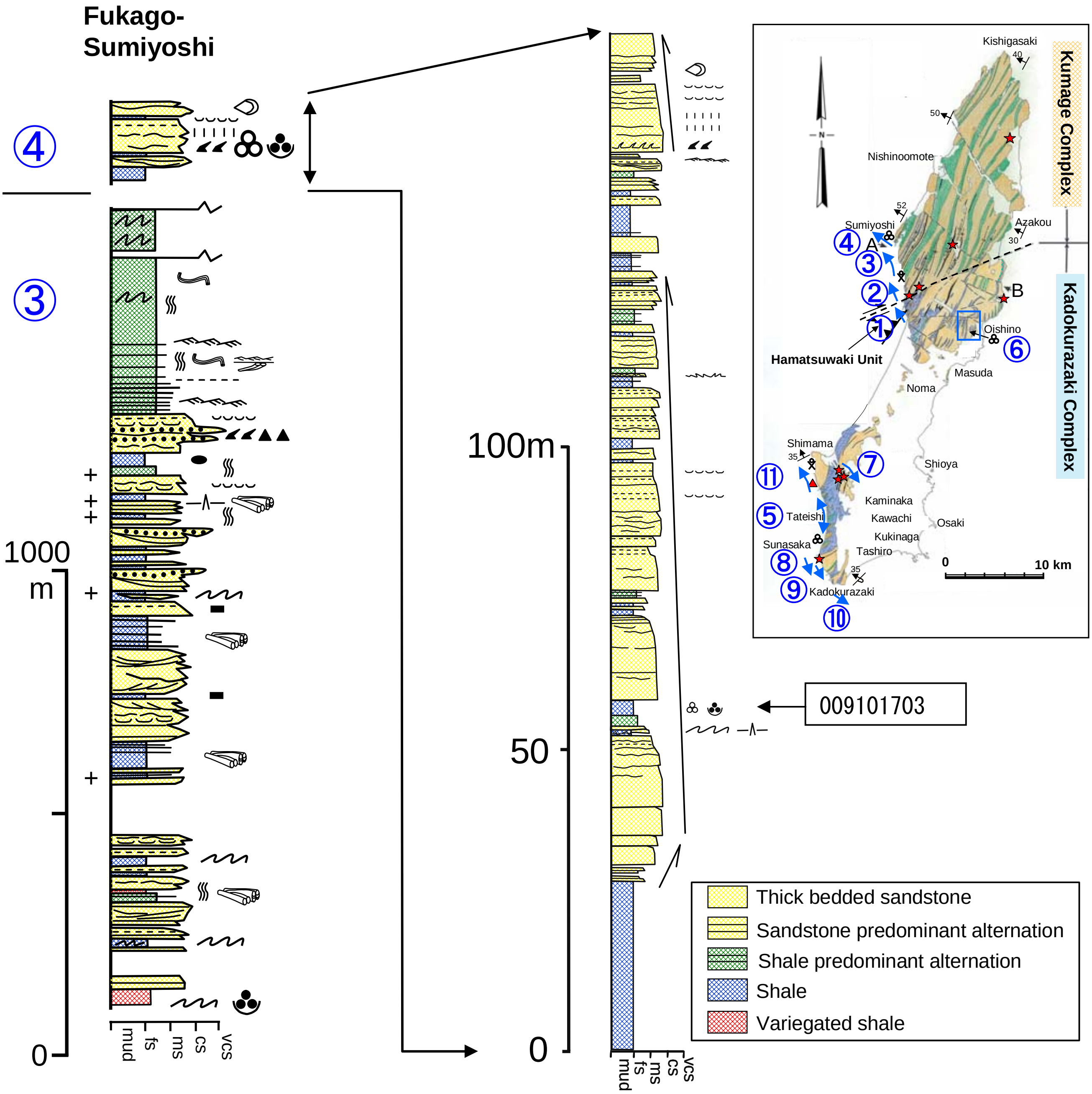

Fig.3.1.12 Columns of Section ③ and Section ④ measured between Fukago and Sumiyoshi. Sequence of Section ④ begins with shale and shows two cycles of sandstone units which are characterized by fining-upward in about 30 to 100m thickness. The shale interval in thick-bedded sandstones yields planktonic foraminiferal fossils (sample 009101703) referable to Early Miocene in age. Location of the ③ and ④sections is shown in the index map inflame.

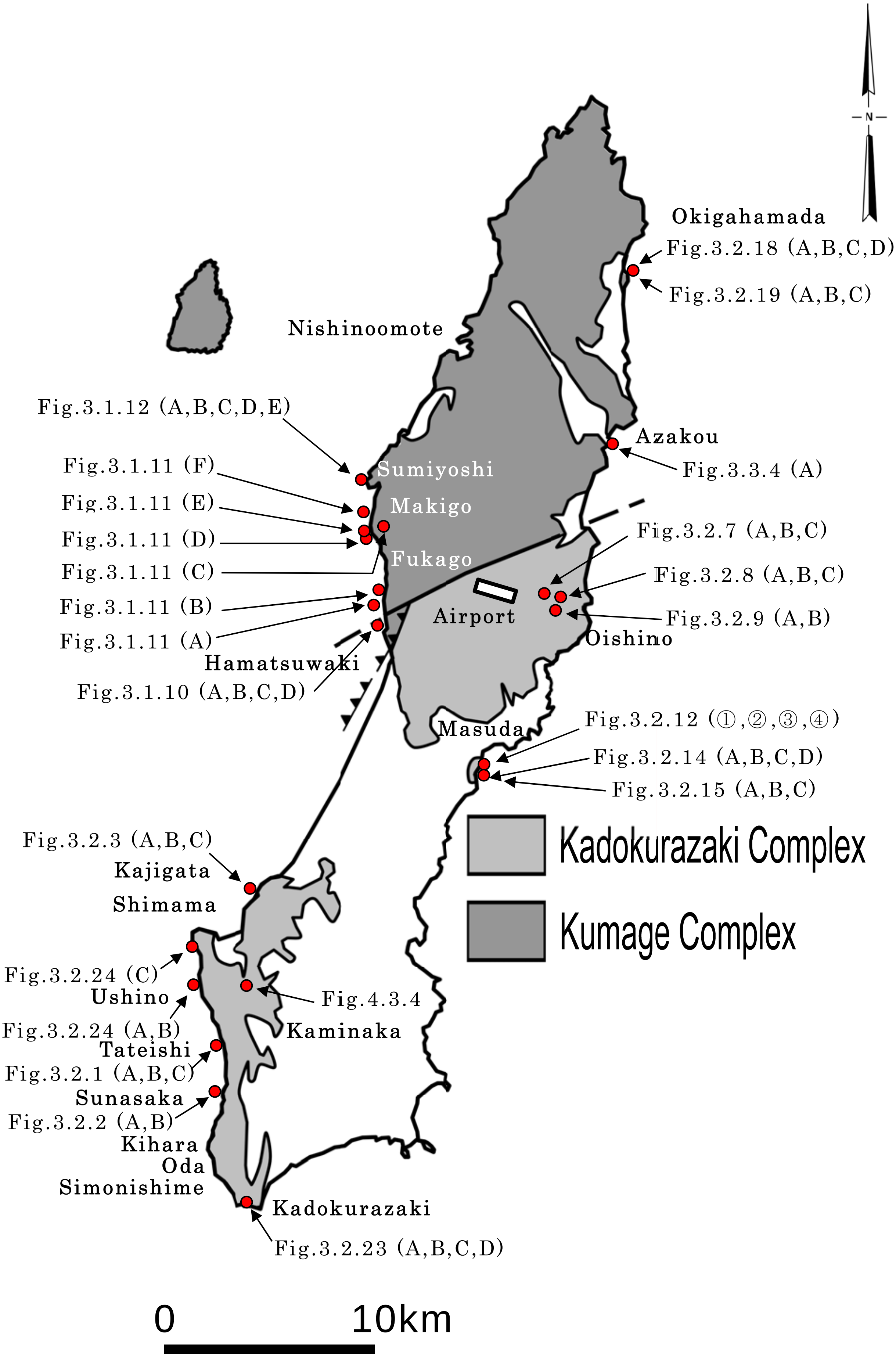

Fig. 3.1.13 Map showing the locations of the outcrop photos in this study area.

3.2 Kadokurazaki Complex

The Kadokurazaki Complex is distributed in the central and southern part of Tanegashima. This complex consists of the chaotic rocks (block-in-matrix) and huge slump sheets (olistoliths). Due to complicated lithofacies with intricate deformation structures such as overturned fold, recumbent fold, and lack of fossil record, the detailed stratigraphy of this complex has been left unstudied except for some local observations (Hashimoto, 1956; Hayasaka *et al*., 1980; Sakai, 1980; Okada *et al.,* 1982).

This chaotic complex in Yakushima (Fig.12 in the Appendix) is distributed in the eastern region of the Ochinokawa fault and the Kusukawa-Kojima fault (Hashimoto, 1956). In Tanegashima, the type localities are at coast of Tateishi and also distributed at coast of Funayuki in Yakushima, where the allochthonous basaltic pillow lavas crop out (Sakai, 1980). The matrix including basaltic rock are the mixture consisting of angular clasts of sandstone and shale, ranging in size from a few centimeters to several hundred meters, in scaly cleaved mudstone. Therefore, this unit is characterized by the block-in-matrix fabrics (Cowan, 1985), produced by the accumulation of debris flows and submarine slides.

On the other hand, large slump sheets (olistoliths) are a few hundred meters to a one kilometer in size. Many of the allochthonous blocks and slump sheets show deep-sea fan turbidite facies. In some allochthonous blocks, their facies imply the shelf deposits that formed by storm or hyperpycnal flows. The deformations of huge slump sheets are characterized by large-scale recumbent folds formed by gravitational gliding.

Two types of lithologic bodies can be distinguished in the Kadokurazaki Complex as shown in the geological maps and the correlation of turbidite sequences (Figs.3.1.3, 3.1.5 and 3.1.8); the chaotic rocks, and the large slide masses. Former is exposed typically along the coast near Tateish (Section ⑤ in Fig.3.1.5), and later appears in the central part (Section ⑥ in Fig.3.1.3) and southern part of Tanegashima (Section ⑦-⑪ in Fig.3.1.5).

3.2.1 Chaotic rocks

The chaotic rock is characterized by the block-in-matrix fabrics with muddy matrix commonly. It shows no clear stratification and is characteristically accompanied by penecontemporaneous deformation such as slump folds, slump breccia or sedimentary boudinage and dewatering structures. These structures and fabrics were formed by failure, brecciation, and accumulation of stratified strata on slope under unstable gravity condition and by hydrostatic brecciation related with abnormal pressure. The strata containing basaltic rocks consist of angular clasts of sandstone and shale, ranging in size from a few centimeters to several hundred meters, in scaly cleaved mudstone.

Exotic block of basalt lava

The basaltic rock (doleritic in composition) exposed at Tateishi area of Tanegashima is composed of pillow lava with volcanic conglomerate. The cracks of pillow lava have been filled up with micritic limestone (Fig.3.2.1). The rock body having a size of 13-20m shows an oval shape with long axis east to west.

On the other hand, basaltic rock at Funayuki in Yakushima consists mainly of pillow lava, hyaloclastite, and subordinately of intercalations of grayish to reddish claystone and ocher-like deposit (Sakai, 1980, 2010). This rock body in length of 360m and width of 160m shows a long axis in the NE-SW direction. These greenstone bodies occur in scaly cleaved argillaceous strata and show the discontinuous, sub-rounded elliptical in profile. They are assumed as accreted rocks of seamounts on the proto-Philippine Sea Plate (Sakai, 1980).

Block-in- matrix chaotic rocks

The distribution of this unit has been known in west-central area (Hamatsuwaki), the south-west coast (Kajigata; Fig.3.2.2) and the southern coastal area between Kihara-Ushino (Fig.3.2.3). This unit is characterized by containing angular clasts of sandstone and shale

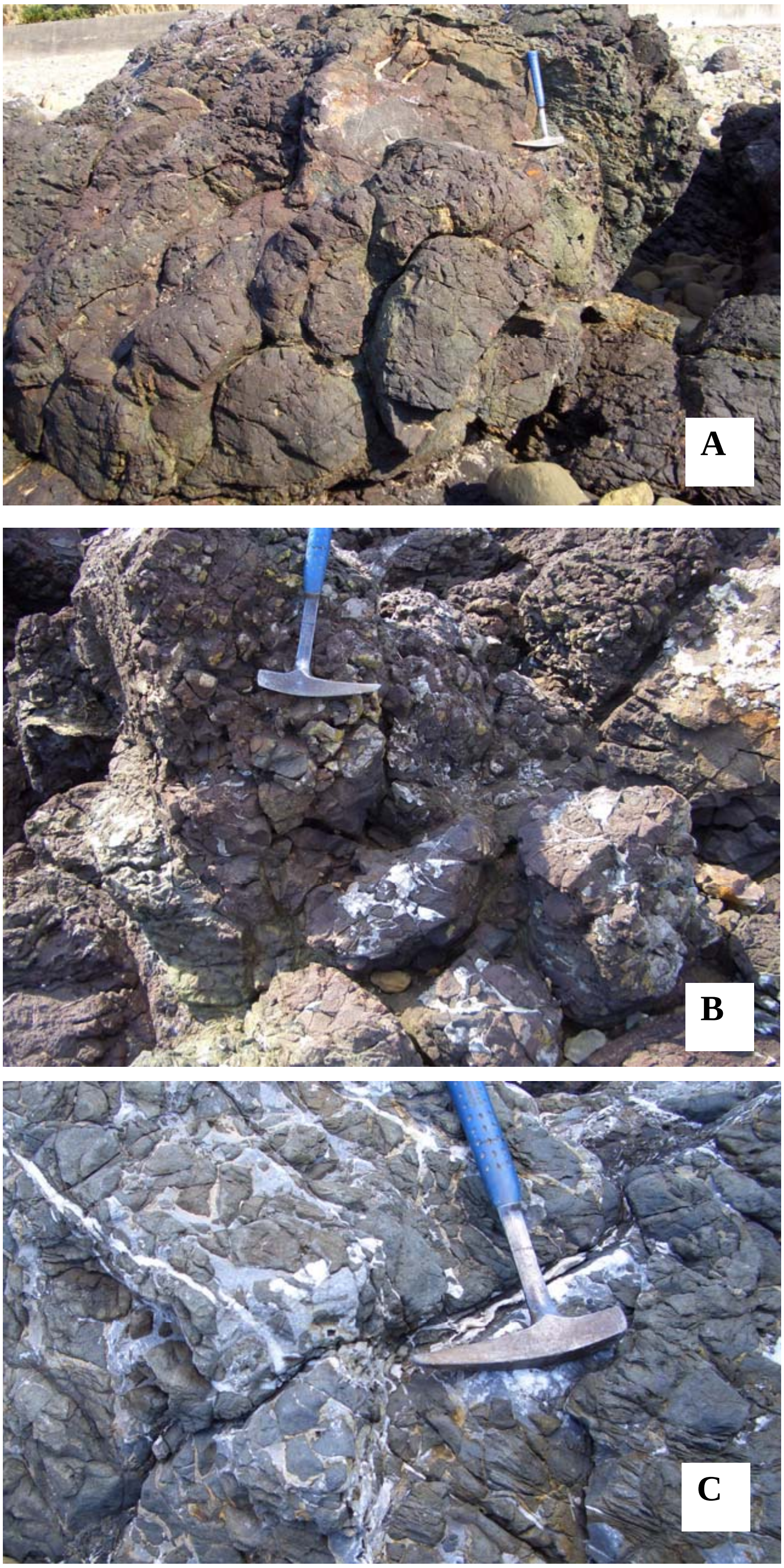

Fig.3.2.1 Olistolith of basalt in pillow lava at the coast of Tateishi, southern part of Tanagashima (Section ⑤). A: Outcrop of the basaltic rock (doleritic rock) body composed mainly of pillow lava. B; Volcanic conglomerate accompanied with pillow basalt. C: Micritic limestone filling the cracks of pillow lavas. The locations of outcrop photos are shown in Fig. 3.1.13.

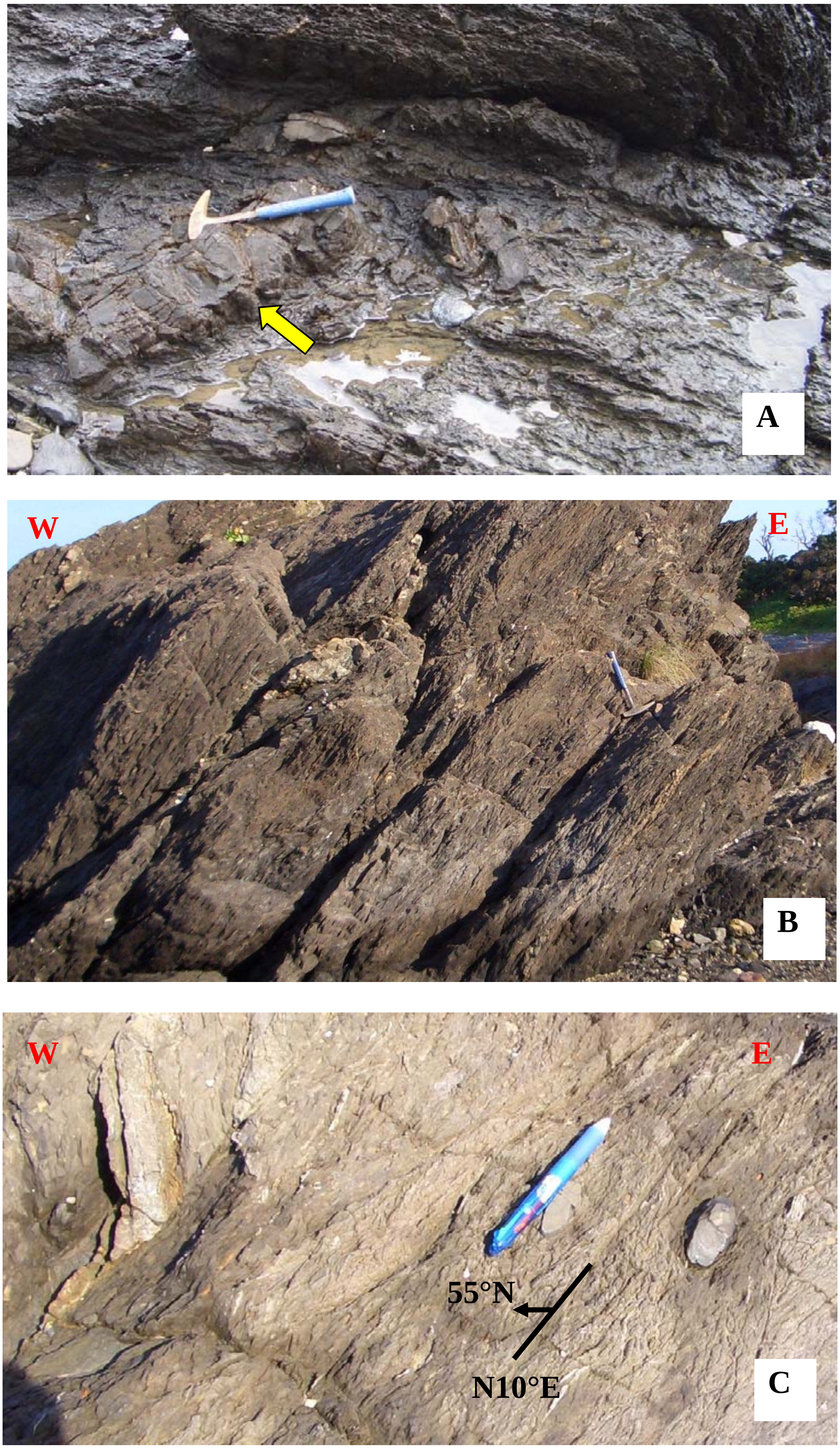

Fig.3.2.2 Outcrop photos showing the occurrence of olistoliths in block-in-matrix chaotic rocks on the Kajigata coast. A: Matrix of the olistostrome containing angular sandstone blocks (arrowed). B and C: Olistoliths of pebbly mudstone penetrative cleavages (strike N10°E/dip 55°N). The locations of outcrop photos are shown in Fig. 3.1.13.

Fig.3.2.3 Outcrop photo showing the occurrence of the chaotic rocks (Section ⑤). A: Chaotic rocks including large sandstone blocks in the northern coast of Sunasaka fishing port. B: Mud stone yielding some planktonic foraminiferal remains of Early Miocene age (Zone N.4-N.6). The locations of outcrop photos are shown in Fig. 3.1.13.

derived mainly from the Kumage complex.

Olistoliths of pebbly mudstone which have development of intensive slaty cleavages that formed under the high confining pressure are contained also. They are probably derived from the pre-Eocene basement, because such a rock has not been recognized in the Kumage complex of Tanegashima.

The matrix surrounding the olistoliths is characterized by scaly fabric which shows polished and slickensided surface. The scaly cleavage probably was generated by emplacement of olistostrome. In this study, planctonic foraminifera are obtained from the muddy matrix in the northern coast of Sunasaka fishing port (Fig.3.2.3). The foraminiferal assemblage is assigned to an Early Miocene age (Zone N.4-N.6).

3.2.2 Large slump sheet (Olistolith)

In Tanegashima, this type of geologic bodies which remains original sedimentary sequences are distributed around Masuda, Kadokurazaki and Shimama areas and is composed of mappable large slump sheets. Large slump sheets having large-scale recumbent folds with southeastwards vergence occur at Masuda and Kadokurazaki areas. Most of these fold styles belong to flexural type and appear restrictive occurrence within the sheeted body which could be recognized as an olistholith. They imply, therefore, that folds were formed within semi consolidated blocks during downslope movement.

Many of the allochthonous blocks and slump sheets showing deep-sea fan turbidite facies could be interpreted that they were derived from the Kumage Complex. Some allochonous blocks, their sedimentary facies and features indicate a self-environment based on the sedimentary facies by storm-related or hyperpycnal flows. These are derived from the slope or near the shelf edge of forearc basin. The result of the field observation on some representative olistoliths is described in detail as follows:

(1) Eastern area of airport (Oishino)

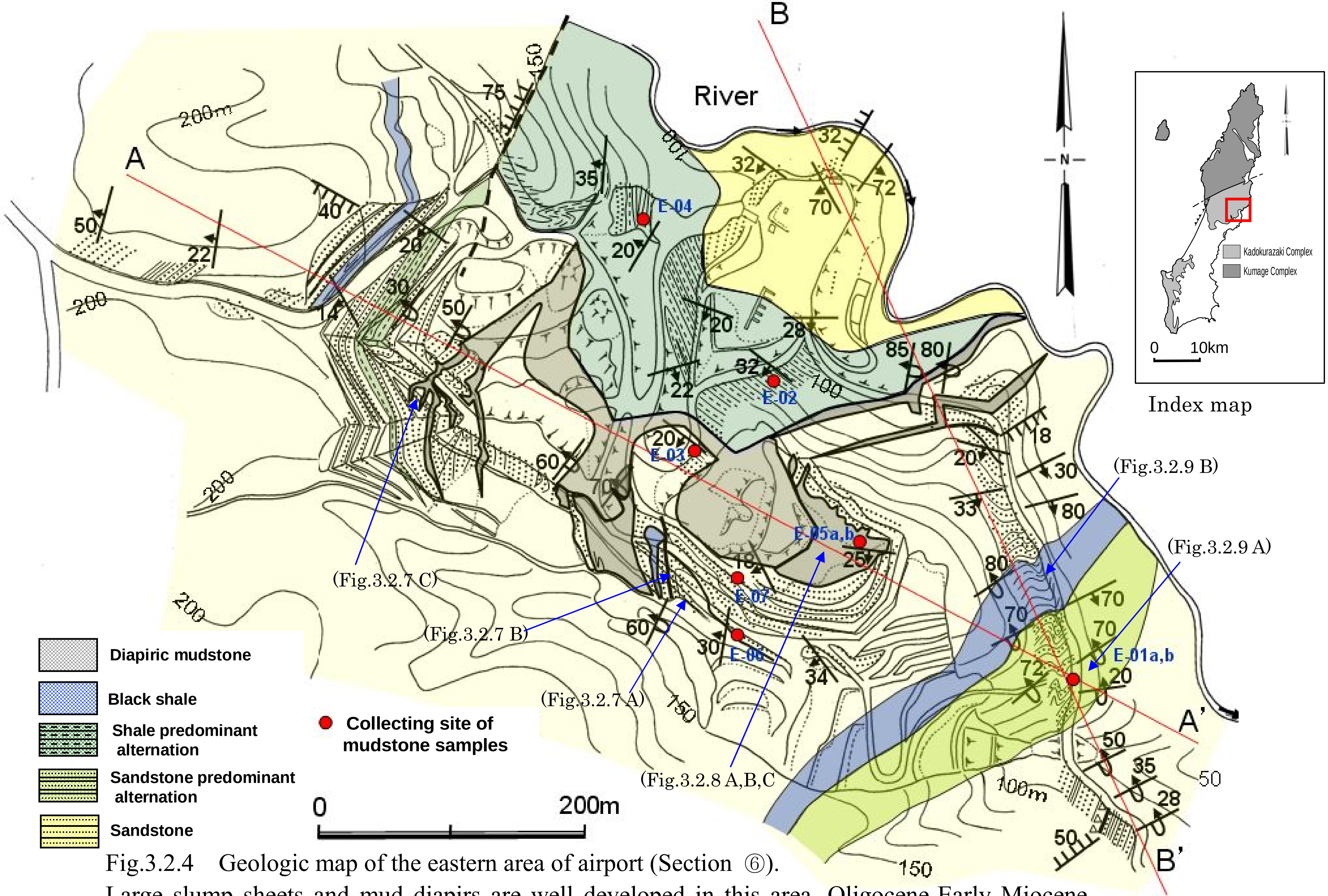

Fig.3.2.4 Geologic map of the eastern area of airport (Section ⑥).
Large slump sheets and mud diapirs are well developed in this area. Oligocene-Early Miocene planktonic foraminifers were obtained from collecting site E-04, E-05 and E-06.

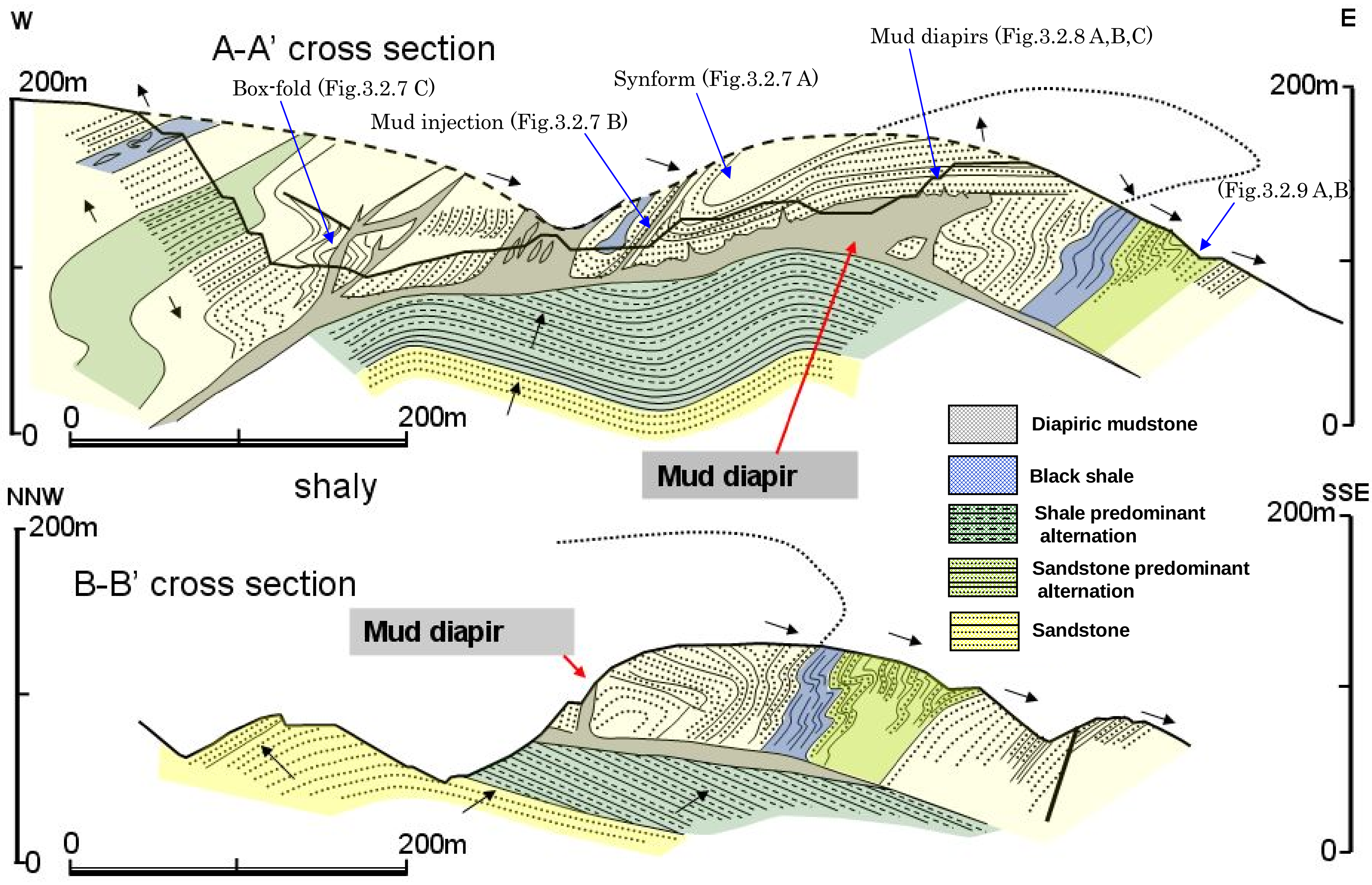

Fig.3.2.5 Geologic profiles of the eastern area of Airport (Section ⑥). See the location for cross-sections in Fig3.2.4. Short black arrows indicate facing of beds.

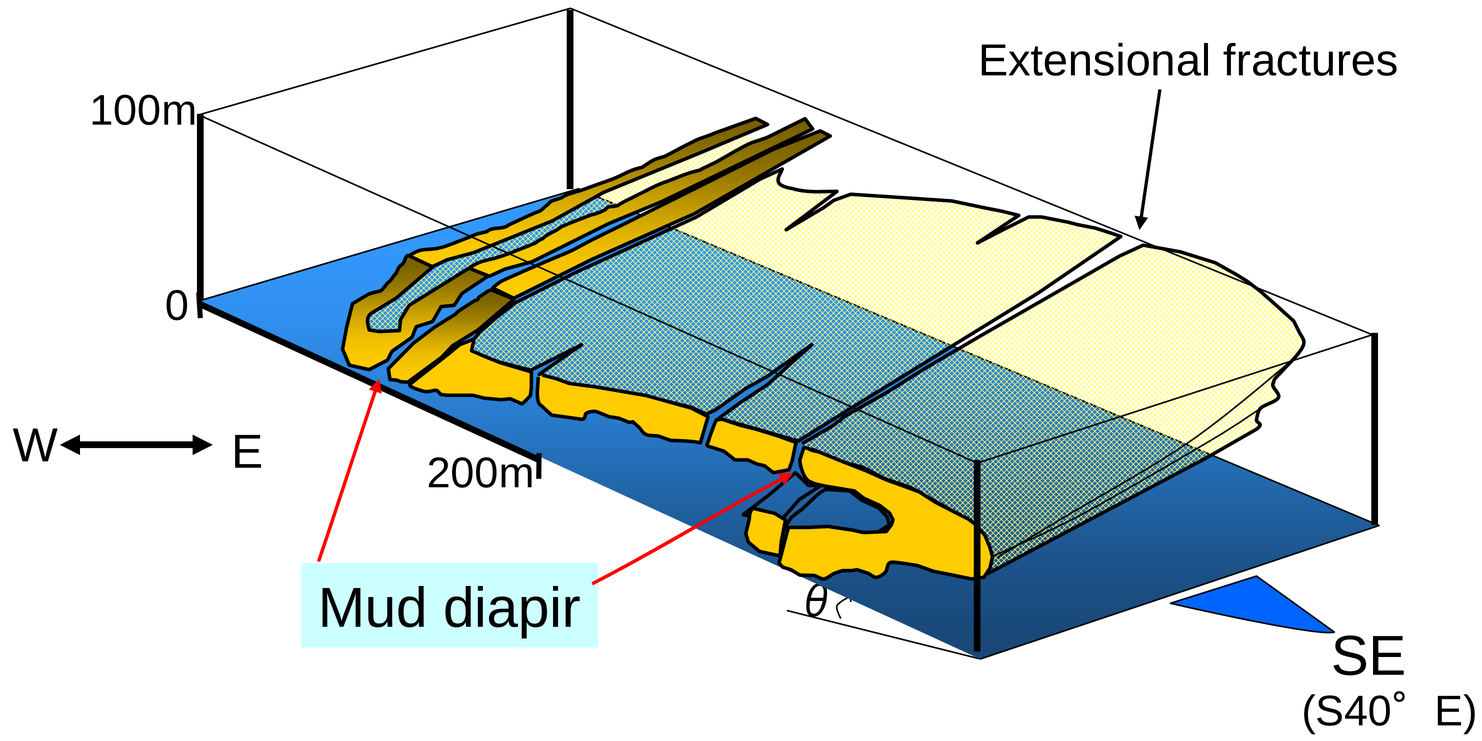

Paleoslope angle: about 2 degrees.
Dip angle of the overlying and underlying strata: about 30 degrees.
Dip angle of the axial plane of recumbent fold: 28 degrees.

Fig.3.2.6 Shematic block diagram showing a reconstructed profile of slump sheet and mud diapirs.

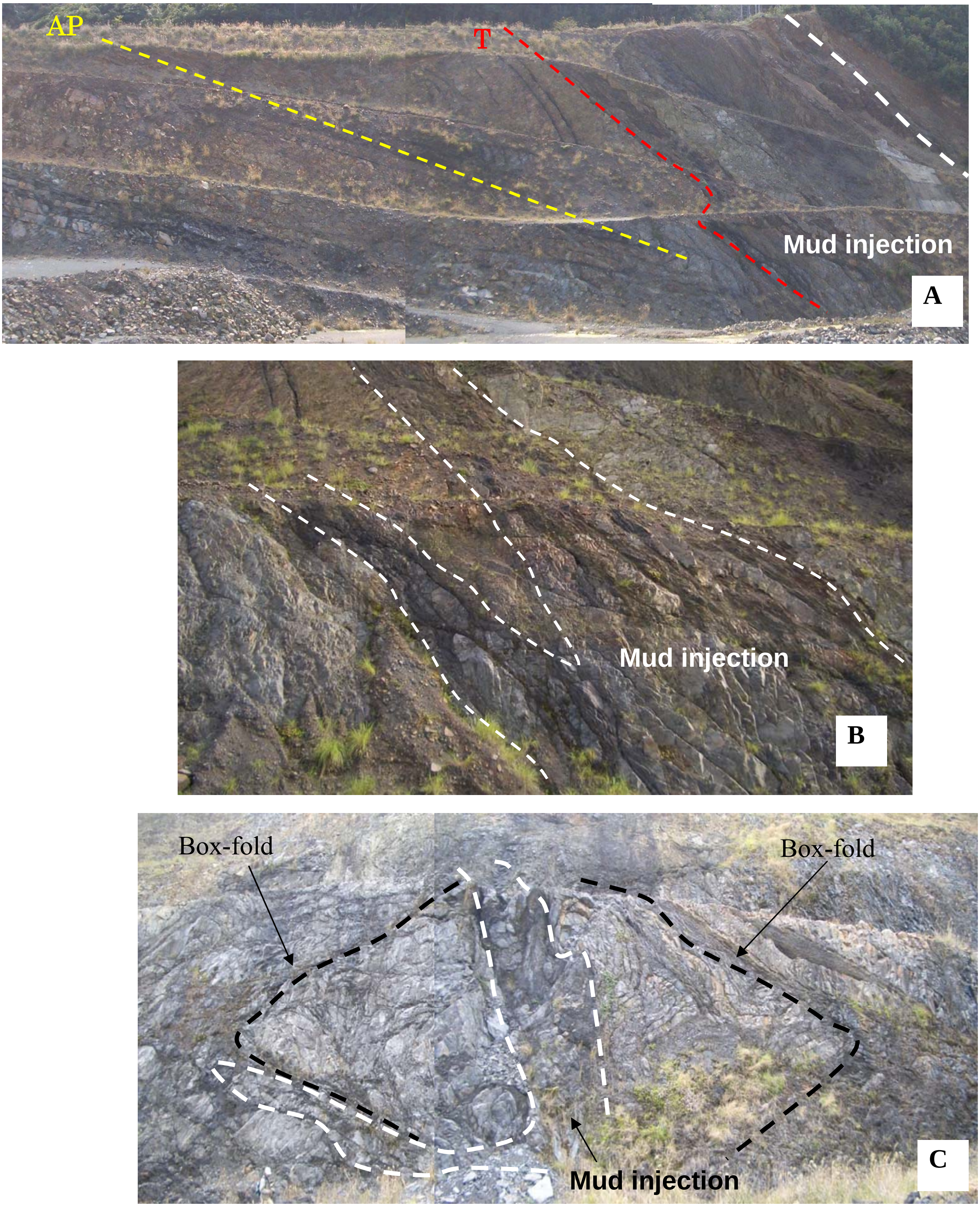

Fig.3.2.7 Folding style in the sheeted olistolith of the Kadokurazaki Complex. A: Overturned flexural fold with axial plane (AP) of synform dipping 30 degrees to WNW (dashed yellow line). The right-hand limb is detached and disrupted by the thrust fault (T: dashed red line). B: Mud injection along the thrust zone. C: Box-fold style occurs above a detachment. The locations of outcrop photos are shown in Fig. 3.1.13, 3.2.4 and 3.2.5.

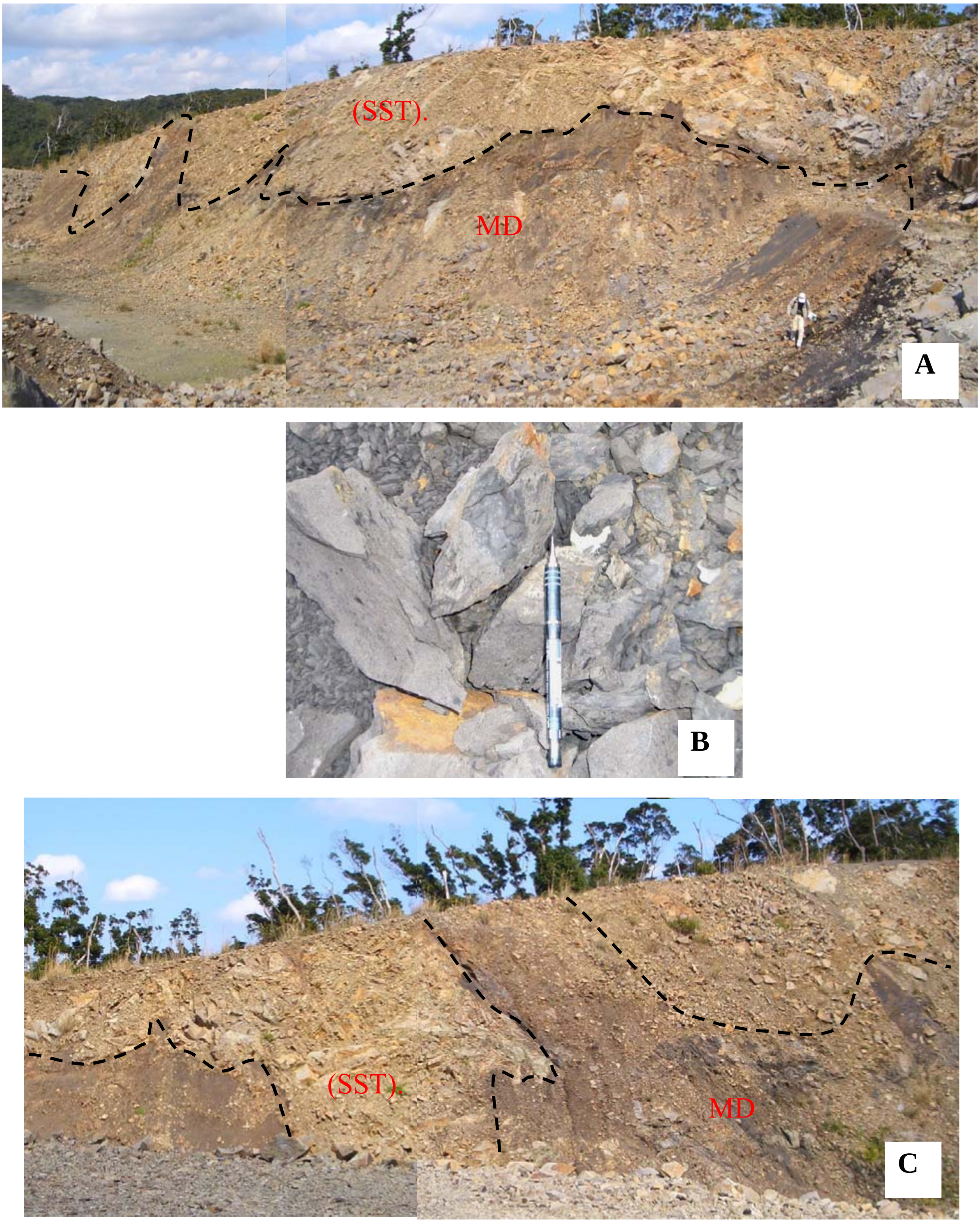

Fig.3.2.8 Mud diapirs (MD) injecting into the slump sheet above. A: Discordant contact (dashed black line) between mudstone and sandstone layers. B: Intrusive mudstone containing black colored sandy shale fragments. C: Mud diapirs (MD) intrusion along the extensional fractures (NE-SW) in the overlaying sandstone (SST). The locations of outcrop photos are shown in Figs. 3.1.13, 3.2.4 and 3.2.5.

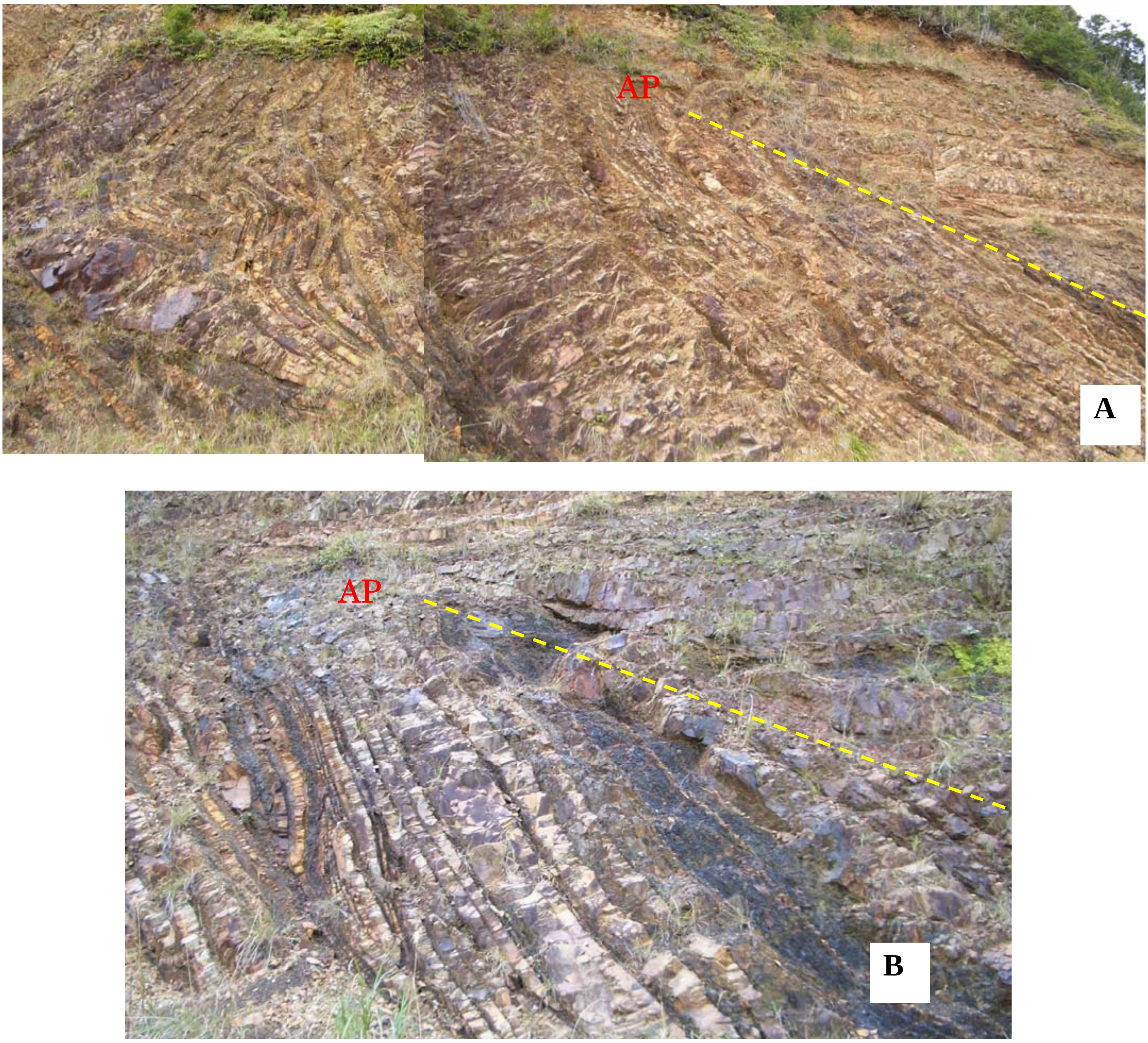

Fig.3.2.9 Large scale southeast-vergent recumbent folds. A and B: Axial plane (AP) of antiform dips inclining at 25 degrees to NW. These strata are composed of sandy alternation which has been deformed by a flexural fold during the gravity sliding. The locations of outcrop photos are shown in Figs. 3.1.13, 3.2.4 and 3.2.5.

Intensely folded olistolith showing a deep-sea fan facies occurs in the quarry on eastern area of airport extensively as shown in Fig 3.2.4. As a result of the analysis of deformation structures, the folded strata of the olistolith can be divided lithologically into the lower, middle and upper parts (Figs. 3.2.4 and 3.2.5; Fig.6 in the Appendix). The lower part is composed of thick sandstone and shale-dominant alternating beds. Some planktonic foraminiferal fossils were obtained (Fig.3.2.4) which assigned to Oligocene to Early Miocene in age.

Synform and box-fold occur in this section (Figs 3.2.5 and 3.2.7). Box fold or conjugate folds have plural axial planes inclined in different angles from each other (Roberts, 1982). These fold types occur generally above the basal detachment zone (decollemant), and are formed in gypsum and salt layer (Ruh *et al*., 2012), glaciogenic deposit (Pedersen, 1996, 2014) and weak mud-rich sediments (Alsop & Mrco, 2013). In the study area, it is likely that the box fold was resulted from the lateral compressional stress field during gravity creep and sliding on gentle slope covered by weak mud-mud rich sediments towards the southeast.

The middle part is characterized by grey colored mudstone including black colored angular shale fragments abundantly. Many mud diapirs intruded into the slided strata above can be observed (Fig.3.2.8). The mud diapirs appear along the extensional fractures (NE-SW) of overlaying slumped sandstone (Fig.3.2.8). The intrusive mud yield planktonic foraminifera indicating Early Miocene age. Similar mud diapir structure has been reported from the Izaki olistolith of Nichinan Group (Sakai *et al*. 1987).

The upper part is composed of thick sandstone and sand-dominant alternating beds showing large-scale recumbent folds (Fig.3.2.9). From the geometric analysis of the orientation of fold axes, southeastwards gravity sliding was inferred (Fig.3.2.6). Planktonic foraminifera obtained from this section are assigned to the Oligocene to Early Miocene (E04, E05 and E06 in Fig.3.2.4).

(2) Southern coast of Masuda

Along the east coast near Masuda, central Tanegashima, the lithofcies of the olistholiths from 100m to 200m in size are pebbly mudstone and shallow marine sediments which were deposited by hyperpycnal flows and wave actions of inner shelf environment. The route map and profile of this area is shown in Fig.3.2.10.

Pebbly mudstone

The pebbly mudstone is characterized by many sandstone pebbles in shale matrix and is produced by the accumulation of subaqueous debris flows (Fig.3.2.10). The pebbles are sub-angular clasts which are 2-4cm in length and 1-2cm in width, and they were probably derived from the Kumage Complex. A slaty cleavage formed parallel to the long axis of the pebbles is developed in the muddy matrix.

Shallow-marine sediments

The slump sheet consists of the alternating beds of thin sandstone and shale. Sandstone beds (5-15cm thick) show climbing-ripple, wave-ripple laminations and storm-included cross-stratification commonly (Figs.3.2.11 and 3.2.12). These sedimentary structures indicate a deposition under shallow-water environments above the fair weather wave base.

Wave-modified sandstone

Wave-modified sandstone is about 33m and consists of the turbidite facies (Tabc) in the lowermost part and the wave-modified facies from the lower to the upper parts (Figs.3.2.13, 3.2.14 and 3.2.15). Flute casts are observable on the bottom surface of turbidite, and large convoluted laminations are developed in Tc and Td divisions in the lowermost of sandstone sequence. The lower to upper part of the sequence above the turbidite horizon, is composed of climbing-rippled and large-scale cross-stratified sandstones. Inverse grading in parallel-laminated sandstones identified with traction carpet flow (Lowe, 1982) were found also.

These sedimentary facies suggest that the sandstone beds were deposited density flows under the fluctuations of flow velocity and

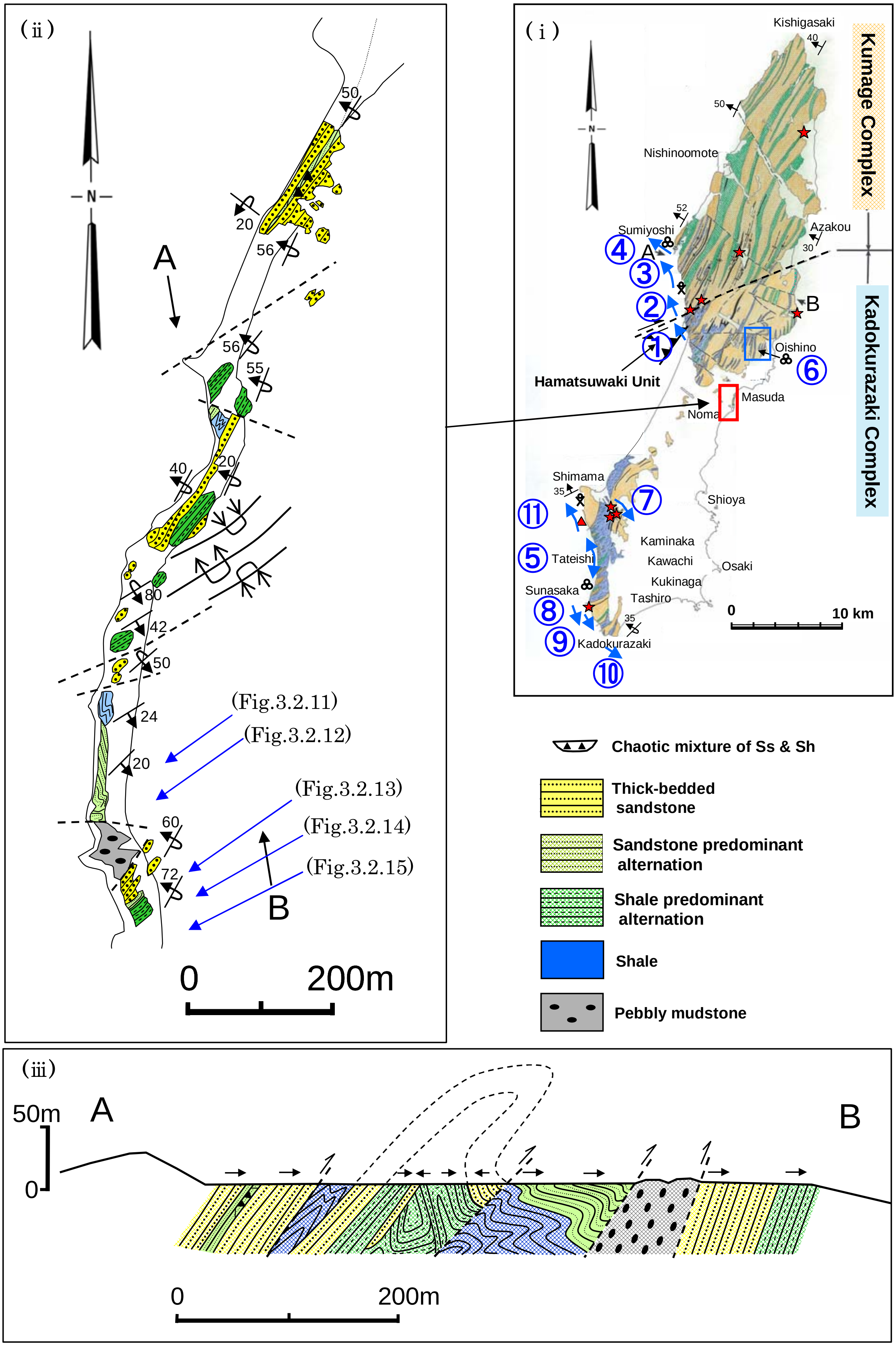

Fig.3.2.10 Route map and profile along the southern coast of Masuda. Black arrows indicate facing of beds. (ⅰ): Index for the route map (ⅱ), (ⅲ): Profile of the route investigated. Short black arrows in the profile indicate facing of beds.

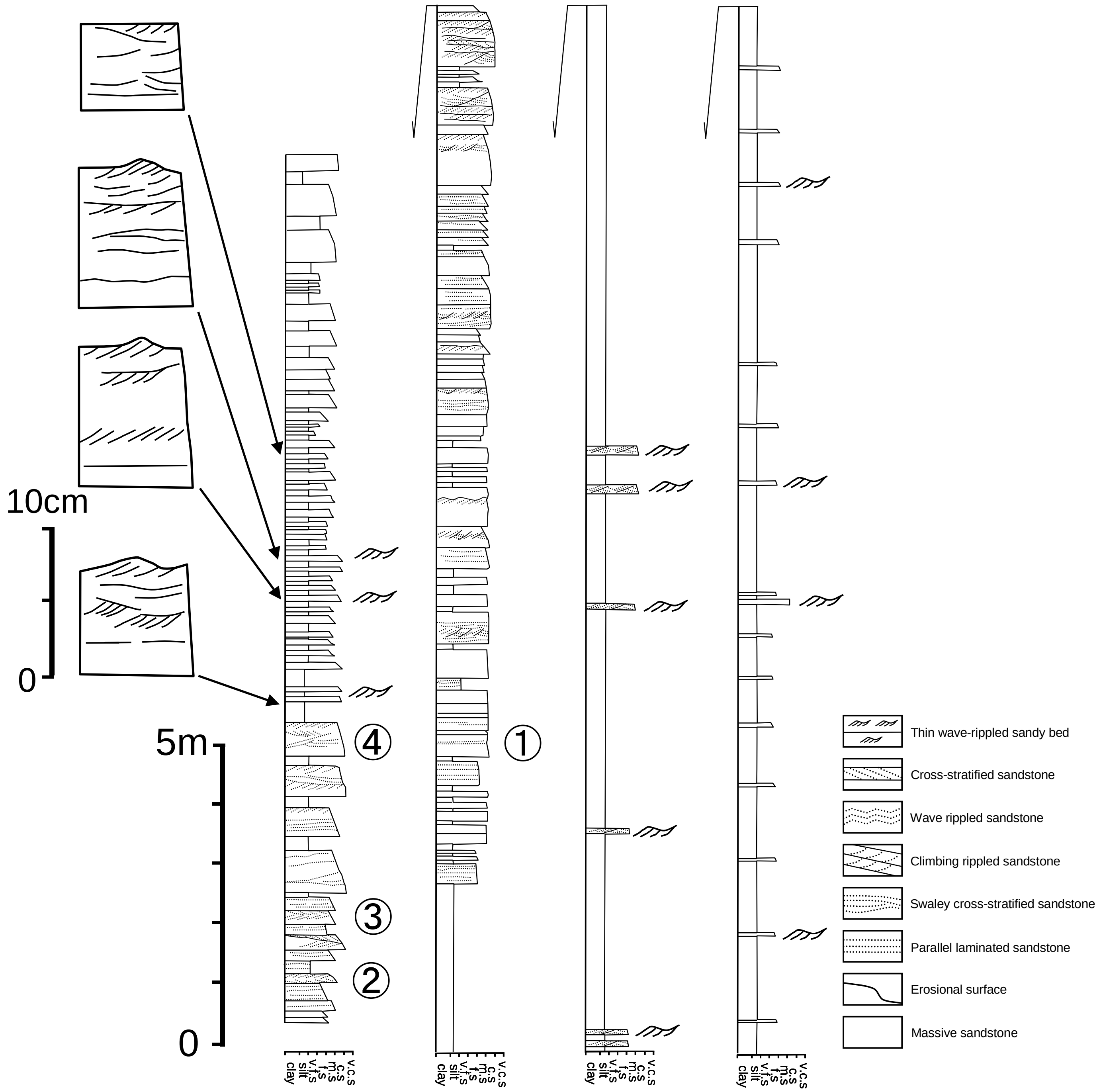

Fig.3.2.11 Measured columnar section of which lithologic unit is interpreted as the shelf environment sequence, on the southern coast of Masuda. See the location in Fig.3.2.10.

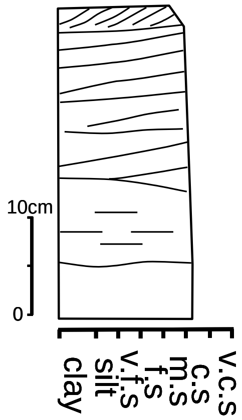

④ Tab and parallel to weakly cross-stratified sandstone.

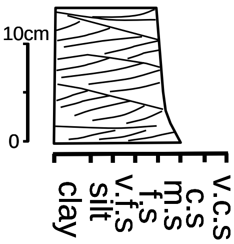

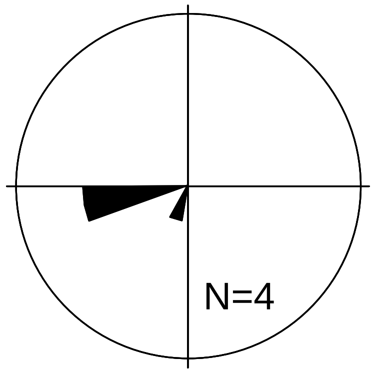

③ Climbing rippled sandstone.

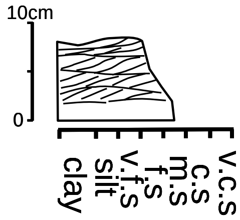

② Ta and climbing rippled sandstone.

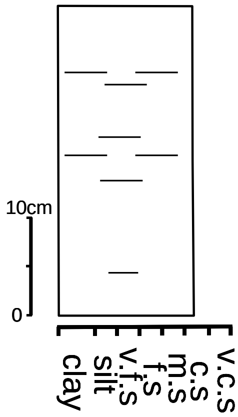

① Turbidite (Ta,Tab).

Fig.3.2.12 Outcrop photos showing internal structures identified with turbidite (①) turbidite and hyperpycnite (② - ④). Paleocurrent rose diagram by photo ③ based on measurement of foreset laminae. See the location in Fig.3.2.10.

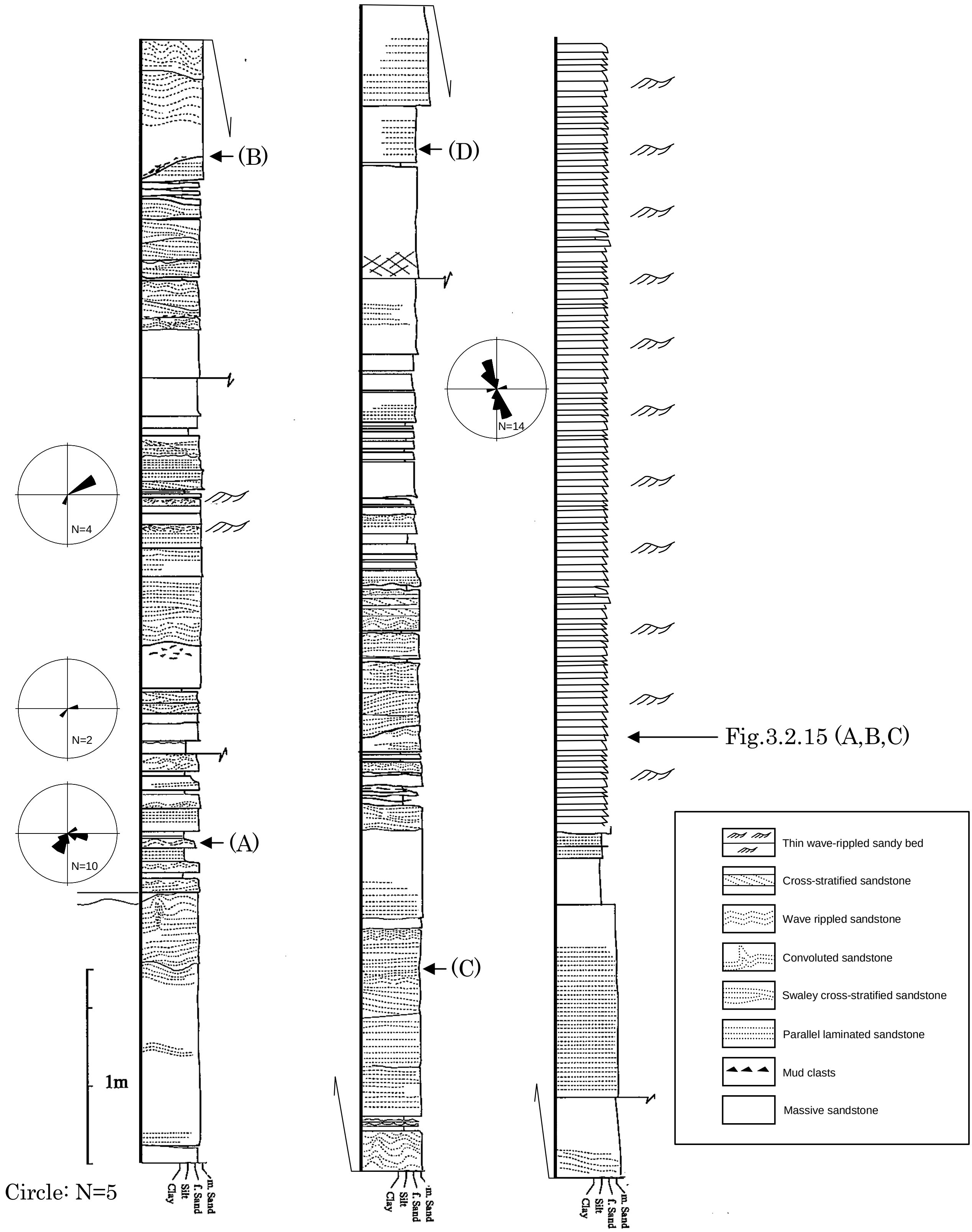

Fig.3.2.13 Measured section of shallow-marine olistolith at the southern coast of Masuda. The current rose diagrams from the foreset lamina of cross-stratified sandstones. See the location in Fig.3.2.10. (A), (B), (C) and (D) stand for outcrop photos in Fig.3.2.14. The sedimentary features of thin-bedded alternation of sandstone and shale are shown in Fig.3.2.15.

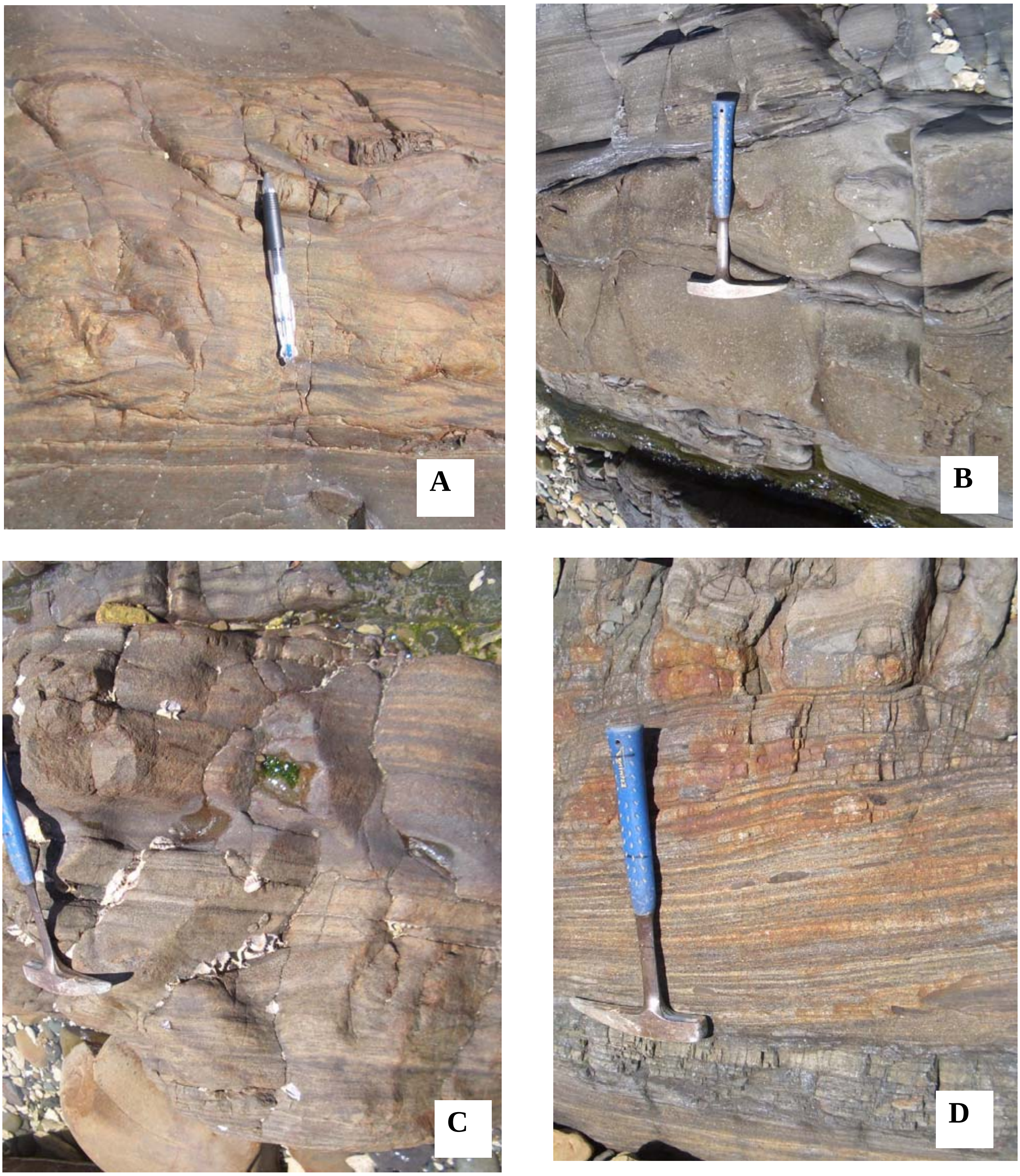

Fig.3.2.14 Outcrop photos show sedimentary structures in wave generated sandstone (hyperpycnite) intercalated in the lower and middle parts of the columnar section (Fig.3.2.13) The total thickness of sandstone bed is about 33m. The sandstone exhibits the turbidite facies in the lowermost part and the wave-modified facies in the lower to upper part. A: Climbing-ripple laminae. B: Large-scale cross-stratified sandstone. C: Repetition of inverse grading in thick sandy laminae. D: Inverse grading in parallel-laminated sandstone. See the locations and stratigraphic positions in Figs.3.2.10 and 3.2.13, respectively.

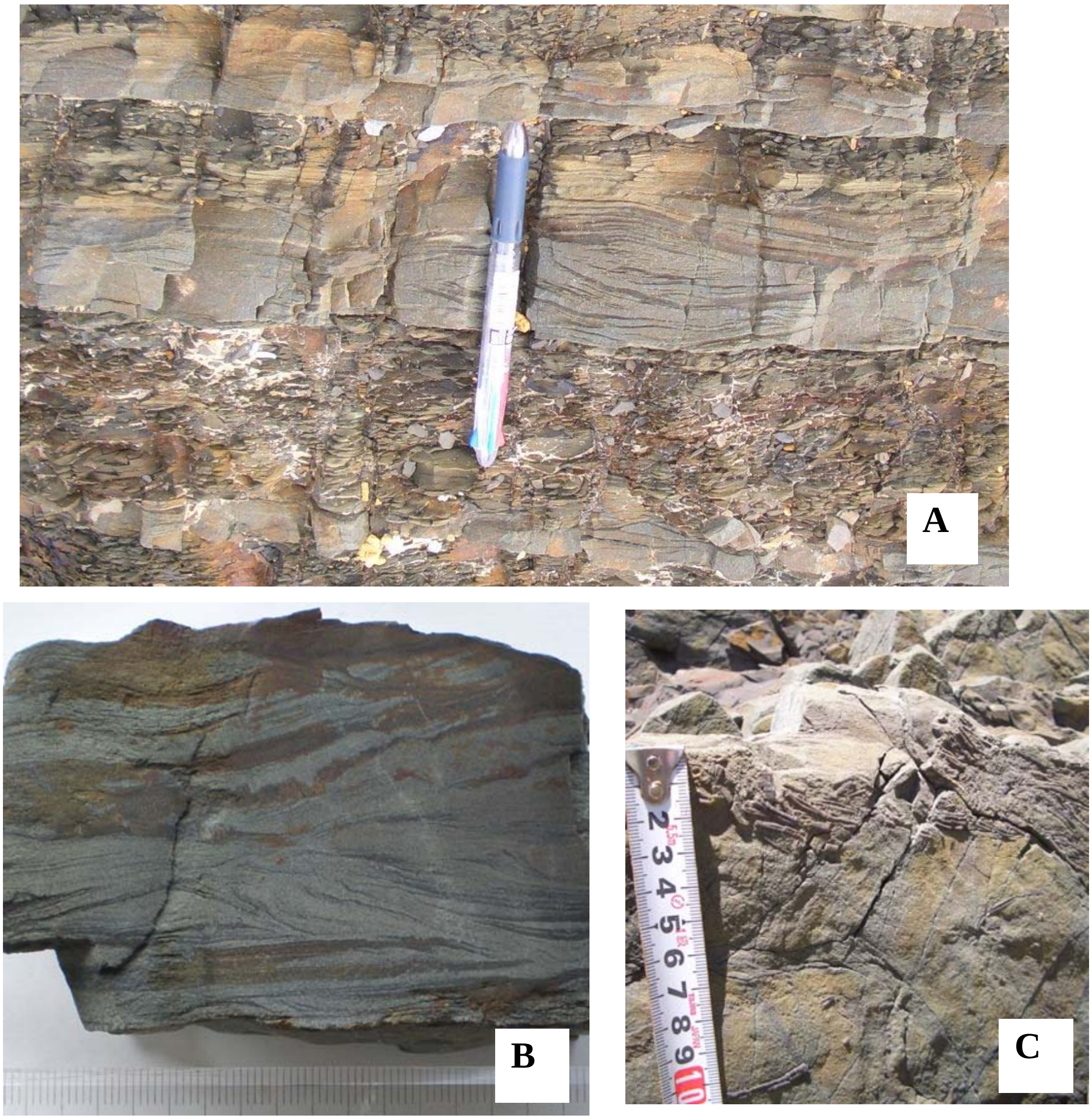

Fig.3.2.15 Outcrop photos show sedimentary features in sandstone on the southern coast of the Masuda. A: The alternation of thin sandstone and shale conformably overlies the thick sandstone bed (Fig.3.2.13). Climbing ripple cross-lamination and parallel-lamination which are reflected by decreasing and increasing flow velocity respectively. B: Wave-generated climbing cross-lamination (polished cross section of sandstone). C: *Tererbellina* preserved on the bottom surface of the thin sandstone bed. See the location and stratigraphic position in Figs.3.2.10 and 3.2.13, respectively.

sediment concentration resemble to hyperpycnal flow (Mulder & Alexander, 2001; Saitoh *et al*. 2005).

The generation of hyperpycnal flow occurs at a river mouth environment when the flood water discharges into marine basin. Therefore, bed type is changeable by a function of the magnitude of the flooding water corresponding to the velocity and amount of discharge at the river mouth (Mulder *et al*, 2001, 2003).

Saitoh *et al*. (2005) suggested that the criteria for identifying hyperpycnal flow deposits are as follows:

"(1) vertical succession composed of 2 parts, inversely-graded lower part and normally-graded upper part,

(2) internal scour surface,

(3) repetitive alternation of fine-grained and coarse-grained layers, or laminated and massive layers,

(4) abrupt pinch-out of beds, and

(5) inclusion of terrestrial materials such as leaves. "

Except number (5), the above all criteria are able to apply in this wave-modified sandstone.

(3) Allochthonous blocks of shallow marine deposits in the Kumage Complex

The olistolith with hyperpycnites was observed also on the coast of Okigahamada of the northeast part Tanegashima, where the Kumage Complex is extensively distributed (Fig.3.2.16).

As shown in Figs.3.2.17 and 3.2.2.18, the lower unit of the olistolith is characterized by thin climbing-ripple laminated sandstone. The middle to upper units are composed of cross-stratified sandstone, parallel-laminated sandstone and climbing-ripple laminated sandstone. Thus, the middle part sandstone is characterized by hyperpycnal flow deposits.

Small vertical burrows are found in the thin wave-rippled sandstone overlaid by the thick bedded sandstone. The vertical burrows which have a diameter of 1 to 4 mm at the bottom, and 2 to 8 mm at the top are filled with very fine grained sand to silt

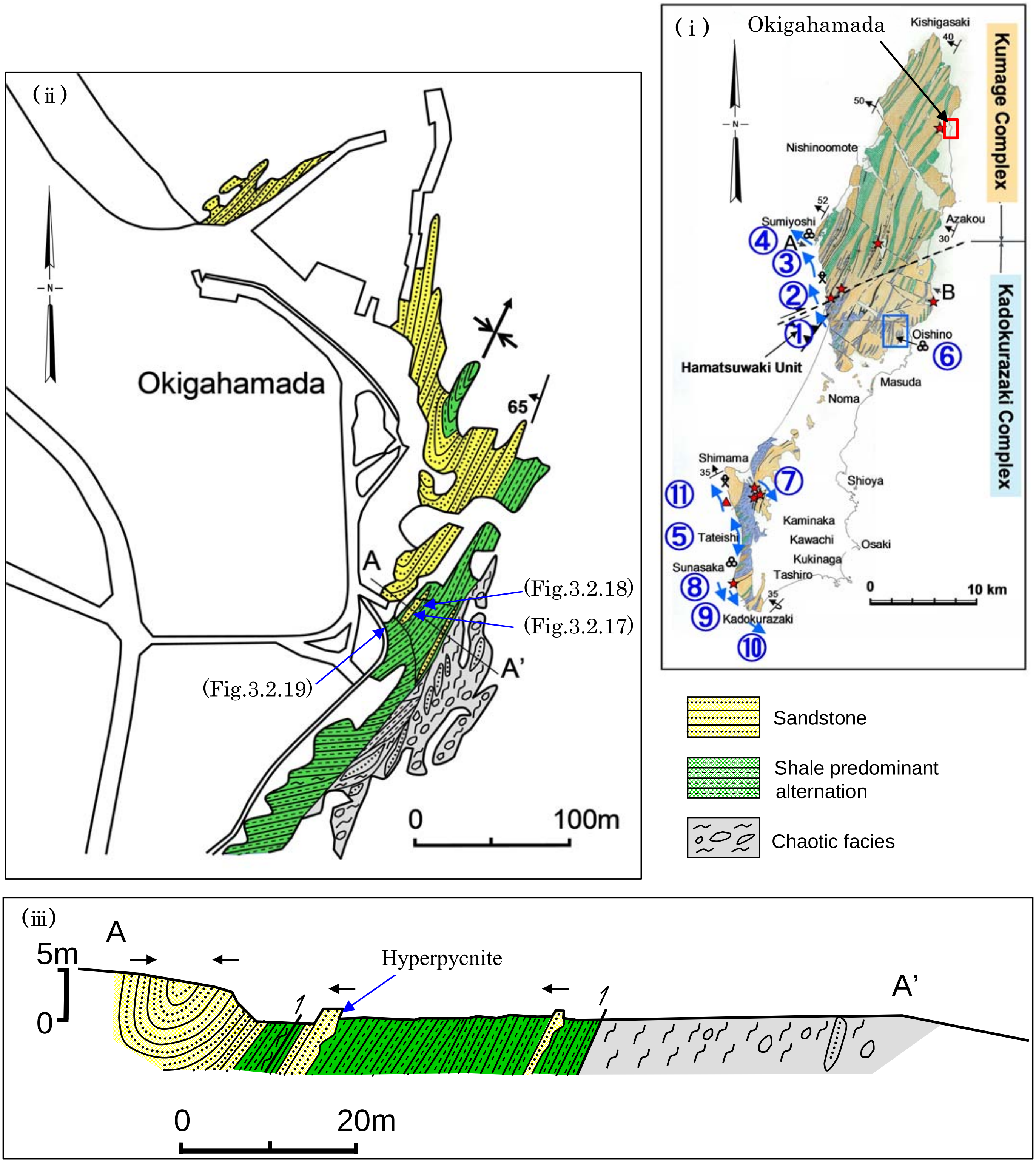

Fig.3.2.16 Route map and profile of shallow-marine olistholith along the coast of Okigahamada. This large slump sheet is shelf environment deposit. Black short arrows in the profile indicate facing of beds. (ⅰ): Index for the route investigated, (ⅱ) and (ⅲ): Rout map and profile, respectively. Short black arrows in the profile indicate facing of beds.

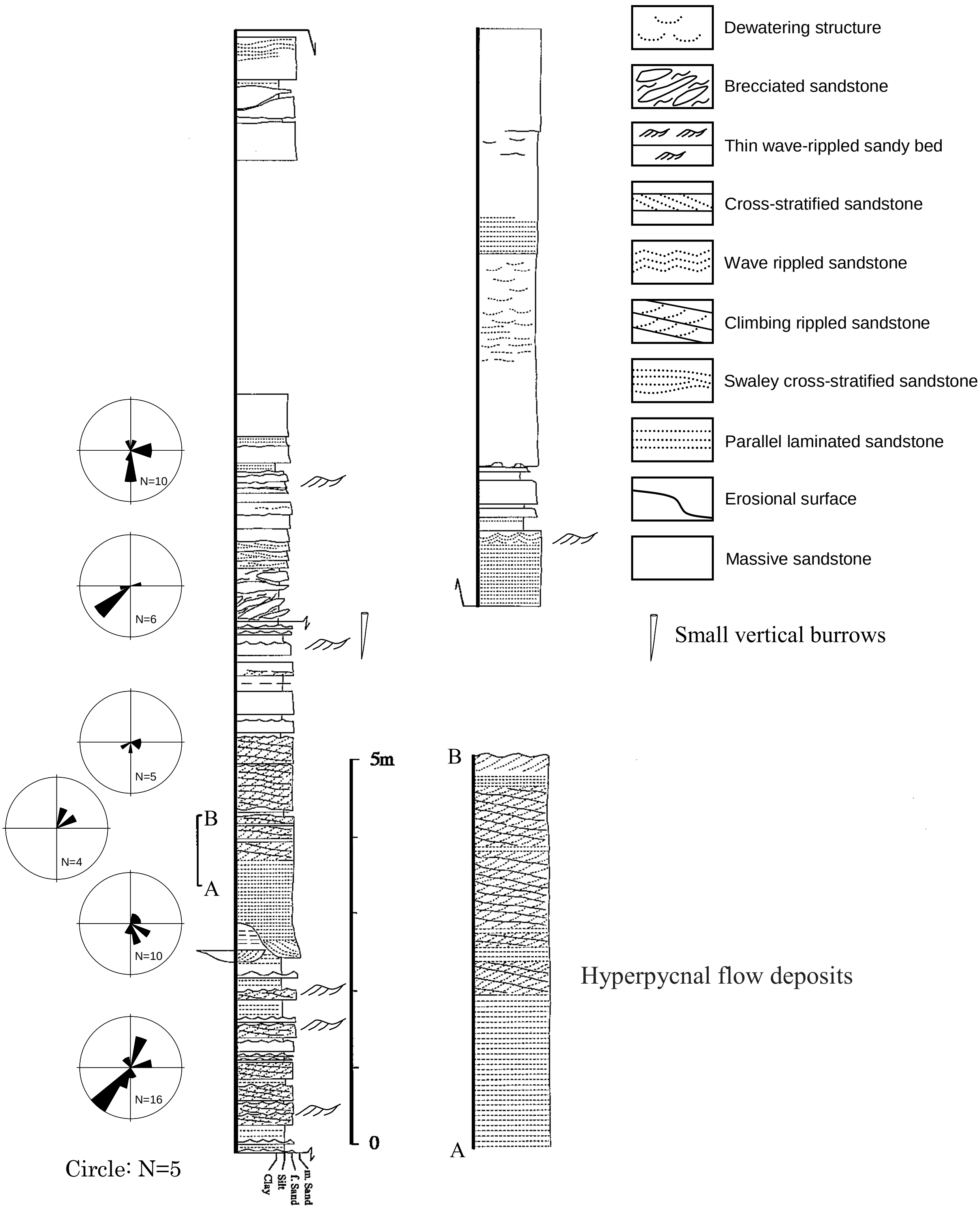

Fig.3.2.17 Columnar section of the slump sheet showing a shallow-marine succession along the Okigahamada coast. The current rose diagrams were measured from cross-bedded sandstones. Location and geologic information for Fig.3.2.16.

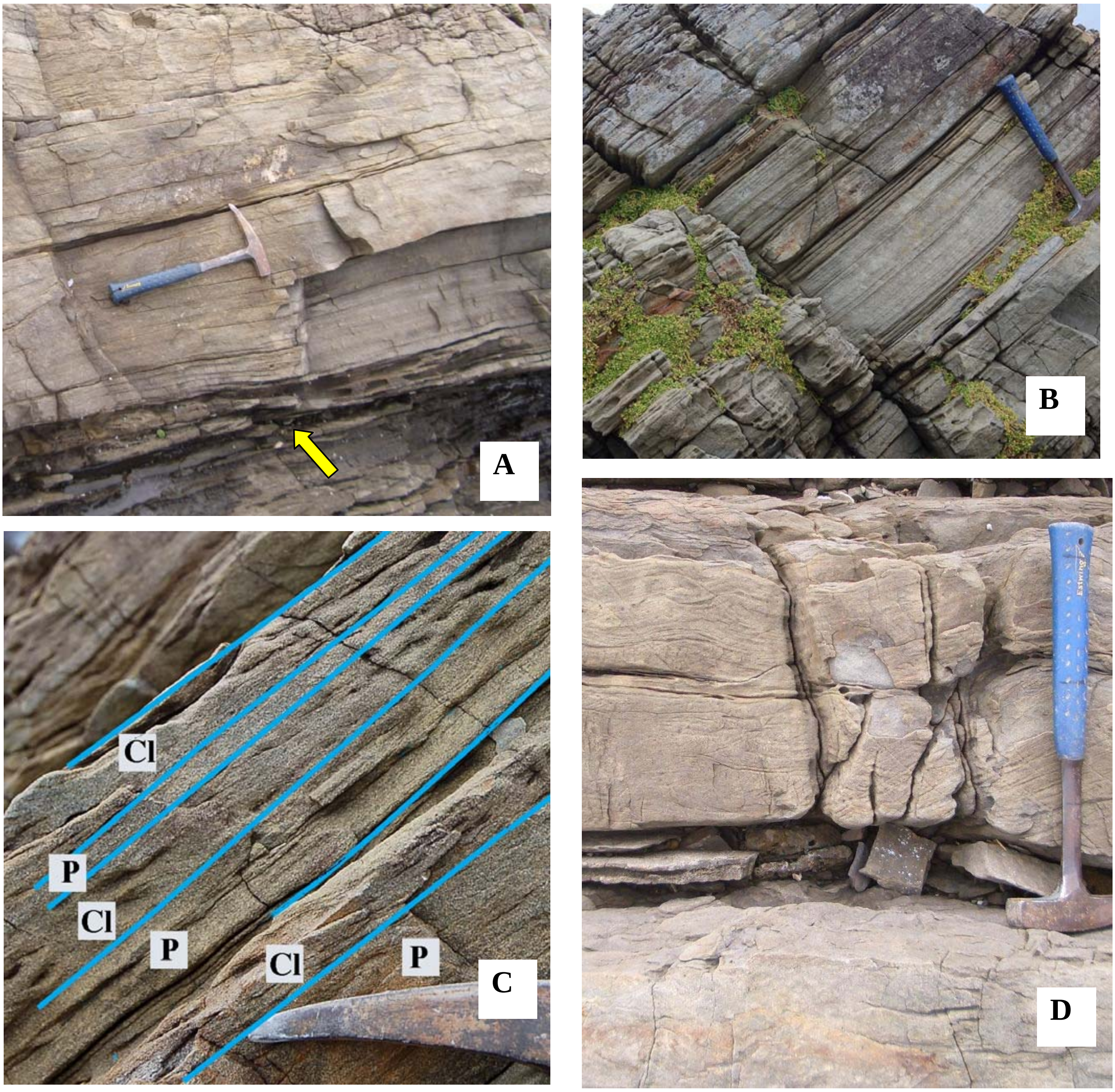

Fig.3.2.18 Outcrop photos show a sandstone bed (hyperpycnite) from the olistolith exposed at the coast of Okigahamada. A: Lower part of the low-angled cross-stratified coarse-grained sandstone above the basal erosional surface (arrowed). B: Distinctive parallel laminations in the middle part of the sandstone bed. C: Frequent repetitions of parallel- (p) and climbing ripple-lamination (Cl) in the upper part indicating deposition under unsteady density flow. D: Uppermost part of the sandstone shows dune and wavy lamination. See the location of phots in Fig.3.2.16.

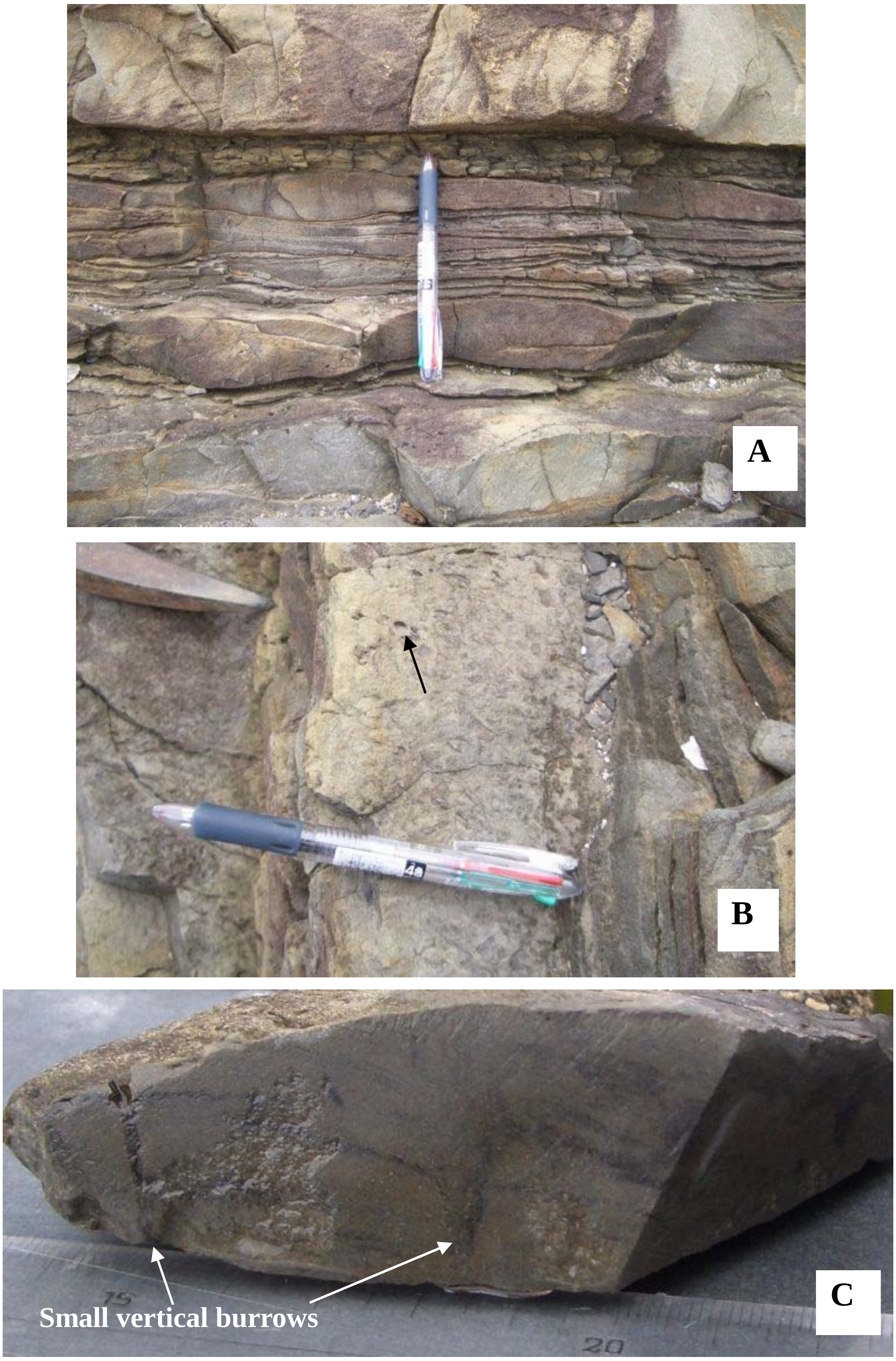

Fig.3.2.19 Outcrop photos show a sand-dominant alternation bed yielding small vertical burrows, in the olistolith exposed along the coast of Okigahamada. A: Thin bedded sandstone with current- and wave-ripple cross-lamination, indicating deposition in shallow-water environments above the fair-weather wave-base. B: The top surface of wavy laminated sandstone recognized many small vertical burrows (diameter of 2 to 8 mm). C: Trace fossil (arrowed) corresponding to *Monocraterion* (Frey, 1975). The funnel opening and concavity of the laminae point to the top surface of the bed. See the location of phots in Fig.3.2.16.

(Fig.3.2.19). Weakly funnel structure are recognized, therefore, this trace fossil is identified to *Monocraterion* isp. (Frey, 1975). Generally, this burrow is coexistent with *Skolithos* ichnospecies. These trace fossils indicate shallow marine environments.

(4) Kadokura fishing port area

Along the coast Kihara and Kadokurazaki areas, the overturned strata younging towards the southeast are well distributed (Figs.3.1.5 and 3.1.6). These strata are almost composed of coherent turbidite sequences with some slump beds. Around the Kadokura fishing port, slump deposits with complicated structure occur from 50 to 200 in size meters (Figs.3.2.20 and 3.2.21). These blocks (olistoliths) consist of the sandstone-dominant alternations. As shown in Fig.3.2.23, the dark grey colored shale interbedded with the sandstone beds yields, occasionally siderite nodules similar to those of northern part of Tanegashima (Hayasaka *et al.*, 1983), suggesting a slide mass derived from the Kumage Complex, probably.

The fold structure developed within each olistolith is highly different. Geometry of folds in this area varies from outcrop to outcrop, locally as shown in route map (Fig.3.2.20). The reconstruction of folds shows recumbent fold in which the axial planes dip up to 15 degrees northwestwards (Figs.3.2.21 and .3.2.22). Judging from the orientation of slump fold axes, southeastwards gravity sliding can be assumed. This study concluded that the fold structures are peculiar to each olistolith that reflected the different slide movement or final strains for emplacement.

(5) Shimama-Kaminaka section (Section ⑦)

This section is exposed along the road between Shimama and Kaminaka. As shown in Figs.3.1.5 and 3.1.7, these strata show antiformal synclines and synformal anticlines caused by gravitational sliding, and are contacted with northeast-trending thrust fault at the

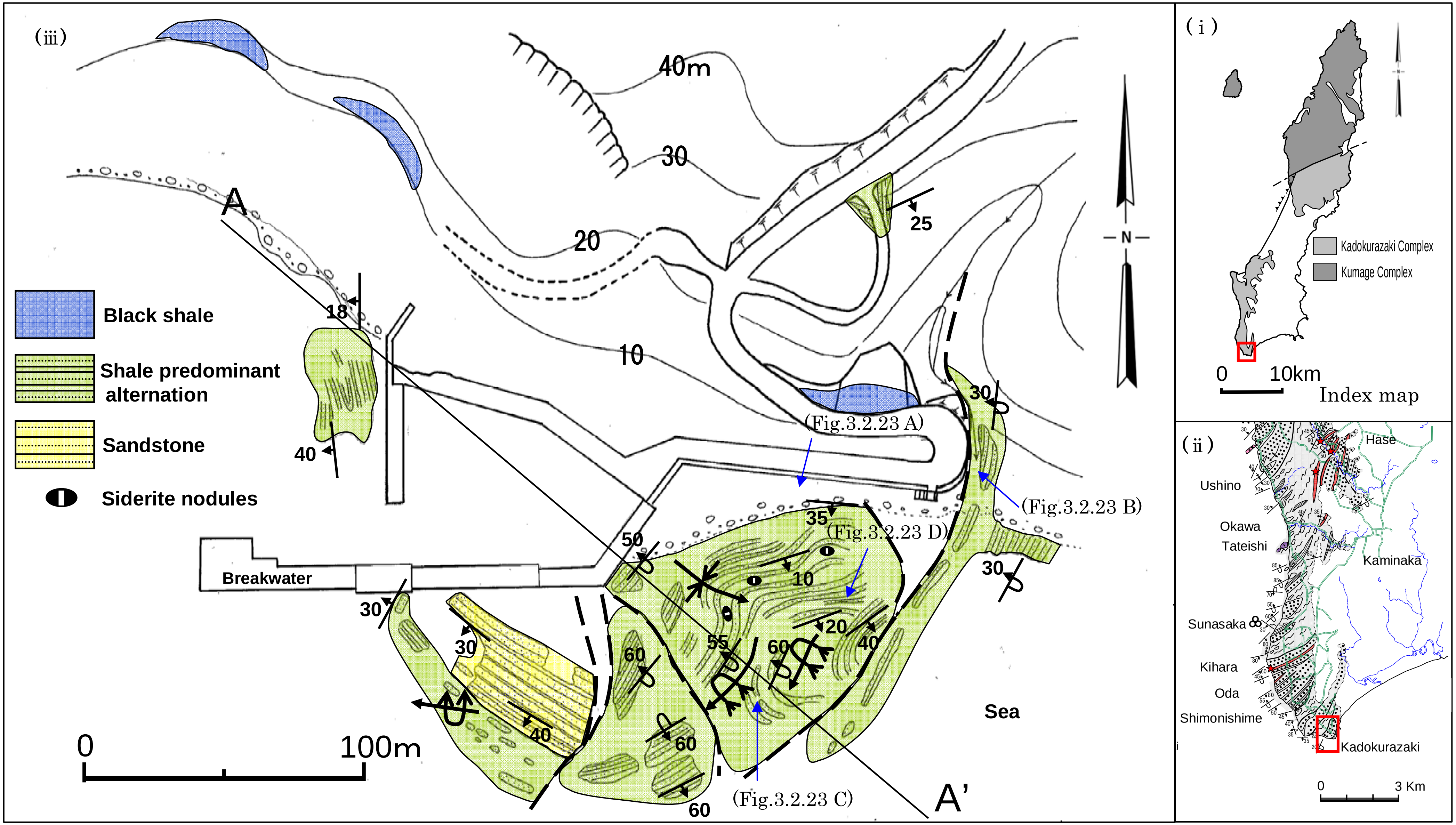

Fig.3.2.20 Map showing slump structure around the Kadokura fishing port in southern part of Tanegashima. (i) and (ii) : Index for the area investigated, (iii): Rout map and guide for profile of Fig.3.2.21.

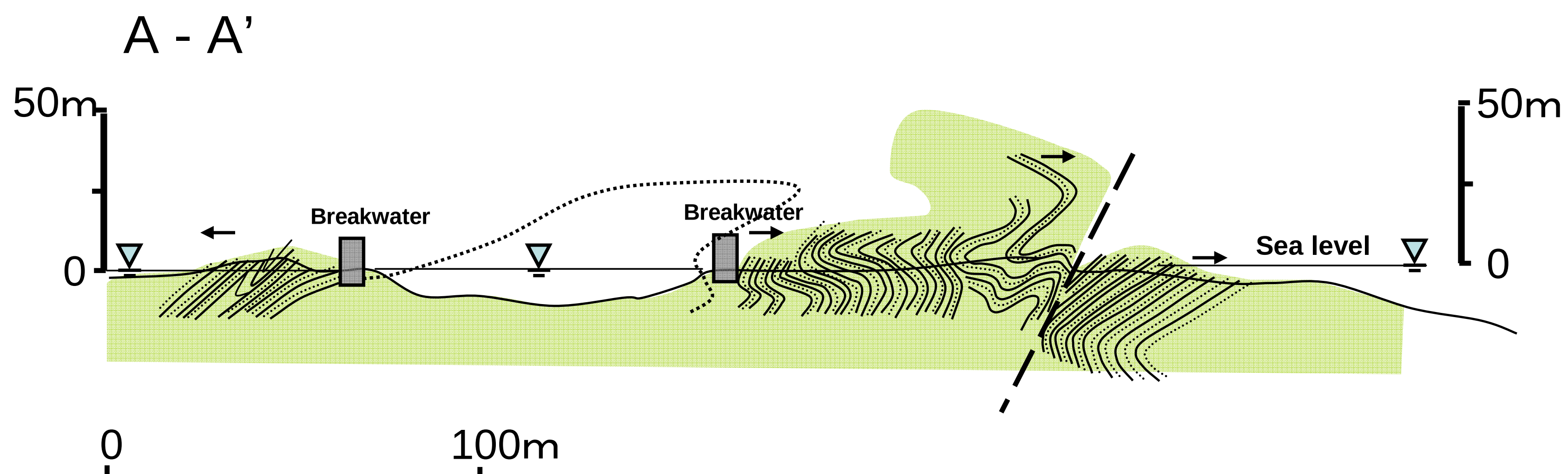

Fig.3.2.21 Cross-section showing very irregular slump folds.
Short black arrows in the profile indicate facing of beds.

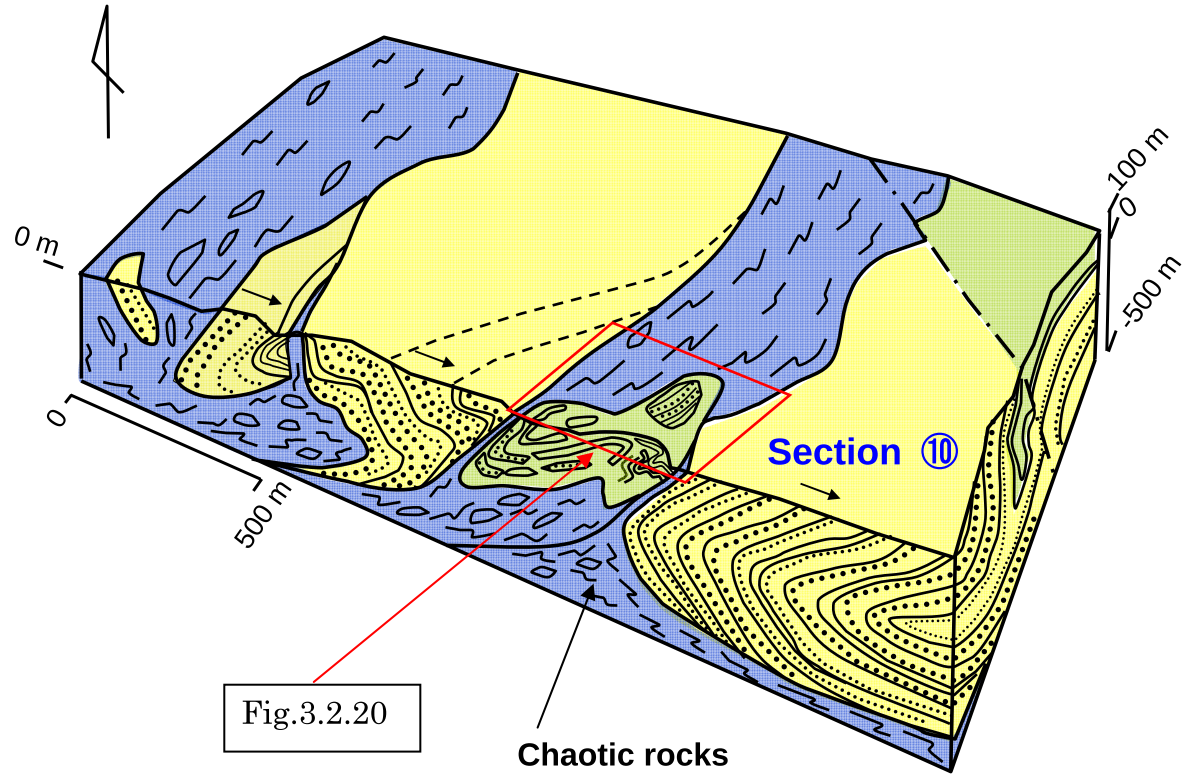

Fig.3.2.22 Schematic block diagram illustrating the geometry of sheeted slump folds in the Kadokurazaki headland. Short black arrows indicate facing of beds. Short black arrows indicate facing of beds.

Fig.3.2.23 Outcrop photos show the slump structures and sedimentary features of olistoliths around the Kadokura fishing port. A: Large-scale slump structure. B: Fold axial plane (AP: arrowed) dips at a low angle. C: Siderite nodule in the dark grey colored shale. D: Longitudinal ridge-and-furrow structures on the bottom surface of the sandstone. The locations of outcrop photos are shown in Fig. 3.1.13 and 3.2.20.

base of west frank. The top of east frank is in fault contact with the very thick sandstone succession. The lower part of this section consists of turbidite succession characterized by coarsening-upward tendency (FA3) (Fig.3.1.8 and Fig.7 in the Appendix). The middle and upper part is intercalated with shale (FA2) and Middle Eocene radiolarian-bearing variegated shale (FA1) (Okada, *et al*, 1982). Furthermore, flysch turbidities overlie these strata in the uppermost part.

(6) Kihara-Oda section (Section ⑧)

The section ⑧ occurs as slump sheets which are overturned beds facing towards the southeast, along the coast between Kihara and Oda (Figs.3.1.5 and 3.1.6). The total thickness of this section is approximately 1200m (Fig.3.1.8 and Fig.8 in the Appendix). The lowermost part of this section contains scaly shale enclosing blocks of various size sandstones from decimeter to meter. In the middle and upper part, this section shows a very thick stratified succession which is made up of slumped shale (FA2) containing sandstone blocks, variegated shale (FA1), sandy turbidite (FA3) and thick-bedded sandstone (FA4). Sandy turbidite and thick-bedded sandstone sequences have many cycles of thickening and coarsening upward to asymmetric successions (Individual sequence thickness: 10-110m). Sand volcanos less than 3cm in diameter occur, occasionally on the upper surfaces of sandy turbidite (FA3). From the variegated shale (FA3), Kuwazuru & Nagatsu (2007) obtained the radiolarian fossils indicating Middle Eocene to early Early Oligocene age.

(7) Shimonishime section (Section ⑨)

The section ⑨ is distributed in the coast area between Oda and Shimonishime (Figs.3.1.5 and 3.1.6). The total thickness of this section is about 1000m (Fig.3.1.8 and Fig.9 in the Appendix). The strata of this section facing towards the southeast mostly strike NE-SW and dip steeply to the SE. This section mainly consist of sandy turbidite (FA3) and thick-bedded sandstone sequences

(Individual thickness: 10-70m) (FA4) which are characterized by thickening and coarsening-upward to asymmetric tendency. Shale dominant beds (FA2) and alternating thin beds of fine-grained sandstone and shale (FA5) recognized in middle to upper part of this section. One specimen of molluscan fossils having similarity to *Nuclidae* was found from the shale dominant beds (FA5).

(8) Kadokurazaki Section (Section ⑩)

The section ⑩ is exposed along the coast between the Kadokura fishing port and the east end of the Kadokurazaki headland (Figs.3.2.5, 3.1.6 and 3.2.22). This section having a thickness of about 250m comprises turbidite (FA3) and thick-bedded sandstone sequences (FA4) containing many cycles of thickening and coarsening upward to asymmetric successions (Individual cycle thickness: 10-110m) (Fig.3.1.8 and Fig.10 in the Appendix). These sandy turbidite sequences are occasionally intercalated with thin coal seams and ichnofossils such as *Terebellina* are found from the bottom surface of the thin sandstone alternated with shale in the upper part of this section. These evidences in this section are similar to FA3 and FA4 in the Fukago Unit of the Kumage Complex.

(9) Shimamasaki Section (Section ⑪)

Along the coast Ushino to Shimamazaki, the northwards younging strata are widely distributed (Figs.3.1.5 and 3.1.6). This sandstone dominant body is exposed 3 km in length and 2 Km in width. Its total thickness attains about 1300m (Figs.3.1.8 and Fig.11 in the Appendix).

The lower part of the section ⑪ overlying on the chaotic rocks of the Kadokurazaki Complex, shows gently folds trending NE-SW (Figs.3.1.5, 3.1.6 and 3.3.5). The uppermost part of this section is unknown because of lacking of exposure on the west of Shimama headland. However, the chaotic rocks appear, in the northern area of the Shimama.

The Section ⑪ is almost composed of turbidite sequences and show a succession which is contact with a chaotic rock of the Kadokurazaki Complex. Within the turbidite sequences, a variety of sedimentary structure such as flute casts, amlgamations, large water-escape structures, pipy water-escape structures, dish structures, ripple marks, and sand volcanoes were observed. Bioturbation could be found in the muddy rocks. In the lower part of the turbidite sequence, the whitish tuffaceous sandstone is intercalated (Fig.3.2.24). In this study, fission-track analysis was carried out for this tuffaceous rock and obtained an age of 48.9±4.1Ma as described later.

On the west coast of Shimamazaki, ill-sorted muddy sandstone bed (6m thick) yields molluscan fossils which has a close alliance to species originally described from the Ashiya Group (Hayasaka *et al*., 1980). Trace fossils (*Tigillites*-like vertical burrows) corresponding to those of shallow neritic type were found also in ill-sorted sandstone. The sequence of the coherent blocks in Shimama headland shows many sedimentary cycles containing a coarsening- and thickening-upward as well as fining- and thinning-upward cycles (see Fig.11 in the Appendix).

As shown in Fig.3.1.5, several quartz-porphyry dikes were found from the west coast and edge of cape. The age of these intrusive rocks, dated 15.6 Ma, seems that of the quartz-porphyry and granitoid body occurred in the northeastern part of Yakushima (Ogasawara, 1997).

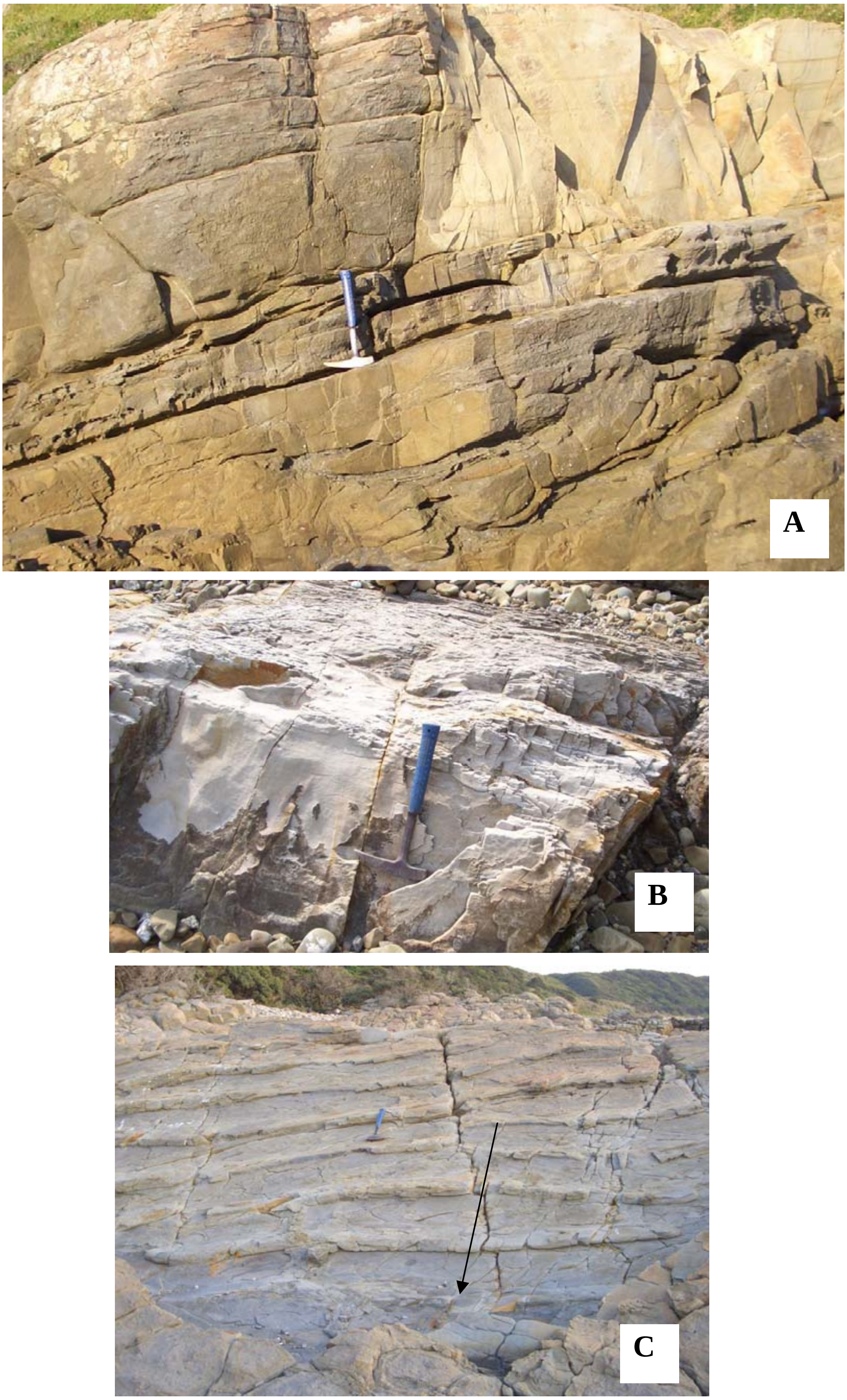

Fig.3.2.24 Outcrop photos show the lithofacies and sedimentary features of the Shimama Olistolith (Section ⑪). A: Parallel-laminated sandstone in the amalgamated sandstone beds. B: Whitish tuffaceous sandstone obtained an age of 48.9±4.1Ma by fission-track method. C: Straight ripple marks on the top surface of the sandstone. Black arrows indicate the flow direction towards the NNW. The locations of outcrop phots are shown in Fig.3.1.13.

3.3 Paleocurrents and slump directions

3.3.1 Paleocurrent directions

Paleocurrent directions are confined and controlled by the morphology of sedimentary basins in general. The paleocurrent data are useful for estimating the directions of sedimentary transport and migrations of depositional sites. However, the paleocurrent directions should differ among the olistoliths due to the rotation and deformation during submarine sliding. In this study, many sedimentary structures with paleocurrent orientations were measured from both turbidite sequences in the Kumage and Kadokuraxaki Complexes. Figs.3.3.1and 3.3.2 show paleocurrent data collected from sole marks such as flute casts, groove casts, gutter casts, and asymmetric current-ripples, cross-stratifications and paleo-channels.

The sandy turbidies (FA3) of the Kumage Complex show generally northeasterly flow directions which imply parallel to the axis of elongated forearc basin. On the other hand, ripple marks on the top of thick sandstone (FA4) show multi-directional flows, however, its sole marks indicate polydirectional paleoflows towards the northeast and southeast. The southeasterly flows suggest that the sediments were supplied from the northwest.

In Kadokurazaki Complex in the central part of Tanegashima, the turbidite sequences comparable to lobe facies (FA3) show a dominated northeasterly paleocurrent directions which seem to be in harmony with those in the Kumage Complex (Fig.3.3.1). Northeasterly and northwesterly paleocurrent directions were shown from some olistoliths distributed in the southern part of Tanegashima.

The northwestwards paleocurrent directions shown in the olistolith of Kadokurazaki area (Fig.3.3.1) are suggested clearly that many olistoliths have rotated anticlockwisely up to 90 degrees. Additionally, paleocurrent data from the lobe facies in the lower part of the Shimama Olistolith (Section ⑪) display northeasterly flows, whereas in the thick sandstone sequences (FA4) of the middle part and the lobe facies (FA3) of the upper part show predominant directions towards the southwest.

3.3.2 Slump directions

Fold structures preserved within the sliding sheets are useful to examine the paleoslope directions which might be reflected as an attitude of sliding sheets. The geometrical analyses of slump folds were carried out in the representative slump zones to compare the paleoslope directions between the Kumage and Kadokurazaki Complexes (Fig.3.3.3).

There are some methods having proposed for the analysis of slump folds: the separation-arc method (Hansen, 1971; Bradley & Hanson, 1998), axial-planar intersection method (Strachan & Alsop, 2006), and mean axis method (Alsop & Marco, 2012, 2013).

As the result of, the sliding directions of the Kumage Complex in Azakou area (Fig.3.3.4) indicate a sliding direction towards the E-ESE, so that the paleoslope was inferred the eastwards (Fig.3.3.3). In contrast, the large slump sheets of the Kadokurazaki Complex in the middle and southern part of Tanegashima suggest a gravitational transport towards the SE (Fig.3.3.3).

The lower part of the Simama Olistolith is accompanied by folds which have fold axes trending NE-SW and plunging gently towards the southwest or the northeast (Fig.3.3.5). Therefore, these folds are also thought to have been formed during a sliding motion towards the SE. It is therefore suggested that paleocurrent directions in each olistolithes does not coincide with one another because of different gravitational sliding directions with block rotation.

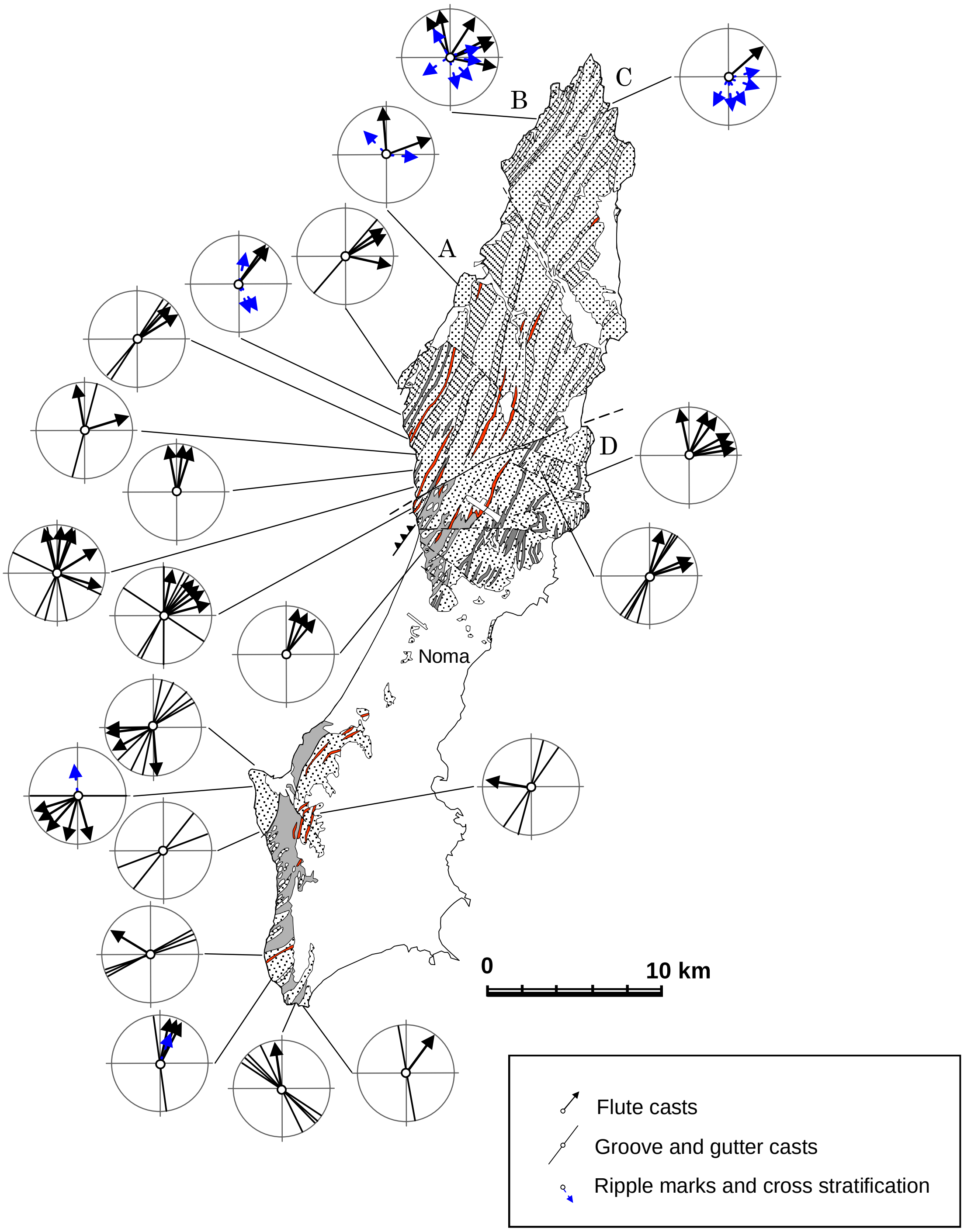

Fig.3.3.1 Paleocurrent directions inferred from solemarks, ripple marks and cross-stratificasions in the Kumage and Kadokurazaki Complexes. Paleocurrent data of A,B,C and D areas were provided by Okada (1983), from “*Geology of Tané-ga-shima*” (Hayasaka *et al.*, 1983).

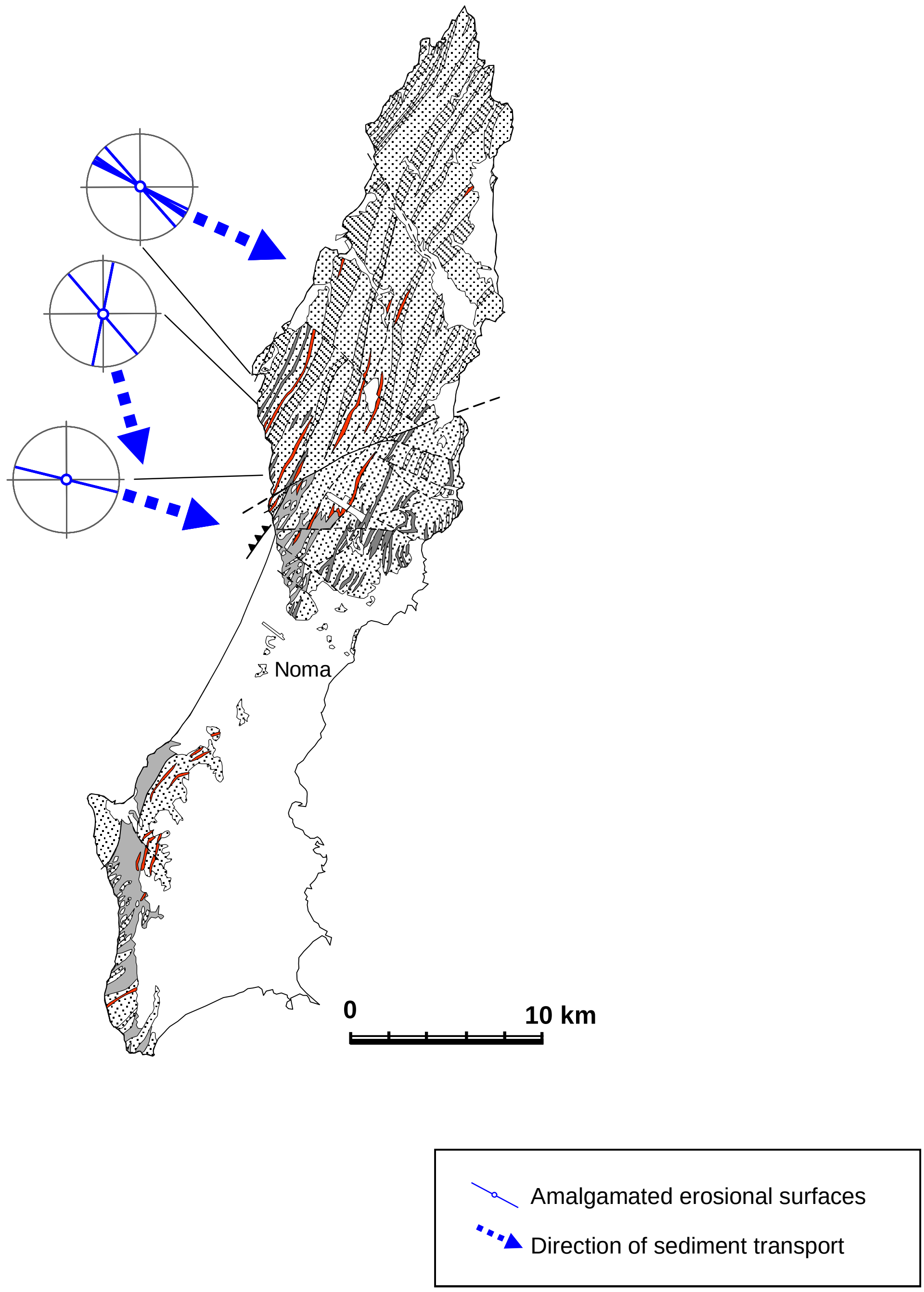

Fig.3.3.2 Paleocurrent directions inferred from channel structures in channel and channel-lobe facies associations of the Kumage Complex.

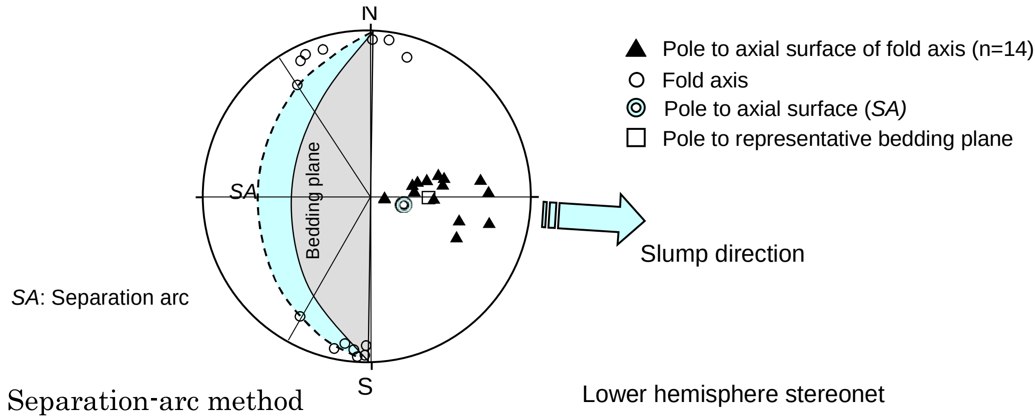

1: Slump direction of the Kumage Complex in the Azakou area.

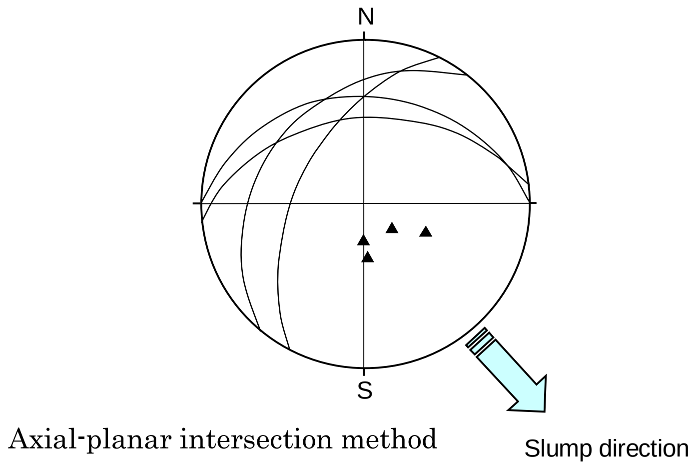

2: Slump direction of the Kadokurazaki Complex around the quarry in the eastern part of airport.

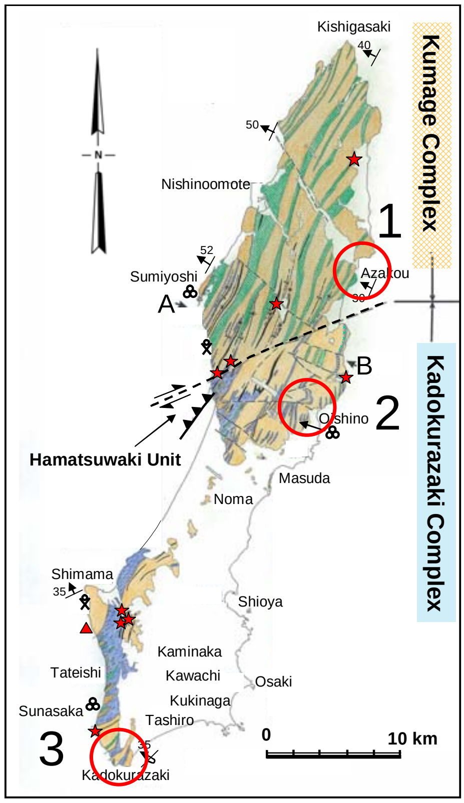

Locality map

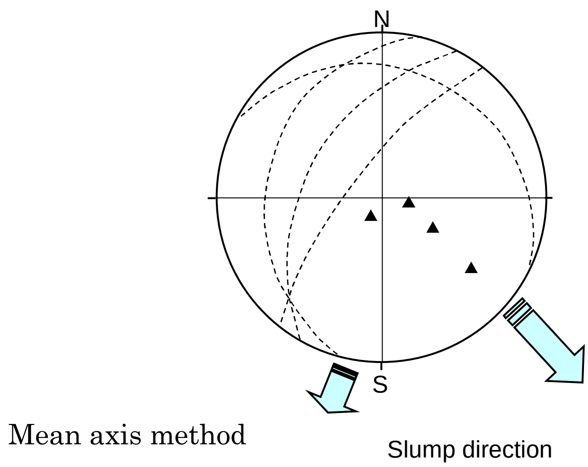

3. Slump direction of the Kadokurazaki Cmplex around Kadokurazaki fishing port.

Fig.3.3.3 Analysis of slump folds. Slump directions (large arrows) inferred form the Kumage and the Kadokurazaki Complexes.

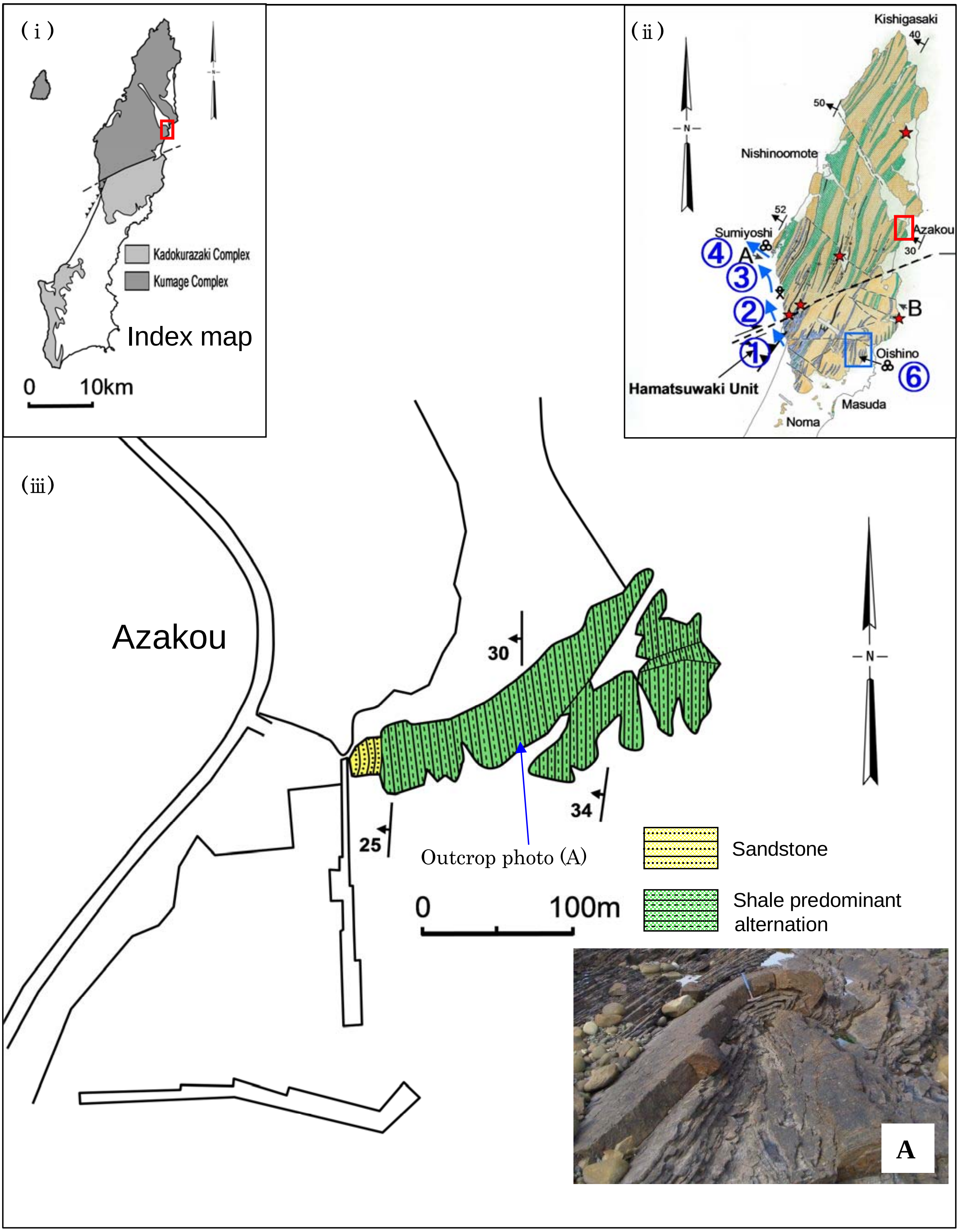

Fig.3.3.4 Geologic sketch map showing the slump zone of the Kumage Complex at the coast of Azakou. Outcrop photo (A) shows slump fold. (i) and (ii) : Index for the area investigated, (iii): Rout map of the slump zone. The location of photo (A) is also shown in Fig.3.1.13.

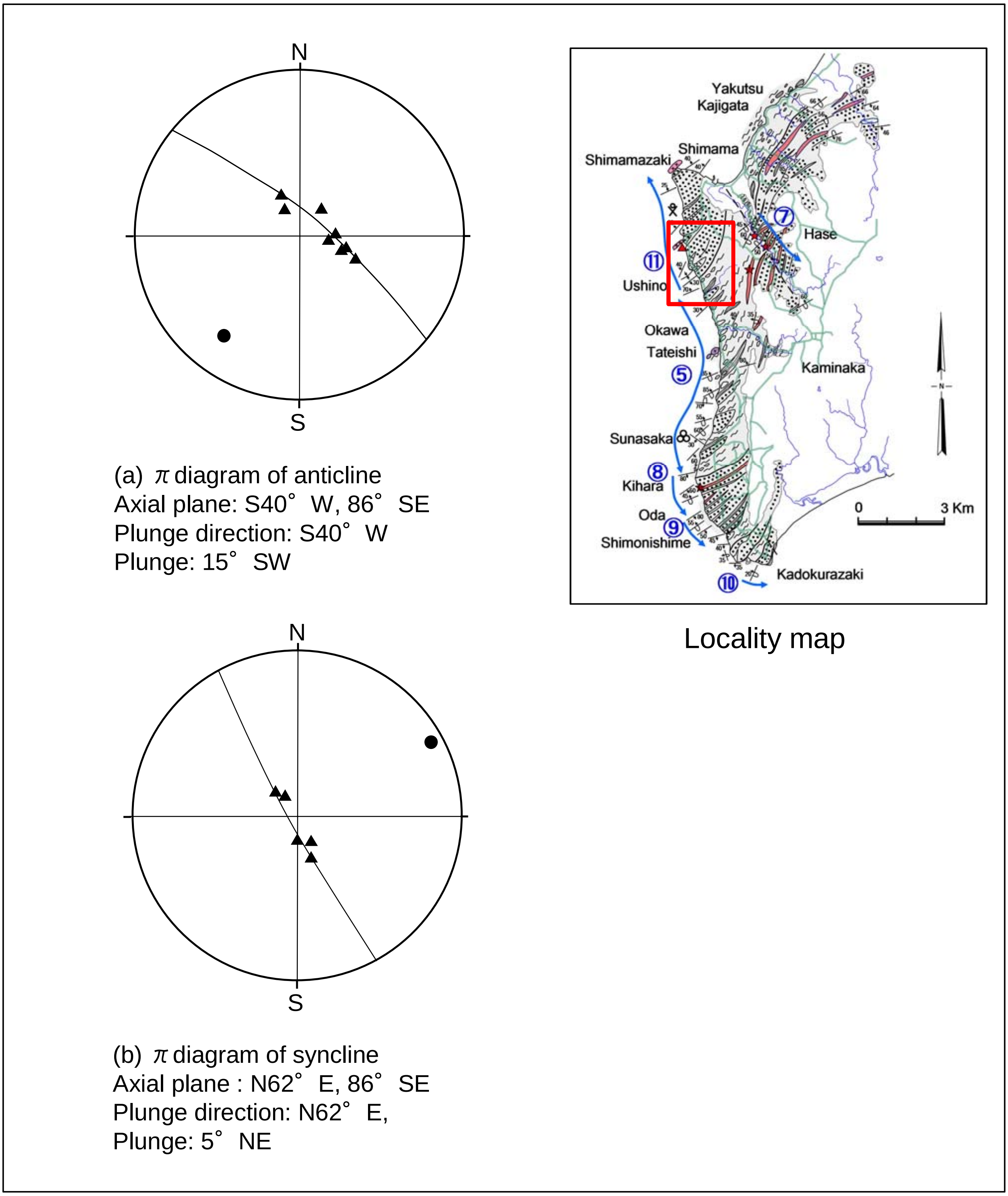

Fig.3.3.5 Lower hemisphere projection of fold data showing the orientation of fold axes of anticline (a) and syncline (b) in the lower part of the Shimama Olistolith (Section ⑪). Black small triangles and circles stand for bedding planes and fold axes respectively.

4. Microfossil evidence and fission-track age

The Southern Shimanto Belt is generally unfossiliferous in spite of the abundance of trace fossils. The fossil records that have been reported so far are a few specimens of molluscs (Hyayasaka *et al*., 1980) and radiolarian fossils obtained at the some regions of Tanegashima and Yakusima (Okada *et al*., 1982; Kuwazuru & Nagatsu, 2007; Saito *et al*, 2007). The radiolarian fossils have been extracted from the variegated shale intercalated with the turbidite sequences and the fossil assemblages range in age from Middle Eocene to Early Oligocene.

In this study, the planktonic foraminifera have been extracted to clarify the age for the uppermost part of the Kumage Complex. As a result, this study could provide a new age assigned to Early Miocene.

4.1 Radiolarian fossils

Tanegashima

The radiolarian fossils shown in Tables 1 and 2 of the Appendix have been previously reported from the Southern Shimanto Belt in Tanegashima (Okada *et al*., 1982; Kuwazru & Nagatsu, 2007).

According to Okada *et al*. (1982), the turbidite sequence is accompanied subordinately by variegated shale which distributed in the middle and south part of Tanegashima, and yields abundant remains of radiolarians (Table 1 in the Appendix). The sequence belongs to the Kadokuraszaki Complex, and the strata distributed around Hamatuwaki and Furuta in the middle part of the island are correlated with the Kumage Complex in this study.

The radiolarian assemblages occurred in the Kadokurazaki Complex was assigned to the *Thyrsocyrtis triacantha* Zone and the *T. bromia* Zone, indicating Middle to Late Eocene in age. The radiolarian assemblage from the equivalent to the Kumage Complex is the *Theocotyle ficus* Zone, indicating Middle to Late Eocene in age.

Kuwazuru & Nagatsu (2007) reported that the radiolarian fossils obtained from the variegated shale of Kadokurazaki Complex which exposed at the coast of Nishinokihara in the south of the island, and from the variegated shale of the Kumage Complex around Okinohamada in the northern part of the island (Table 2 in the Appendix).

The variegated shale of Kazokurazaki Complex in Nishinokihara yields the radiolarian fossil *Theocampe* cf. *mongolfieri* (Ehrenberg) indicating Middle Eocene to early Early Oligocene in age. On the other hand, the variegated shale of Kumage Complex in Okinohamada also yields the radiolarian fossil *Theocyrtis tuberosa* Riedel indicating late Late Eocene to early Late Oligocene in age.

Yakushima

As shown in Fig.12 and Table 3 in the Appendix, the red shale in the Kadokurazaki Complex near Anbo northeast of Yakushima, yields radiolarian fossils such as *Dictyoprora mongolfieri*, *Theocyrtis* cf. *perpumila* and *Calocycloma* cf. *ampulla* indicating Middle to early Late Eocene (Saito *et al*., 2007). *Dictyoprora mongolfieri* can be assigned to early Middle Eocene to Early Oligocene, and it has been reported from the Kumage Complex in Tanegashma by Okada *et al*. (1982).

Considering the radiolarian fossils which had been obtained from the chaotic complex, however, the red shale of Yakushima bearing the radiolarian fossils were derived from the Kumage Complex.

4.2 Planktonic foraminifera

Treatment of samples

The extraction of the foraminifera was carried out by HF (5%) method on 111 samples collected from the Kumage and Kadokurazaki Complexes in the middle and southern part of Tanegashima. Each sample of muddy rocks was 1.5-2.0kg in weight.

After washing through an 80-mesh and a 200-mesh screen, all the planktonic and benthic foraminiferal specimens were picked up from the washed residues. The preservation of fossil was not good in general due to diagenetic effect. Therefore, well-preserved specimens of the foraminifera have been further extracted by means of NaTPB (sodium tetraphenylborate).

As a result of the above-mentioned extraction work, the identifiable planktonic foraminiferal specimens (Table 4.2.1) were obtained from three localities: Sumiyoshi, eastern area of airport and Sunasaka (Fig.4.2.1).

The planktonic foraminifera obtained from each area are described as follows:

(1) Sumiyoshi area

Geological setting

The strata of the Sumiyoshi area (Section ④) are placed on the uppermost part of the stratigraphic horizon in the Kumage Complex. The turbidite sequences are composed of the intermediate to coarse-grained sandstone beds with subordinate shale and alternating beds of sandstone and shale.

The geological structure shows an anticline, which hinge line plunges 40-50° in NE direction. The dark grey shale and bluish grey shale near the fold axis yield the following planktonic foraminifera remains (Fig. 4.2.1).

Globoquadrina venezuelana (Hedberg)
Globigerinoides cf. *subquadratus* Broennimann
Dentoglobigerina larmeui (Akers)

Catapsydrax dissimilis (Cushman and Bermudez)
Catapsydrax unicavus Bolli, Loeblich and Tappan
Catapsydrax spp
Dentoglobigerina spp.

This foraminiferal assemblage suggests that these strata are assigned to Early Miocene in age. The last occurrence of *Catapsydrax dissimilis* (Cushman and Bermudez) (Fig.4.2.2) defines N6/N7 boundary (Blow, 1969). Therefore, these strata are older than ca.17.5 Ma.

(2) Eastern area of airport (Oishino)

Geological setting

This area is characterized by large slump sheets belonging to the Kadokurazaki Complex (Section ⑥). The planktonic foraminifera remains were obtained from three sites: E-04, E-05a and E-06) (Figs.3.2.4 and 4.2.1).

The specimen number E-04 was collected from the muddy rocks of the shale predominant alternation characterized by the thin turbidite sequence of the lower unit (Fig.6 in the Appendix). The specimen number E-05a was collected from the grey colored mudstone with black colored shale fragments, and shows a body of mud diapirs. The specimen number E-06 was collected from the dark grey shale which was intercalated in the thick-bedded sandstone showing slump structure.

E-04:

Globoquadrina venezuelana (Hedberg)

E-05a:

Globigerinoides quadrilobatus (d'Orbigny)
Globoquadrina venezuelana (Hedberg)
Dentoglobigerina larmeui (Akers)

The joint occurrence of these species indicates an Early Miocene age.

E-06:

Paragloborotalia nana (Bolli)

The occurrence of this species ranges from Oligocene to

Early Miocene in age.

(3) Sunasaka area

Geological setting

This area is located at the northern side of Sunasaka fishing port in the southern part of Tanegashima where the Kadokurazaki Complex is distributed broadly (Fig.4.2.1). The strata show the block-in-matrix fabrics which are composed of many angular clasts of sandstone and shale, ranging in size from a few centimeters to several ten meters. The matrix of the olistostrome is characterized by scaly cleavage.

009061803a:

Globigerinoides cf. *quadrilobatus*

The first appearance of this species has been since the Miocene.

009061803b:

Globigerina praebulloides
Catapsydrax dissimilis (Cushman and Bermudez)
Catapsydrax unicavus Bolli, Loeblich and Tappan
Dentoglobigerina altispira
Dentoglobigerina larmeui (Akers)
Globigerinoides trilobus
Globoquadrina venezuelana
Globoturborotalita cf. obliquus
Globoturborotalita woodi
Paragloborotalia sp.

This fomraminiferal assemblage is assigned to Early Miocene. Because of the occurrence of *Catapsydrax dissimilis* (Cushman and Bermudez, 1937) (Fig4.2.2), these strata are older than ca.17.5 Ma. In addition, the first occurrence of *Globigerinoides trilobus* (Fig.4.2.2) has been since ca.23Ma.

009061803b’:

Catapsydrax unicavus Bolli, Loeblich and Tappan
Catapsydrax spp.
Globigerinita glutinata (Egger)

The joint occurrence of these species is assigned to Late Oligocene to Early Miocene in age.

As mentioned above, it was clarified that the planktonic foraminiferal faunas obtained from the Sumiyoshi Unit (Section ④) of the Kumage Complex and the chaotic rocks (Section ⑤) of the Kadokurazaki Complex represent zone N.4-N.6 as summary in Fig.4.2.3.

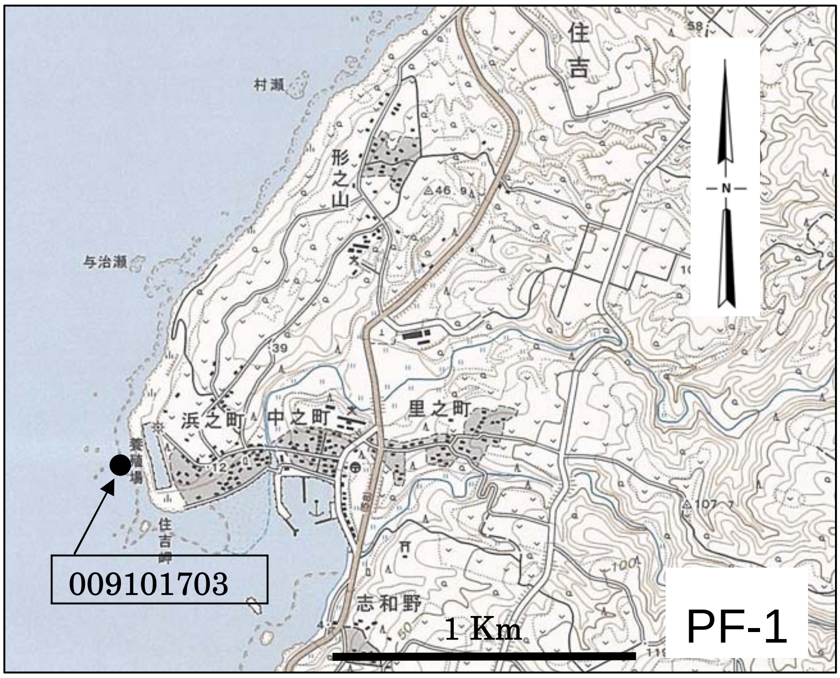

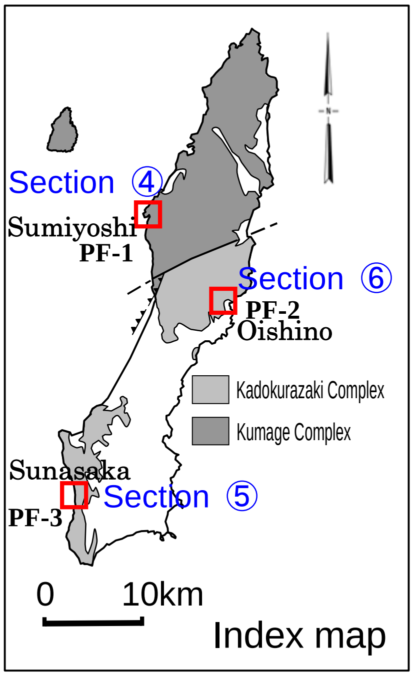

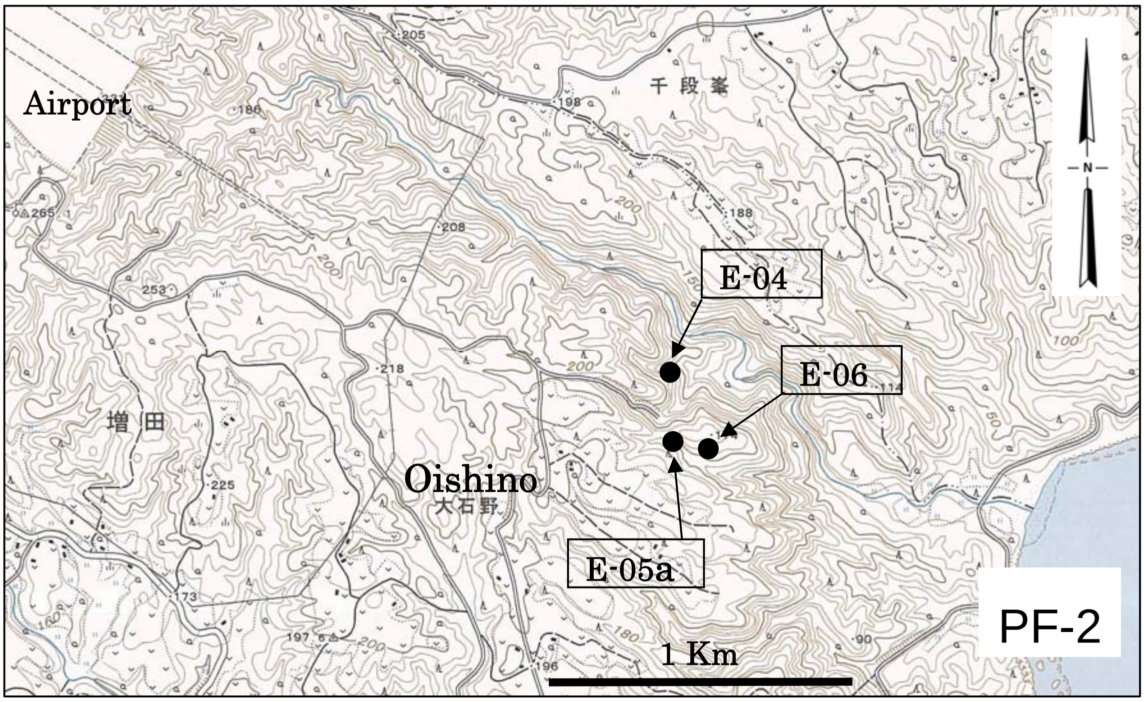

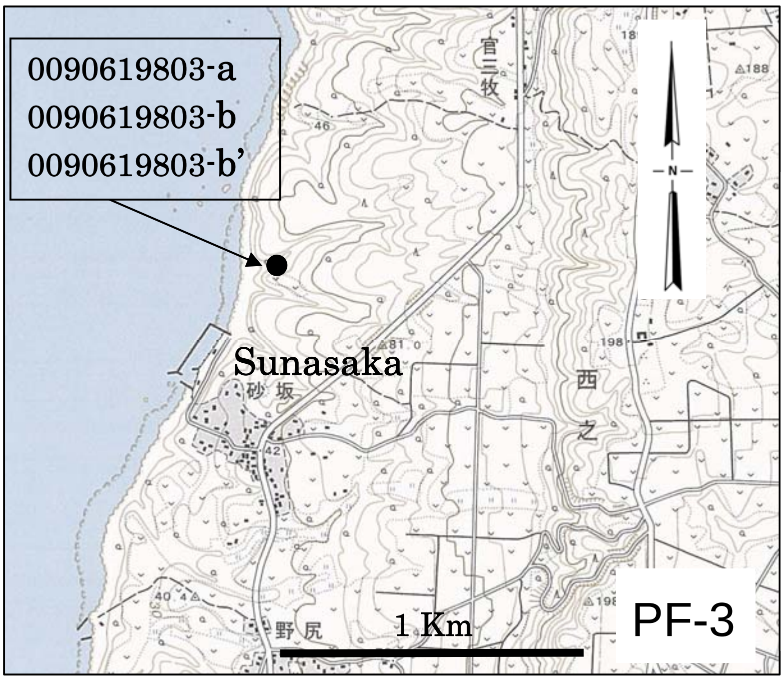

Fig.4.2.1 Map showing locations of samples for planktonic foraminiferal studies.

The topographic maps "Nishinoomote","Hamatuwaki" ,and "Kadokurazaki" (scale 1:25,000) published by the Geographical Survey Institute.

Table 4.2.1 List of planktonic foraminifera from the Kumage and Kadokurazaki Complexes. (Identified by Dr. Hayashi, Shimane University)

Tanegashima							
Complex	**Kumage Complex**	**Kadokurazaki Complex**					
Locality No.	**PF-1(Sec. ④)**	**PF-2 (Sec. ⑥)**			**PF-3 (Sec. ⑤)**		
Specimen No.	**00910 1703**	**E-04**	**E-05 a**	**E-06**	**00906 1803a**	**00906 1803b**	**00906 1803b'**
Globigerina praebulloides						●	
Catapsydrax dissimilis (Cushman and Bermudez)	●					●	
Catapsydrax unicavus Bolli, Loeblich and Tappan	●					●	●
Catapsydrax spp.	●						●
Globigerinita glutinata (Egger)							●
Dentoglobigerina altispira						●	
Dentoglobigerina larmeui (Akers)	●		●			●	
Dentoglobigerina spp.	●						
Globigerinoides trilobus						●	
Globigerinoides quadrilobatus (d'Orbigny)			●				
G. cf. *quadrilobatus*					●		
Globigerinoides cf. *subquadratus* Broennimann	●						
Globoquadrina venezuelana (Hedberg)	●						
Globoquadrina venezuelana		●	●			●	
Globoturborotalita cf. *obliquus*						●	
Globoturborotalita woodi						●	
Paragloborotalia nana (Bolli)				●			
Paragloborotalia sp.						●	
Age	**Early Mioc. (Older than an age of ca.17.5Ma)**	**—**	**Early Mioc.**	**Oligoc. - Early Mioc.**	**Since the Mioc.**	**Early Mioc. (N.4-N.6) (Older than an age of ca.17.5Ma)**	**Late Oligoc. - Early Mioc.**

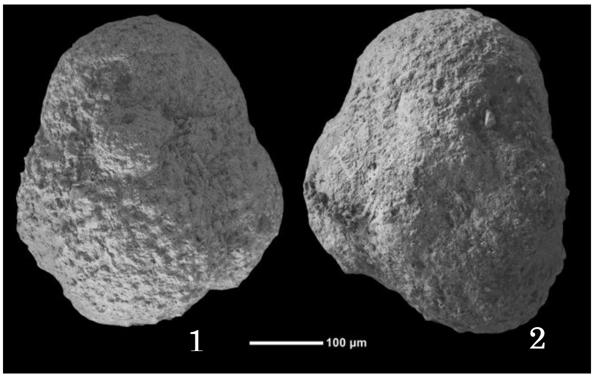

1-2: *Catapsydrax dissimillis* (Cushman and Bermudez), umbilical and spiral side views; Sample 009101703, Sumiyoshi. Kumage Complex.

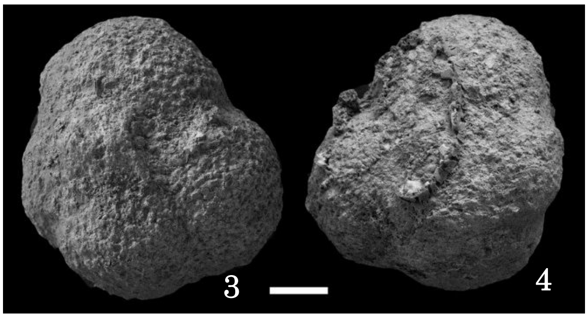

3-4: *Catapsydrax dissimilis*, umbilical and spiral side views; Sample 009061803b, Sunasaka, Kadokurazaki Complex.

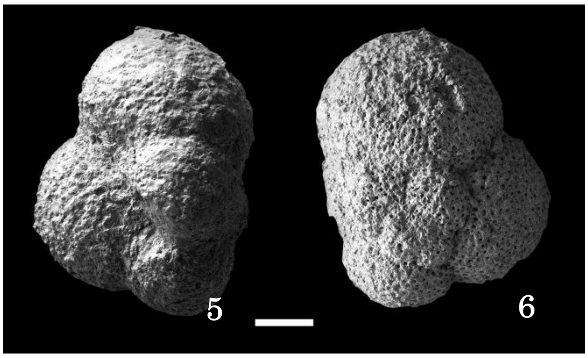

5-6: Catapsydrax unicavus, umbilical and spiral side views; Sample 009061803b, Sunasaka, Kadokurazaki Complex.

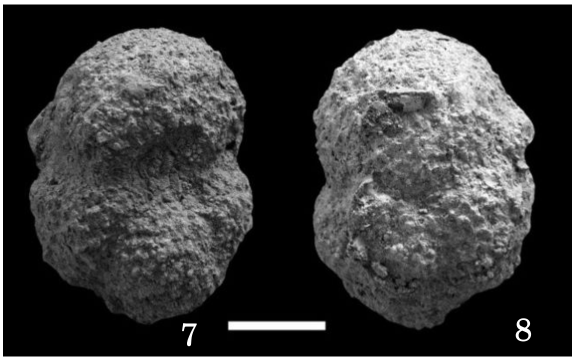

7-8: *Globoturborotalita woodi*, umbilical and spiral side views; Sample 009061803b, Sunasaka, Kadokurazaki Complex.

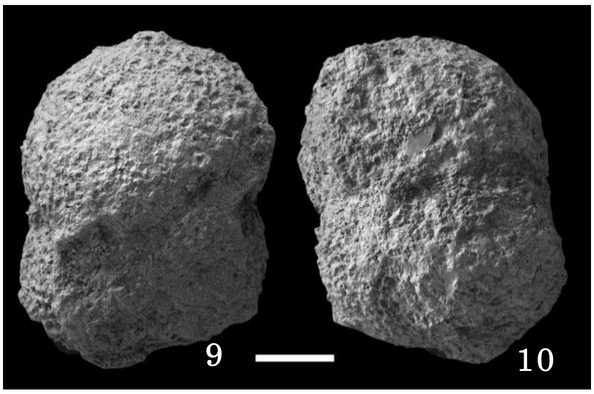

9-10: *Globigerinoides trilobus*, umbilical and spiral side views; Sample 009061803b, Sunasaka, Kadokurazaki Complex.

Scale bar 100 µm

Fig.4.2.2 Micrographs of planktonic foraminifera from the Kumage and Kadokurazaki Complexes in Tanegashima.

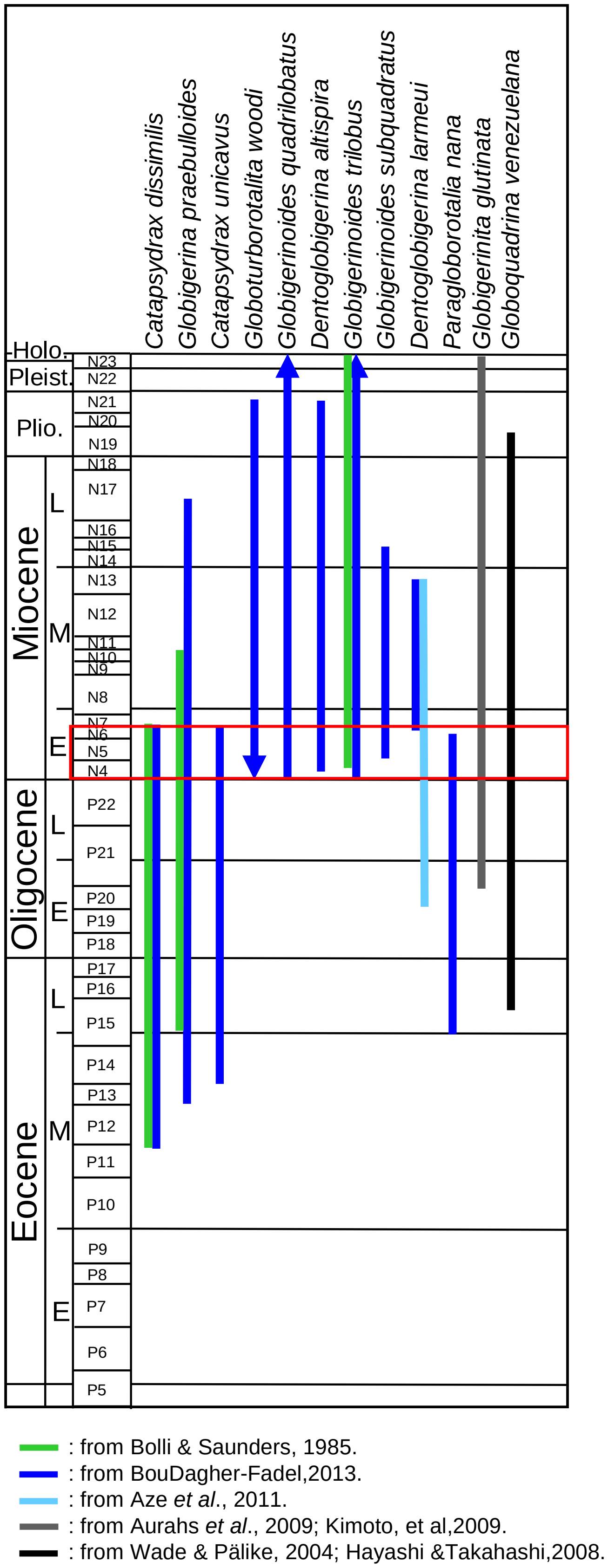

Fig.4.2.3 Biostratigraphic distributions of planktonic foraminifera from the Kumage and Kadokurazaki Complexes.

4.3 Benthic foraminifera

The benthic foraminifera are used to presume a water depth, though they are not available for determining of the geological age. Well preserved benthic foraminiferal specimens were obtained from the variegated shale which is distributed in the northwestern part of Kaminaka and in the Fruta area (Fig.4.3.1). The planktonic foraminiferal fossils were rarely found from these strata.

Variegated shale of Middle to Late Eocene in the northwestern part of Kaminaka belongs to the Kadokurazaki Complex. On the other hand, similar shale of the Kumage Complex in the Furuta area, the northern part of Tanegashiam, yields the radiolarian fossils that can be assigned to Middle Eocene-early Early Oligocene.

(1) Western part of Kaminaka

Figs.4.3.1, 4.3.2, 4.3.3 and 4.3.4 show sampling sites, their stratigraphic positions and outcrop phots of the variegated shale, respectively. The obtained agglutinated benthic foraminiferal fossils are as follows:

Ammodiscus sp.
Haplophragmoides sp.
Alveolophragmium sp.
Trochammina sp.
Cyclammina sp.
Glomospira goldials
Glomospira charoides
Bathysiphon sp.

(2) Furuta area

The obtained benthic foraminiferal specimens are as follows:

Ammodiscus sp.
Trochammina sp.
Cyclammina sp
Glomospira charoides

The relative abundance of benthic foraminifera in these areas is shown in Tables 4.3.1-4.3.3 and Fig.4.3.5. These assemblages are almost agglutinated species, but no calcareous foraminifera are found in these strata. Due to the abundant occurrence of these agglutinated specimens, the variegated shale was deposited below the calcite compensation depth (CCD) in the basin. The *Glomospira* sp. of the recent foraminifera occurs at the depth from about 5,000 to 5,500m in the north Philippine Sea (Akimoto, 1990, 1996; Inoue, 1989) (Fig.13 in the Appendix).

(3) Deep-sea benthic foraminiferal assemblage of the Southern Shimanto Belt

Although the benthic foraminiferal remains from the Southern Shimanto Belt are less well documented, they have been studied previously in four regions as follows.

Wano formation in Amami-Oshima

Aoyagi & Inoue (1979) obtained the benthic foraminifera from the Eocene dark grey shale and they argued that the Wano Formation was deposited in bathyal to neritic environment based on the following benthic foraminiferal assemblage.

Trochammina sp. indet.
Cyclammina cf. *pusilla* Brady
Glomospira sp. indet.
Bathysiphon eocenica Cushman & Hanna
Bolivinopsis cf. *ichodaensis* Asano & Murata
Silicosigmoilina sakasegawaensis (Asano & Murata)

Nichinan Group in Osumi Peninsula

The following benthic foraminifera and some planktonic foraminifera have been extracted from the Eocene variegated shale (Kuwano, 1960).

Ammodiscus sp.
Cyclammina sp.
Trochammina sp. indet.

Silicosigmoilina calfornica Cushman & Hanna

Glomospira charoides

Tashiro lower subunit of the Hyuga Group in East Kyushu

The following benthic foraminifera and abundant planktonic foraminifera have been extracted from the Middle Eocene-Early Oligocene muddy rocks of the Tashiro Formation which is composed mainly of massive mudstone (Nishi, 1987, 1988).

Bathysiphon sp.

Cyclammina sp.

Silicosigmoilina sp.

Pullenia bulloides (d'Orbigny)

Stilostomella sp.

Uvigerina sp.

Nishi (1987, 1988) concluded that the benthic foraminifera, scanty occurrence of calcareous microfossils in claystones and *Nereites* ichnofacies of crawling and grazing types from the Tashiro Fromation suggested deposition at depths greater than the bathyal zone.

Setogawa Group in Shizuoka

The Early Miocene tuffaceous mudstone of the Setogawa Group yields the following benthic foraminiferal fossil assemblage (Kitazato, 1980).

Glomospra sp

Reophax sp.

Cyclammina sp.

Ammodiscus sp.

Haplophragmoides spp.

Bathysiphon sp.

Tolypammina sp.

Lituotuba sp.

Kitazato (1980) presumed that most of the species of this assemblage now live in deep sea, below 3000m, in modern Pacific Ocean suggesting that the deposition took place on the similar deep sea floor.

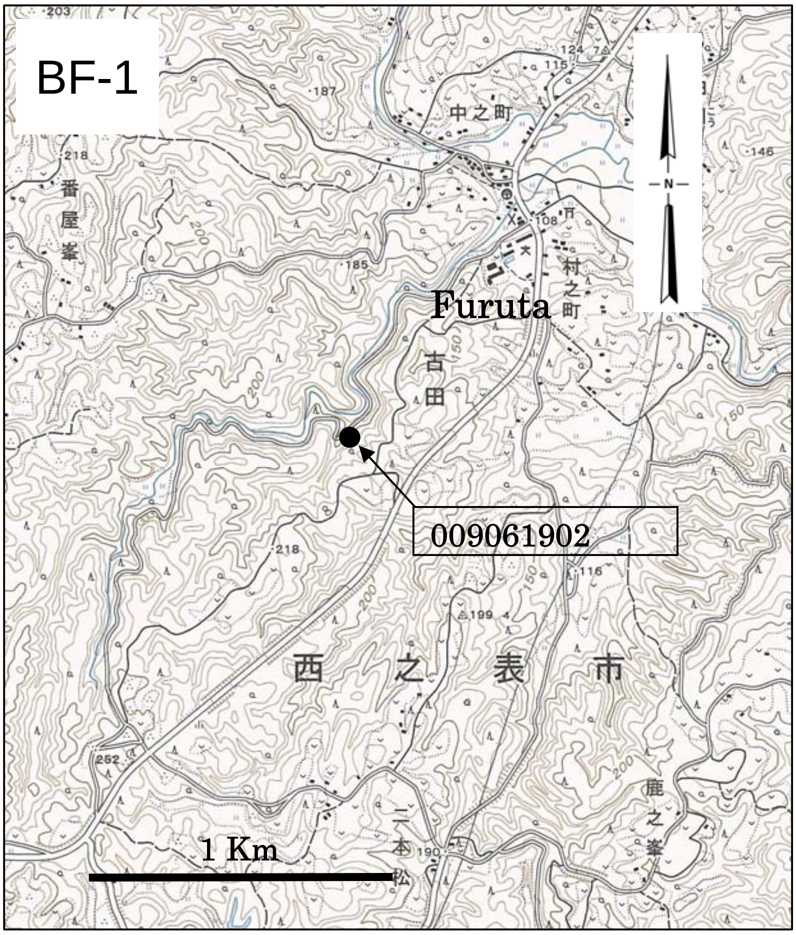

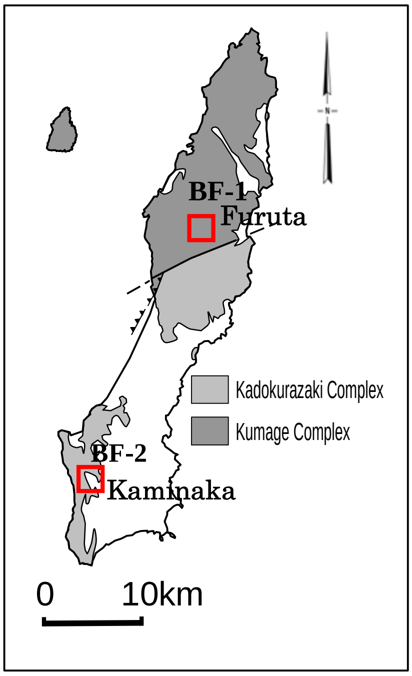

Index map

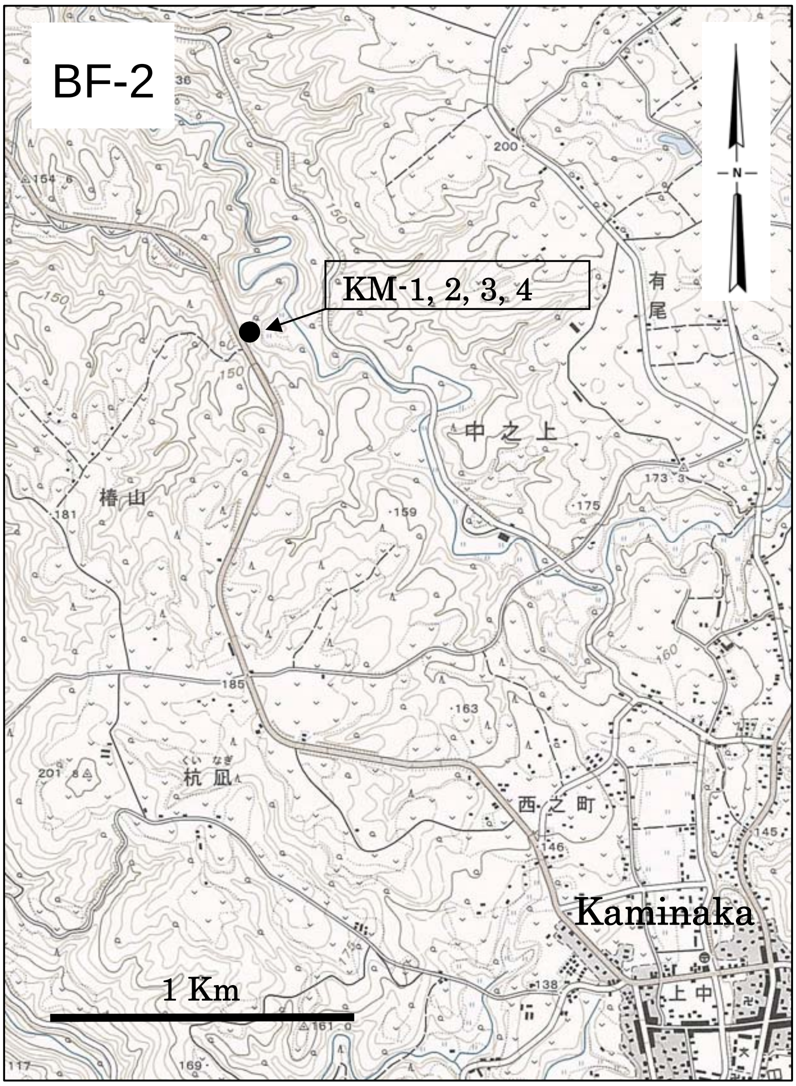

Fig.4.3.1 Map showing locations of samples for benthic foraminiferal studies.

The topographic maps “Hamatuwaki”,and “Kadokurazaki” (scale 1:25,000) published by the Geographical Survey. Institute.

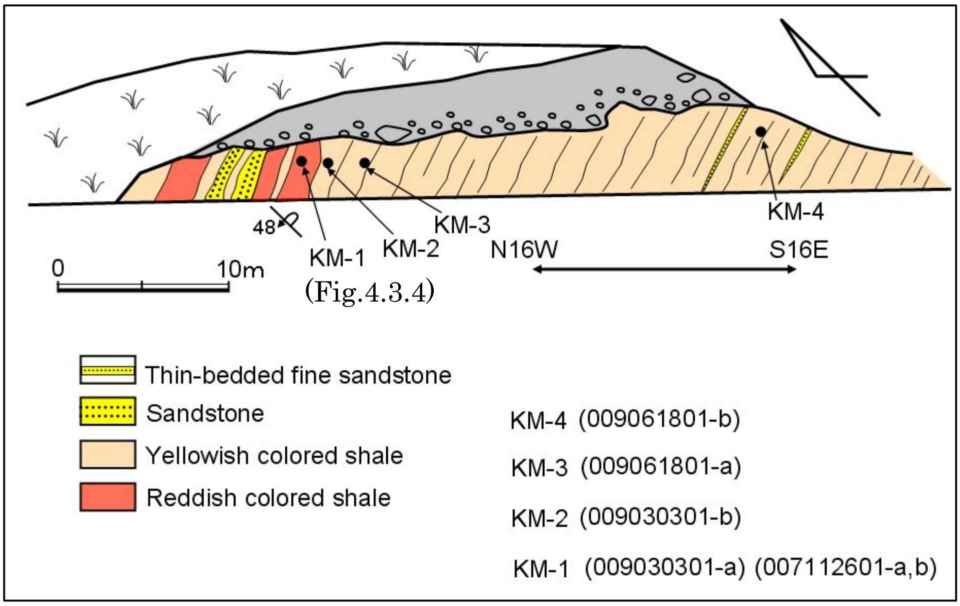

Fig.4.3.2 Sketch showing the road-cut exposure of the variegated shale and location of samples. See the location in Figs.3.1.13 and 4.3.1.

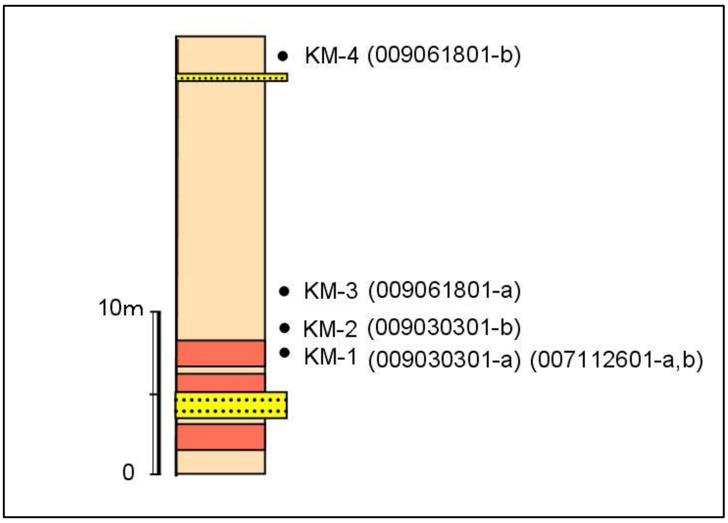

Fig.4.3.3 Columnar section of the variegated shale and sample horizons.

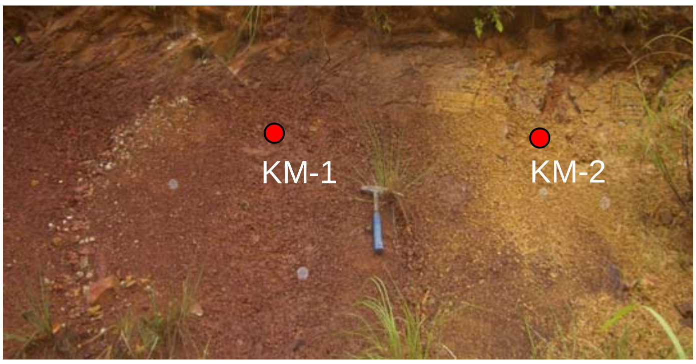

Fig.4.3.4 Outcrop photos of the variegated shale in the western part of Kaminaka. This variegated shale yields the abundant benthic foraminifera and radiolarians indicating Middle to Late Eocene in age. The location is shown in Figs.3.1.13, 4.3.1 and 4.3.2.

Table 4.3.1 Benthic foraminiferal assemblages from the red shale in the Kaminaka area. Sample number: KM-1 (009030301-a).

NO.	Species	Number of specimens	%
1	*Cyclammina ezoensis* Asano	41	25.8%
2	*Cyclammina cancellata* Brady	4	2.5%
4	*Haplophragmoides* sp.	3	1.9%
5	*Trochammina* sp.	1	0.6%
6	*Glomospira charoides* (Jones and Parker)	3	1.9%
7	*Glomospira gordialis* (Jones and Parker)	25	15.7%
8	*Ammodiscus* sp.	18	11.3%
9	*Bathysiphon* sp.	64	40.3%
		159	100.0%

Table 4.3.2 Benthic foraminiferal assemblages from the yellow shale in the Kaminaka area. Sample number: KM-2 (009030301-b).

NO.	Species	Number of specimens	%
1	*Cyclammina ezoensis* Asano	10	10.1%
3	*Alveolophragmium subglobosum*	2	2.0%
4	*Haplophragmoides* sp.	6	6.1%
6	*Glomospira charoides* (Jones and Parker)	12	12.1%
7	*Glomospira gordialis* (Jones and Parker)	4	4.0%
9	*Bathysiphon* sp.	65	65.7%
		99	100.0%

Table 4.3.3 Benthic foraminiferal assemblages from the yellow shale in the Furuta area. Sample number: 009061902.

NO.	Species	Number of specimens	%
1	*Cyclammina ezoensis* Asano	5	2.1%
5	*Trochammina* globigerinaformis	13	5.5%
9	*Bathysiphon* sp.	45	19.0%
10	*Agglutinated foraminefera* gen. et. sp. indet.	174	73.4%
		237	100.0%

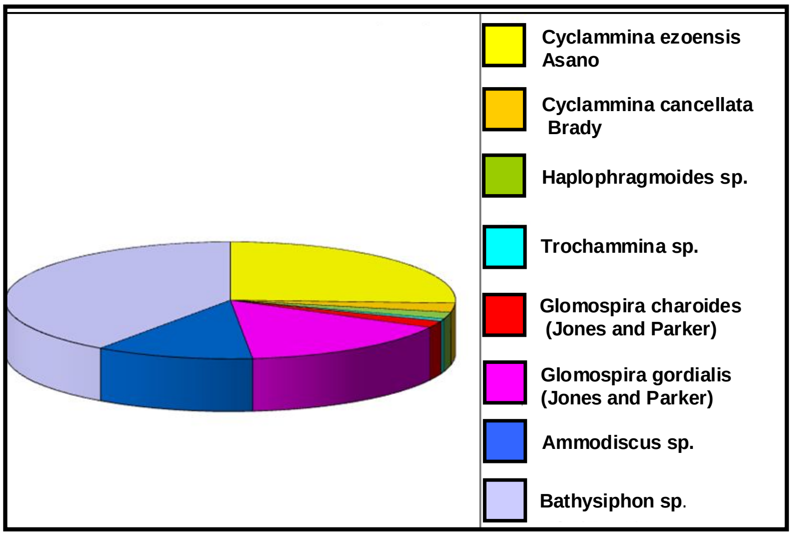

A: Reddish shale in the northwest of Kaminaka (KM-1; 009030301-a)

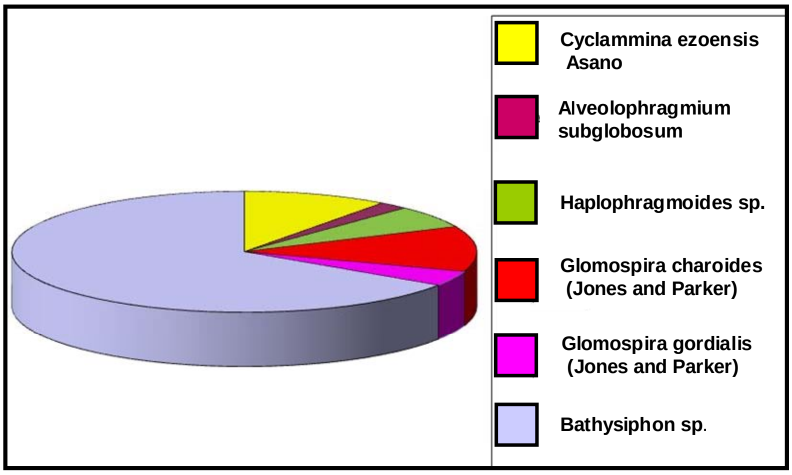

B: Yellowish shale in the northwest of Kaminaka (KM-2; 009030301-b)

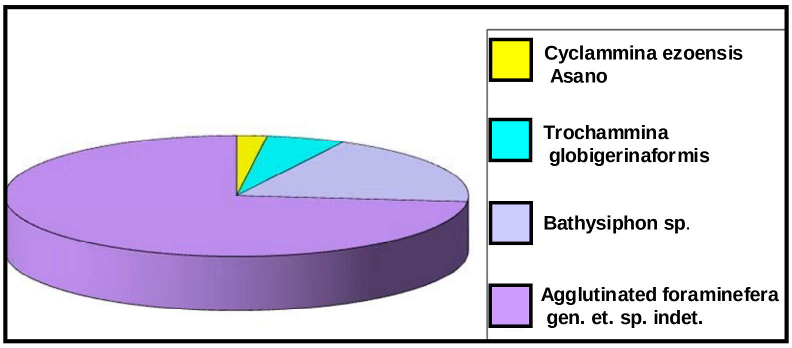

C: Yellowish shale in the southwest of Furuta (009061902)

Fig.4.3.5 Percent abundance of benthic foraminifers in variegated shale. See the locations of samples in Figs.4.3.1, 4.3.2 and 4.3.3.

4.4 Fission-track dating

In this study, zircon fission-track age was measured on the tuffaceous sandstone collected from the lower part of the Shimama Olistolith (Section ⑪) (Fig.4.1.1). This rock consists of pale greenish gray colored fragile small particles (Fig.14 in the Appendix). The mineral composition shows an appearance of glassy detritus as a whole always as well as quartz, plagioclase and iron minerals. Alteration of all colored minerals and the groundmass are considerably progressed.

The fission-track age determination was done by Geochronology Japan Inc., Osaka, Japan. The experimental method and processing are explained in the flowchart of Fig. 4.4.2. The fission-age obtained from the tuffaceous sandstione is 48.9 ± 4.1 Ma as shown in Table 4.4.1.

(1) Method

Fission-track dating was carried out by the External-surface Internal-detector (muscovite) method (ESID) (Daishi *et al*., 1986; Daishi, 1989). This Grain-by-Grain dating method generally uses on a sample which has spontaneous track density and induced tracks can be counted on the same plain of zircon.

The experimental procedure and condition of the fission-track age determination are different in each experimenter. In this experiment, the methods and conditions are adopted as follows.

Separation and selection of zircon crystals

A proper weight (5-10kg) of the rock sample was shattered with a crusher and then pulverized sample was sieved through 48-200 meshes. Heavy mineral grains were concentrated by panning, and were separated using Hallimond's magnetic separator. Selected heavy mineral grains were passed through a bromoform heavy liquid (specific gravity of 2.85). The weak magnetic minerals were eliminated by isodynamic-separator. Selected samples were heated in hydrofluoric acid which added few drops of H_2O and H_2SO_4 to resolve silica minerals.

Selected zircon grains which may be contaminated with iron oxide, were boiled in dilute hydrochloric acid. The uranium content varies greatly in proportion of form and particle size of crystals, and therefore, the zircon grains were selected in accordance with the similar form and diameter. The deeper colored zircon grains were hand-picked out to prevent mixing with other color crystals.

Etching

The selected 50 grains of zircon were mounted on the polyhexafluoroethylene (teflon hexafluoride) sheet and each crystal plains of zircon were cleaned using a DP-cloth without diamond-paste. The zircon grains were etched for 25 hours in eutectic mixture of 50.6 mol% of KOH and 49.4 mol% of NaOH (Gleadow *et al*., 1976) at 220 ± 1°C. Muscovite, external detector was etched for 60 minutes in 48% of HF kept at 25°C in constant-temperature water bath.

Neutron irradiation

The muscovite external detector was attached to the zircons in order to check the induced track density. In the same way the muscovite detector was attached to the standard glass (NBS SRM-913) to monitor neutron dose. They are put together in a capsule, and thermal neutrons were irradiated for 10 minutes in the rotation specimen rack of the McMaster University nuclear reactor.

Thermal neutron dose was determined by the muscovite as an external detector attached to the standard glass, and thermal neutron dose φ is expressed by the following formula.

$$\varphi = \varphi_k \times \rho_u / \rho_k$$

where

φ_k= thermal neutron dose of standard glass irradiated at NBS nuclear reactor

ρ_u= track density of muscovite attached to standard glass irradiated with sample

ρ_k= track density of muscovite attached to standard glass which irradiated at NBS nuclear reactor

Counting of tracks

Fission-track counting was carried out with an optical microscope under 1000× magnification. These tracks were counted in the 2π geometry field except for the area with inclusions and the part damaged by etching.

Numerical formula of the fission-track dating

The following expression was obtained when the constants are substituted into the fission-track dating numerical formula proposed by Price & Walker (1963).

For example, the ^{238}U fission-track decay constant is generally taken as 8.30×10^{-17}/yr.

$$Age = 6.45 \times 10^{9} \times ln\ (1 + 7.68 \times 10^{-18} \times \Phi \times \rho_s / \rho_i)$$

where

Φ= the thermal neutron dose received in the nuclear reactor ($n \cdot cm^{-2}$)

ρ_s= the measured spontaneous track density of ^{238}U

ρ_i= the measured induced track density o$^{f\ 235}U$

The calculation using the above mentioned methods were statistically verified by F-value (actual variance / expected variance) (Hayashi & Sugiyama, 1987) and P I (precision index) statistics (Hayashi & Fujii, 1985).

The following equation included the 'Zeta' calibration method (Hurford & Green, 1983) is used as the standard means to determine the fission-track ages.

$$A = 1 / \lambda_D \times ln\ (1 + \lambda_D \times \zeta \times \rho_s / \rho_i \times \rho_u)$$

where

λ_D : the decay constant of ^{238}U (1.55125×10^{-10} year^{-1}) (Jaffey *et al.*, 1971)

ζ: the value of zeta (ζ is 323±5 when the NBS-612 standard glass was used at the McMater University nuclear reactor.)

(2) Result

Table 4.1.1 shows the fission-track age. The dating of 50 zircon grains obtained from the sample was carried out by the above-mentioned method, whereas 35 grains of those were unable to measure due to high density of spontaneous tracks of ^{238}U.

Fission-track age measurements on the 15 zircon grains give the age of 48.9±4.1Ma, and these grains were considered to be essential grains tested by F-value and P I statistics.

Table 4.1.1 Fission-track ages of zircon

Sample No.	Spontaneous track number	Spontaneous track density $\times 10^6 cm^{-2}$	Induced track number	Induced track density $\times 10^6 cm^{-2}$	Thermal[*1] neutron dose $\times 10^{14} cm^{-2}$	F[*2]	PI[*3]	Number of grains	Age[*4] and std. error (Ma)	Relative std. error (%)	Method[*5]	ID
007SH01	739	4.5061 ± 0.1658	226	1.3780 ± 0.0917	3.03 ± 0.11	0.55	81	15	**48.9 ± 4.12**	8.4	ESED	D1401010

[*1] thermal neutron dose $\varphi = \varphi k \times \rho u / \rho k$
φk : thermal neutron dose of standard glass (NBS SRM-913) irradiated at NBS nuclear reactor
$= 4.75 \pm 0.05 \ (\times 10^{14} cm^{-2})$
ρu : track density of muscovite attached to standard glass irradiated with sample
$= 5.645 \times 10^4 cm^{-2}$ = 1694 tracks / $3.0 \times 10^{-2} cm^2$
ρk : track density of muscovite attached to standard glass which irradiated at NBS nuclear reactor
$= 8.850 \times 10^4 cm^{-2}$ = 2655 tracks / $3.0 \times 10^{-2} cm^2$

[*2] F, F value, Hayashi and Sugiyama, 1987

[*3] PI, precision index, Hayashi and Fujii, 1985

[*4] Age $= 6.45 \times 10^9 \, ln\,(1 + 7.68 \times 10^{-18} \times \varphi \times \rho s / \rho i)$
ρs = spontaneous track density of ^{238}U
ρi = induced track density of ^{235}U

[*5] ESED, External-Surface External-Detector method (Daishi *et al*., 1986; Daishi, 1989)

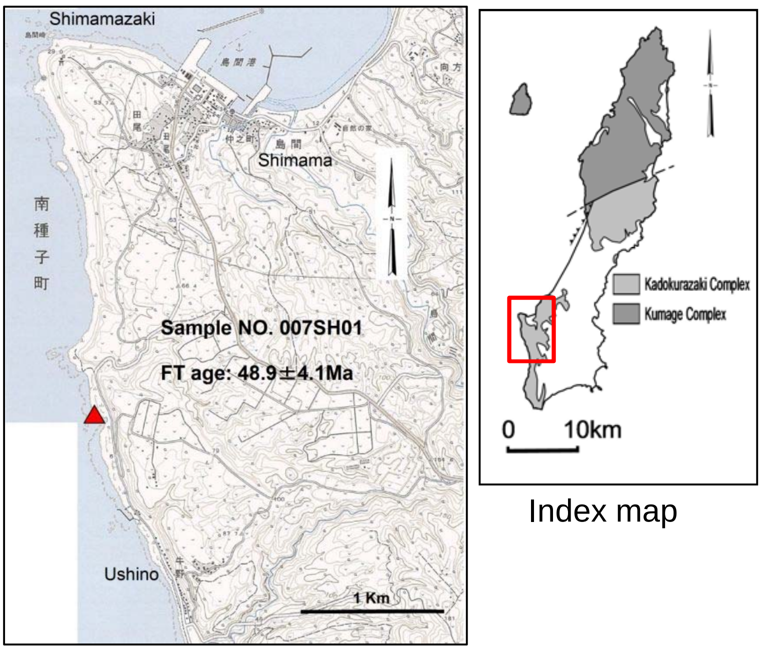

Fig4.4.1 Fission-track age and locality of the whitish tuffaceous sandstone from the lower part of the Shimama Olistolith. Sampling locality is situated at lat.30°26′39.8″N and long.130°51′14.2″E.

The topographic map “Shimama”, scale 1:25,000 published by the Geographical Survey Institute was used.

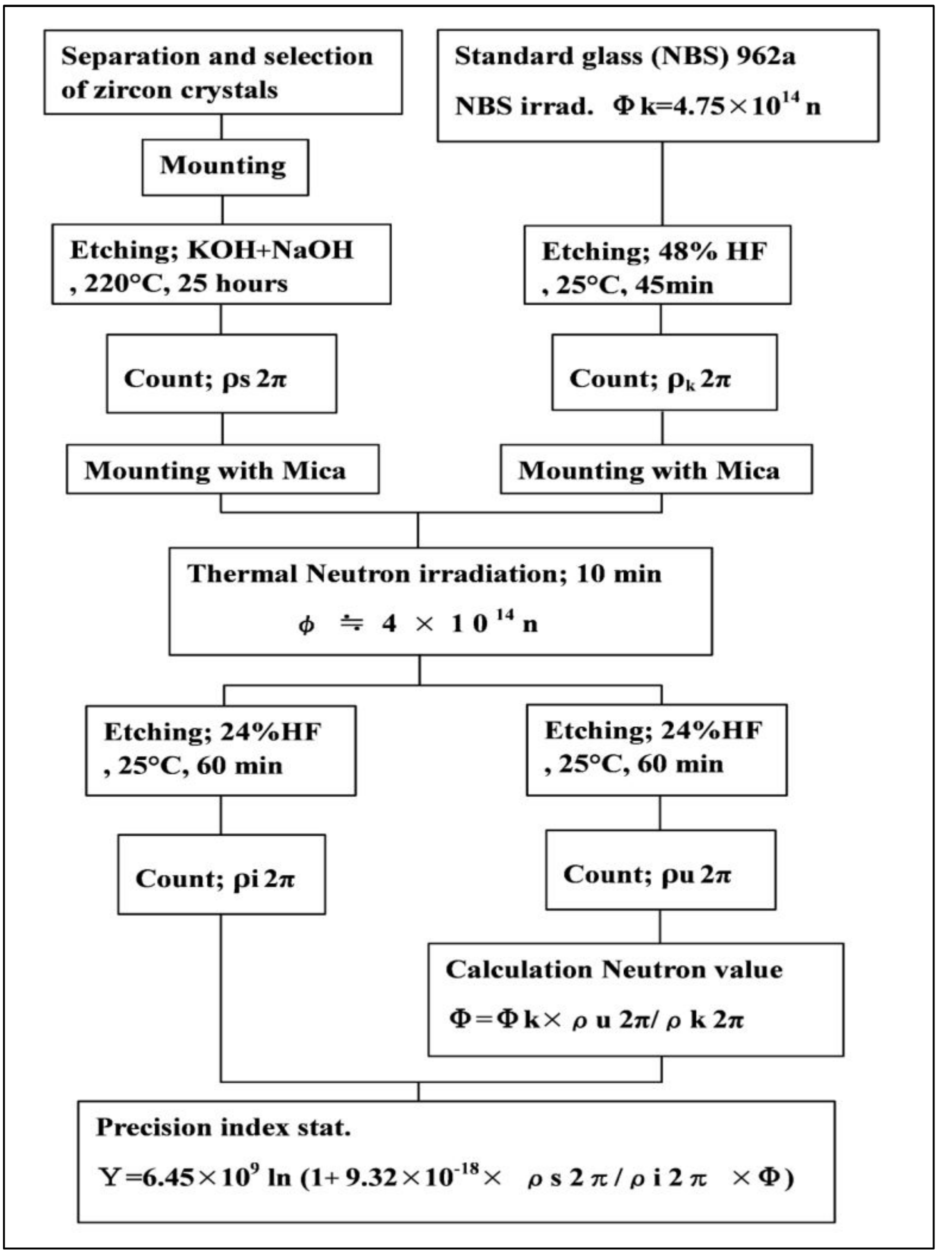

Fig.4.4.2. Flowchart showing the method and processes of fission-track age dating measurement.

5. Southern Shimanto Belt in Central Ryukyu

The Wano Formation and Kayo Formation of Central Ryukyu have been considered to be Eocene in age based on the occurrence of *Nummulites* sp. (Ishida, 1969, Konishi *et al.*, 1973). These strata are comparable to the forearc basin-fill deposits that composed of turbidite sequence accompanied by conglomerates in lower part (Sakai *et al.*, 1977, Sakai, 1988, 1994).

5.1 Wano Formation

The distribution of the Eocene Wano Formation is 2 km in width exposed on the eastern part of the Kasari Peninsula of Amami-Oshima. The western and eastern flanks are in fault contacts with the Cretaceous rocks of the Shimanto Belt. The geological structure of this formation shows a synclinorium whit axial plane dipping towards the northwest (Figs.15 and 16 in the Appendix).

Ishida (1969) studied the lithostratigraphy of the Wano Formation and obtained specimens of *Nummulites* sp., from the alternating thin beds of sandstone and mudstone near Setta. Aoyagi & Inoue (1979) extracted benthic foraminifera from the mudstone and suggested the bathyal to neritic environment. Sakai (1994) studied further in detail on the structural, sedimentological features and planktonic microfossils (Fig.16 in the Appendix). On the basis of planktonic foraminiferal data, this formation was assigned to the middle to late Middle Eocene (P.13-P.14) (Sakai, 1994).

The basal part of this Formation is composed of chaotic mudstone and is overlain by turbidite sequences which consist of three fining- and thinning-upward cycles with total thickness about 900 m (Ishida, 1969; Sakai, 1994; Saki & Fukuda, 1994). Occasionally, trace fossils of *Nereites* sp. and *Helminthoida* sp. were recognized on the bottom surface of thin-bedded sandstone in this unit. Paleocurrent directions from flute-casts indicate predominantly north-northwestwards direction (Ishida, 1969). According to Sakai (1994), the lithofacies and sedimentary features of this formation are briefly summarized as follows:

"The chaotic rock unit includes many blocks of sandstone, massive mudstone, sandy alternation, muddy alternation and acidic tuff in the scaly mud matrix. Major blocks derived from deep-sea fan deposits, are contained glauconitic sandstone (more than 5 m thick). This chaotic rock facies is probably comparable to the slope failure of shelf deposits.

The lower cycle is characterized by channel facies and consists of stratified conglomerate, thick-bedded pebbly sandstone and intermediate to coarse-grained sandstone. The middle unit is changed upwards into levee-deposit with lenticular sandy conglomerate and slump deposit. The top unit consists of thin-bedded alternation and massive mudstone containing nodule.

From the thin-bedded alternation, *Nummulites* sp. was collected by Ishida (1969). This top unit is comparable to lobe or lobe-fringe environments. The middle cycle is made up of pebbly sandstone with small channeled thick-bedded sandstones, suggesting channeled lobe environments. The middle and upper part of this cycle, which are composed of sandy alternation, muddy alternation, mudstone and interbedded acidic tuff, are compared with lobe-fringe environments (Sakai, 1994). The upper cycle consists of sandstone dominant facies (channeled lobe) and sandy and muddy alternations (smooth lobe). The lower sandstone sequence is interbedded with slump beds. These sandstones are characterized by amalgamation and convolution."

5.2 Kayo Formation

The Kayo Formation defined first by Flint *et al.* (1959) for the basement rocks exposed in the east-central part of Okinawa Island (Figs.17 and 18 in the Appendix). *Nummulites* sp. has been found from the lower part of this formation by Konishi *et al*. (1973), and assigned to the Eocene strata of the Southern Sub-belt of Shimanto Supergroup. Suzuki & Ujiie (1985) re-examined these specimens of *Nummulites* derived from the other shallower region as portions of debris flow, and consequently identified these species as *Nummulites amaksaensis* Yabe and Hanzawa, 1925.

The west flank of this formation contacts with the underlying Nago

Fromation by northwest dipping thrust fault named Futami thrust (Hashimoto *et al*., 1978). This formation represents synclinorium accompanied with many parasitic folds, of which fold axial planes show the dip direction towards the northwest (Fig.17 in the Appendix). Total thickness is about 830m (Fukuda *et al*., 1978; Fukuda & Hayasaka, 1978) (Fig.18 in the Appendix). Concerning the geological structure, however, there have been proposed some different interpretations, for example, slump structure of unconsolidated sediments (Hayashi, 1988), imbricated thrust-fold (Ujiie & Iwasaki, 1987; Ujiie, 1989), and accretionary fold and thrust resulting from off-scraping (K. Ujiie, 1997).

As seen in the lithologic profile (Fig.17 in the Appendix), however, the fold axis of synclinorium is approximately parallel to the strike of the Futami thrust. In the northwestern area, the map-scaled fold axis, overturned strata and S-shaped mesoscopic folds are associated, whereas, normal strata and Z-shape mesoscopic folds predominantly occur in the southeast area (Sakai, 1994).

Therefore, the deformation structures of the Kayo Formation are not resulted in progressive accretionary process, but lateral shortening process after the deposition of total succession. The lithofacies and sedimentary features of this formation are briefly summarized in the following.

The Kayo formation is composed of the alternation of quartz-rich, fine- to intermediate-grained sandstone and shale, and subordinate intraformational conglomerates with limestone cobbles and orthoquartzite pebbles. On the lower surface of sandstone beds, small-scale flute casts and various kinds of trace fossils, such as *Spirorhaphe* sp., *Spirodesmos* sp., *Helminthoida* sp., *Helminthopsis* sp., *Cosmorhaphe* sp., *Paleomeandron* sp., *Belorhaphe* sp. and *Paleodictyon* sp. are observed. In the Kayo Formation, five successive units were discriminated based on detailed observation of lithofacies (Fig.18 in the Appendix). These units are characterized by fining-upward cycles of sedimentation, respectively.

The sandstones referred as the feldspathic arenite in composition are most representative in the formation. They are characterized by base-missing nature and dominated by parallel-laminated sandstone

(Tb-e), current ripple-laminated sandstone (Tc-e) and laminated fine-grained sandstone (Td-e). Parallel lamination is the most common sedimentary features observed in the sandstone beds. From the flute casts measurement, a lateral palaeocurrent direction indicates the sediment transportation from west or southwest.

As mentioned above, the paleocurrent patterns and deposits of the Southern Shimanto Belt in Central Ryukyu suggest that those basins were structurally controlled by older basement rocks as shown in narrow and synformal configuration (Fig.5.2.1). Such a basin profile is likely reflect that the basin floors were inclined towards the northeast and showing high subsidence because of northeastern turbidity currents characterized by finning- and thinning-upward sequential stacking patterns. Consequently, there are differences between the Southern Shimant Belt of North Ryukyu and Central Ryukyu in the sedimentary systems and environments due to the spatial distribution of source of sediment supply and delta-fed-fan (Sakai, 1994; Sakai & Fukuda, 1994). Furthermore, Sakai (1994) explained that the oblique subduction or lateral slip of plate subduction systems affected on the formation of the basins in Central Ryukyu such as perched basin which were parallel to the trench. In contrast, in the South Kyushu and North Ryukyu, orthogonal subduction was continued during the Eocene because of occurrence of the tectonic mélange in the Southern Shimanto Belt (Sakai, 1989).

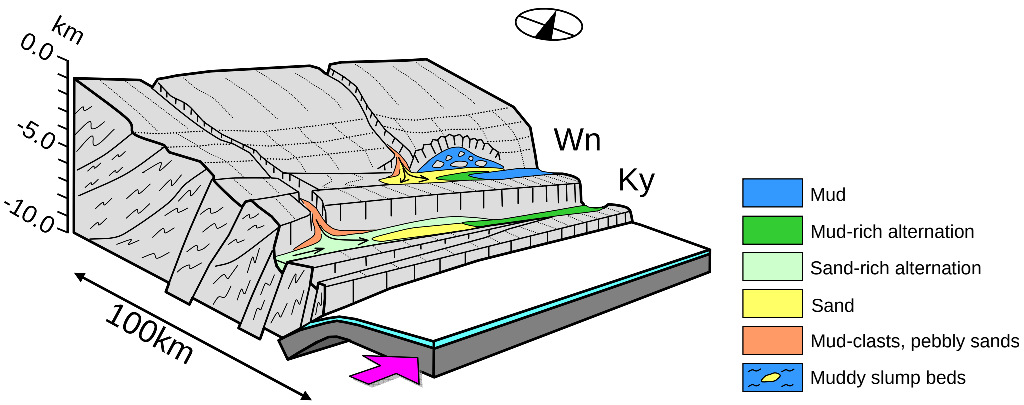

Fig.5.2.1 Schematic block diagram showing an inferred depositional environments of the Wano and Kayo Formations. Wn: Wano Formation. Ky: Kayo Formation.

6. Discussion

6.1 Age of the Kadokurazaki Complex

In this study, planktonic foraminiferal fossils obtained from three localities belonging to the uppermost of the Kumage Complex and Kadokurazaki Complex of Tanegashima. The main components of these fossil assemblages are the genus *Globoquadrina*, *Dentoglobigerina* and *Catapsydrax*. It is a global tendency that these fossil genera are recognized as characteristics of Early Miocene.

Particularly, the planktonic foraminiferal assemblage obtained from the muddy matrix of the olistostrome that is exposed along the coast of Sunasaka in Minamitane can be correlated with N.4 - N.6 of Blow (1969) (equivalent to ca.23 - 18 Ma), and it has became clear that the uppermost of Kumage Complex includes the Early Miocene rocks. Therefore, it is firstly interpreted that the sedimentation of the Southern Shimanto Belt in North Ryukyu continued from Middle Eocene until Early Miocene time.

On the other hand, the Nichinan Group in Southern Kyushu yields abundant planktonic foraminifers. On the basis of the planktonic foraminifer obtained from the olistoliths and muddy matrix, the Nichinan Group has been divided into three Zones, *Globorotalia (Turborotalia) opima opima* Zone, *Globigerina angulisuturalis* Zone, *Globorotalia (Turborotalia) kugleri* Zone in ascending order (Sakai *et al.,* 1984; Nishi, 1985). These Zones are correlated with P21 (= N2), P22 (=N3) and N4 of Blow (1969) respectively and each of Zones is correlated with Late Oligocene, latest Oligocene and earliest Miocene (Sakai *et al.,* 1984). This is therefore first report to provide the information of the planktonic foraminiferal Zone of N.4-N.6 form the Southern Shimanto Belt in South Kyusyu and North Ryukyu (Fig.6.1.1).

The coherent turbidite sequence of the Kumage Comprex distributed in the northern part of Tnegashima, is correlated with forearc basin and trench depositional setting. The variegated shale occurred at the lower member of this coherent sequence, yields radiolarian fossils indicating Middle Eocene to Early Oligocene age.

In contrast, the Kadokurazaki Complex distributed in the middle and southern areas of Tanegashima, has features of block-in-matrix fabric macroscopically containing clasts of sandstone, alternation of sandstone and shale, and pillow lavas of basaltic rock. These rocks are considered to be the result of mass-wasting processes, such as debris flows at paleo-slope area.

The chaotic unit is overlain by the large slump sheets, most of which are derived from the Kumage Complex. The large slump sheets as olistholith show structural complexity due to sliding processes under the force of gravity. In particular, recumbent folds are observed in the southeast region of the Hamatsuwaki fault. Moreover, antifomal syncline and synformal anticline were recognized along the load leading from Kaminaka to Shimama, and around Kadokurazaki in southern Tanegashima.

These slump sheets were characterized by SE-vergent fault in internal structure. The Shimama Olistolith, however, represents a general trend of strike in NE-SW direction and mostly dips 30-40 degree NW. The lower part of the Shimama Olistolith is accompanied by folds. These fold structures may be caused by gravity sliding of mega-slump sheet.

From the above-mentioned facts, the thick bedded sandstone of the uppermost of the Kumage Complex in Sumiyoshi, the diapiric mudstone underlying recumbent folded thick-sandstone in the eastern area of airport (Oishino area) and the chaotic rocks of the Kadokurazaki Complex are considered to be in a relation of contemporaneous heterotopic facies (Fig.6.1.2).

6.2 Intrusive igneous rocks

Lamprophyre

Intrusive igneous rocks of lamprophyre (camptonite) that is assumed to be derived from alkali-basalt magma source occurred in the northwest part of Tanegashima (Taneda & Kinoshita, 1972; Yagi *et al*., 1975). The trend of its distribution is showing NNE-SSW direction which almost coincides with general strike of the Kumage Complex. The contact surface of intrusive rock and host rock is high angle. Generally, the dyke rocks intruded along the bedding plane, but there are some outcrops where the intrusive rocks cut the host strata at a high angle (Taneda & Kinoshita, 1972).

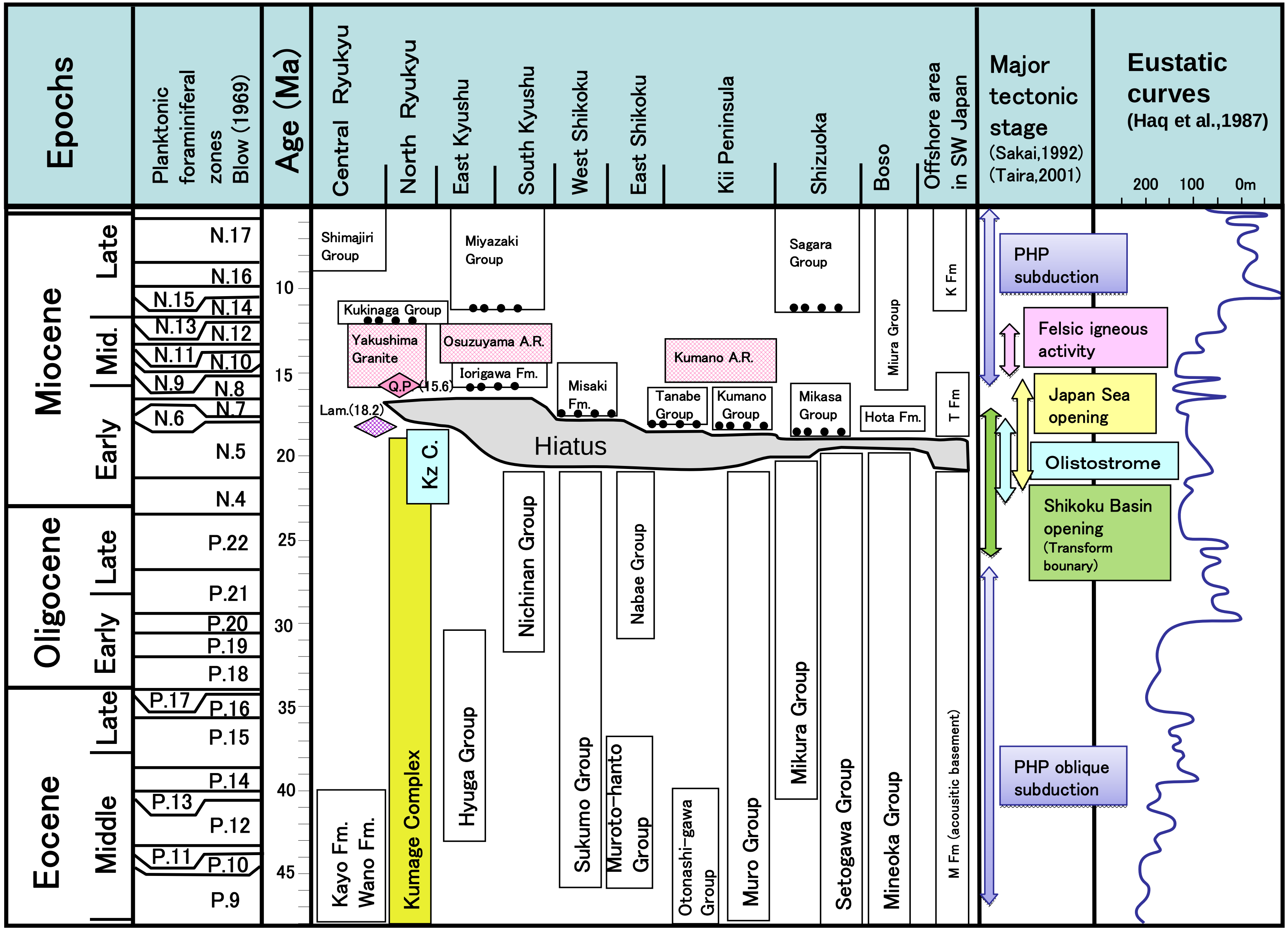

Chronostratigraphy by Hilgen *et al.* (2012)　Kz C.:Kadokurazaki Complex　● ● ● Basal conglomerate　A.R.: Acidic Rocks

Fig.6.1.1　Comparison of the Cenozoic tectono-stratigraphic evolution Central-North Ryukyu and SW Japan. Modified from Sakai (1992).

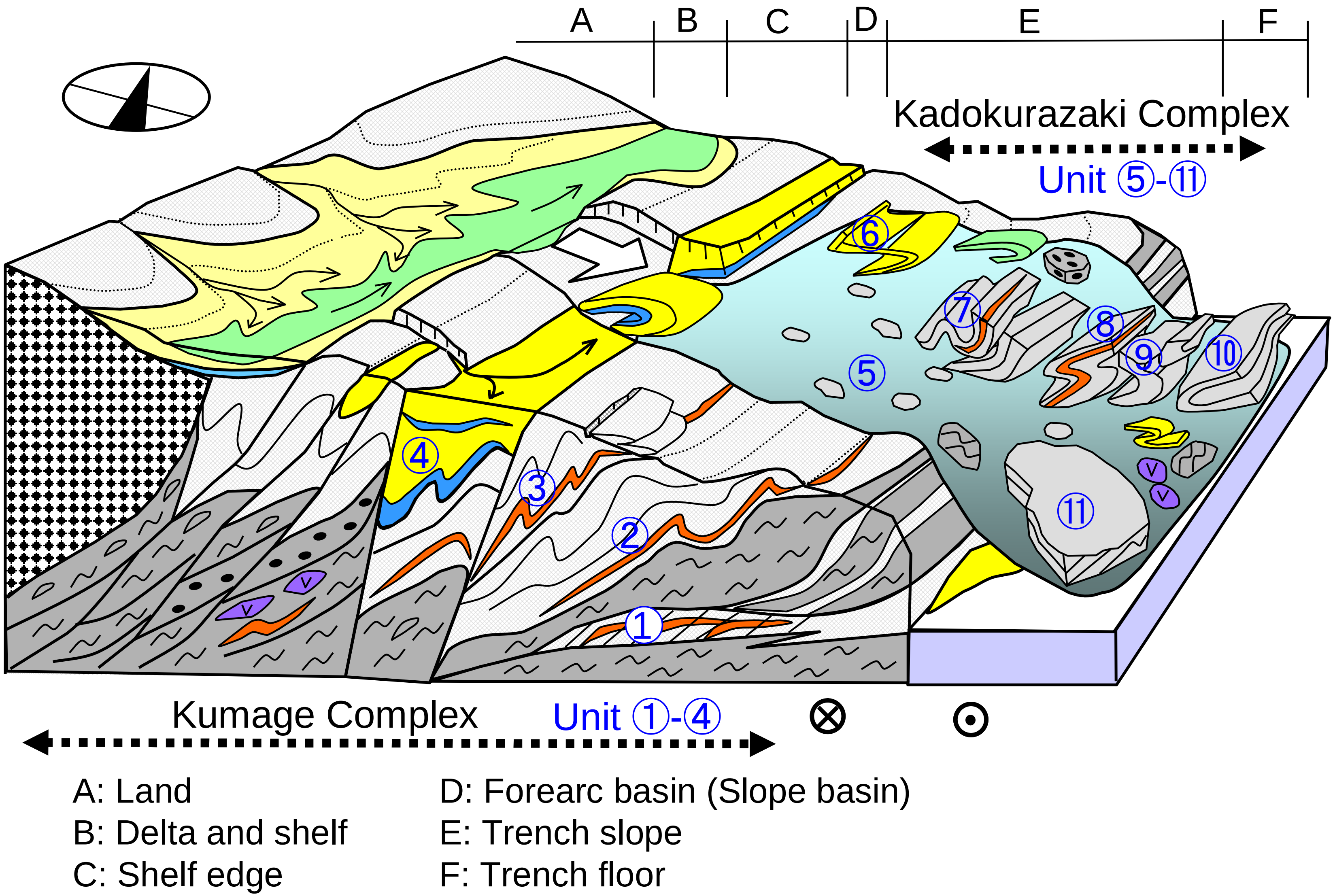

Fig.6.1.2 Schematic block diagram showing an inferred depositional environments (A to B) and collapse between the shelf edge and the trench slope (E and F) under right-lateral transformal plate boundary.

Taneda & Kinoshita (1972) measured the K-Ar ages on the lamprophyre sample of the Sumiyoshi neighborhood and obtained the age of 16 ± 2 Ma. Afterwards, Ogasawara (1997) carried out precise K-Ar dating of lamprophyre in the southern part of Nishinoomote and dyke rock of quartz porphyry of Shimamazaki in Minamitane, and obtained ages of 18.2 ± 0.9 Ma and 15.6 ± 0.8 Ma, respectively.

In the outer zone of Southwest Japan, it is known that the lamprophyre of Shingu in Ehime (Takamura, 1978), which intruded at the same time as in Tanegashima. Lamprophyre of Shingu is the intrusive sheet which penetrated to the black schist of the Sanbagawa belt, and it implies that it came from the upper part of mantle including the xenoliths of the ultramafic rock and mafic rock (Takamura, 1978). This intrusive rock has yielded a K-Ar age of 17.7 ± 0.5 Ma (Uto *et al.*, 1987).

The rock magnetism of the lamprophyre in Tanegashima measured by Tanedda & Kinoshita (1972) are showing reverse with large deviation angle in declination. According to the standard (Cande & Kent, 1995), this alkali volcanism probably corresponds to a reverse geomagnetic polarity interval of chron C5Dr (18.28-17.62 Ma) (Ogasawara, 1997).

Therefore, it is suggested that these two lamprophyre dykes of Tanegashima and Shingu were penetrated into the basement locks at the approximately same time as ca.18Ma. This magmatic activity of alkaline rock is earlier than clockwise rotation of southwest Japan (Ogasawara, 1997).

Quartz porphyry

The quartz porphyry dated as 15.6Ma was occurred in Shimamazaki of southern Tanegashima and in Ochinokawa of northeastern Yakushima (Ogasawara, 1997). These dykes indicate in the N60-70W direction and show that this acidic igneous activity began at 15.5Ma just before instrusion of S-type Yakushima granite dated 13-14Ma (Shibata & Nozawa, 1968). The Shimamazaki quartz porphyry has been injected along the bedding plane of the coherent turbidite of the Shimamazaki olistolith, therefore an emplacement of the olistolith of the Kadokurazaki Complex can be obviously predated more than an age of 15.6 Ma.

6.3 Paleostress fields

Generally, fossil tension cracks are formed perpendicularly to axis of the minimum principal compressional stress, and parasitic craters and dykes concentrate in the direction of the maximum principal stress axis (Nakamura, 1969). In other words, a horizontal growth direction of the dyke shows the maximum principal stress axis in the paleostress field.

Late Cenozoic dike swarms

Yamamoto (1991) examined the interaction of tectonic stress field and igneous activity, referred to the late Cenozoic dike swarms (55 places in total) in Japanese islands. From the examination of tectonic stress field at 15-22Ma, he presumed that " The Southwest Japan Arc and the Northeast Honshu Arc were under an extensional stress, which caused many along-arc trending dike swarms".

Paleostress fields of SW Japan in Early Miocene

The directions of the alkaline dykes almost show E-W direction at Shingu of Shikoku and N20°E direction in Tanegashima, respectively. It is suggested that the difference of these directions resulted from the rotation of SW Japan to 47degrees associated with the rapid opening of the Sea of Japan at ca. 15 Ma (Torii *et al.*, 1985). The dyke of Shingu of Shikoku showed a direction of N43°E before to rotate clockwise and as a result, a current direction is almost E-W after rotation.

On the other hand, the Ryukyu Arc was originally continental margin arc, but separated from the Chinese continental margin by the rifting of the Okinawa trough which began at before about 10 Ma. South Ryukyu rotated 19 degrees clockwise during 10-4 Ma, and North Ryukyu rotated in succession 30 degrees counterclockwise at 6-2 Ma. During this time, Okinawa trough was opened approximately 70 km by Central Ryukyu (Miki, 1991; Kodama & Nakayama, 1993; Kamata & Kodama, 1994).

As mentioned above, it can be postulated that North Ryukyu rotated 30 degrees counterclockwise after 6 Ma, and the dyke orientation of lamprophyre in Tanegashima showed the N50°E direction at ca. 18 Ma. Therefore, these data suggested that the directions of the dikes of two areas in Shingu and Tanegashima coincide with NE-SW direction at ca.18 Ma, and the island arc oriented in the same direction. In other words, ENE-WSW direction is maximum horizontal compressive stress (σH max) at ca. 18 Ma and NWN-SES direction is assigned to σ 3 (minimum horizontal stress). These facts support the idea that the extensional stress perpendicular to the island-arc crust existed in SW Japan during 15-22 Ma from the analysis on intrusive rocks (Yamamoto, 1991).

Considering the intrusion of the lamprophyre of Shingu parallel to the island arc, the Shikoku Basin was continued spreading in the ENE-WSW direction to 24-18 Ma (Uto, 1995). The plate motion implies that the forearc sliver of SW Japan has contacted with Philippine Sea plate by a transform fault. The 18.2 Ma lamprophyre dyke at Tanegashima (Ogasawara, 1997) can be explained that SW Japan and North Ryukyu were under the extensional stress field at ca. 18 Ma.

Fault strikes usually have been formed perpendicular to the extensional stress, and submarine slope destabilization would occur in the forearc region of SW Japan. Particularly, at the forearc basin and trench-slope break to trench parts, the fracturing and creep deformation may be promoted under the extensional condition.

Moreover, re-initiation of subduction associated with back-arc basin opening began ca. 17 Ma was the critical event responsible for the forming of the modern SW Japan volcanic arc (Kimura *et al*, 2005). Kimura *et al.* (2005) further stated that a convergent plate boundary along SW Japan is required to accommodate opening of the Sea of Japan and to give force for large-scale rotation of the arc during subduction have been under way by 17 Ma (Fig.6.3.1).

The first few million years of subduction must have been very rapid (>10 cm/year) in order for the Philippine Sea lithosphere to arrive beneath the Setouchi Zone and cause HMA (high-magnesium andesites) magmatism by 16-15 Ma (Kimura *et al*, 2005). Considering these facts of the late Cenozoic volcanic activity in SW Japan, it is suggested that the trigger of olistostrome in Tanegashima was a change from extensional into compressional stress field caused by initiation of subduction of the Philippine Sea plate (Fig.6.3.2).

6.4 Timing of initiation of olistostrome in Tanegashima

The olistostromal Kadokurazaki Complex representing a huge collapse of forearc region was resulted from the re-subduction the Philippine Sea Plate just after the opening of the Shikoku Basin. The timing of the emplacement of olistostrome could be assigned precisely to the end of Early Miocene between the youngest age (N.4-N.6 zones: ca. 23-17.5Ma) of the complexes and the intrusive rocks (18.2Ma) prior to the shallow marine Kukinaga Formation in Middle Miocene. It is suggested strongly, therefore, that the opening of Japan Sea during 17 to 15Ma could be inferred as the most possible driving force for the extensive large-scaled failure and subsequent rapid elevation of forearc region.

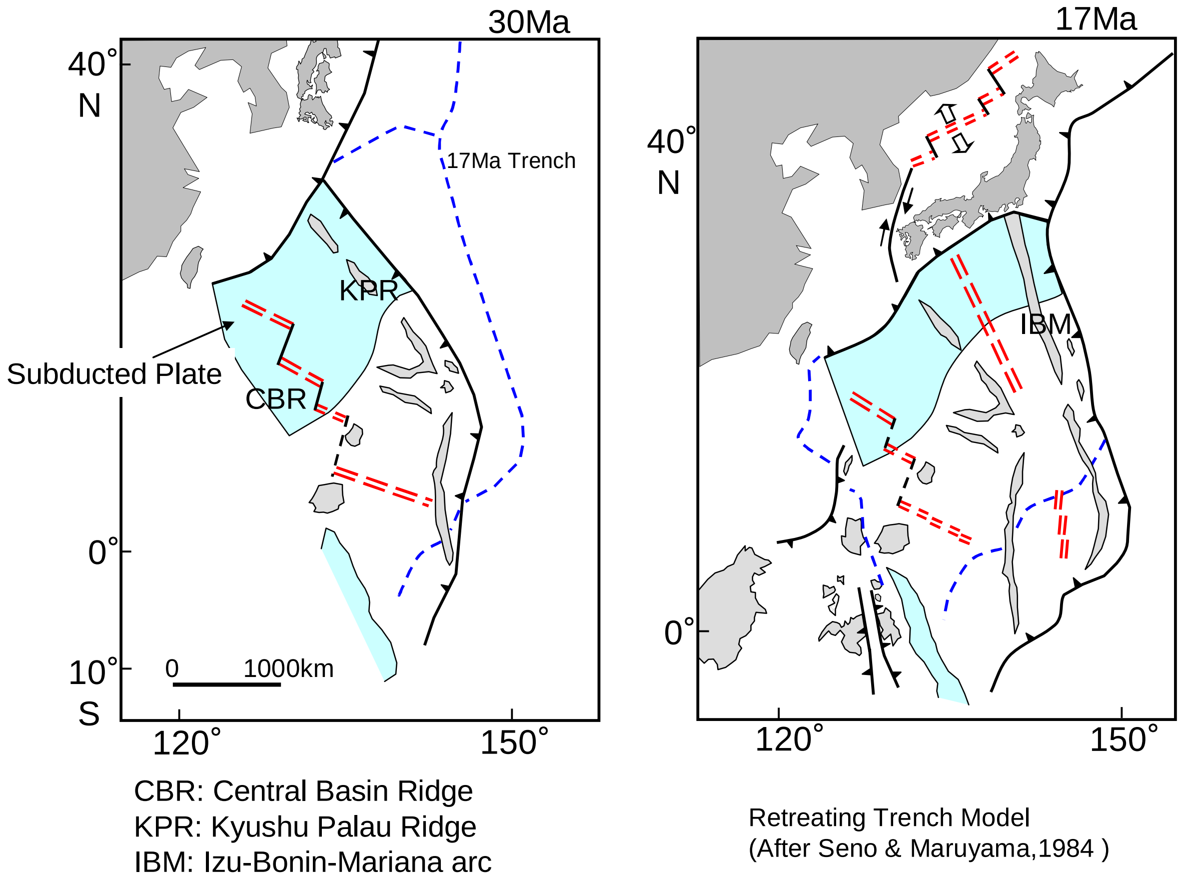

Fig.6.3.1 Reconstructions of Philippine Sea Plate motion in Oligocene to Middle Miocene time. After Seno & Maruyama (1984).

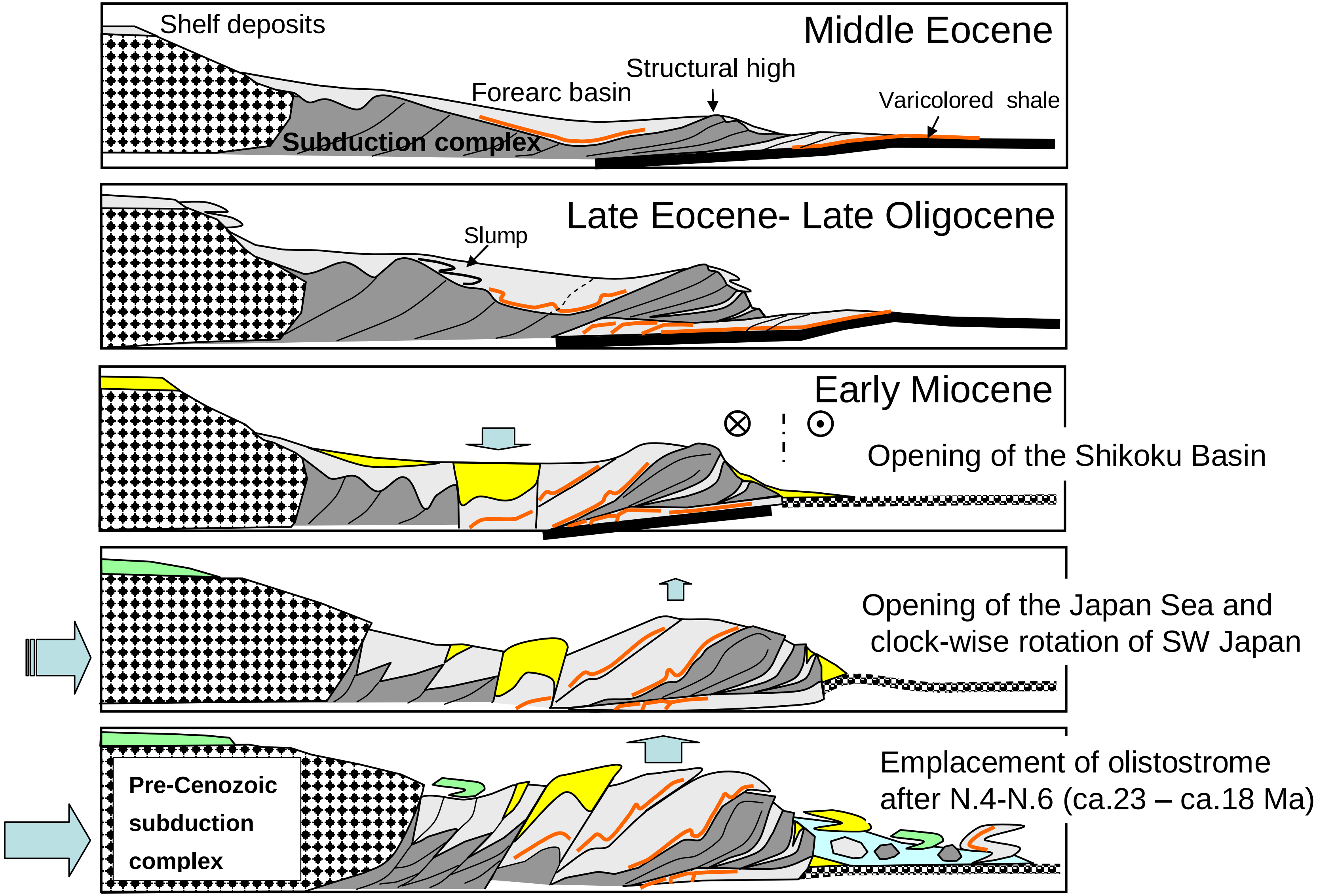

Fig.6.3.2 Evolution in the forarc region of North Ryukyu during the Middle Eocene to Early Miocene.

7. Conclusion

In this study, the geologic structures and sedimentologic feature of the Southern Shimanto Belt of North Ryukyu were described and the tectonic evolution of the Ryukyu Arc during Middle Eocene to Early Miocene was discussed. Furthermore, the evolutions of sedimentary basins in forearc region of Ryukyu Arc were examined comparatively to those of Kyushu.

The results of this study are summarized as follows:

(1) The Kumage Group of Tanegashima in North Ryukyu is able to divide into the coherent stratum in the middle to northern region named Kumage Complex and the mapable chaotic deposits in the middle to southern region, named Kadokurazaki Complex. In the middle part of Tanegashima, these Complexes were in contact with strike-slip fault (the Hamatsuwaki fault) trending NNE-SSW in direction and steeply dipping. Most part of this fault has been cut by dextral strike-slip faults oriented in NE-SW direction.

(2) The pelitic phyllite (Hamatsuwaki Unit) occurs as coherent turbidte sequences in the lowest part of the Kumage Complex. The most striking features of this unit are intensely development of shear folding corresponding to the accretinary wedge within the arc-trench system. This unit is overlain by a thick turbidite successions compared to sand-rich fan, composed of sandstones, alternating beds of sandstone and shale and mudstone (Fukago and Sumiyoshi Units).

(3) The Kadokurazaki Complex is made up of matrix-dominated olistostrome consisting mudstone mixture associated with pebbly mudstone, and various sizes of olistholiths composed of clastic rocks derived from the Kumage Complex, and pillow basaltic rocks and varicolored shale as allochthonous slabs. Storm and hyperpycnal flow deposits indicating shelf environment were recognized as sheeted olistoliths, however, most of these olistholiths have shown features of turbidite facies formed on the deep-sea fan.

Based on both geometric properties and deformation grade, the overturned beds are interpreted that the inclined to overturned bending folds were caused by gravity gliding in the huge olistoliths, and these deformation structures are different from flexural-slip folds and related thrust fault in the Kumage Complex. Pebbly mudstones in the megaliths caused by diapiric injection during gravitational gliding took place as poor continuity of stratification extremely complicated structure.

(4) In this study, planktonic foraminifers were extracted from the mudstones collected from 111 locations in Tanegashima. As the results, the identifiable planktonic foraminifers were obtained from the uppermost part of coherent sequences in the west coast area, the slump terrane in the east area of the middle part of the island, and the chaotic rocks in the southern part of the island. From the examination of these microfossils, it was made clear that the Southern Shimanto Belt has unconventional stratigraphic relationships as follows.

The coherent sequence in the Kumage Complex of the west coast of middle part of Tanegashima, can be assigned in the uppermost part of the stratigraphic horizon. Therefore, the sedimentation of the Kumage Complex continued until Early Miocene based on the foraminiferal N.4-N.6 zones (ca.23-17.5Ma) of Blow (1969).

According to the previous study (Okada *et al*., 1982; Kuwazuru & Nagatsu, 2007; Saito *et al*, 2007), most of the radiolarians have been found from varicolored shale of both Kumage and Kadokurazaki Complexes in this study, and could be assigned ages ranging from Middle Eocene to Oligocene (48-23Ma). However, the planktonic foraminifers obtained from the pelitic matrix in the Kadokurazaki Complex distributed in the middle and southern region of Tanegashima are comparable to N.4-N.6, as same as the uppermost part of the Kumage Complex.

From these evidences of micro-fossils mentioned above, it could be concluded that the uppermost turbidite sequence of the Kumage complex is a contemporaneous heterotopic facies of the muddy matrix of the Kadokurazaki Complex and the Kadokurazaki Complex has been formed at Early Miocene.

(5) The timing of emplacement of olistostrome can be constrained by the intrusive alkali-rock (Lamprophyre) extending along the long axis of the island. Consequently, the time of olistostrome emplacement could be estimated during ca. 23-18Ma which is shorter period than previous interpretations from South Kyushu.

(6) In this period, the spreading speed of the Shikoku Basin had gradually decelerated, and Southwest Japan started to rotate clockwise, while the back-arc basin initiated opening at Japan Sea.

The rapid emplacement of a large-scale olistostrome was caused by riding of Southwest Japan at the forearc region on the Philippine Sea plate, soon after the Shikoku Basin ceased the opening. This event probably has triggered by the upward rising of the accretional wedges of the Southern Simanto Belt and instability of forearc slope.

Acknowledgements

I would like to express my cordial thanks to Dr. Takashi Sakai of Kyushu University for his valuable suggestions in field observations and critical reading of the manuscript. I am grateful to Prof. Hiroyoshi Sano for his criticism on the manuscript, continuous advice and encouragement throughout the study. And also, I would like to thank to Prof. Koji Wakita of Yamaguchi University for his valuable comments and critical reading of the manuscript.

I would extend my sincere appreciation to Associate Prof. Kazumi Akimoto of Kumamoto University for many helpful advices on the taxonomic studies of planktonic and benthic foraminifera. Finally, I would express my deep appreciation to Associate Prof. Hiroki Hayashi of Shimane University for identification of the planktonic foraminifera.

References

Akimoto, K., 1990, Distribution of Recent benthic foraminiferal faunas in the Pacific off southwest Japan and around Hachijojima Island. *Sci. Rep., Tohoku Univ., 2nd ser. (Geol.*), **60**, 139-223, pls.11-24.

Akimoto, K., Uematsu, K., Hattori, M. and Kato, C., 1996, Recent benthic foraminiferal assemblage discovered from the hidal zone of Mariana Trench, Northwest Pacific Ocean. *JAMSTEC J. Deep Sea Res.*, **12**, 263-273.

Allen, J.P. and Fielding, C.R., 2007, Sedimentology and stratigraphic architecture of the Late Permian Betts Creek Beds, Queensland, Australia. *Sedimentary Geology*, **202**, 5-34. Doi:10.1016/j.sedgeo.2006.12.010

Alsop, G.I. and Marco, S., 2012, A large-scale radial pattern of seismogenic slumping towards the Dead Sea Basin. *Journal of the Geological Society, London*, **169**, 99-110. Doi: 10.1144/0016-76492011-032

Alsop, G.I. and Marco, S., 2013, Seismogenic slump folds formed by gravity-driven tectonics down a negligible subaqueous slope. *Tectonophysics*, **605**, 48-69. http://dx.doi.org/10.1016/j.tecto.2013.04.004

Aoyagi, K. and Inoue, Y., 1979, Micro-paleontology and Sedimentary Petrology of the Eocene Wano Formation in North of Amami-ohshima, Kagoshima, Japan. *In* Geological studies of the Ryukyu Islands, edited by Kizaki, K., **4**, 23-28 (in Japanese with English abstract).

Aurahs, R., Göker, M., Grimm, G.W., Hemleben, V., Hemleben, C., Schiebel, R. and Kučera, M., 2009, Using the multiple analysis approach to reconstruct phylogenetic relationships among planktonic foraminifera from highly divergent and length-polymorphic SSU rDNA sequences. *Bioinform Biol Insights*, **3**, 155-177.

Aze,T. Ezard, T.H.G, Purvis, A., Coxall, H.K., Stewart, D.R.M., Wade, B.S. and Pearson, P.N., 2011, A phylogeny of Cenozoic macroperforate planktonic foraminifera from fossil data. *Biol. Rev*., **86**, 900-927. Doi:10.1111/j.1469-185X.2011.00178.x

Blow, W.H., 1969, Late middle Eocene to Recent planktonic foraminiferal biostratigraphy. *In* Brönnimann, P. and Renz, H. H., eds.: *1st Int. Conf.*

Plankton. Microfossils, Geneva, 1967**,** **1**, 199-422, Brill, Leiden.

Bolli, H.M. and Saunders, J.B., 1985, Oligocene to Holocene low latitude planktonic foraminifera. *In* Bolli, H. M., Saunders, J. B., and Perch-Nielsen, K., eds., *Plankton stratigraphy, Cambridge Univ. Press*, 155-262.

BouDagher-Fadel, M.K., 2013, Biostratigraphic and Geological Significance of Planktonic Foraminifera (2nd ed.). Office of the Vice Provost (Research), UCL: London, UK. Doi: http://dx.doi.org/10.14324/99.1

Bradley, D. and Hanson, L., 1998, Paleoslope analysis of slump folds in the Devonian flysch of Maine. *Jour. Geol.*, **106**, 305-318.

Bridge, J.S., and Best, J.L., 1988, Flow, sediment transport and bedform dynamics over the transition from dunes to upper-stage plane beds: implications for the formation of planar laminae. *Sedimentology*, **35**, 153-163.

Byrne, T. and DiTullo, L., 1992, Evidence for changing plate motions in southwest Japan and reconstructions of the Philippine Sea plate. *The Island Arc*, **1**, 148-165. DOI: 10.1111/j.1440-1738.1992.tb00066.x

Cande, S.C. and Kent, D.V., 1995, Revised calibration of the geomagnetic polarity timescale for the Late Cretaceous and Cenozoic: *Journal of Geophysical Research,* **100**, 6093-6095.

Cowan, D.S., 1985, Structural styles in Mesozoic and Cenozoic melanges in the western Cordillera of North America. *Bull. Geol. Soc. Amer*., 96, 451-462.

Daishi, M., 1989, Volcanic geology and rocks of Nakanoshima, Tokara Islands, Kagoshima Prefecture, Japan. *Jour. Geosci., Okaka City Univ*., **32**, 1-22.

Daishi, M., Hayashi M. and Kato, Y., 1986, Fission track ages of some Cenozoic acidic intrusive rocks from Ryukyu Islands. *Jour. Japan Assoc. M in. Petro. Econ. Geol.*, **81**,324-332 (in Japanese with English abstract).

Fielding, C.R., 2006, Upper flow regime sheets, lenses and scour fills: Extending the range of architectural elements for fluvial sediment bodies. *Sedimentary Geology*, **190**, 227-240. Doi:10.1016/j.sedgeo.2006.05.009

Flint, D. E., Saplis, R. A, and Corwin, G., 1959, *Military geology of Okinawa Jima, Ryukyu-retto.* **5**, Geol., **88**, *U.S. Army Pacific Off. Eng., Intell. Div., with personnel of U.S. Geol Surv.*

Frey, P.W., 1975, *The study of trace fossils. A synthesis of principles, problems and procedures in Ichnology*. Springer-Verlag. 562p.

Fukuda, Y. and Hayasaka, S., 1978, Trace fossils from the Eocene Kayo Formation in Okinawa-shima, Ryukyu Islands, Japan. *Rep. Fac. Sci., Kagoshima Univ.* (*Earth Sci. & Biol.*), **11**, 13-25.

Fukuda, Y. and Sakai, T., 2009, Olistostrome Belt in Tanega-shima, North Ryukyu. *Geol. Soc. Japan, Abstracts, **116th** Ann. Meeting.*, 68 (in Japanese).

Fukuda, Y., 2008, Sedimentary facies and system of the Eocene Shimanto Belt along the Ryukyu Arc. *Geol. Soc. Japan, Abstracts, **115th** Ann. Meeting.*, 94 (in Japanese).

Fukuda, Y., Kaihori, A., Otsuka, H. and Hayasak, S., 1978, A note on the sedimentological features of the Kayo Formation in Okinawa-shima, Ryukyu Islands. *In* Geological studies of the Ryukyu Islands, edited by Kizaki, K., **3**, 39-52 (in Japanese with English abstract).

Gleadow, A.J.W., Hurford, A.J. and Quaife, R.D., 1976, Fission track dating of zircon: improved etching techniques. *Earth Planet. Sci. Lett.*, **33**, 273-276.

Hansen, E., 1971, Strain Facies. Springer-Verlag Berlin, Heidelberg, New York.

Hanzawa, S., 1935, Topography and geology of the Riukiu Islands. *Sci. Rep. Tohoku Univ.*, *2 nd Ser*, (Geol), **17**, 1-61.

Haraguchi, S., Ishizuka, H., Ishii, T., Fujioka, K., Yuasa, M. and Shibasaki, H., 2014, Low- and high-temperature alterations of volcanic rocks in the northwestern Philippine Sea, and association with volcanic settings. *Island Arc*, **23**, 324-343.

Hasegawa, A., Nakajima, J., Uchida, N., Hirose, F., Kita, S. and Matsuzawa, T., 2010, Slab Structure beneath the Japanese Islands and Earthquake Generation. *J. Geography,* **119**, 190-204 (in Japanese with English abstract).

Hashimoto, I., 1956, Geological succession and structure of the undated strata in Yaku-shima, and some facts concerning the Kumage Group in the western part of Tané-ga-shima, Kagoshima Prefecture. *Rep.*

Earth Sci. Dept. Gen. Educ., Kyushu Univ., **2**, 23-34 (in Japanese with English abstract).

Hashimoto, S. and Nakagawa, H., 1978, Geology of the northern part of Okinawa-jima Ⅲ- On the geologic structure of the central part of the Ryukyu Islands. *In* Geological studies of the Ryukyu Islands, edited by Kizaki, K., **3**, 23-29 (in Japanese with English abstract).

Hayasaka, S., 1969, Molluscan fauna of the Kukinaga Group in Tané-ga-shima, South Kyushu, Japan. *Rep. Fac. Sci., Kagoshima Univ. (Earth Sci., Biol.)*, **2**, 33-52.

Hayasaka, S., 1973, Pliocene marine fauna from Tané-ga-shima, South Kyushu, Japan. *Sci. Rep. Tohoku Univ. 2nd Ser. (Geol.), Spec. Vol.***6**, 97-108.

Hayasaka, S., 1985, Yakushima. *In* Kizaki**,** K., ed., Geology of the Ryukyu Island Arc, Okinawa Times, 29-34 (in. Japanese).

Hayasaka, S., 1988, Geology of Tané-ga-shima. *Modern Geology*, **12**, 169-183.

Hayasaka, S., Fukuda, Y., and Hayama, A., 1980, Discovery of molluscan fossils and the paleoenvironmental aspects of the Kumage Group, in Tané-ga-shima, South Kyushu, Japan. *Prof. Saburo Kanno Mem. Vol.*, 59-70.

Hayasaka, S., Okada, H., Fukuda, Y., and Kojima, M., 1983, Geology of Tané-ga-shima. *Geol. Soc. Japan, Field Guide Book****, 90th*** *Ann. Meeting, Kagoshima*, 113-134 (in Japanese).

Hayashi, D., 1988, Three dimensional finite strain analysis -with reference to Kayo Formation, Kunchan Group, Okinawa-jima- *Jour. Geol. Soc. Japan*, **94**, 757-768 (in Japanese with English abstract).

Hayashi, H. and Takahashi, H., 2008, Numerical age of the planktonic foraminiferal zonal boundary between N.15 and N.16 in the mid-latitude northwest Pacific region. *Bull. Geol. Surv. Japan,* **59**, 415-422.

Hayashi, M. and Fujii, M., 1985, Statistical procedure to estimate the presence of detritus grains from the grain-by-grain fission track dating data. *Jour. Geol. Soc. Japan*, **91**, 403-409 (in Japanese with English abstract).

Hayashi, M. and Sugiyama, H., 1987, A sample statistical test for fission track counts obtained by the grain-by-grain dating method. *Jour.*

Japan Assoc. M in. Petro. Econ. Geol., **82**, 370-381 (in Japanese with English abstract).

Hilgen, F.J., Lourens, L.J. and van Dam, J.A., 2012, The Neogene Period. *In*: Grandstein, F.M., Ogg, J.G., Schmitz, M.D. and Ogg, G.M. (eds.). The Geologic Time Scale 2012. Elsevier, 923-978.

Holloway, N.H., 1981, The North Palawan Blocks, Philippines: its relation to the Asian Mainland and its role in the evolution of South China Sea. Geol. Soc. Malaysia, Bulletin **14**, 19-58.

Honza, E. and Fujioka, K., 2004, Formation of arcs and backarc basin inferred from the tectonic evolution of Southeast Asia since the Late Cretaceous. *Tectonophysics*, **384**, 23-53. Doi:10.1016/j.tecto.2004.02.006

Hufford, A.J. and Green, P.F., 1983, The zeta age caliblration of fission-track dating. *Isotope Geosci.*, **1**, 285-317.

Inoue, Y., 1989, Northwest Pacific foraminifera as paleoenvironmental indicators. *Sci. Rep., Inst. Geol., Univ. Tsukuba, Sec. B*, **10**, 57-162, pls. 18-33.

Ishida, S., 1969, Wano Formation (Eocene) in Amami-oshima, Ryukyu Islands, Japan. *Jour. Geol. Soc. Japan*, **75**, 141-156.

Jaffey, A.H., Flynn, K.F., Glendenin, L.E., Bentley, W. C. and Essling, A.M., 1971, Precision measurement of half-lives and specific activities of ^{235}U and ^{238}U, *Phys. Rev.*, **C4**, 1889–1906.

Kagoshima Prefecture, 1990, *Geological map of Kagoshima Prefecture, with Geological Sheet Map at 1:100,000.*

Kamata, H. and Kodama, K., 1994, Tectonics of an arc-arc junction: an example from Kyushu Island at the junction of the Southwest Japan Arc and the Ryukyu Arc. *Tectonophysics*, **233**, 69-81.

Kamata, H. and Kodama, K., 1999, Volcanic history and tectonics of the Southwest Japan Arc. *The Island arc*, **8**, 393-403.

Karig, D. E., 1975, Basin genesis in the Philippine Sea. *In* Initial Reports of the Deep-Sea Drilling Project, vol. **31**, D. E. Karig, J. C. Ingle, Jr. et al., pp. 857-879, U. S. Government Printing Office, Washington, D. C.

Kimoto, K., Ishimura, T., Tsunogai, U., Itaki, T. and Ujiié, 2009, The living triserial planktic foraminifer *Gallitellia vivans* (Cushman): Distribution, stable isotopes, and paleoecological implications. *Marine*

Micropaleontology, **71**, 71-79. Doi:10.1016/j.marmicro.2009.01.006

Kimura, J., Stern, R.J. and Yoshida, T., 2005, Reinitiation of subduction and magmatic responses in SW Japan during Neogene time. *GSA Bulletin* **117**, 7-8, 969-986.

Kitazato, H., 1980, Deep sea foraminiferal assemblage of the Setogawa Group. *In* Taira, A., and Tashiro, M., *eds*., Geology and Paleontology of the Shimanto Belt, Selected Papers in Honor of Prof. Jiro Katto, 219-225, pls. 26, 27 (in Japanese with English abstract).

Kizaki, K., 1978, Problems on the tectonics of the Ryukyu Islands Arc. *In* Geological studies of the Ryukyu Islands, edited by Kizaki, K., **3**, 1-9 (in Japanese with English abstract).

Kizaki, K., 1979, Kyushu western marginal shear and its significance. *Chikyukagaku* (*Earth Sci.*), **33**, 144-151(in Japanese with English abstract).

Kizaki, K., 1986, Geology and tectonics of the Ryukyu Islands. *Tectonophysics*, **125**, 193-207.

Kodama, K. and Nakayama, K., 1993, Paleomagnetic evidence for post-Late Miocene intra-arc rotation of South Kyushu, Japan. *Tectonics*, **12**, 35–47. DOI: 10.1029/92TC01712

Konishi, K., 1963, Pre-Miocene basement complex of Okinawa, and the tectonic belts of Ryukyu Islands. *Sci. Rep. Kanazawa Univ.,* **8**. 569-602.

Konishi, K., 1965, Geotectonic framework of the Ryukyu Islands (Nansei-shoto). *Jour. Geol. Soc. Japan,* **71**, 437-457 (in Japanese with English abstract).

Konishi, K., Ishibashi, T. and Tsuruyama, K., 1973, Find of *Nummulites* and orthoquorzitic pebbles from the Eocene turbidites in Shimajiri belt, Okinawa. *Sci., Rep. Kanazawa univ.,* **18**(1), 43-53.

Kuwano, Y., 1960, A Paleogene foraminiferal faunule from Osumi peninsula, Southern Kyushu, Japan. *Misc. Rep. Res. Inst. Natur. Resources*, **52-53**, 136-147.

Kuwazuru, J. and Nagatsu, M., 2007, Paleogene radiolarians from the Kumage group in the Northern Tanegashima Island, Kagoshima Prefecture, Japan. *Kagoshima prefectural museum research report*, **26**, 1-11 (in Japanese).

Letouzey, J. and Kimura, M., 1987, Okinawa Trough genesis: structure and evolution of a backarc basin developed in a continent. *Marine and Petroleum Geology*, **2**, 111-130.

Lowe, D.R., 1982, Sediment gravity flows: II. Depositional models with special reference to the deposits of high-density turbidity currents. *Journal of Sedimentary Petrology*, **52**, 279-297.

Miki, M., Matsuda, T. and Otofuji, Y., 1990, Opening mode of the Okinawa Trough: paleomagnetic evidence from the South Ryukyu Arc. *Tectonophysics*, **175**, 335-347.

Mulder, T. and Alexander, J., 2001, The physical character of subaqueous sedimentary density flows and their deposits. Sedimentology, 48, 269-299. DOI: 10.1046/j.1365-3091.2001.00360.x

Mulder, T., Migeon, S., Savoye, B. and Faugères, J.-C., 2001, Inversely graded turbidite sequences in the deep Mediterranean:a record of deposits from flood-generated turbidity currents? *Geo-Marine Letters*, 21, 86-93. Doi: 10.1007/s003670100071

Mulder, T., Syvitski, J.P.M., Migeon, S., Faugeres, J.-C., and Savoye, B., 2003, Marine hyperpycnal flow: initiation, behavior and related deposits. A review. *Marine and Petroleum Geology.* **20**, 861-882. Doi:10.1016/j.marpetgeo.2003.01.003

Mutti, E**.** and Normark W.R.,1987, Comparing examples of modern and ancient turbidite systems: problems and concepts, *in* Legget J. K., Zuffa G. G., eds., Marine clastic sedimentology: concepts and case studies (Graham and Trotman, London), 1–38.

Nagahama, H. and Sakai, T., 1972, Sedimentary structures in the Shimanto Group in Yaku-shima, Kagoshima Prefecture. *Bull. Geol. Surv. Japan*, **23**, 445-455, pls18-39 (in Japanese with English abstract).

Nakamura, K., 1969, Arrangement of parasitic cones as a possible key to regional stress field. *Bull. Volcanol. Soc. Japan*, **14**, 8-20 (in Japanese with English abstract).

Nishi, H., 1985, Litho- and biostratigraphy of the Oligocene-Miocene Nichinan Group in the Miyazaki Prefecture, Kyusyu. *Mem. Fac. Sci., Kyushu Univ., Ser. D, Geol.*, **25**, 289-317.

Nishi, H., 1987, Structural analysis of Tashiro Formation of Hyuga Group based on planktonic foraminiferal zonation -An example of structural analysis of accretionary prism-. *Sci. Rep., Dept. Geol., Kyushu Univ.,* **15**, 59-81 (in Japanese).

Nishi, H., 1988, Structural analysis of part of the Shimanto accretionary complex, Kyusyu, Japan, based on planktonic foraminiferal zonation. *Modern Geology*, **12**, 47-69.

Ogasawara, M., 1997, K-Ar age and geochemical characteristics of the quartz-porphyry at Shimama, southern Tanegashima, and K-Ar age of a lamprophyre from northern Tanegashima: implications for Miocene igneous activities in the Outer Zone of Southwest Japan. *Jour. Japan. Min. Pet. Eco. Geol*., **92,** 454-464 (in Japanese with English abstract).

Okada, H. and Whitaker, J. H. McD., 1979, Sand Volcanoes of the Palaeogene Kumage Group, Tanegashima, Southwest Japan. *Jour. Geol. Soc. Japan*, **85**, 187-196.

Okada, H., 1982, Depositional environments of sedimentary rocks in the Shimanto Belt: the case of the Kumage Group in Tanegashima Island. *Geol. Soc. Japan, Abstracts, **89th** Ann. Meeting.*, 80-81 (in Japanese).

Okada, H., Okabe, K. Suzuki, K. and Nakaseko, K., 1982, Radiolarian assemblages of the Kumage Group (Shimanto belt) in Tanegashima, Southwest Japan. *News Osaka Micropaleont. Spec. Vol.**5**,* 409-413 (in Japanese with English abstract).

Okino, K., Ohara,Y., Kasuga, S. and Kato, Y., 1999, The Philippine Sea: New survey results reveal the structure and the history of the marginal basins *Geophys. Res. Lett*., **26,** 2287-2290.

Park, J.-O., Tokuyama, H., Shinohara, M. and Taira, A., 1998, Seismic record of tectonic evolution and backarc rifting in the southern Ryukyu island arc system. *Tectonophysics*, **294**, 21-42.

Pedersen, S.A.S., 1996, Progressive glaciotectonic deformation in Weichselian and Palaeogene deposits at Feggeklit, northern Denmark. *Bulletin of the Geological Society of Denmark*, **42**, 153–174.

Pedersen, S.A.S., 2014, Architecture of Glacial complexes. *Geosciences*, **4**, 269-296. Doi:10.3390/geosciences4040269

Pickering, K.T., Hiscott, R.N. and Hein, F.J., 1989, Deep-marine environments: clastic sedimentation and tectonics. *Unwin Hyman, London,* 416.

Price, P.B. and Walker, R.M., 1963, Fossil tracks of charged particles in gneiss and age of minerals. *Jour. Geophys. Res*., **68**, 4847-4862.

Roberts, J.L., 1982, introduction to geological maps and structures. Pergamon Press Ltd.

Ruh, J.B., Kaus, B.J.P. and Burg, J.-P. (2012), Numerical investigation of deformation mechanics in fold-and-thrust belts: Influence of rheology of single and multiple dИcollements, *Tectonics*, **31**, TC3005 Doi:10.1029/2011TC003047

Saito, M., Kawakami, S. and Ogasawara, M., 2007a, Establishment of stratigraphic framework of the Shimanto accretionary complex in Yakushima Island, Japan, based on newly found Eocene radiolarian fossils. *Jour. Geol. Soc. Japan*, **113**, 266-269.

Saito, M., Ogasawara, M., Nagamori, H., Geshi, N. and Komazawa, M., 2007b, *Geological map of Japan 1:200,000, Yakushima*. Geol. Surv. Japan (in Japanese with English abstract).

Saitoh, Y., Tamura, T. and Masuda, F., 2005, Characteristics of hyperpycnal flow and its deposits as an innovative factor for the turbidite paradigm. *Journal of Geography*, **114**, 687-704 (in Japanese with English abstract).

Sakai, H., 1988a, Toi-misaki olistostrome of the Southern Belt of the Shimanto Terrane, South Kyushu - Ⅰ. Reconstruction of depositional environments and stratigraphy before the collapse. *Jour. Geol. Soc. Japan*, **94**, 733-747 (in Japanese with English abstract).

Sakai, H., 1988b, Toi-misaki olistostrome of the Southern Belt of the Shimanto Terrane, South Kyushu - Ⅱ. Deformation structures of huge submarine slides and their processes of formation. *Jour. Geol. Soc. Japan*, **94**, 837-853 (in Japanese with English abstract).

Sakai, H., 1988c, Origin of the Misaki Olistostrome Belt and re-examination of the Takachiho Orogeny. *Jour. Geol. Soc. Japan*, **94**, 945-961 (in Japanese with English abstract).

Sakai, T. and Fukuda, Y., 1994, Eocene sedimentary tectonics along the convergent margin of the Philippine Sea Plate: axial and lateral flows in forearc region. *Geol. Soc. Japan, Abstracts, **101th** Ann. Meeting.*, 145-145 (in Japanese).

Sakai, T., 1980, Mode of occurrence and origin of greenstones in the Shimanto Terrain in Tane-ga-shima and Yaku-shima Island, Ryukyu Arc. *In Geological Studies of the Ryukyu Island*, edited by Kizaki, K., **5**, 27-37 (in Japanese with English abstract).

Sakai, T., 1985, Geology of the Nichinan Group and the process of production of the outermargin olistostrome belt of the Shimanto

Terrane. *In* Memoirs of the Symposium on Formation of Slump Facies and Its Relation to Tectonics - Some Problems on the Deformation of unconsolidated sediments - *,Tectonic Research Group of Japan , Research Group of the Clastic Sediments in Japan*, 95-116 (in Japanese with English abstract)..

Sakai, T., 1988, Tectono-stratigraphic feature of the Paleogene subduction complex in Kyushu and Ryukyu arc and their comparison. *Geol. Soc. Japan, Abstracts, **95th** Ann. Meeting.*, 484(in Japanese).

Sakai, T., 1989, Accretionary deformation and their tectonic environments of the Shimanto Terrane in Kyusyu. *Jour. Tectonics Res. Japan*, **34**, 157-171 (in Japanese).

Sakai, T., 1992, Examination of the Takachiho Disturbance and plate tectonics along the margin of Southwest Japan in late Cenozoic time. *Prof. Yukio Matsumoto Mem. Vol.*, 95-106 (in Japanese with English abstract).

Sakai, T., 2010, The Southern Shimanto Belt in the Ryukyu Islands. *In* The Geological Society of Japan (ed.) *Regional Geology of Japan–Kyushu and Okinawa*, 141-149 , Asakura Publishing Co., Ltd., Tokyo (in Japanese).

Sakai, T., Nishi, H., Saito, T., Nakaseko, K. and Nishimura, A., 1984, Microfossil stratigraphy of the Paleogene System in Kyusyu Shimanto Belt. *In*, Saito, T., Okada, H., and Kaiho, K. eds., *Biostratigraphy and International Correlation of the Paleogene System in Japan*, 95-112. Yamagata Univ. (in Japanese).

Sakai, T., Ono, K., Momoki, Y., Otsuka, H. and Hayasaka, S., 1977, Geology of the Northern part of Amami-Oshima. *In* Geological studies of the Ryukyu Islands, edited by Kizaki, K., **2**, 11-23 (in Japanese with English abstract).

Sakai,T., 1994, Sedimentation of the Eocene forearc basins along the Kyushu-Ryukyu regions and spreading of the Philippine Sea Plate. *In*: *Effect of the ridge passings along the margin of Japan Arc. Grant-in-Aid for Co-operative Resarch News Lett.*, **2**, 83-102 (in Japanese).

Scott, R., and L. Kroenke, 1980, Evolution of back arc spreading and arc volcanism in the Philippine Sea: Interpretation of Leg 59 DSDP results. *In* The Tectonic and Geologic Evolution of Southeast Asian

Seas and Islands, Geophys. Monogr. Ser., **23**, (edited by D. E. Hayes), 283-291, AGU, Washington, D. C.

Seno, T. and Maruyma, S., 1984, Paleogeographic reconstruction and origin of the Philippine Sea. *Tectonophysics*, **102**, 53-84.

Seno, T. and Maruyma, S., 1985, Tectonics of the Philippine Sea. *Jour. Geogr.,* 94, 141-155.

Shibata, K. and Nozawa, T., 1968, K-Ar ages of Yakujima Granite,Kyushu, Japan. *Bull. Geol. Surv. Japan*, **19**, 237-241.

Stow, D.A.V., 2010, Sedimentary rocks in the field: A colour guide. *Manson publishing,* 1-320.

Strachan, L.J. and Also, G.I., 2006, Slump folds as estimators of paleoslope: a case study from the Fisherstreet Slump of County Clare, Ireland. *Basin Research*, 18, 451-470. Doi:10.1111/j.1365-2117.2006.00302.x

Suzuki, Y. and Ujiie, H., 1985, *Nummulites amakusaensis* from the Kayo Formation and its significance on the Ryukyu Island arc development. *Chikyukagaku* (*Earth Sci.*)*,* **39**, 385-388.

Taira, A., 2001, Tectonic evolution of the Japanese Island arc system: *Annu. Rev. Earth Planet. Sci.*, **29**, 109-134.

Taira, A., Okada, H. and Whitaker, J.H. McD., 1988, The Shimanto belt of Japan: Cretaceous-lower Miocene active-margin sedimentation. *Modern Geology*, **12**, 5-26.

Takamura, H., 1978, Finding of spinel-lherzolite xenolith in basaltic sheets from Shingu, Ehime Prefecture, Japan. *Jour. Geol. Soc. Japan*, **84**, 475-479 (in Japanese).

Taneda, S. and Kinoshita, K., 1972, An Alkaline Rock Body in Tanegashima Island, South Kyushu, Japan. *Bull. Volcanol. Soc. Japan, Ser.* 2, **17**, 88-97 (in Japanese).

Taylor, B., 1992, Rifting and the volcanic-tectonic evolution of the Izu-Bonin-Mariana Arc. *In* Taylor, B., Fujioka, K., et al., *Proc. ODP, Sci. Results,* **126**: College Station, TX (Ocean Drilling Program), 627–651.

Teraoka, Y., Okumura, K., Suzuki, M. and Kawakami, K., 1999, Clastic sediments of the Shimanto Supergroup in Southwest Japan. *Bull. Geol. Surv. Japan*, **50**, 559-590.

Torii, M., Hayashida, A. and Otofuji, Y.,1985, Rotation of

Southwest Japan and the origin of Japan Sea, *Kagaku (Science), Iwanami Book Co*, **55**, 47-52 (in Japanese).
Ujiie, H. and Iwasaki, T., 1987, Imbricated thrust-fold zone recognized in the Eocene Kayo formation of the northern Okinawa Islands. *Bull. fac. Sci. Univ. Ryukyus,* **45**, 253-278 (in Japanese with English abstract).
Ujiie, H., 1989, Eocene foreland thrust-fold belt of the central Ryukyu Island Arc: Deduced from sedimentary structures in the Kayo Formation. *Facies in the Active Margin,* edited by Taira, A. and Masuda, F., 711-722.
Ujiie, K., 1997, Off-scraping accretionary process under the subduction of young oceanic crust: The Shimanto Belt of Okinawa Island, Ryukyu arc. *Tectonics*, **16**, 305-322.
Uto, K., 1995, Volcanoes and age determination: Now and future of K-Ar and $^{40}Ar/^{39}Ar$ dating *Bull. Volcanol. Soc. Japan*, **40**, s27-s46 (in Japanese with English abstract).
Uto, K., Hirai, H., Goto, K. and Arai, S., 1987, K-Ar ages of carbonate- and mantle nodule-bearing lamprophyre dikes from Shingu, central Shikoku, Southwest Japan. *Geochem. J.*, **21**, 283-290.
Wade, B.S. and Pälike, H., 2004, Oligocene climate dynamics. Paleoceanography, **19**, PA4019. Doi:10.1029/2004PA001042
Watts, A.B., Weissel, J.K. and Larson, R.L., 1977, Sea-floor spreading in marginal basins of the Western Pacific. *Tectonophysics*, **37**, 167-181. DOI: 10.1016/0040-1951(77)90046-4
Yagi, K., Ishikawa, H. and Kojima, M., 1975, Petrology of a lamprophyre sheet in Tanegashima Island , Kagoshima Prefecture, Japan. *Jour. Japan. Min. Pet. Eco. Geol*., **70** (7) 213-224.
Yagishita, K., 1992, Recent studies on some sedimentary structures formed under upper-flow-regime condition: review and discussion. *Ann. Rep. Fac. Educ., Iwate Univ.*, **52**, 85-95.
Yagishita, K., Nakazato, H., Igarashi, C. and Taira, A., 1988, Grain fabric of a laboratory antidune. *Jour. Geol. Soc. Japan*, **94**, 55-57 (in Japanese with English abstract).
Yamamoto, T., 1991, Late Cenozoic dike swarms and tectonic stress field in Japan. *Bull. Geol. Surv. Japan*, **42**, 131-148.

Appendix

List of Figures

List of Tables

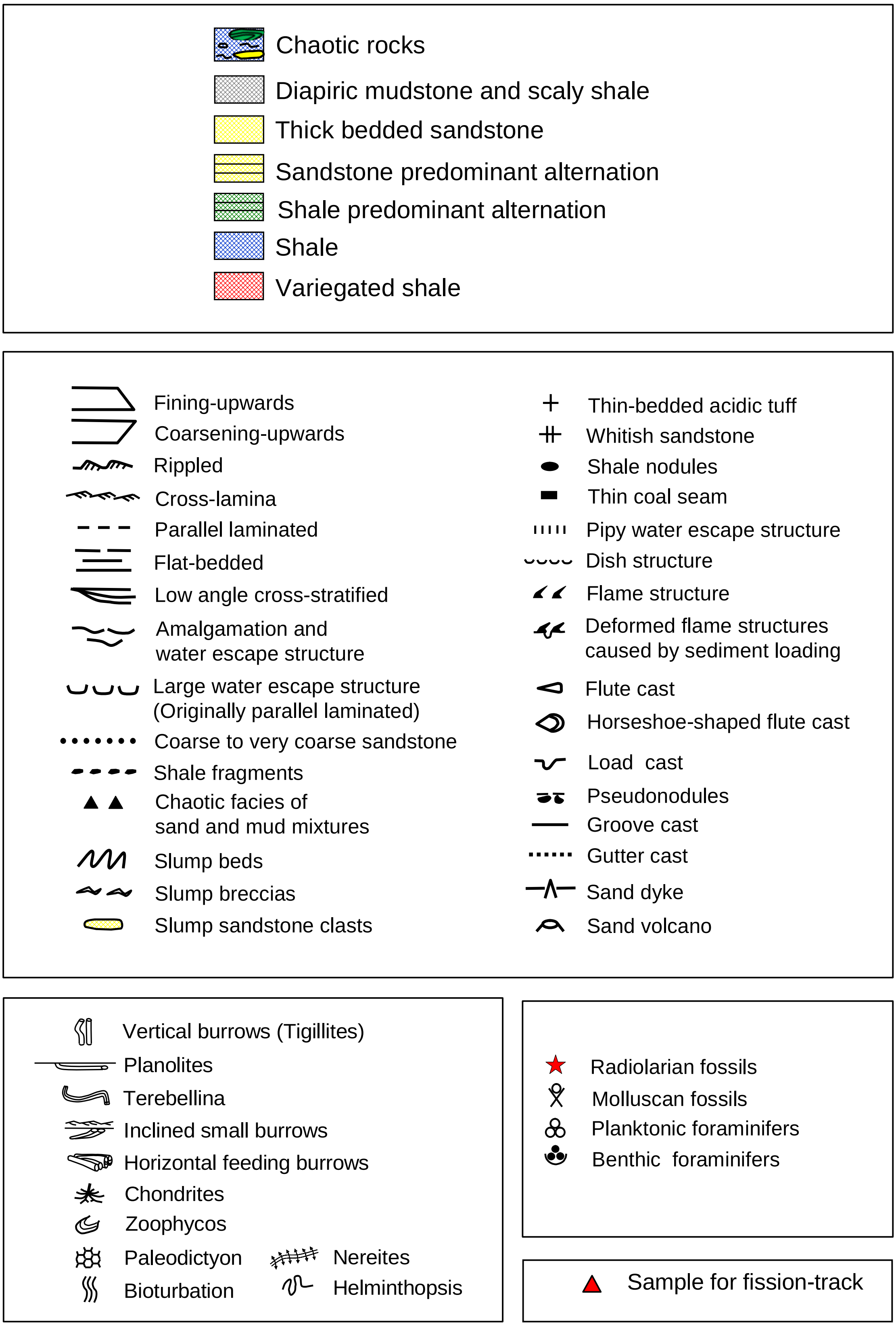

Fig.1 Legend for lithologic columns.

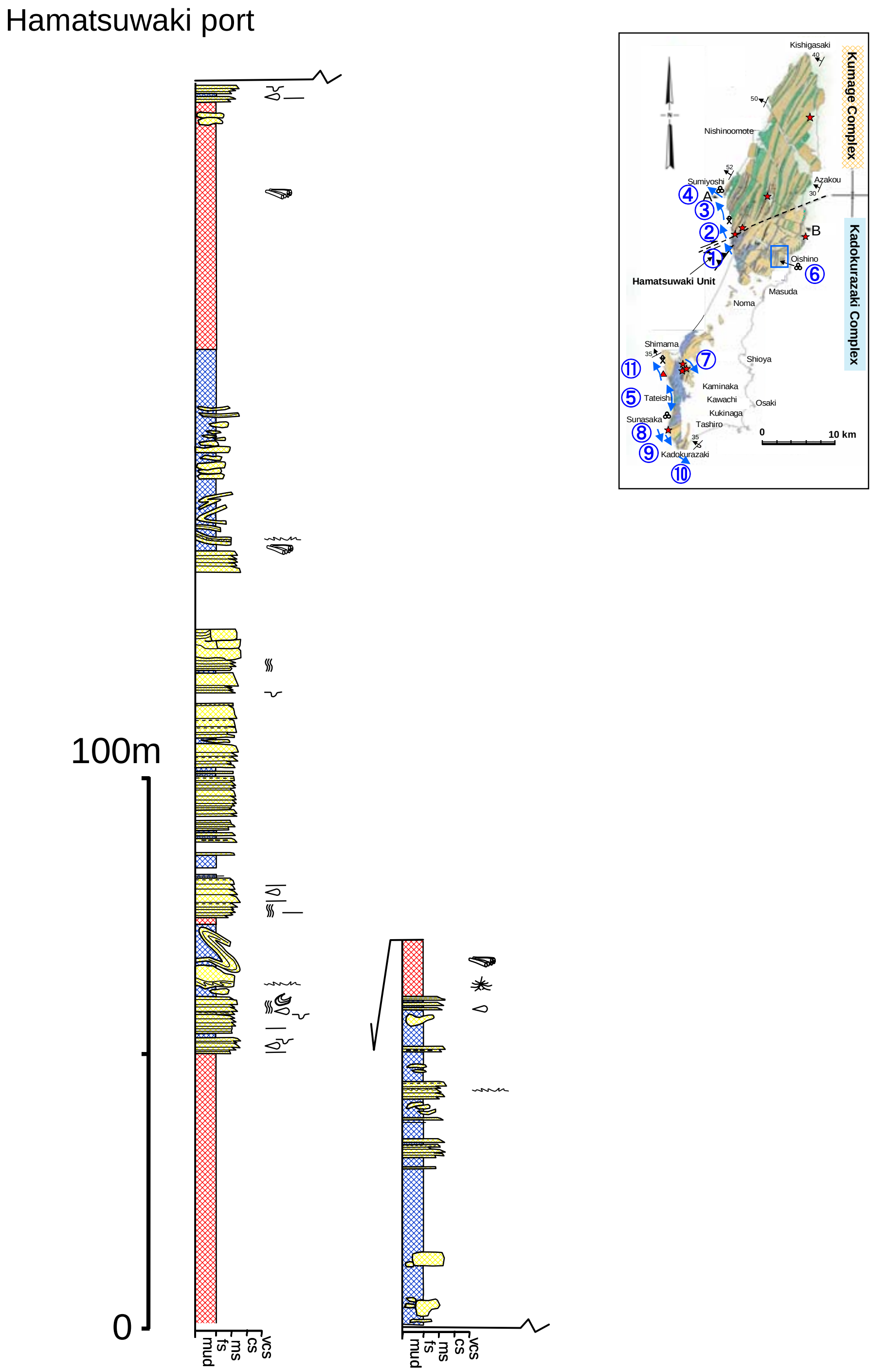

Fig.2 Lithologic columns of Section ①. This section named the Hamatsuwaki Unit in the Kumage Complex was measured along the Hamatsuwaki coast area, showing the variegated shale containing slump beds and sandy turbidite.

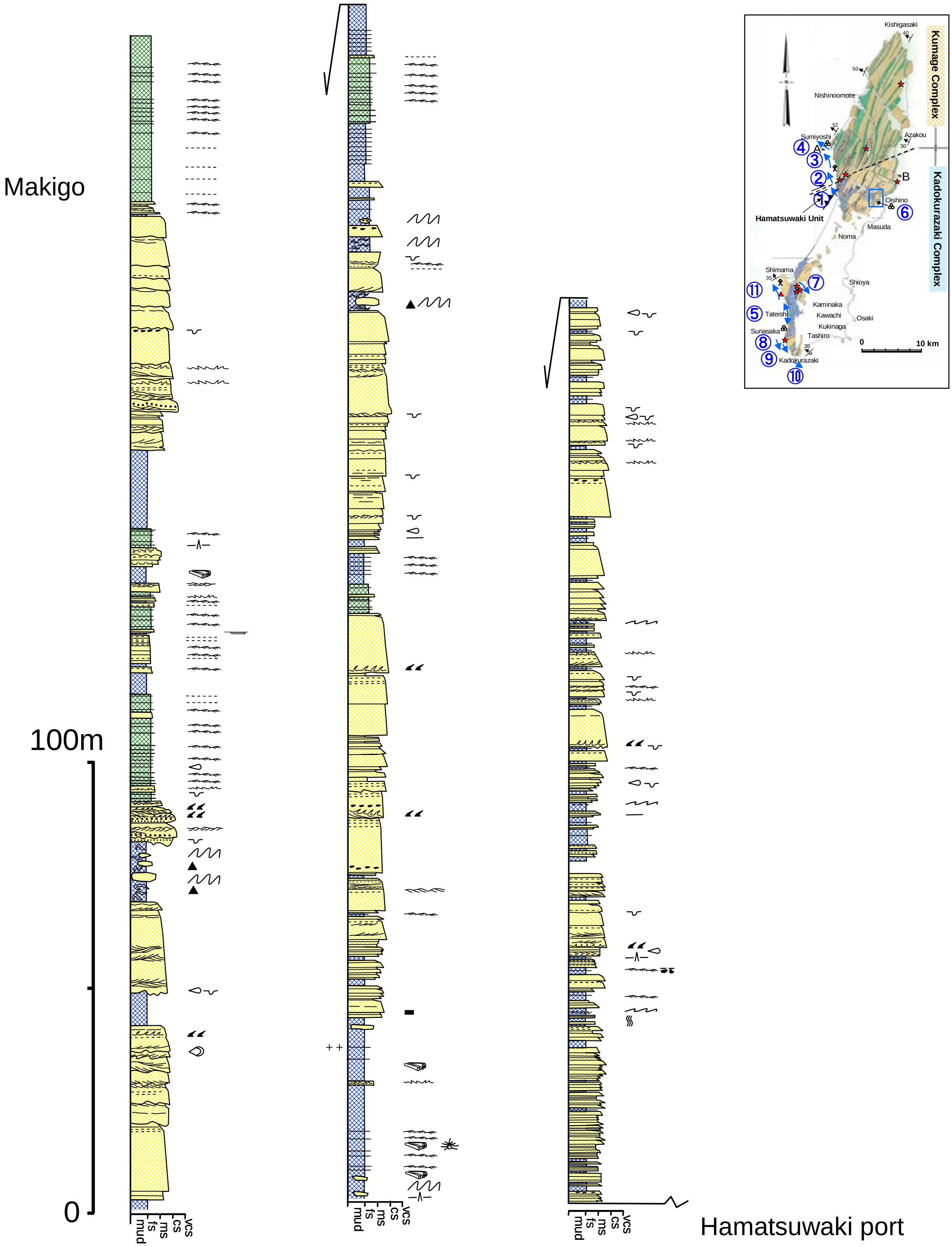

Fig.3 Lithologic columns of the lower and middle part of Section ②. This section named the Fukago Unit in the Kumage Complex was measured along the Hamatsuwaki and Makigo coastal areas.

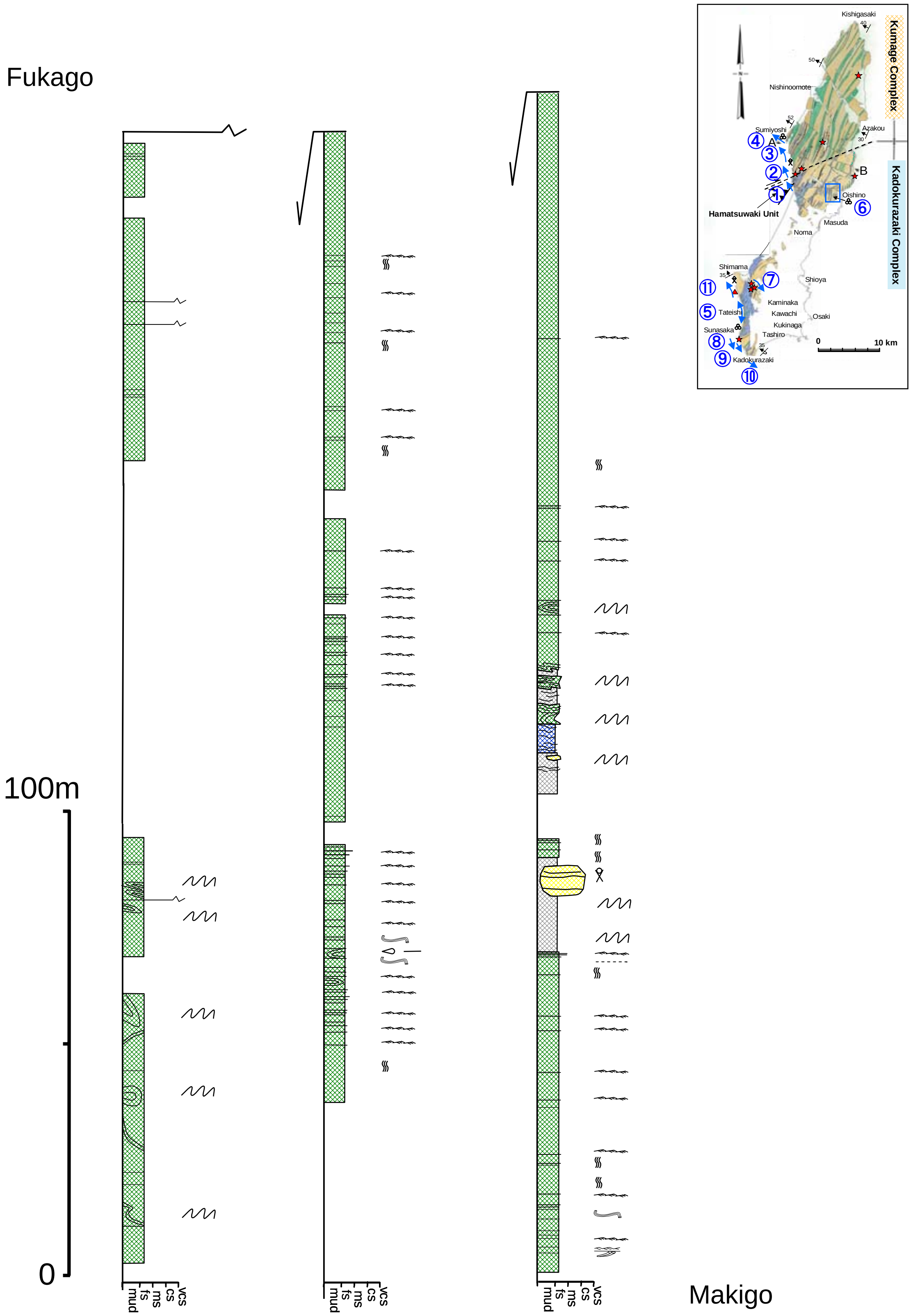

Fig.3 (continued). Lithologic columns of the upper part of Section ②. The Fukago Unit in the Kumage Complex was measured between the Makigo and Fukago coastal areas.

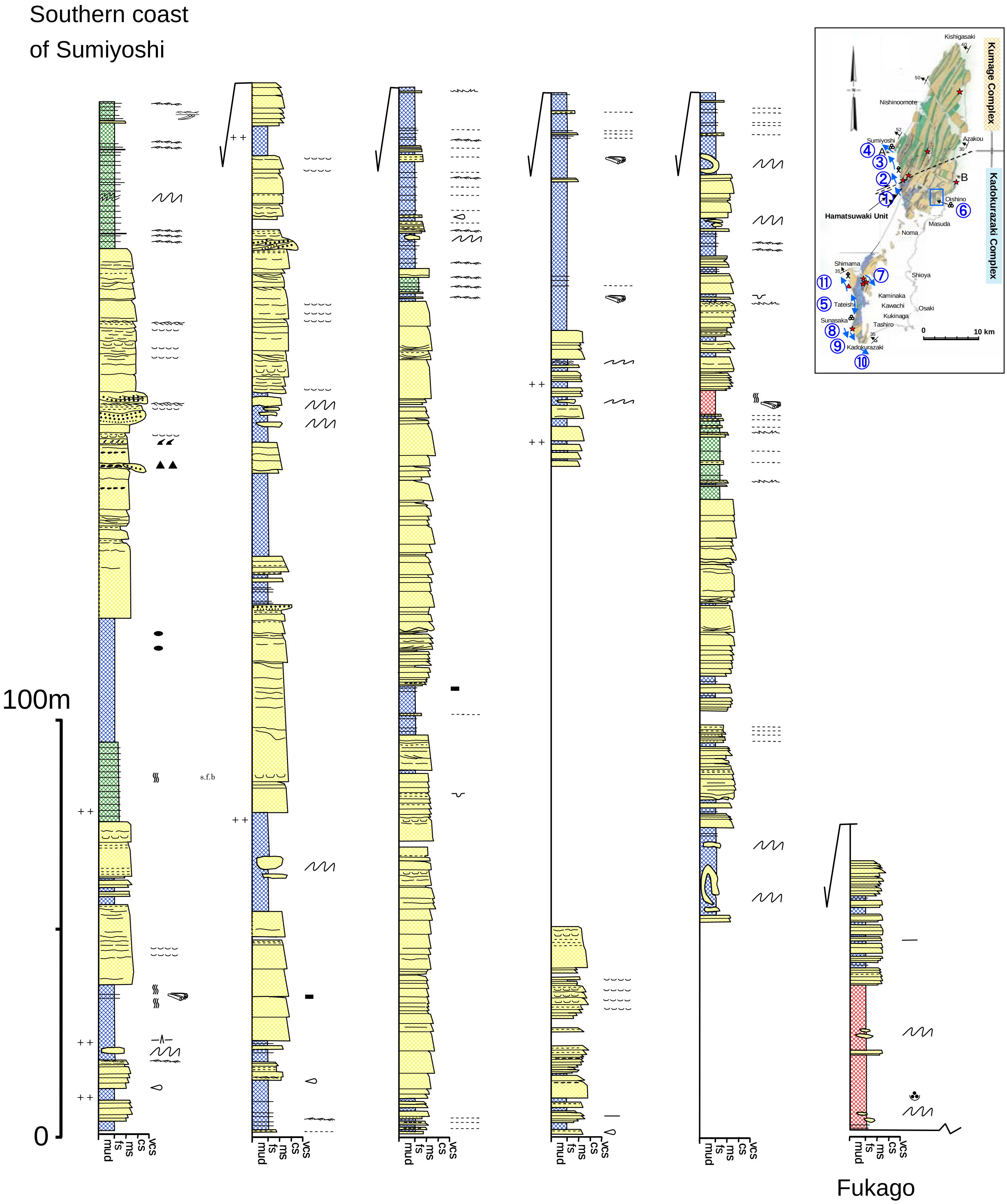

Fig.4 Lithologic columns of the lower part and middle part of Section ③. The Fukago Unit in the Kumage Complex was measured between the Fukago and Sumiyoshi coastal area. (s.f.b : small feeding bullows).

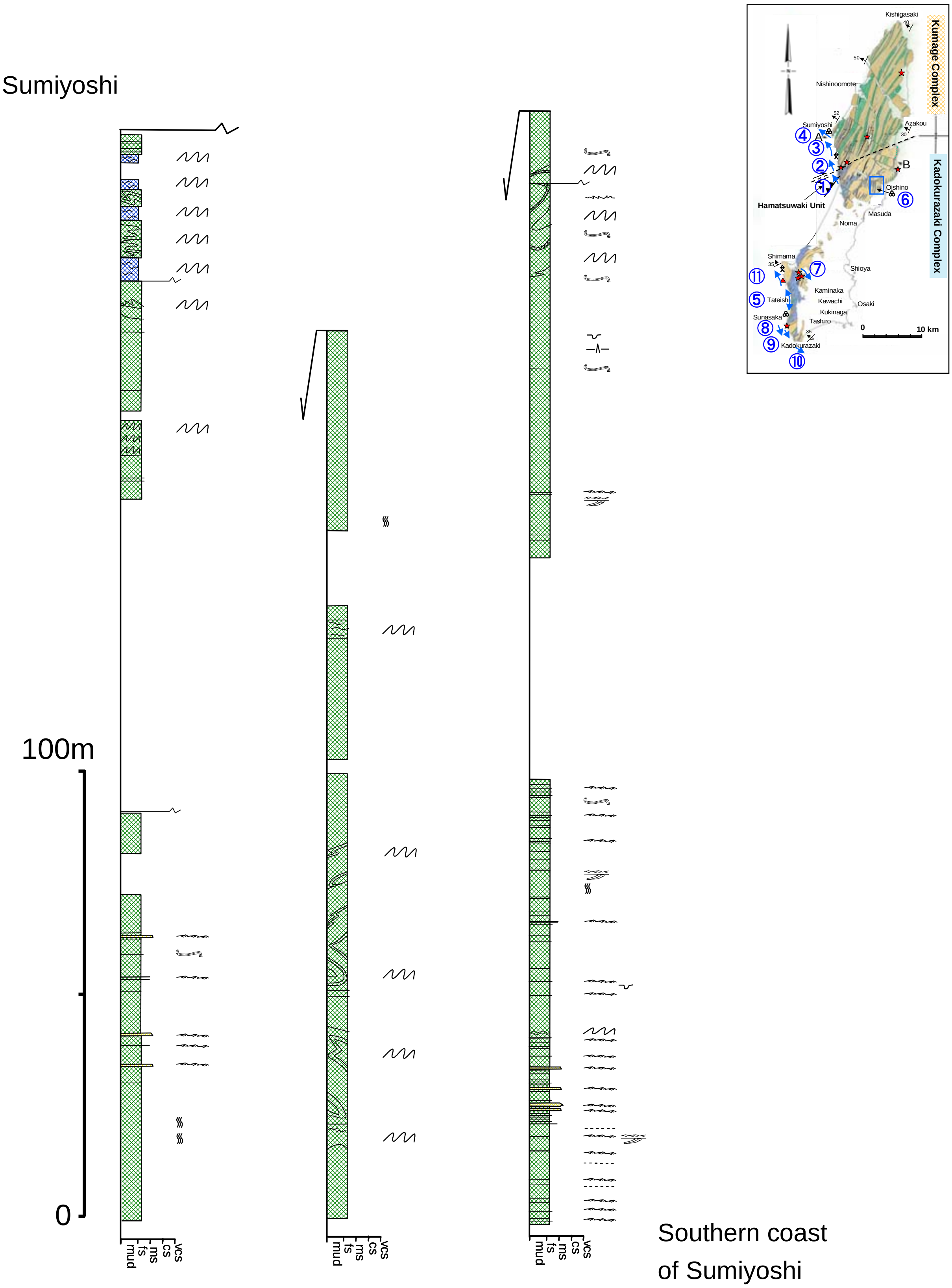

Fig.4 (continued). Lithologic columns of the upper part of Section ③. The Fukago Unit in the Kumage Complex was measured between the Fukago and Sumiyoshi coastal areas.

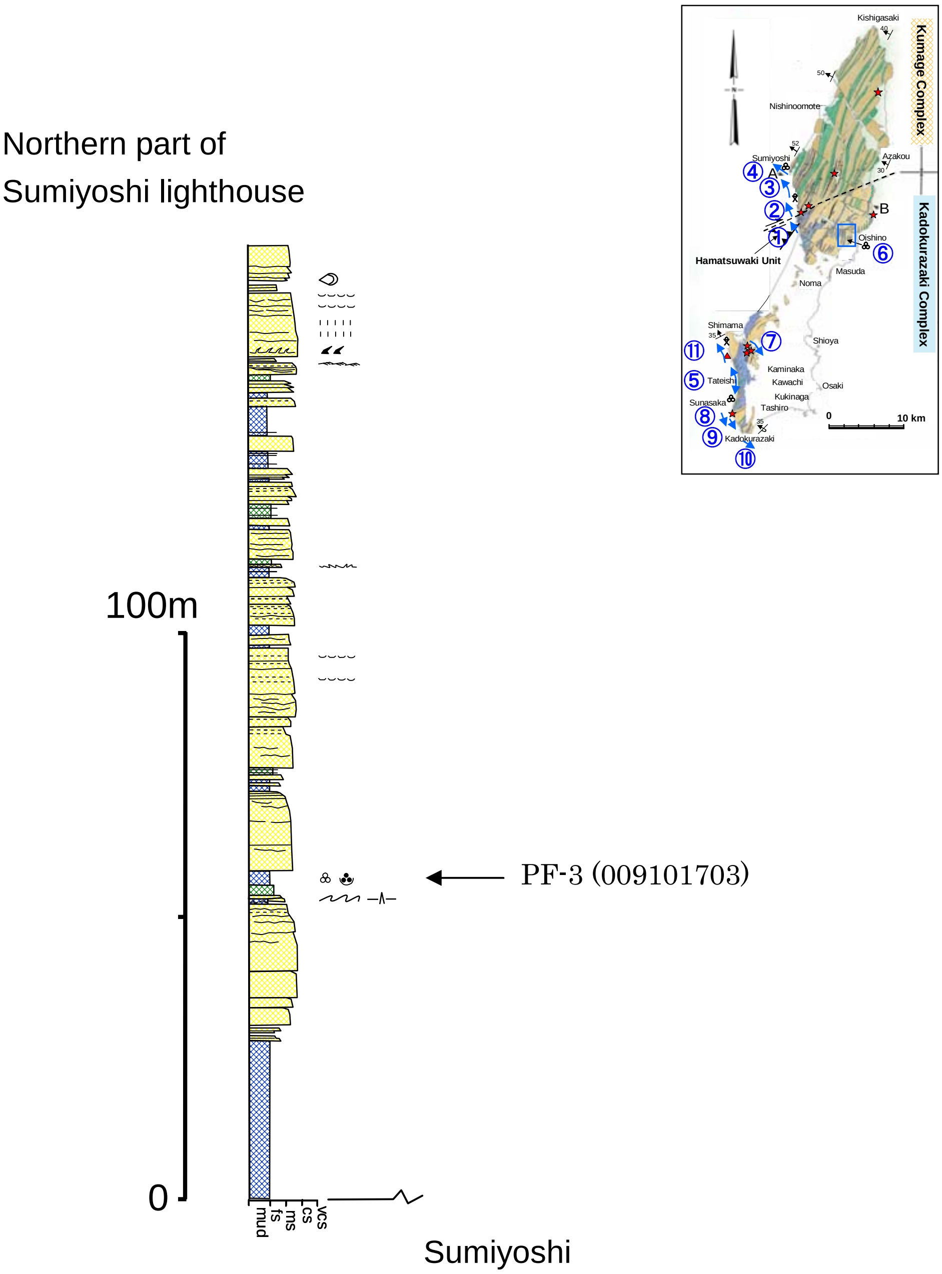

Fig.5 Lithologic column of Section ④. This section named the Sumiyoshi Unit in the Kumage Complex was measured on the Sumiyoshi coastal area. This Section yields planktonic foraminifers and benthic foraminifers (PF-3).

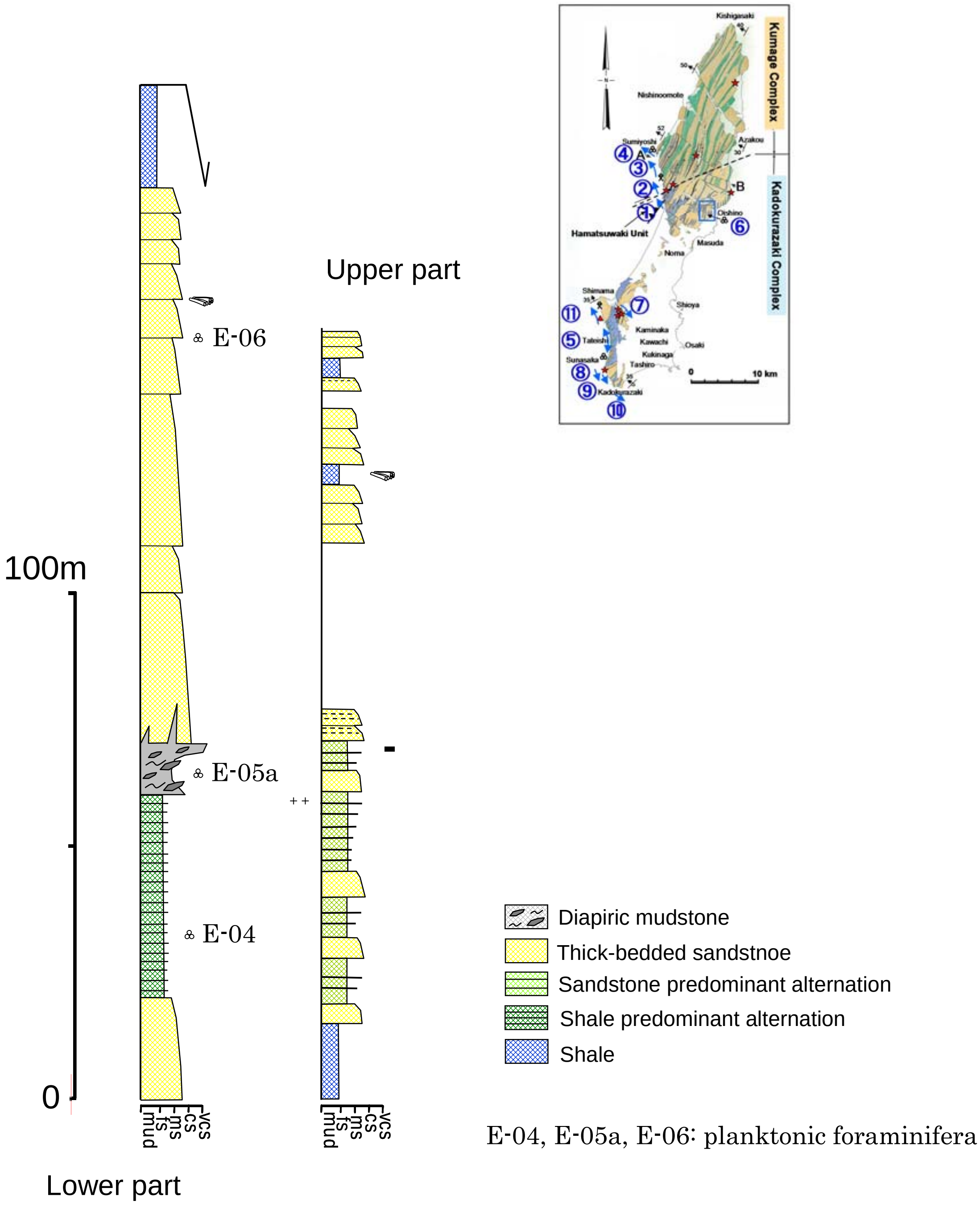

Fig.6 Lithologic columns of Section ⑥. This section is lcated in the eastern aria of airport (Oishino area) belonging to the Kadokurazaki Complex and contains the diapiric mudstone. Sample numbers (E-04, E-05a and E-6) indicate stratigraphic positions of samples yielding planktonic foraminifers.

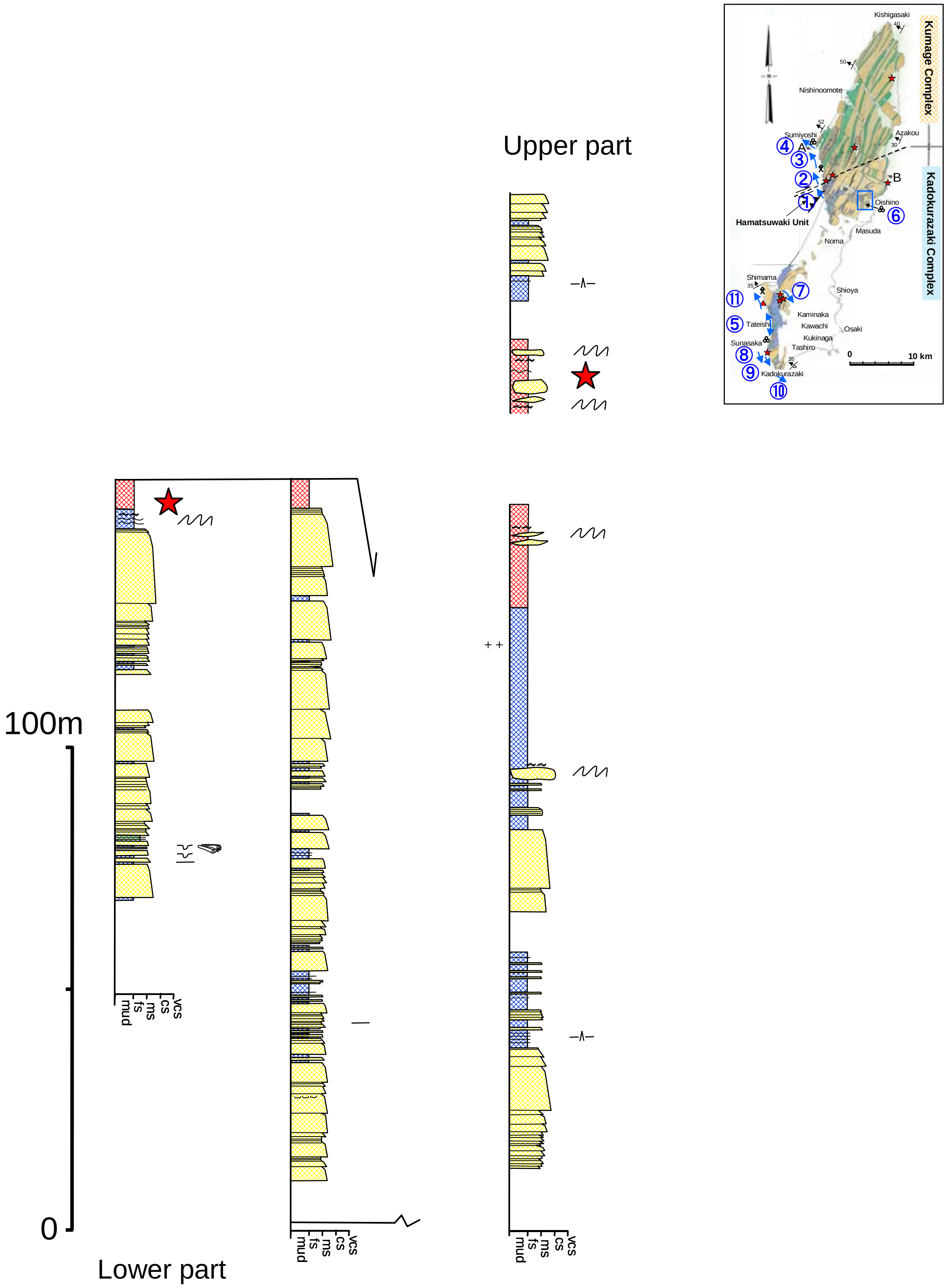

Fig.7 Lthologic columns of Section ⑦. This section in the Kadokurazaki Complex was measured along the road between Shimama and Kaminaka, showing the turbidite sequences intercalated with shale and variegated shale beds.

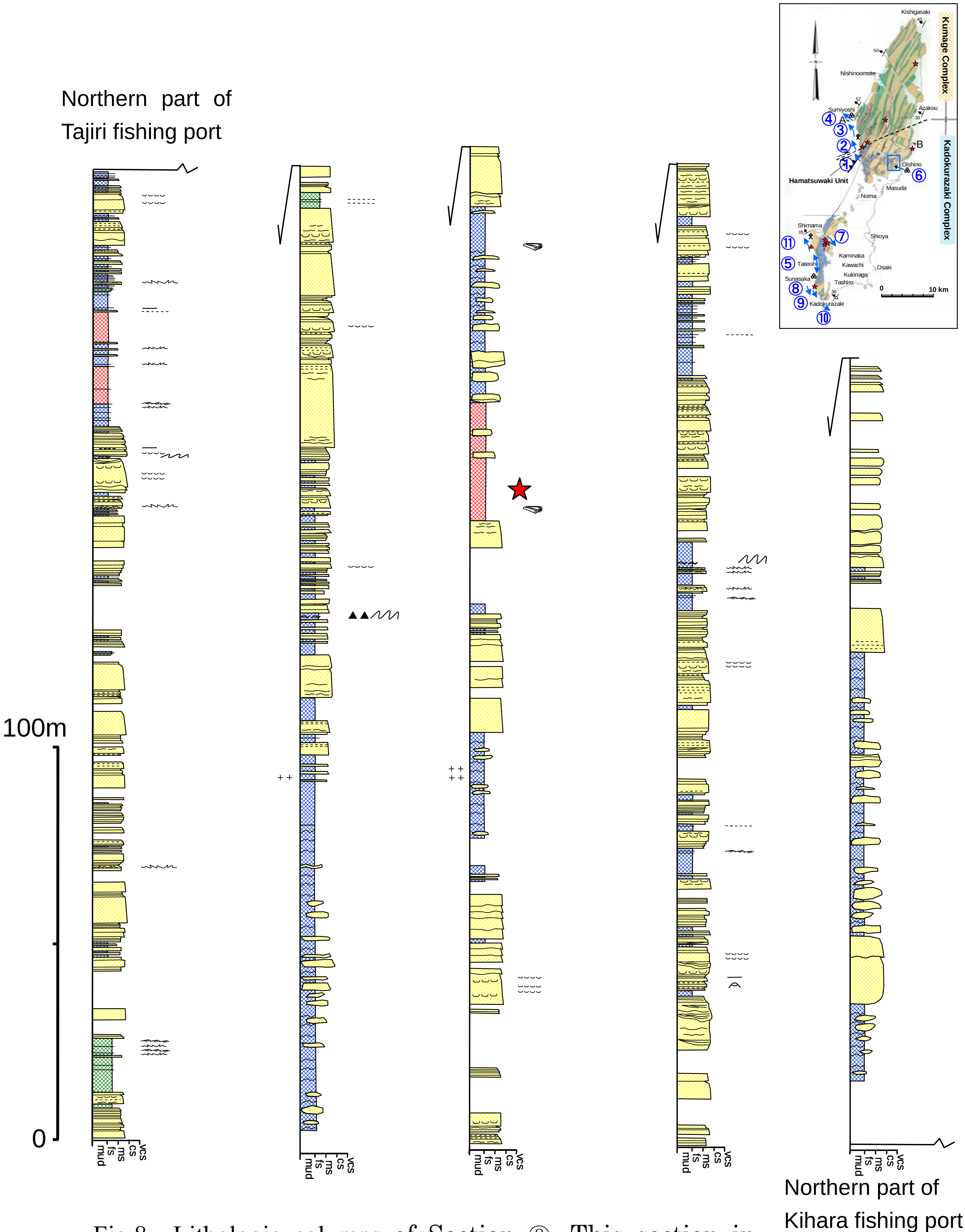

Fig.8 Lithologic columns of Section ⑧. This section in the Kadokurazaki Complex was measured between the Kihara and Oda coastal areas. This Section ⑧ contains intercalations of variegated shale beds in the middle and upper parts.

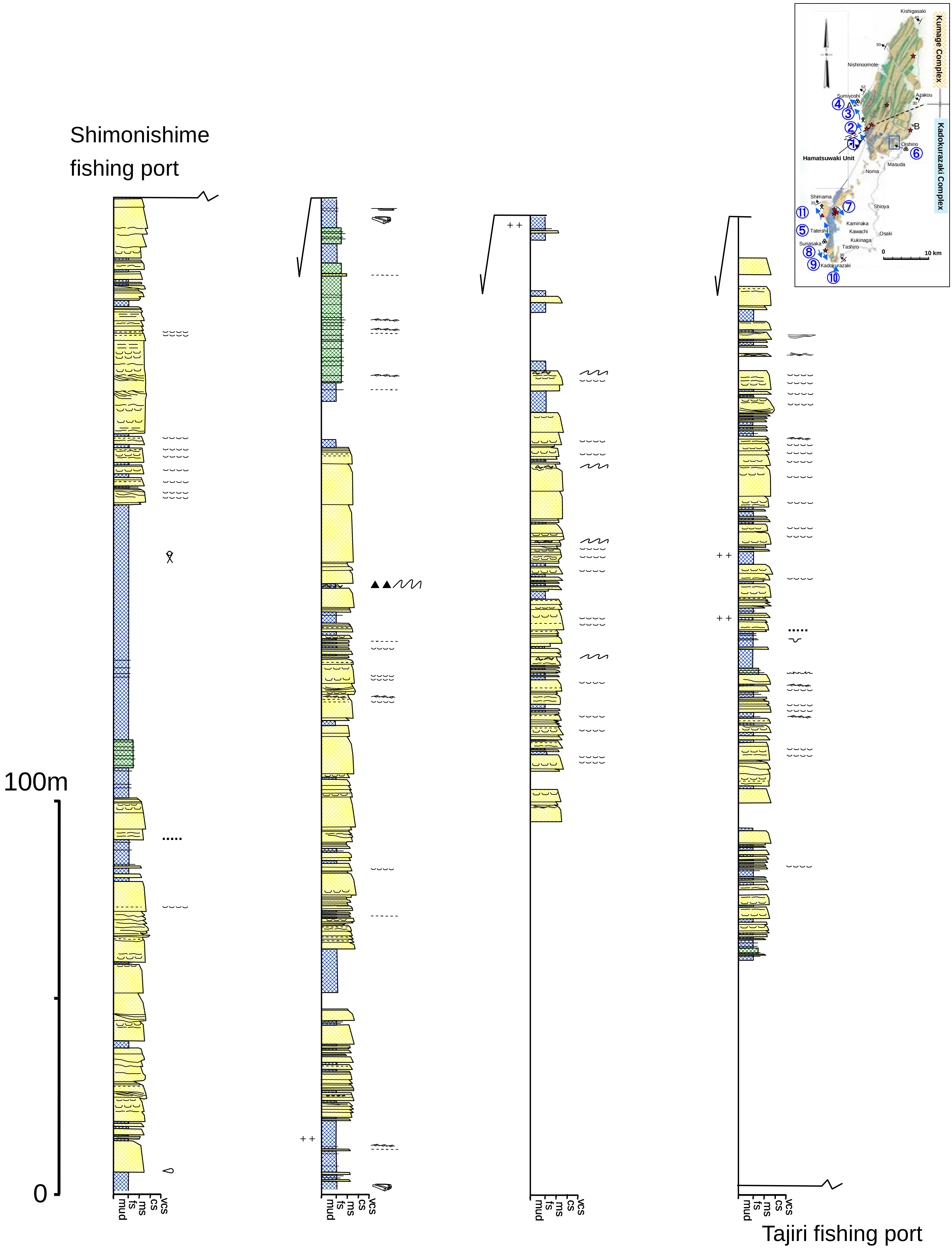

Fig.9　Lithologic columns of Section ⑨. This section in the Kadokurazaki Complex was measured between the Oda and Shimonishime coastal areas. The shale dominant beds in the upper part yield small molluscan fossils (probably *Nuculidae*).

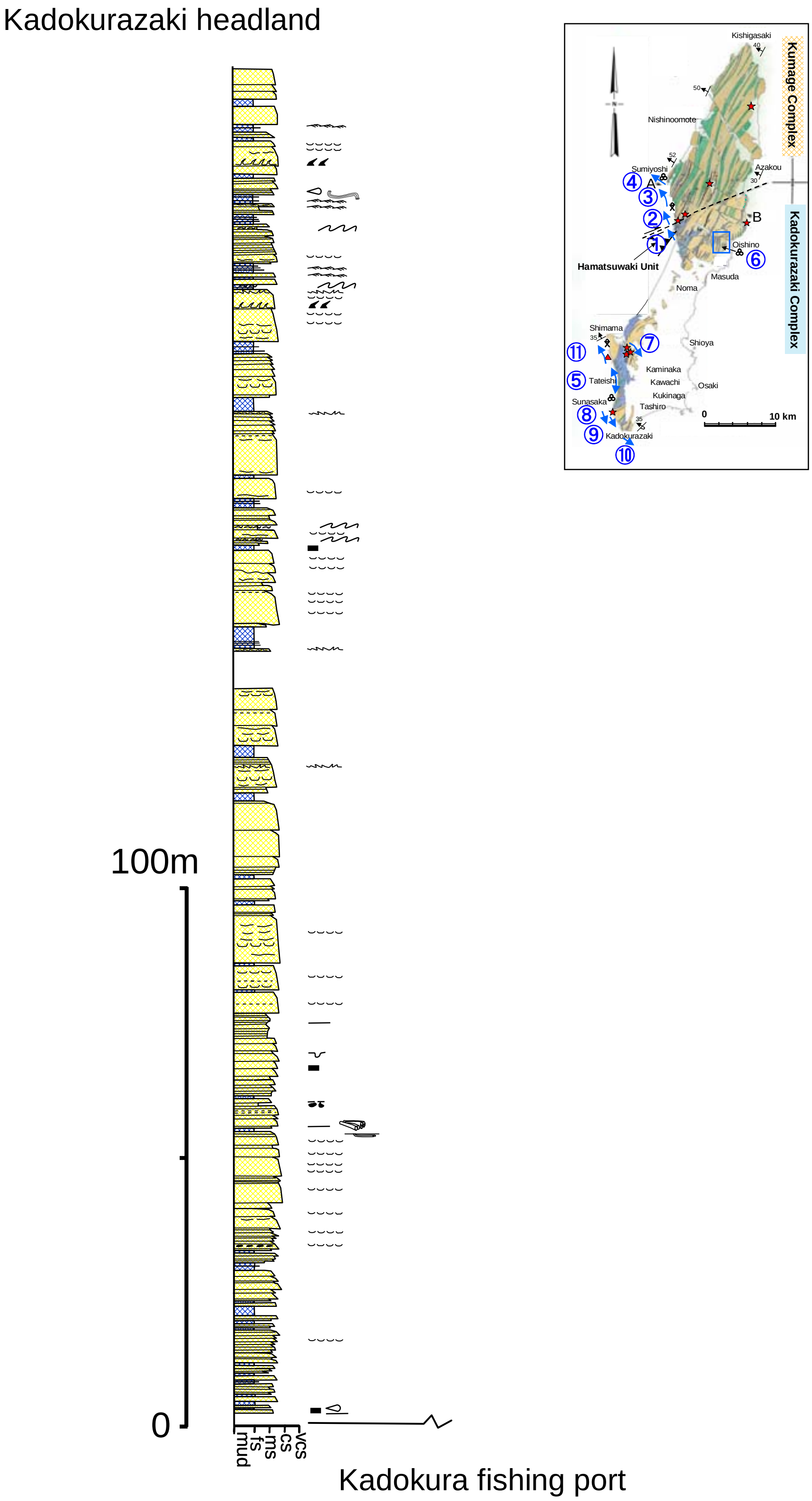

Fig.10 Lithologic column of Section ⑩. This section in the Kadokurazaki Complex was measured along the coast between the Kadokura fishing port and the Kadokurazaki headland.

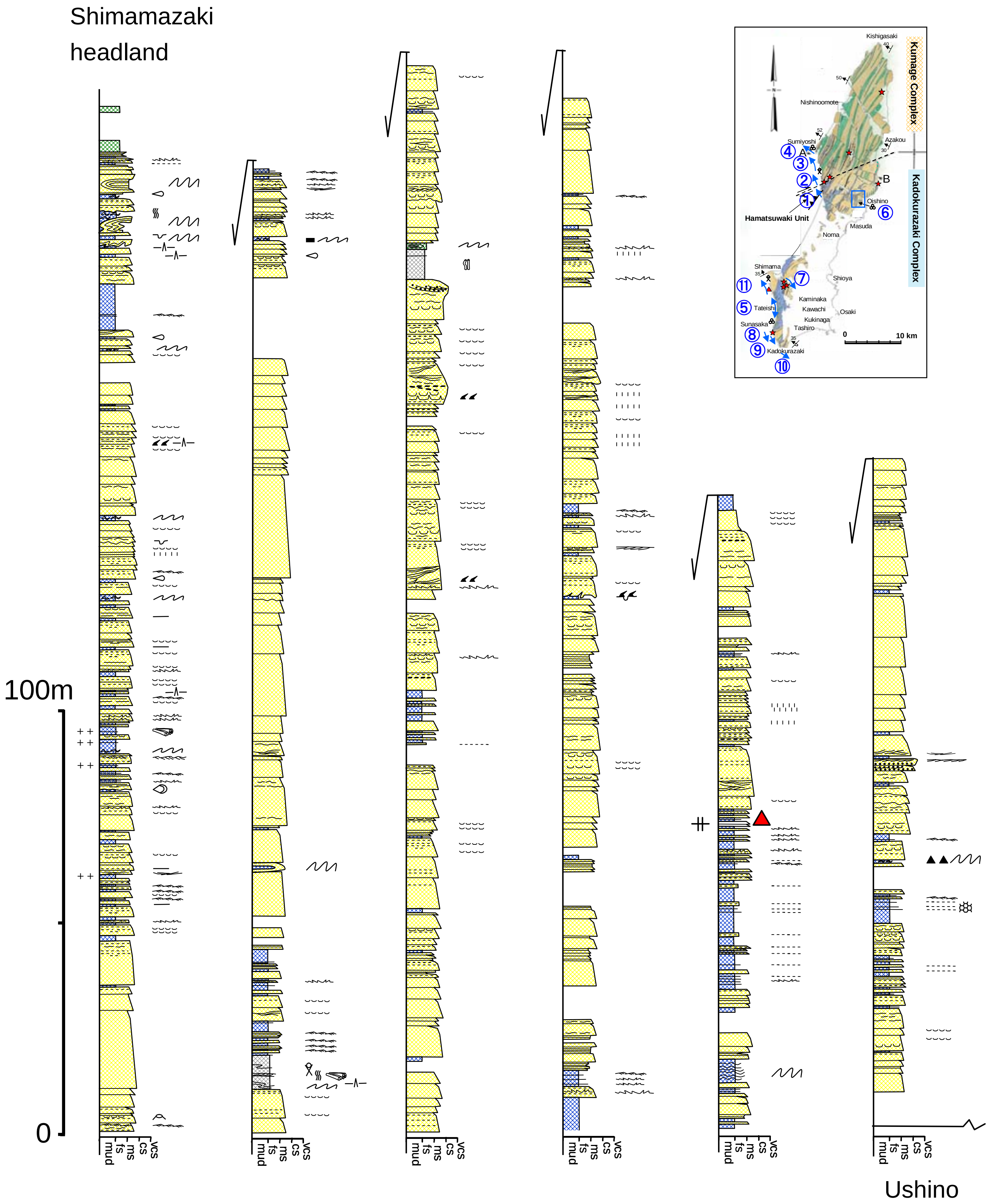

Fig.11 Lithologic columns of Section ⑪. This section named the Shimamazaki Olistolith in the Kadokurazaki Complex was measured along the coast between the Ushino and Shimamazaki headland. Red triangle stands for the stratigraphic position of fission-track dating.

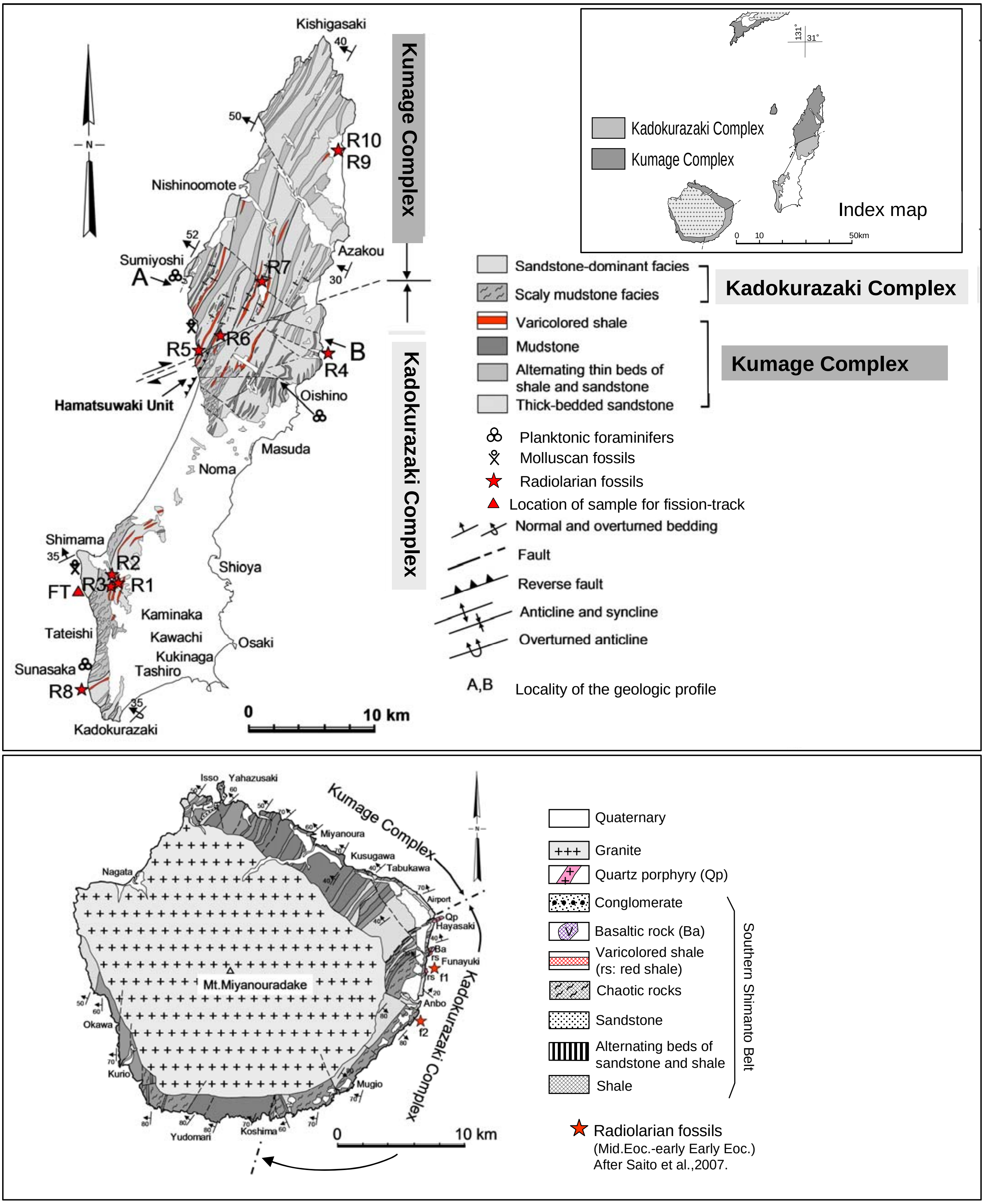

Fig.12 Locality of radiolarian fossils in Tanegasima and Yakushima. Base map of Yakushima after Sakai (2010). f1 and f2: Radiolarian-bearing localities reported by Saito et al. (2007).

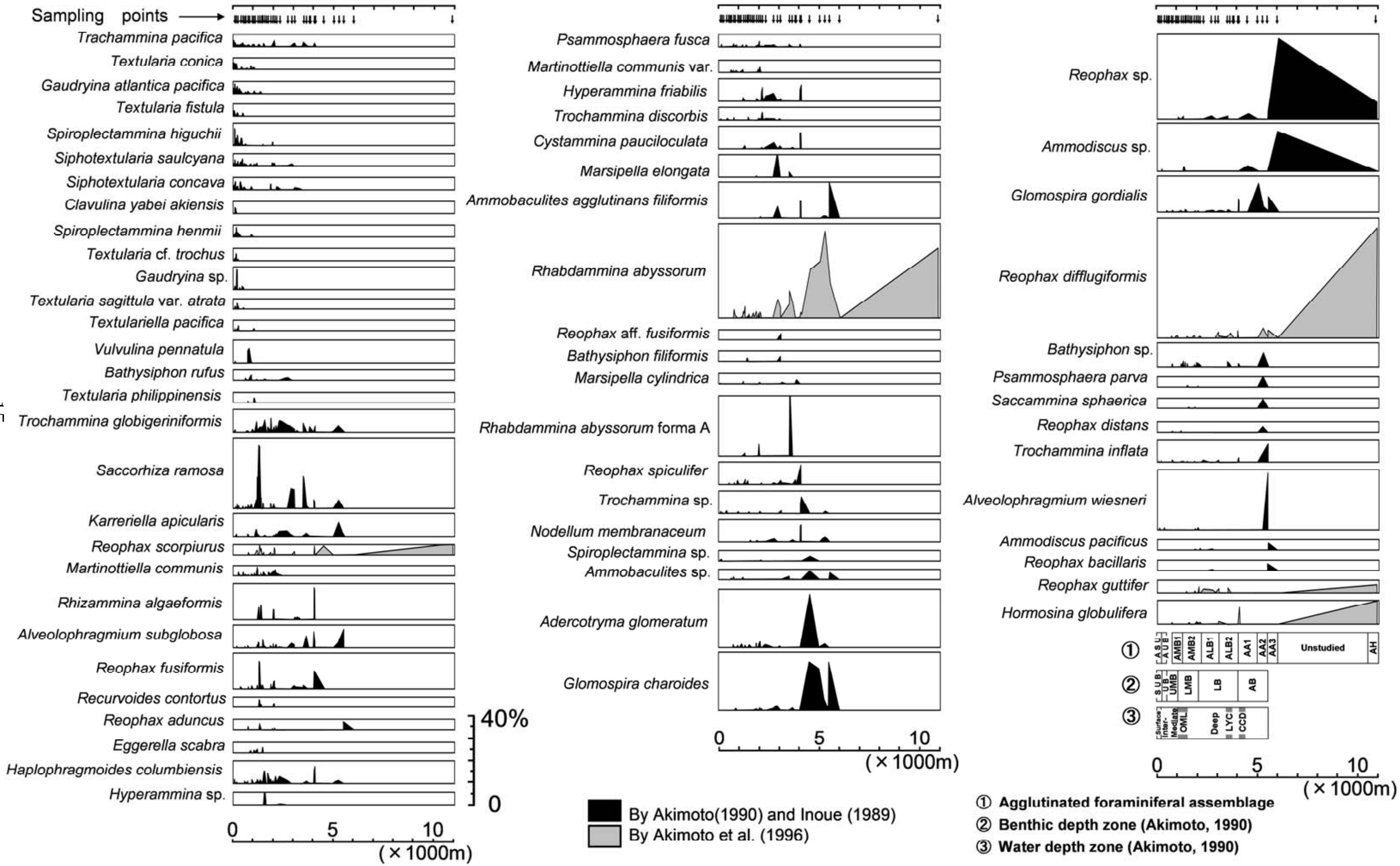

Fig.13 Depth distribution of modern agglutinated benthic foraminifers. After Akimoto *et al*. (1996).

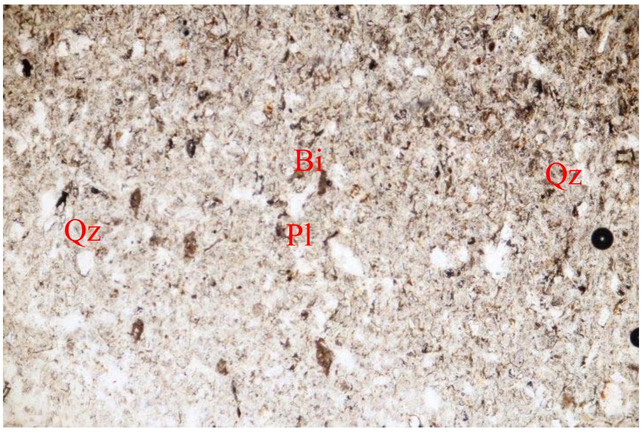

0 1mm

Parallel nicols

Crossed nicols

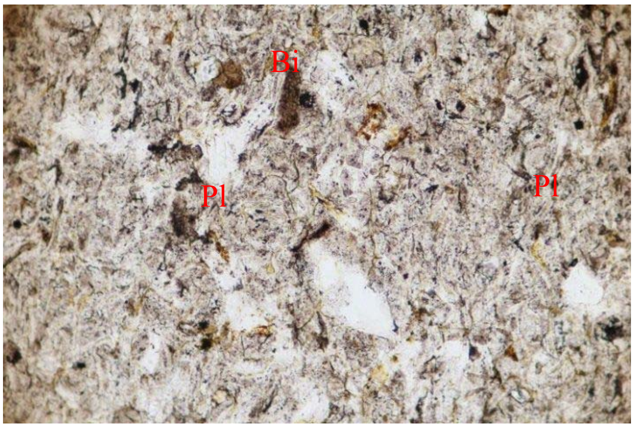

0 0.5mm

Parallel nicols

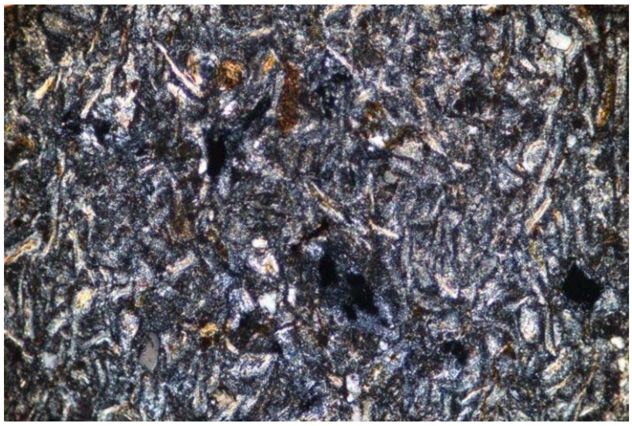

Crossed nicols

Qz: Quartz, Pl: Plagioclase, Bi: Biotite

Fig.14 Photomicrographs of grain textures in the tuffaceous sandstone.

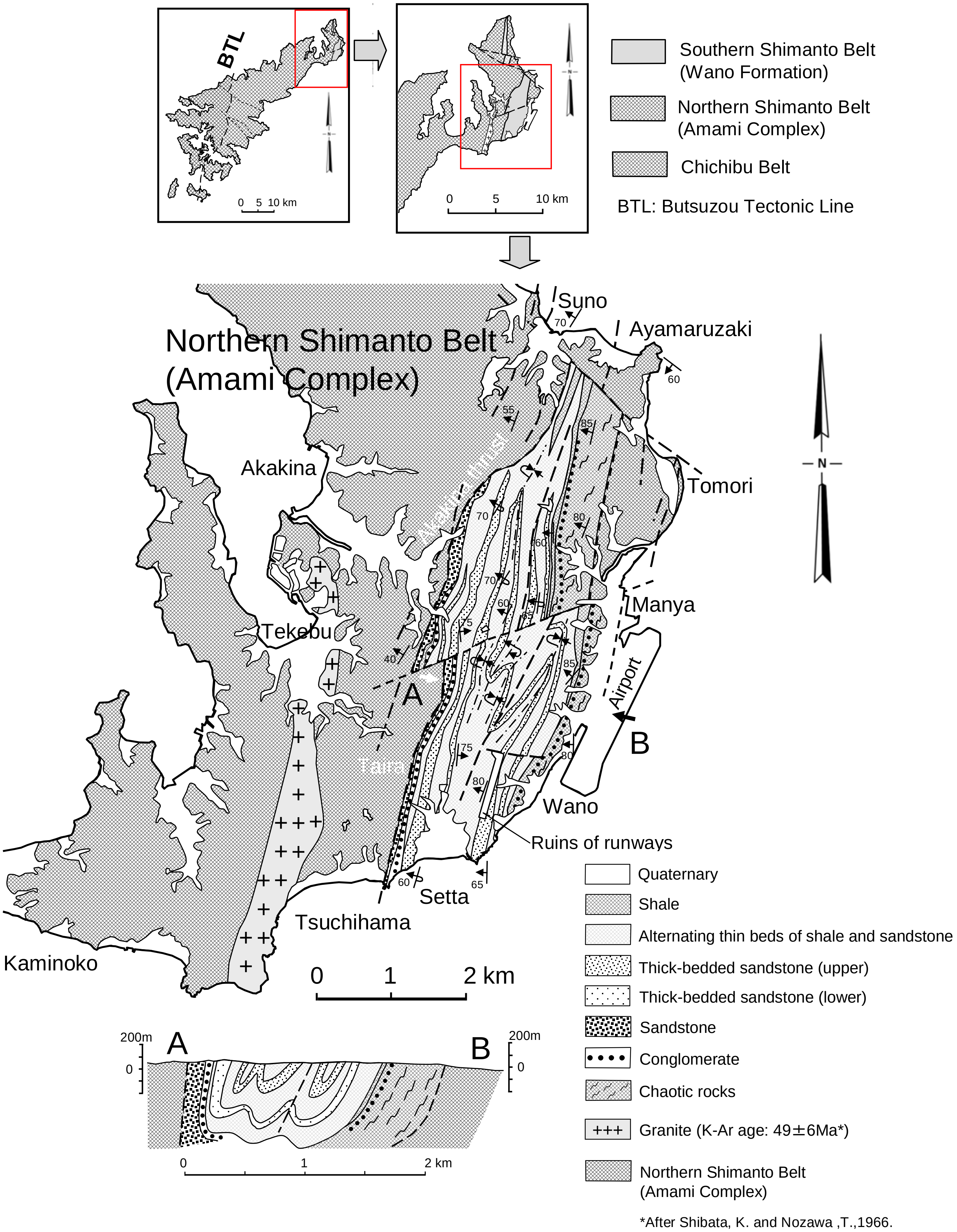

Fig.15 Geological map and profile of the Wano Formation in Amami-Oshima. Modified from Sakai (1994).

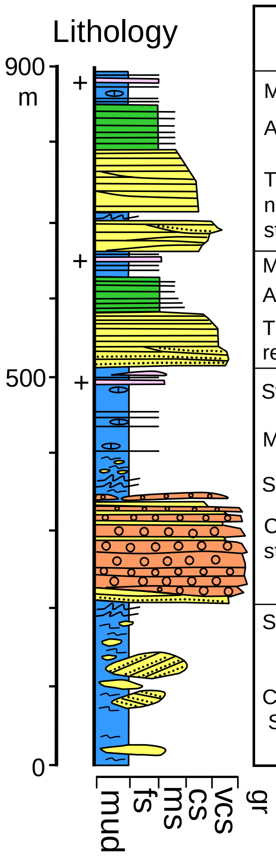

Sedimentary Facies	Interpretation
Massive to stratified mudstone containing thin acidic tuff and nodules.	Lobe fringe
Alternating thin beds of shale and sandstone (Ta,Tab).	Non channeled lobe
Thick-bedded, coarse- to medium-grained sandstone with channelized structures, normal-to-reverse grading, dish structures, convolution, and large-scale cross-stratifications.	Channeled lobe
Mudstone intercalated with thin acidic tuff	Lobe fringe
Alternating thin beds of shale and sandstone (Bouma Ta and Tab divisions).	Non channeled lobe
Thick-bedded, medium-grained sandstone with channelized structures, normal-to-reverse grading, dish structures, convolution, and large-scale cross-stratifications.	Channeled lobe
Stratified mudstone with some acidic tuff intercalations.	Lobe fringe
Massive mudstone intercalated with thin-bedded sandstone, and nodules.	Levee
Slump beds with pebbly mudstone.	
Conglomerate with reverse and normal grading, amalgamation, channelized structures.	Deep submarine channel
Slump beds.	
Chaotic mudstone including blocks of sandstone and sandy lobe deposits. Sometimes containing blocks of glauconitic sandstone.	Submarine slope failure deposits

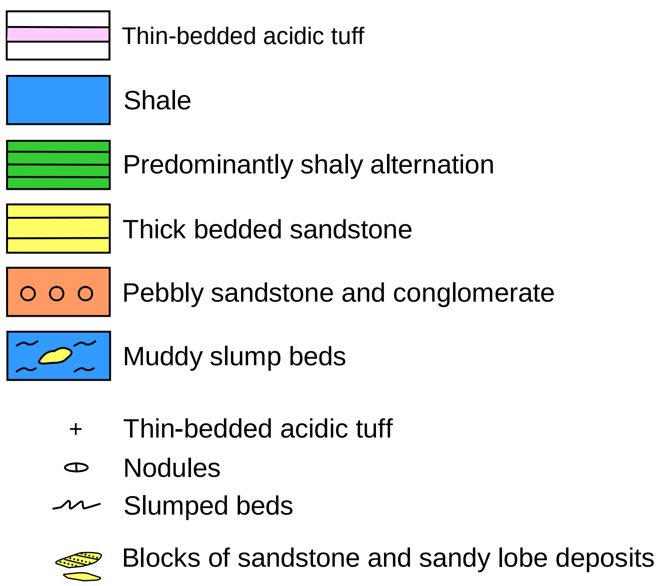

Fig.16 Sedimentary facies and depositional environments of the Wano Formation. Modified from Sakai (1994).

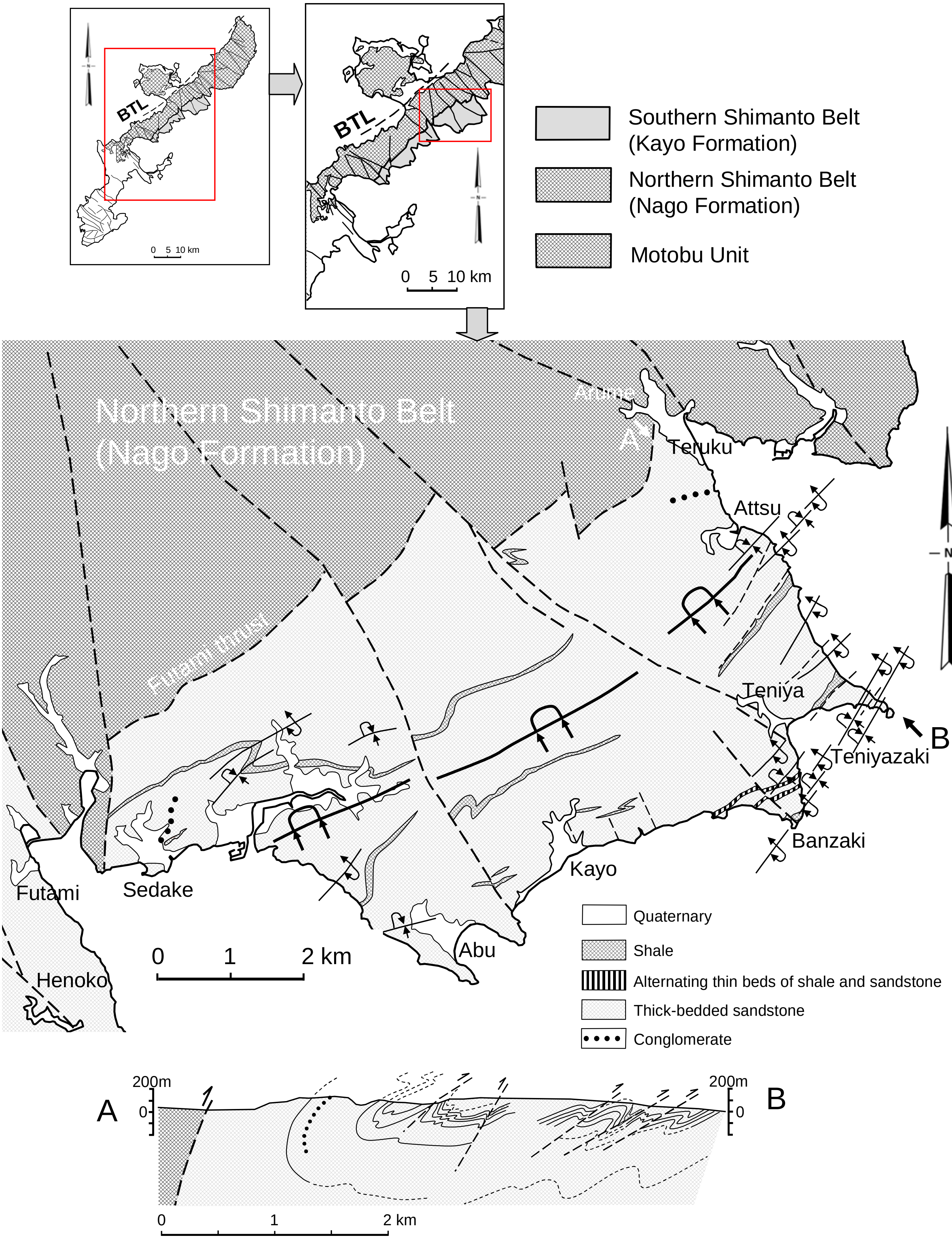

Fig.17 Geological map and profile of the Kayo Formation. Modified from Fukuda *et al*. (1978) and Fukuda & Hayasaka (1978).

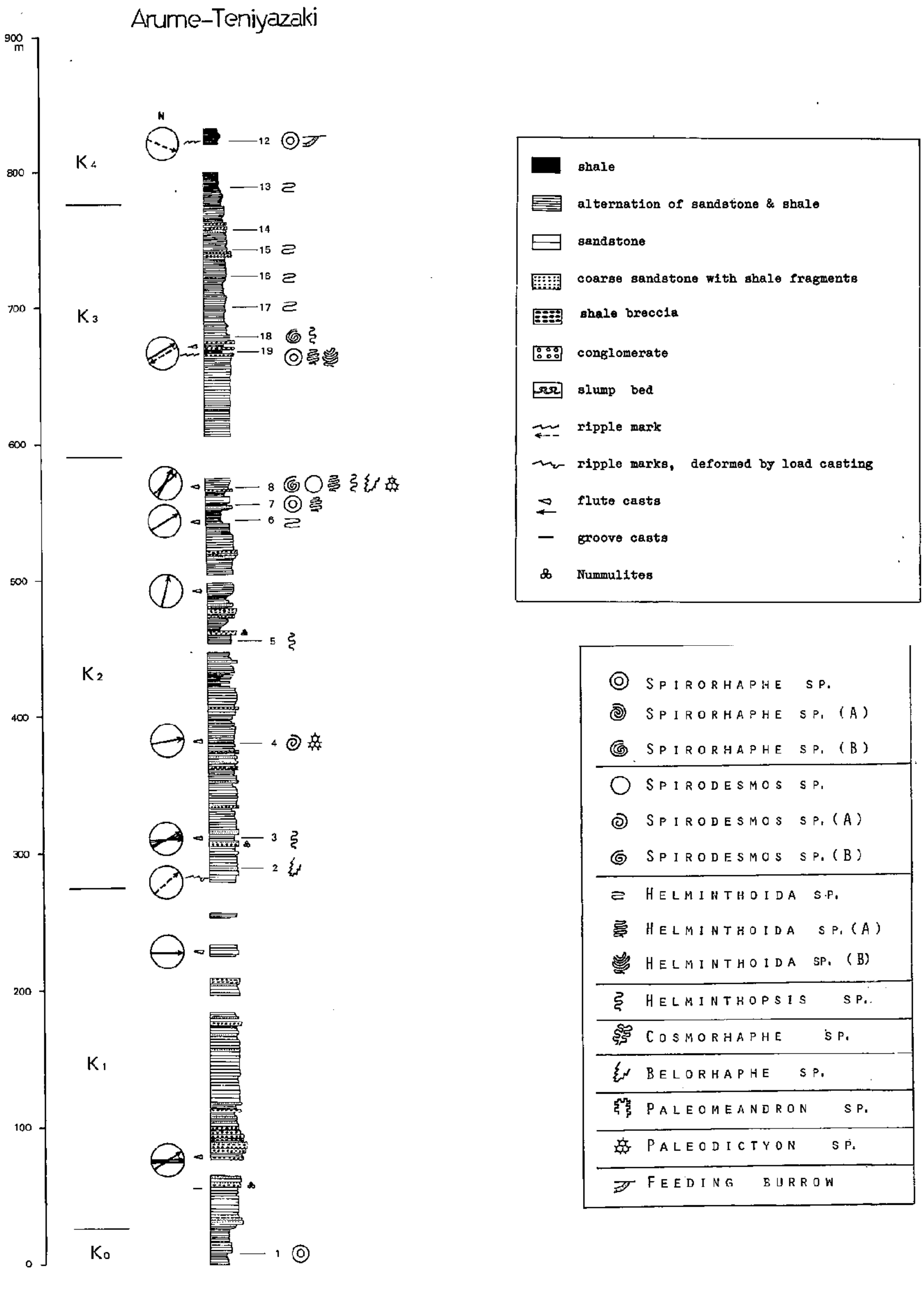

Fig.18 Vertical change of lithofacies of the Kayo Fornation. (◎○: Ill-preserved trace fosills and undistinguishable speciments.) After Fukuda *et al*. (1978) and Fukuda & Hayasaka (1978).

Table 1 List of radiolarian from the Southern Shimanto Belt in Tanegashima (after Okada *et al.*, 1982).

	Tanegashima						
Formation	Kadokurazaki Complex				Kumage Complex		
Locality No.	**R-1**	**R-2**	**R-3**	**R-4**	**R-5**	**R-6**	**R-7**
Specimen No.	92-5	96-2	831-5	901	31105	31209	504
Theocampe mongolfieri		●					
Theocampe armadillo			●				
Thyrsocyrtis bromia			●			●	
Thyrsocyrtis triacantha		●	●	●		●	
Podocyrtis (Lampterium) *sinuosa*	●	●	●				
Cycladophora turris		●				●	
Bekoma sp. (?)		●					
Lychnocanium sp.		●	●		●	●	
Nassellaria gen. et sp. indet.	●	●	●				
Sumellaria gen. et sp. indet.		●	●				
Dictyoprora armadillo					●	●	●
Dictyoprora mongolfieri					●		
Teocotyle ficus				●	●		●
Actinommid gen. et sp. indet				●	●		
Spongodiscid gen. et sp. indet.					●	●	

Table 2 List of radiolarian from the Southern Shimanto Belt in Tanegashima (after Kuwazuru and Nagatsu, 2007).

	Tanegashima		
Formation	Kadokurazaki Complex	Kumage Complex	
Locality No.	**R-8**	**R-9**	**R-10**
Specimen No.	Tg-64	Tg-85	Tg-96
Amhisphaera cf. *minor* Clark and Campbell			●
Discoid gen. et sp. indet.		●	
Eucytidiidae gen. et sp. indet.	●		
Eusyringium cf. *fistuligerum* (Ehrenberg)			●
Lithocyclia (?) sp. aff. L. *crux* Moore			●
Lychnocanium (?) sp.			●
Nassellaria gen. et sp. indet.		●	●
Periphaena (?) sp.	●		●
Periphaena (?) spp.			●
Phormocyrtis (?) sp.			●
Spumellaria gen. et sp. indet.	●	●	●
Stylosphaera (?) spp.			●
Stylosphaerid gen. et sp. indet.			●
Theocampe cf. *amphora* (Haeckel)			●
Theocampe cf.*mongolfieri* (Ehrenberg)	●		
Theocampe (?) sp.			●
Teocotyle cf. *ficus*		●	
Theocyrtis cf. *tuberosa* Riedel			●
Theocyrtis (?) sp.			●
Theoperidae gen. et sp. indet.	●	●	●

Table 3 List of radiolarian from the Southern Shimanto Belt in Yakushima (after Saito *et al.*, 2007).

	Yakushima	
Formation	Kadokurazaki Complex	
Locality No.	**R-11**	**R-12**
Specimen No.	f-1 (GSJ R81918)	f-2 (GSJ R81919)
Host rock	Red shale	Nodule in mudstone
Dictyoprora mongolfieri (Ehrenberg)	●	
Nassellaria gen. et sp. indet.	●	
Calocyclas sp.	●	
Calocycloma sp. cf. *ampulla* Ehrenberg	●	
Calocycloma sp.	●	
Theocyrtis sp. cf. *perpumila* Sanfilippo	●	
Spumellaria gen. et sp. indet.		●
Disk-shaped Spumellaria gen. et sp. indet.		●